PHD

Novel aspects of alkyne substituted transition metal complexes

Cairns, Gareth Alan

Award date:
1998

Awarding institution:
University of Bath

Novel Aspects of Alkyne Substituted Transition Metal Complexes.

submitted by Gareth Alan Cairns

for the degree of Ph.D.

of the University of Bath

1998.

COPYRIGHT

G A Cairns

ProQuest LLC
789 East Eisenhower Parkway
P.O. Box 1346
Ann Arbor, MI 48106-1346

Memorandum.

The work described in this thesis was carried out by the author between October 1993 and October 1996 within the School of Chemistry at the University of Bath, under the supervision of Professor Michael Green. Unless otherwise indicated, the work is original and has not been submitted for any other degree.

Acknowledgements.

I would like to thank my supervisor Professor Michael Green for his guidance, encouragement and patience throughout my studies.

Thanks are due to Dr. Mary Mahon for the crystallographic studies reported within this work. Further thanks go to the technical staff of the Inorganic department Alan Carver, Robert Stevens and Ahmed Sheibani not just for technical support but for their conversation.

To the lab for keeping me sane, going to tea, playing skittles and providing help and friendship, my thanks goes to Simon, Chris, Alan, Jackie, Georg, Steve, Nick, Claire, Harish, Andy, Mark, Jason and Chris.

To the bar for four years enjoyable employment, cheers to Adrian, Ronnie, Tim, Sean, Jo and all in the Union.

I thank EPSRC for the funding to carry out this work.

Finally, I would like to thank Mum and Dad for all their support through my Ph.D. I couldn't have done it without you and Cathy for not nagging too much and proof reading, ta monster.

Summary.

This thesis describes some novel results from the reactions between tris alkyne complexes and co-ordinating chelating phosphines. A new synthetic route into substituted transition metal carborane complexes has also been explored.

The reaction of [W(NCMe)(η^2-PhC≡CPh)$_3$] **15** with *o*-diphenylphosphinostyrene (dpps) yielded an unexpected alkenecarbyne product **I**. Complex **I** exists as two isomers and its structure was confirmed, by a single crystal X-ray diffraction study, to display a tetraphenylcyclopentadienyl ligand, a metal carbyne and a surprisingly modified dpps ligand. Isotopic labelling experiments confirmed that cleavage of both carbon-carbon double and triple bonds had occurred followed by couplings of the fragments to produce **Ia, b**. A possible reaction pathway, suggesting a role for an η^2-vinyl intermediate, is outlined.

In order to extend our understanding of the reaction that had taken place *o*-diphenylphosphinoallylbenzene (dppa) was prepared and reacted with [W(NCMe)(η^2-PhC≡CPh)$_3$] **15** in a similar manner to the dpps. The product **II** was characterised by a single crystal X-ray diffraction study. Surprisingly the complex contains a metal carbene, a diphenylacetylene ligand and a butadienyl ligand. The most interesting structural feature is the two carbon unit which forms a bridge between the carbene carbon and the carbon atom that had as its origin the allylic CH_2 carbon of the dppa ligand. It is again suggested that the reaction pathway involves an η^2-vinyl intermediate.

In attempting to synthesise a cycloheptatrienyl/carborane mixed sandwich species, the complex [NEt_4][*closo*-3,3-$(CO)_2$-3-(η^3-C_7H_7)-3,1,2-$MoC_2B_9H_{11}$] **V** was formed, which upon protonation produced a labile leaving group allowing a number of molecules to fill the vacant co-ordination site yielding complexes of the general formula [*closo*-3-$(CO)_x$-3-$(L)_y$-3,1,2-$MoC_2B_9H_{11}$]. Further reactions produced the complex [*closo*-3-(CO)-3-(η^2-PhC≡CPh)-3-(PPh_3)-3,1,2-$MoC_2B_9H_{11}$].

The preparation of a four electron donor phosphaalkyne complex of tantalum is also reported within.

Contents.

Abbreviations.

General		**NMR**	
acac	acetylacetonate	at	apparent triplet
Bu^n	n-butyl	br	broad
Bu^t	tert-butyl	d	doublet
Cp	cyclopentadienyl	dd	doublet of doublets
dmpe	1,2- bis-(dimethylphosphino)ethane	hept	heptet
dppa	*o*-diphenylphosphinoallylbenzene	J	Coupling constant in Hertz
dppe	1,2-bis-(diphenylphosphino)ethane	m	multiplet
dppm	*bis*-(diphenylphosphino)methane	ppm	parts per million
dpps	*o*-diphenylphosphinostyrene	q	quartet
Et	ethyl	s	singlet
Me	methyl	t	triplet
Ph	phenyl	tt	triplet of triplets
^iPr	isopropyl		
py	pyridine		
r.t.	room temperature		

.... And he respects Owl, because you can't help respecting anybody who can spell TUESDAY, even if he doesn't spell it right; but spelling isn't everything. There are days when spelling Tuesday simply doesn't count.

A.A. Milne

The House at Pooh Corner.

CHAPTER 1

Introduction to Tris Alkyne Chemistry

1 Introduction.

1.1 Tris Alkyne Chemistry.

Since the beginning of organo-transition metal chemistry interest has been shown in the bonding and reactivity of transition metal alkyne complexes. Initially in this chemistry the alkyne was considered to be acting in a similar fashion to an alkene [1,2], *i.e.* that the metal to alkene bond consists of L→M π donation and M→L back donation into the π^* orbitals of the alkene, Figure 1.1.

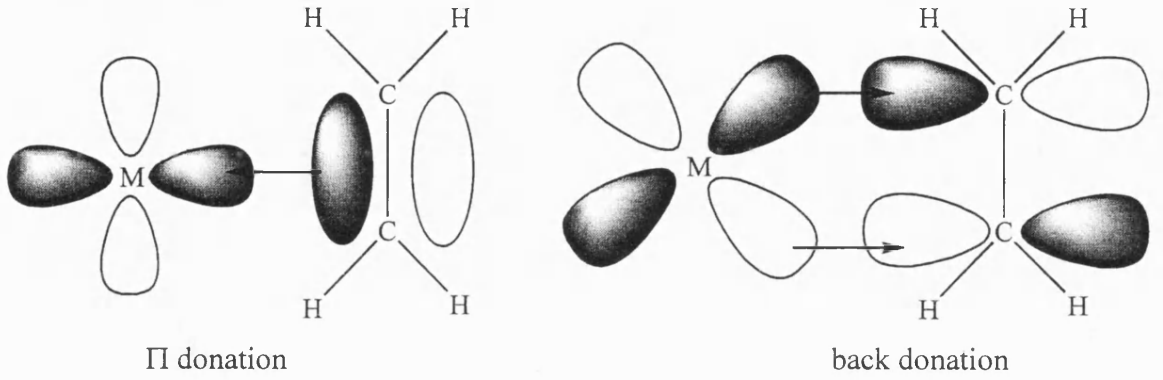

Π donation back donation

Figure 1.1.

This type of bond interaction was observed for alkynes where the alkyne utilises one of its pair of π orbitals in a bonding mode.

This was accepted as the bonding nature of alkynes until 1963 when Tate and Augl [3] published the results of a study into the reaction between $[W(NCMe)_3(CO)_3]$ **1** and hex-3-yne, which produced a new alkyne complex of tungsten that exhibited "a very unusual structural and electronic arrangement". In order to account for the physical and chemical properties of the complex, they proposed the product of the reaction to be $[W(CO)(\eta^2\text{-}EtC{\equiv}CEt)_3]$ **2**, Scheme 1.1. They made the following statements about the new complex:-

1 The geometry about the tungsten must be "pseudotetrahedral".

2 The alkyne was "doubly π bonded to the tungsten atoms".

3 In order to achieve the effective atomic number for tungsten, two of the three alkyne ligands must be serving in "the unusual capacity of four electron donors".

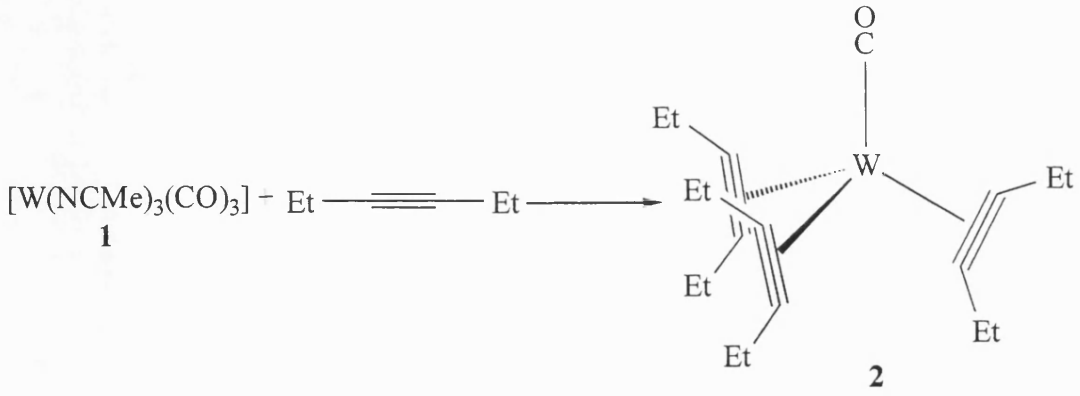

Scheme 1.1.

Infra-red studies showed a single strong absorption at 2036cm^{-1} for the terminal metal carbonyl and a band at 1702cm^{-1} which was compared to a series of complexes synthesised by Chatt [4]. This series of platinum alkyne complexes all exhibited infra-red absorption bands at 1700cm^{-1}, attributed to the alkyne ligand, which indicated that the triple bond had been reduced in strength to a double bond. Tate inferred that this meant that the alkyne in **2** was doubly π bonded, *i.e.* acting as a four electron donor, to the metal centre, though, it has since been shown that this cannot be ascertained by infra-red alone. Proton NMR studies showed that, though all three alkynes were equivalent, the terminal ethyl groups were in different environments. The ethyl groups nearer to the carbonyl group having a different chemical shift to those further away. The NMR study also ruled out the formation of a benzene type ring. The electronic equivalence of the alkyne groups can be explained by delocalisation throughout the hydrocarbon system.

The chemistry of these complexes was expanded in 1964 [5] when further trisalkyne tungsten analogues were prepared, Scheme 1.2, highlighting the accessibility of these new complexes.

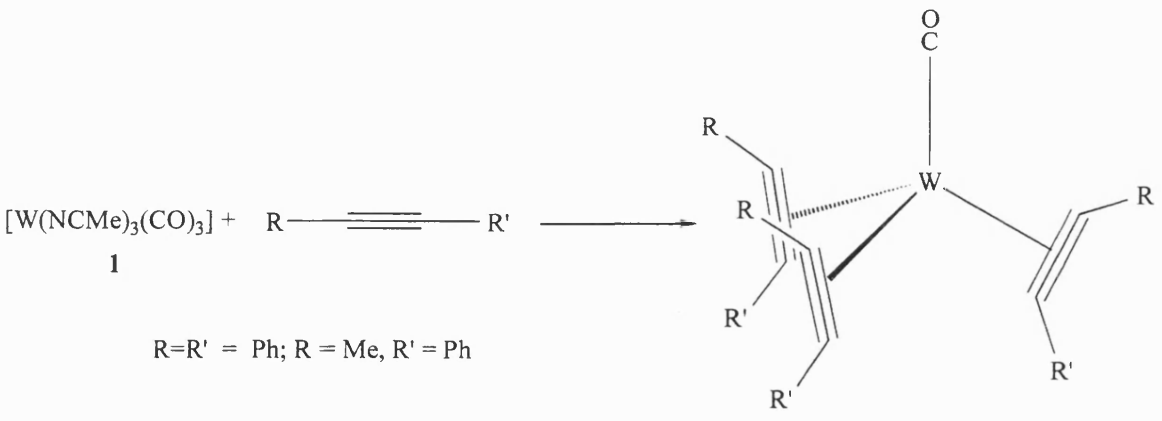

Scheme 1.2.

In attempting to extend this chemistry to molybdenum and chromium, completely different results were observed. The molybdenum system lead to the formation of hexaethylbenzene from hex-3-yne *via* cyclotrimerization and the chromium system produced highly air sensitive products.

These unusual products promoted increased interest in the area of alkyne transition metal chemistry and King [6] reported the production of a similar complex from the reaction of **1** with hexafluorobut-2-yne. This differed slightly from Tate's original complexes in being the acetonitrile adduct rather than the carbonyl, Scheme 1.3.

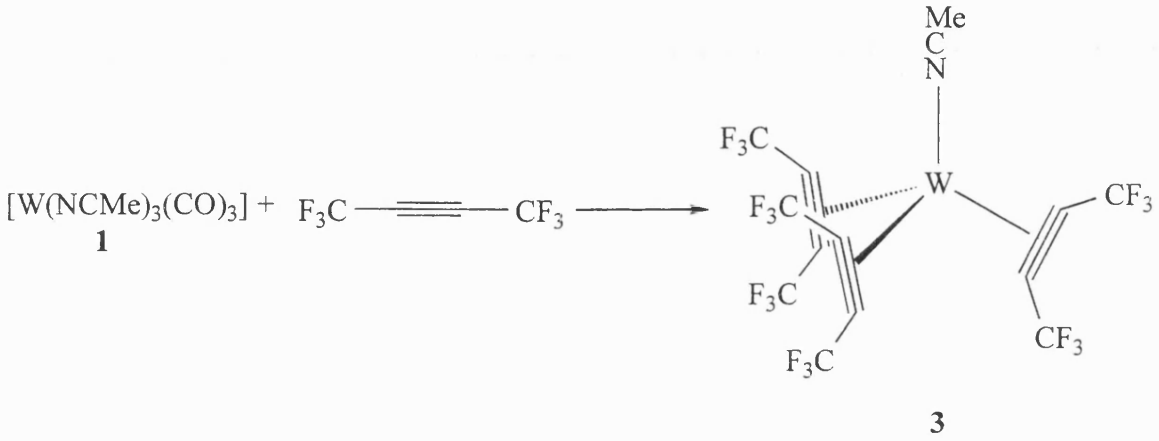

Scheme 1.3.

The formation of an acetonitrile product instead of a carbonyl complex was explained by the electronegativity of the hexafluorobut-2-yne ligands. These ligands may withdraw d electrons from the tungsten atom in the $[WL(\eta^2\text{-}CF_3C{\equiv}CCF_3)_3]$ complex to the extent that insufficient electron density remains for the stabilisation of the tungsten carbonyl bond by the partial pπ-dπ multiple bonding. Thus, the remaining ligand is the acetonitrile because it does not require any pπ-dπ multiple bonding to form a stable bond to tungsten. The molybdenum analogue was prepared in a similar manner [7].

King was concerned that if an alkyne had the ability to act as a four electron donor, as suggested by the complexes described above, why was the product $[WL(alkyne)_3]$ and not $[W(alkyne)_3]$ because the latter would also achieve the effective atomic number for tungsten. He studied the molecular orbital interactions of the $[W(alkyne)_3]$ system and suggested the answer to this problem which is summarised below [8].

King suggested that alkyne four electron donation is achieved by a reversal of the synergic bonding encountered in carbon monoxide and alkenes. One of the molecular orbitals ($\pi_{||}$) of the alkyne creates a σ bond to the metal then a perpendicular filled molecular orbital ($\pi_{\perp}$) of the alkyne is of the correct symmetry to form a π bond with an empty metal d orbital thus donating 4 electrons to the metal atom, Figure 1.2

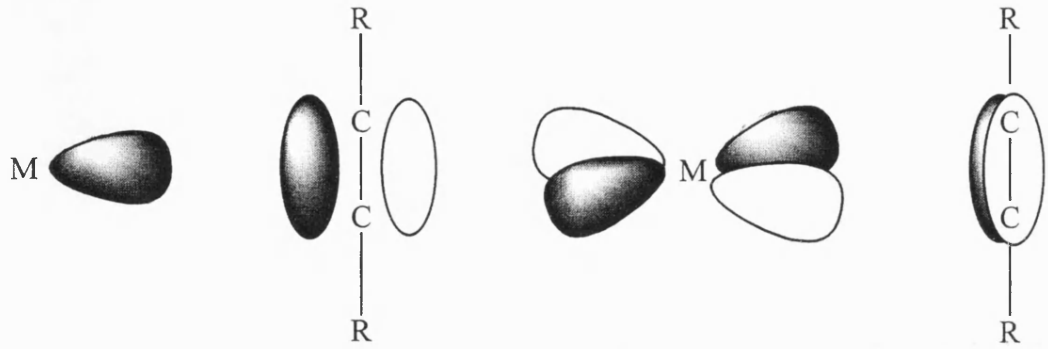

$\pi_{||} \rightarrow M\sigma$ $\pi_{\perp} \rightarrow M(d_{\pi})$

Figure 1.2.

King then went on to consider the possible configurations that a $W(alkyne)_3$ system could hypothetically obtain, Figure 1.3.

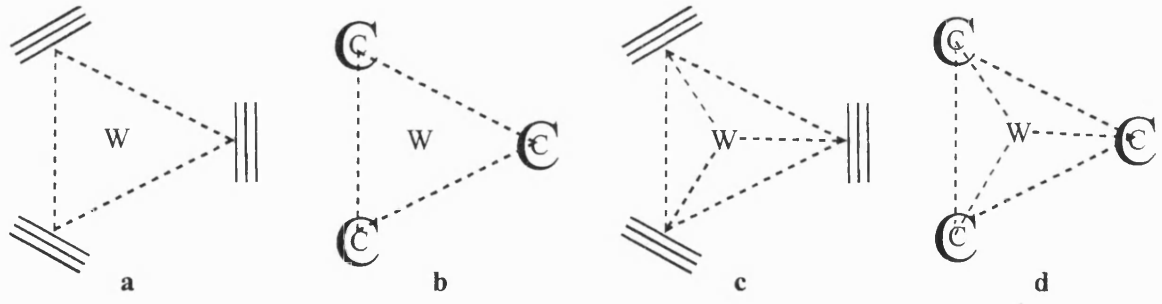

a D_3h **b** D_3h **c** C_3v **d** C_3v

Figure 1.3.

These configurations fall into two symmetry groups; D_{3h}, where the centres of the alkyne ligands and the tungsten are in the same plane (**a** and **b**), and C_{3v}, where the centres of the alkynes are not in the same plane as the tungsten atom in (**c** and **d**). In the cases of **a** and **c** where the alkynes lie parallel to the plane of the molecule there is severe steric hindrance and trimerisation is likely to occur, hence ruling them out of the study.

The other two cases, **b** and **d**, can be reduced to an irreducible representation in which only two appropriate metal orbitals are available for two of the alkynes to donate four electrons whilst the third can only donate two electrons.

This treatment showed that $[W(alkyne)_3]$ would be two electrons short of the favoured noble gas configuration, thus to obtain this desired state a fourth ligand is incorporated into the complex, apparently explaining the prevalence of $[WL(alkyne)_3]$ complexes.

Both Tate's original work and King's above was justified when the first single crystal X-ray structure determination of one of these molecules was completed by Bau [9] in 1972, Figure 1.4.

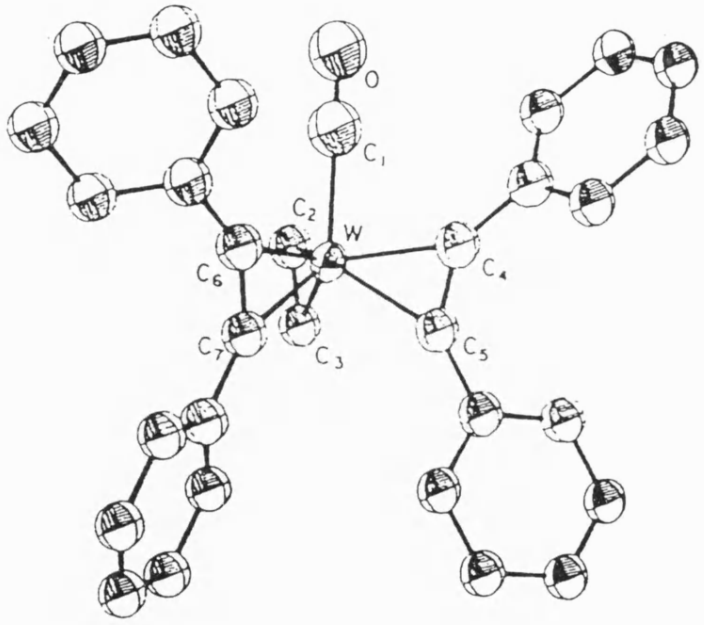

Figure 1.4 The molecular geometry of $[W(CO)(\eta^2\text{-}PhC{\equiv}CPh)_3]$ **4**, the phenyl rings on carbons C_2 and C_3 have been omitted for clarity.

The structure proved the pseudo tetrahedral nature of this group of complexes, with C_{3v} symmetry and supports the proposals made above.

The next significant step forward for trisalkyne chemistry was reported by Green et al [10], when a anionic molybdenum trisalkyne system was prepared, Scheme 1.4. The product of this reaction **5** was identified by a single crystal X-ray diffraction study which disclosed that the crystal contained discrete $[(\eta^7\text{-}C_7H_7)Mo(\mu\text{-}Cl)_3Mo(\eta^7\text{-}C_7H_7)]^+$ and $[MoCl(\eta^2\text{-}CF_3C_2CF_3)_3]^-$ ions.

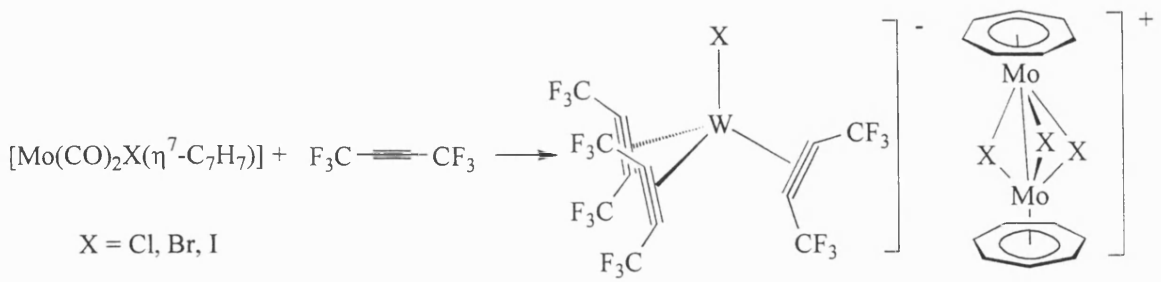

5

Scheme 1.4.

The binuclear cation has two molybdenum atoms each co-ordinated by a η^7-bonded cycloheptatrienyl ligand, and linked by three chlorine bridges. The anion contains one molybdenum atom co-ordinated by three hexafluorobut-2-yne molecules, and one chlorine atom, with the geometry about the molybdenum being described as either a distorted tetrahedron or a tapered mono-capped prism, *i.e.* four or seven co-ordinate.

1.2 Physical Properties of Alkyne Complexes.

There is a much larger body of research relating to the mono and bis alkyne transition metal complexes [11] and the physical properties of these complexes have been analysed for common factors. Templeton found that for terminal four electron donor alkynes the proton NMR would exhibit low field resonances for the alkynic protons. Some examples of this are given in Table 1.1.

A correlation was recognised between ^{13}C-$\{^1H\}$ NMR chemical shift and the number of electrons donated by an alkyne to a metal centre [12], Table 1.2. It should be noted that the alkyne donation of three and one third electrons results from delocalisation of the electrons in the bis and trisalkyne systems, in bisalkyne complexes the alkynes are acting as one four electron donor and one two, which averages out at three electrons per alkyne, and in the trisalkyne case, two alkynes act as four electron donors and one as a two electron donor giving and average of three and one third. A much larger number of complexes were reviewed by Templeton [12] and a graphical representation of the results is shown in Figure 1.5.

Complex	^{1}H NMR shift (ppm)
$[Mo(Br)_2(CO)(PEt_3)_2(\eta^2\text{-}PhC{\equiv}CH)]$	13.0
cis-$[W(CO)_2I_2(PMe_3)(\eta^2\text{-}PhC{\equiv}CH)]$	12.5
trans-$[W(CO)_2I_2(PMe_3)(\eta^2\text{-}PhC{\equiv}CH)]$	13.0
$[Mo(Br)_2(CO)(\eta^2\text{-}PhC{\equiv}CH)(dppe)]$	10.9, 10.8 (isomer)
$[Mo(CO)(PMe_3)_2(\eta^2\text{-}Bu^tC{\equiv}CH)(Cp)][BF_4]$	11.6

Table 1.1 Proton NMR data for selected terminal alkyne complexes.

Complex	^{13}C-{^{1}H} NMR shift (ppm)	No. of electrons donated
$[W(CH_3)(CO)(\eta^2\text{-}HC{\equiv}CH)(Cp)]$	192.5, 187.4.	4
$[W(CO)(\eta^2\text{-}EtC{\equiv}CEt)_3]$	191.1, 170.8.	$3^1/_3$
$[W(CO)(\eta^2\text{-}MeC{\equiv}CBu^n)_2(Cp)]^+$	162.2, 159.4, 144.8, 141.5.	3
$[Mo(\eta^2\text{-}MeC{\equiv}CMe)(Cp)_2]$	115.3.	2

Table 1.2 Selected ^{13}C-{^{1}H} NMR data for internal alkyne complexes.

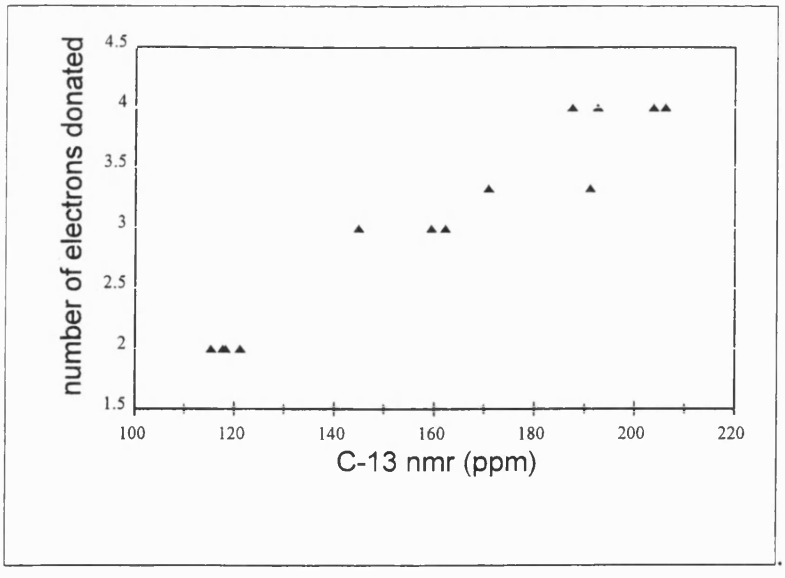

Figure 1.5.

1.3 Reactions of Tris-Alkyne Systems.

1.3.1 Substitution.

The first report of a tris-alkyne substitution reaction was by Shaw [13]. He was investigating organo-transition metal complexes containing crown ether groups, concentrating on substituted crown ether groups. Shaw prepared some benzo-crown ethers substituted in the arene ring, one of the substitutions he described was with C≡CPh, Figure 1.6.

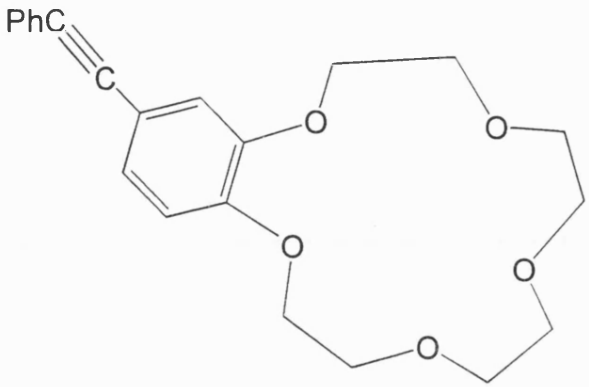

6

Figure 1.6.

He investigated the bridging characteristics of this alkyne by comparing it to PhC≡C$C_6H_3(OMe)_2$-3,4 **7** in nickel and cobalt systems, producing $[Co_2(CO)_6(\eta^2$-PhC≡CR)] and $[Ni_2(\eta^2$-PhC≡CR)$(\eta$-$C_5H_5)_2]$ where R= **7** or **6**, less the PhC≡C unit. Having recognised the unusual chemistry of the tungsten trisalkyne systems described earlier [3,5,9], the reaction of $W(CO)_6$ with both of these alkynes in refluxing acetonitrile for 20 hours was carried out, producing the expected tris-alkyne products, Scheme 1.5.

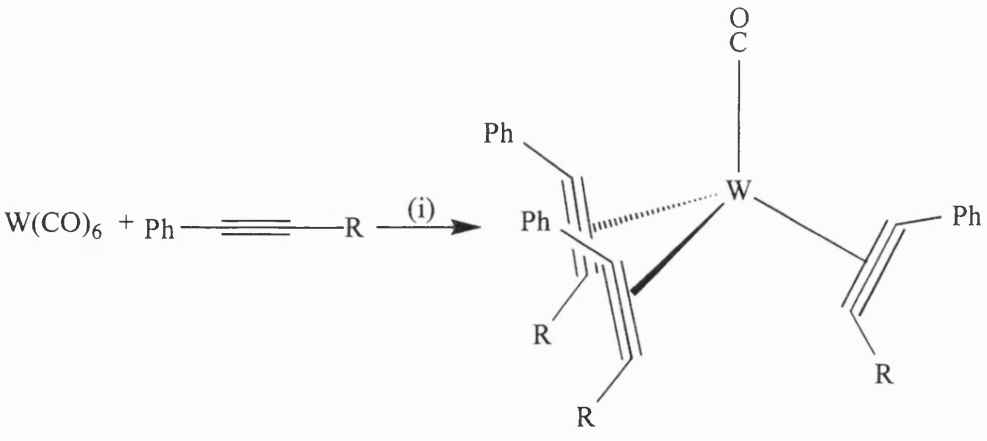

Scheme 1.5 (i) MeCN, reflux; R= **7**→**8a**; R=**6**→**8b**.

He further reacted both **8a,b** with phenyldimethylphosphine (PMe_2Ph), in refluxing benzene for 20 hours, producing the phosphine substituted tris-alkyne tungsten complex $[W(PMe_2Ph)(\eta^2\text{-}PhC{\equiv}CR)_3]$ **9a,b**. The complex **9a**, the **7** derivative, exhibited an $^{31}P\text{-}\{^1H\}$ NMR spectra of two peaks at δ 5.17 and 5.23 ppm each with satellites due to ^{183}W, indicative of two isomers of **9a**, these being with either the phenyl groups in the positions closest to the phosphine or with the **7** grouping closest to the phosphine. The complex **9b**, the **6** derivative, was much less stable than **9a** and could not be isolated pure, though two peaks were again observed in the $^{31}P\text{-}\{^1H\}$ NMR spectrum, at δ 4.97 and 5.03 ppm. In this case the satellites due to coupling to the tungsten were not observed due to decomposition of the complex. These two peaks are again due to isomers of the complex based upon the orientation of the alkyne with respect to the phosphine.

The preparation of the first phosphine substituted tris-alkyne complex, as described above, lead Connor and Hudson [14] to investigate the reaction between a tris-alkyne system and a chelating (2 + 2) electron heteroatom donor ligand. They investigated the reaction of the tungsten complexes $[W(CO)(\eta^2\text{-}RC{\equiv}CR)_3]$, where R= Ph (**4**) and SMe (**10**) [15] with both monodentate and bidentate ligands, no reaction was observed with either triphenylphosphine or 1,2-bis-(diphenylphosphino)ethane (dppe) though reaction of 1,2-bis-(dimethylphosphino)ethane (dmpe) was observed under mild conditions. The reaction of dmpe with **10** in dichloromethane at ambient temperature lead to the formation of the bright pink complex $[W(CO)(\eta^2\text{-}MeSC{\equiv}CSMe)_2(dmpe)]$ **11**, Scheme 1.6. The proton NMR of **11** showed signals for both dithiahex-3-yne (δ 2.86 ppm) and co-ordinated dmpe (δ 1.70 ppm) and an infra-red absorption of $1902cm^{-1}$ for the carbonyl stretch.

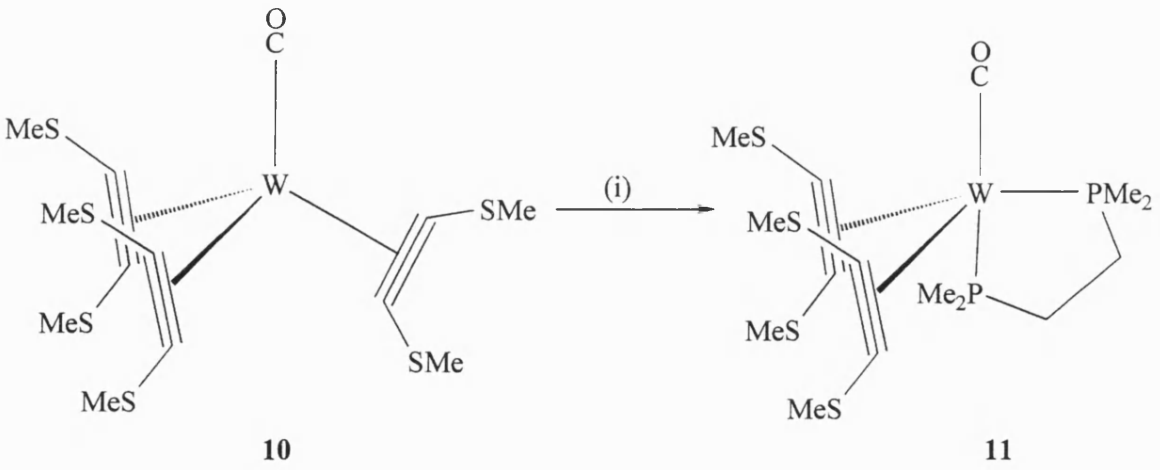

10 **11**

Scheme 1.6 (i) dmpe, CH_2Cl_2.

If this complex is left in a dichloromethane solution the infra-red band at 1902cm^{-1} is observed to disappear and a yellow air stable solid can be isolated from the solution. This yellow solid was shown to be [W(η^2-MeSC≡CSMe)$_2$(dmpe)] **12**. The alkynes display their ability to act in different bonding modes if we compare the electron counts for the complexes [W(CO)(η^2-MeSC≡CSMe)$_2$(dmpe)] **11** and [W(MeSC≡CSMe)$_2$(dmpe)] **12**. For complex **11** to achieve a noble gas electron configuration around the tungsten, one of the alkynes must be acting as a four electron donor and the other must be acting as a two electron donor alkyne. Whereas, in complex **12** both alkynes are acting as four electron donors. It was suggested that the decarbonylation observed occurs because both alkynes wish to stay as four electron donor ligands to the tungsten.

Repeating the reaction of **10** with dmpe in acetone instead of dichloromethane yields a pink air stable complex, again of the composition [W(CO)(η^2-MeSC≡CSMe)$_2$(dmpe)] **13**. However, it was found that complex **13** has a different decomposition temperature compared to that of complex **11** (**11** decomposition temperature of 418K, **13** decomposition temperature of 464K). It was suggested that **13** had a polymeric structure as shown in Figure 1.7. The reactions of **4** with dmpe lead to the formation of [W(CO)(dmpe)$_3$], [W(dmpe)$_3$] and [W(CO)$_2$(dmpe)$_2$].

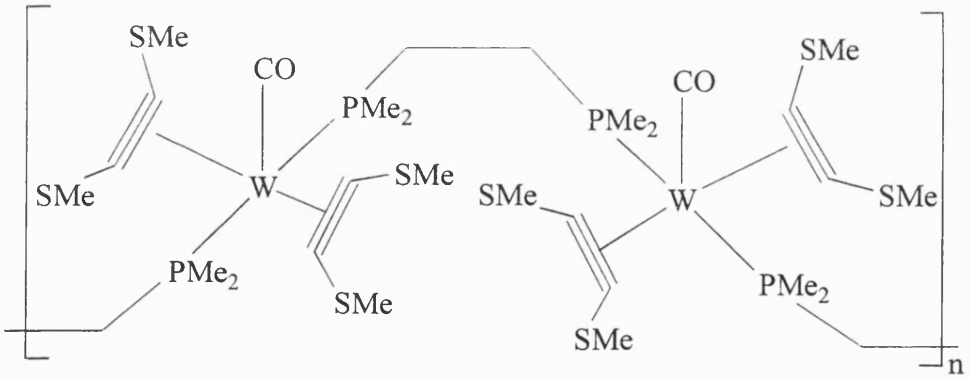

13

Figure 1.7.

The next example of a phosphine substituted tris-alkyne system highlights a second synthetic route into tris-alkyne chemistry [16]. Wilkinson reduced [WCl$_4$(PMe$_3$)$_3$] [17] with sodium amalgam in the presence of phenylacetylene to produce [W(PMe$_3$)(η^2-PhC≡CH)$_3$] **14**, Scheme 1.7. This complex's NMR spectra are as to be expected for a tris-alkyne complex.

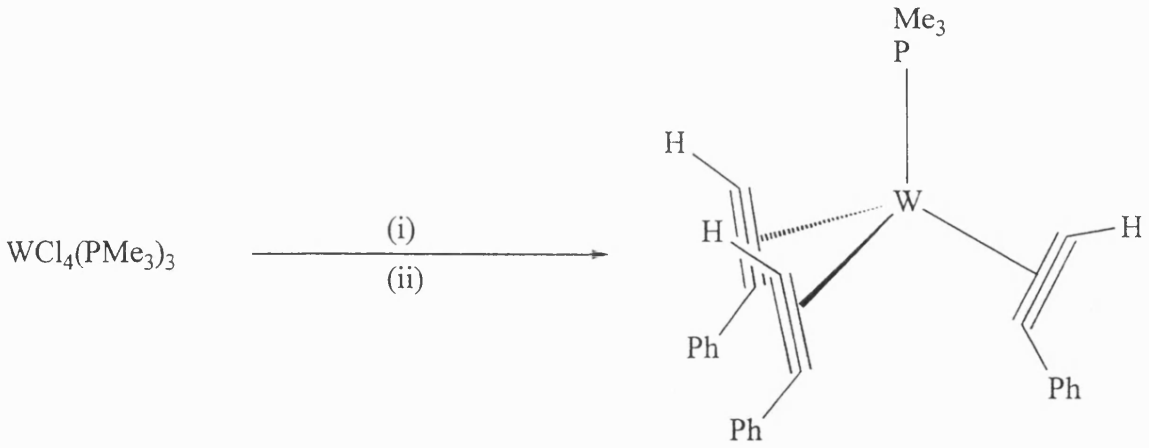

14

Scheme 1.7 (i) Na/Hg, thf; (ii) PhC≡CH.

The main features of the ^{13}C-{^{1}H} NMR are a doublet at δ 201.4 ppm ($^{2}J(CP)$ = 5 Hz; $^{1}J(CW)$ = 41 Hz) assigned to Ph*C*≡CH, a doublet at δ 164.2 ppm ($^{2}J(CP)$ = 16 Hz; $^{1}J(CW)$ = 32.8 Hz) assigned to PhC≡*C*H and another doublet at δ 17.5 ppm ($^{1}J(CP)$ = 14.7 Hz) due to P*Me*$_3$. These assignments were confirmed by a ^{13}C coupled spectrum where the peak at δ 164.2 ppm appears as a doublet of doublets due to coupling both to phosphorus and hydrogen. The ^{31}P-{^{1}H} NMR spectra showed a single peak at δ 0.62 ppm with tungsten satellites, the tungsten-phosphorus coupling being 140Hz. The pseudo-tetrahedral geometry of this family of complexes was again confirmed by a single crystal X-ray diffraction study, the result of which is shown in Figure 1.8.

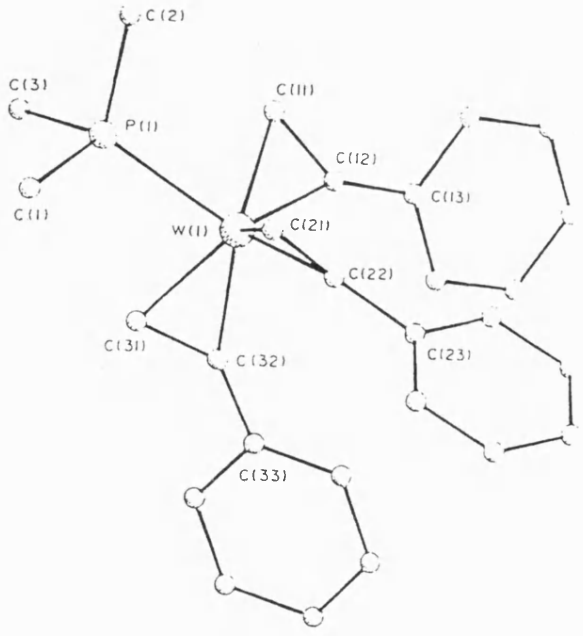

Selected parameters for [W(PhC≡CH)$_3$(PMe$_3$)]:- W-P(1) 2.455(4), W-C(11) 2.076(1), W-C(12) 2.078(13), W-C(21) 20.93(25), W-C(22) 2.035(19), W-C(31) 2.070(23), W-C(32) 2.072(23), C(11)-C(12) 1.299(22), C(21)-C(22) 1.336(24), C(31)-C(32) 1.292(19).

Figure 1.8 Molecular Structure of [W(PMe$_3$)(η^2-PhC≡CH)$_3$].

Previous studies had found the preparation of aryl substituted phosphine trisalkyne complexes to be impossible, fortunately a synthetic route into these complexes was produced by Wen-Yann [18]. The methodology devised involved the conversion of the carbonyl trisalkyne to an acetonitrile trisalkyne complex $[W(NCMe)(\eta^2\text{-}PhC{\equiv}CPh)_3]$ **15**, using trimethylamine-N-oxide in acetonitrile solution. The acetonitrile product was isolated as a white solid which under went facile substitution reactions with phosphines. This was demonstrated by the reaction of **15** with triphenylphosphine or bis-(diphenylphosphino)methane (dppm) in refluxing toluene to give the products $[W(PPh_3)(\eta^2\text{-}PhC{\equiv}CPh)_3]$ **16** and $[W(\eta^1\text{-}PPh_2CH_2PPh_2)(\eta^2\text{-}PhC{\equiv}CPh)_3]$ **17** as shown in Scheme 1.8. The NMR spectra of **16** and **17** showed the expected characteristics and selected data are summarised in Table 1.3.

NMR	$[W(PPh_3)(\eta^2\text{-}PhC{\equiv}CPh)_3]$ **16**	$[W(\eta^1\text{-dppm})(\eta^2\text{-}PhC{\equiv}CPh)_3]$ **17**
$^{13}C\text{-}\{^1H\}$ NMR	δ 198.7, d, C≡C, $^2J(PC)$ = 3.3Hz, $^1J(WC)$ = 32Hz; 180.9, m, C≡C, $^2J(PC)$ = 19Hz, $^1J(WC)$ = 45Hz.	δ 197.2, b, C≡C; 180.3, b, C≡C; 28.0, m, PCH_2P.
$^{31}P\text{-}\{^1H\}$ NMR	δ 36.03, s, $^1J(WP)$ = 128.2Hz	δ 27.48, d, $^2J(PP)$ = 13Hz, $^1J(WP)$ = 125Hz; -23.77, d, $^2J(PP)$ = 13Hz.

Table 1.3 Selected NMR data for complexes 16 and 17.

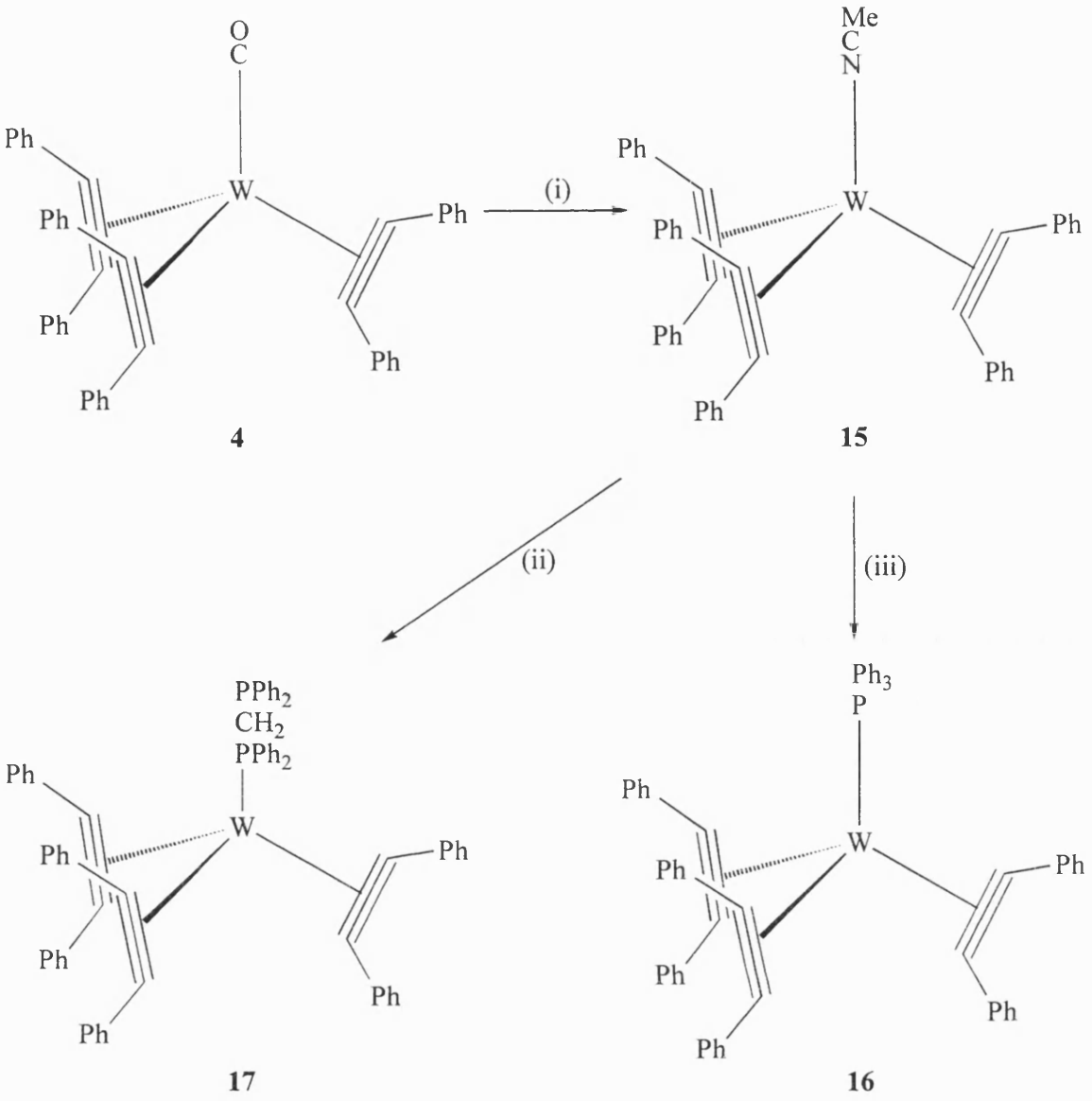

Scheme 1.8 (i) Me_3NO, MeCN, $-CO_2$; (ii) $Ph_2PCH_2PPh_2$; (iii) PPh_3.

There has been little interest in tris-alkyne chemistry outside of the chromium triad, one exception to this though is the work of Mayer. He has been able to prepare a series of rhenium tris-alkyne complexes, $[ReI(\eta^2\text{-}RC{\equiv}CR)_3]$ from $KReO_4$ [19], where R = Me (**18**) or Et (**19**), Scheme 1.9. The alkyne carbons show $^{13}C\text{-}\{^1H\}$ NMR chemical shifts at δ 168.25, 157.08 and δ 171.81, 162.79 for **18** and **19** respectively, typical for the resonance stabilised $3^1/_3$ electron donor alkynes expected for these systems on the basis of symmetry arguments and the 18-electron rule.

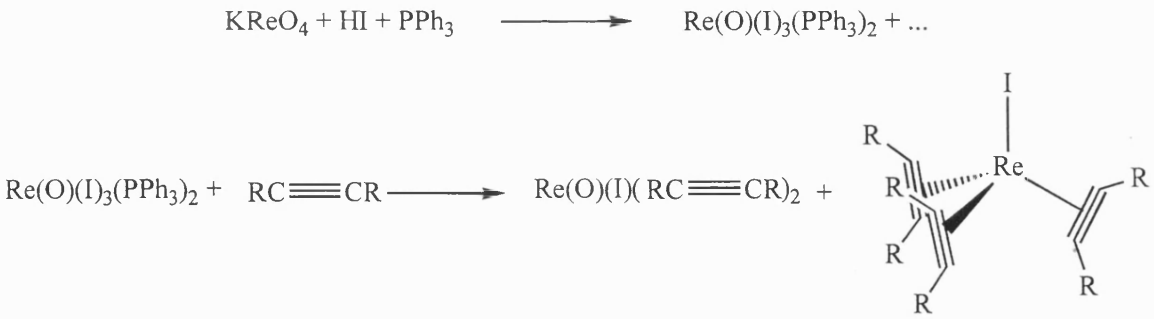

R= Me or Et.

Scheme 1.9.

The principal site of reactivity in these complexes is the iodide ligand, it can be removed with $AgSbF_6$ or replaced by a methyl group, upon reaction with methyl lithium [19]. Utilising this reactivity has lead to a number of derivatives of the initial trisalkyne system being prepared [19,20], Scheme 1.10.

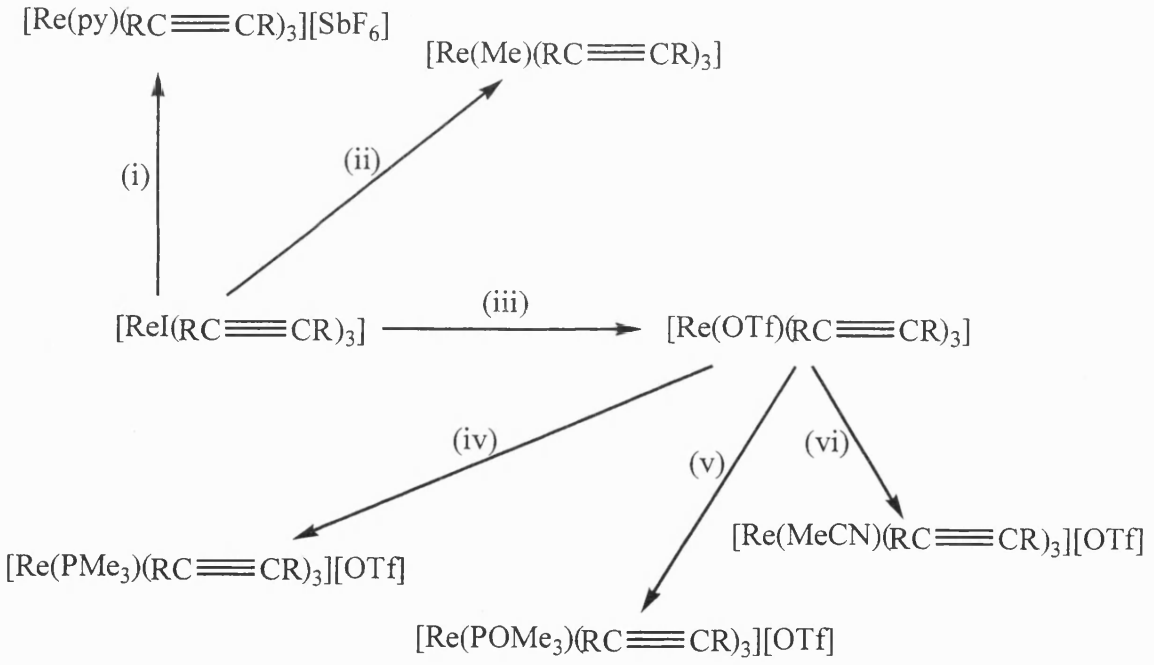

R = Me or Et.

Scheme 1.10 (i) $AgSbF_6$, Pyridine (py); (ii) MeLi; (iii) AgOTf; (iv) PMe_3; (v) $OPMe_3$; (vi) MeCN.

1.3.2 Reduction of Trisalkyne Complexes.

The reduction of $[W(CO)(\eta^2\text{-PhC}\equiv\text{CPh})_3]$ **4** with lithium naphthalenide at -78°C has been investigated by Cooper [21,22] to prepare the dianion $[W(\eta^2\text{-PhC}\equiv\text{CPh})_3]^{2-}$, which exhibits a

dark red-purple colour in thf solution. The formation of the dianion was monitored by the loss of the carbonyl stretch in the infra-red at 2070 cm^{-1}. The colour of the solution did not vary upon warming to room temperature but no products could be isolated. To isolate the dianion it was trapped with triphenyltin chloride, which was added to the reduced solution whilst still at low temperature, a lightening of the solution was observed to red. To further aid the work up of the products of this reaction counter cation exchange was carried out with tetraethylammonium bromide from which analytically pure $[W(SnPh_3)(\eta^2\text{-}PhC{\equiv}CPh)_3][NEt_4]$ **20** could be isolated, Scheme 1.11.

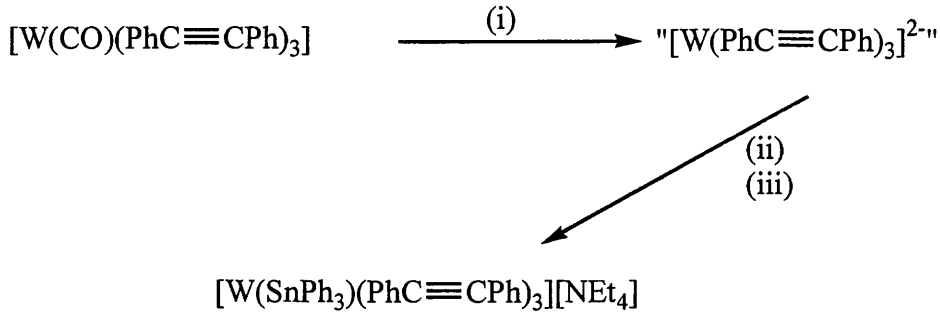

20

Scheme 1.11 (i) $LiC_{10}H_8$, -CO; (ii) Ph_3SnCl; (iii) $[NEt_4]Br$.

The isolation of **20** from the reaction of the reduced solution with Ph_3SnCl does not conclusively prove the formation of $[W(\eta^2\text{-}PhC{\equiv}CPh)_3]^{2-}$ since previous reports [23] have shown that $[W(CO)_5SnPh_3]^-$ can be formed from the reaction of Ph_3SnCl with either $[W(CO)_5]^{2-}$ or its first oxidation product $[W_2(CO)_{10}]^{2-}$, but it does seem probable that the reduction product in the case of **4** is the expected $[W(\eta^2\text{-}PhC{\equiv}CPh)_3]^{2-}$. A similar method was used to produce the trimethyltin derivative of this complex, $[W(SnMe_3)(\eta^2\text{-}PhC{\equiv}CPh)_3][NEt_4]$ **21**. Both these compounds exhibited no signals relating to the alkyne carbons in the $^{13}C\{^1H\}$ NMR at room temperature. These signals can, however, be observed at low temperature (213K), Table 1.4, suggesting that both **20** and **21** are fluxional and that the alkyne resonances are near coalescence at room temperature. Using this information the barrier to rotation for these alkynes was calculated, being 13.1 kcal mol^{-1} and 12.7 kcal mol^{-1} for **20** and **21** respectively, suggesting that steric factors do not dominate the barriers to rotation for $[WL(alkyne)_3]$ complexes.

$[W(SnPh_3)(\eta^2\text{-}PhC{\equiv}CPh)_3][NEt_4]$	$[W(SnMe_3)(\eta^2\text{-}PhC{\equiv}CPh)_3][NEt_4]$
δ 197.3[a]	δ 196.1 ($^1J(WC)$ = 23Hz, $^2J(SnC)$ = 23Hz.)
δ 183.3[a]	δ 186.9 ($^1J(WC)$ = 36Hz, $^2J(SnC)$ = 104Hz.)

[a] satellites for tungsten and tin observed but no couplings reported.

Table 1.4 Alkyne carbon NMR data at 213K for 20 and 21.

1.3.3 Alkyne Coupling Reactions.

Recently there has been some very interesting reports of alkyne coupling reactions involving tris-alkyne systems. These reactions have lead to the formation of cyclobutadienes [24], cyclopentadienylvinylcarbenes [25] and η^4-butadienyls [26]. Below is a brief review of the chemistry involved in the formation of each of these products.

It was reported that it was possible to promote a reaction between $[W(CO)(\eta^2\text{-}PhC{\equiv}CPh)_3]$ **4** and further diphenylacetylene, forming a cyclobutadiene product [24]. The reaction conditions involve sealing **4** and diphenylacetylene in a glass tube under vacuum, heating to 120°C and dissolving **4** in the molten diphenylacetylene forming a dark red solution. After cooling and chromatographic work up red crystals of $[W(CO)(\eta^2\text{-}PhC{\equiv}CPh)_2(\eta^4\text{-}C_4Ph_4)]$ **22** were obtained in a 41% yield, Scheme 1.12.

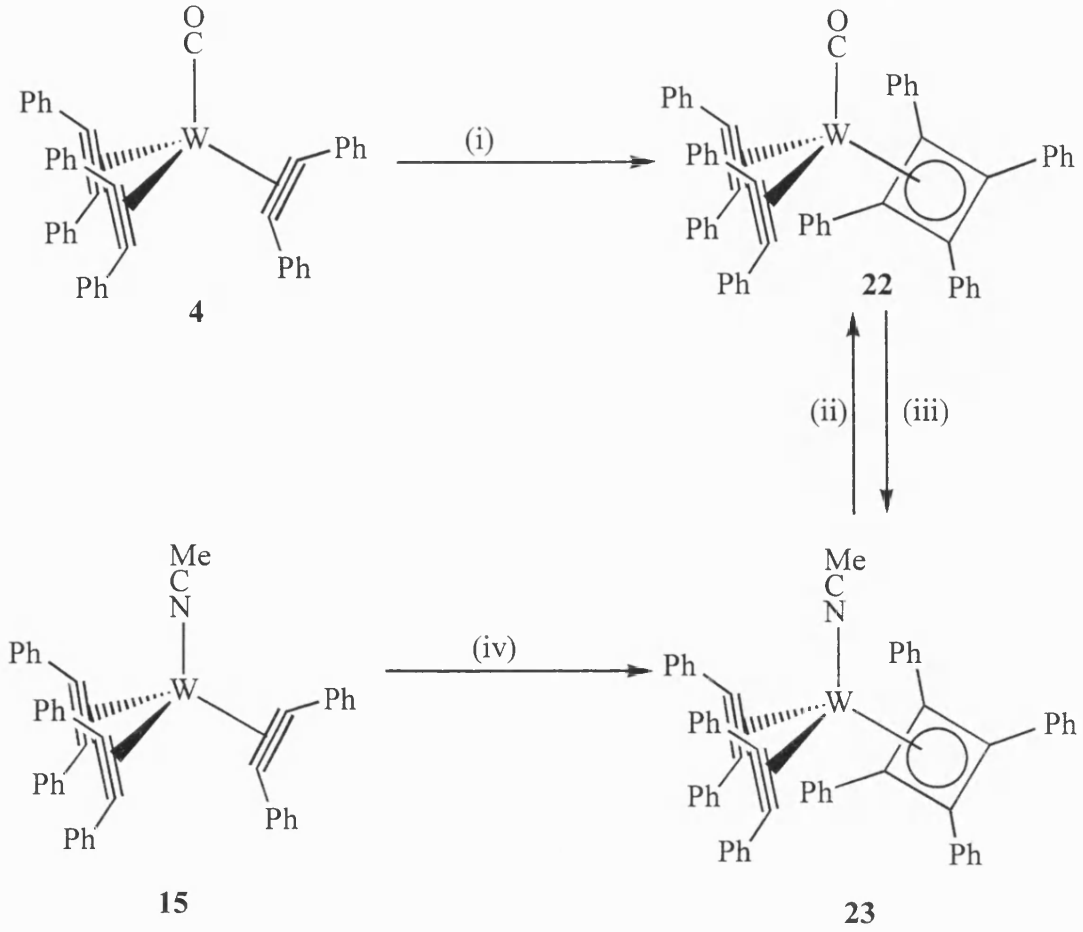

Scheme 1.12 (i) PhC≡CPh; (ii) CO; (iii) Me_3NO, MeCN; (iv) PhC≡CPh, $ClCH_2CH_2Cl$, reflux.

Attempting to mimic this reaction, **4** and diphenylacetylene where refluxed in toluene under nitrogen producing **22** but in less than 10% yield. The physical properties of this product include a carbonyl stretch in the infra-red at 2030 cm^{-1}, the expected alkyne signals at δ 175.9 and 158.9 ppm in the ^{13}C-{^{1}H} NMR and a further signal at δ 83.8 ppm for the carbons of the cyclobutadiene. A single crystal of **22** was subjected to an X-ray structure determination which showed a distorted tetrahedral arrangement of the ligands around the tungsten, Figure 1.9. It is possible to carry out this reaction with the acetonitrile complex **15** in refluxing 1,2-dichloroethane or by treating **22** with trimethylamine-N-oxide, giving [W(NCMe)(η^2-PhC≡CPh)$_2$(η^4-C_4Ph_4)] **23**, Scheme 1.12.

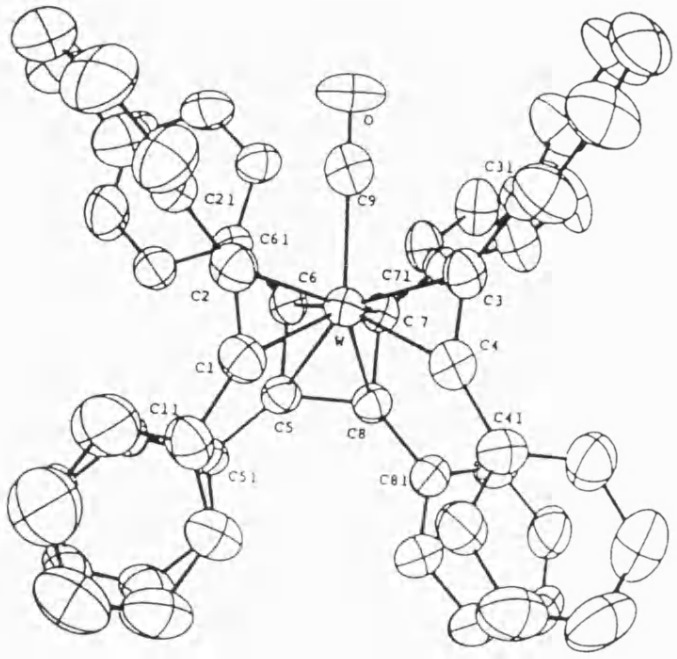

Figure 1.9 Molecular structure of **22**.

If the above reaction is carried out at a slightly higher temperature, 130°C [25], two bands are isolated during the chromatographic work up, the first orange band being the expected $[W(CO)(\eta^2\text{-PhC}\equiv\text{CPh})_2(\eta^4\text{-}C_4Ph_4)]$ **22** and the second product yielding dark red crystals of $[W(CO)(\eta^2\text{-PhC}\equiv\text{CPh})\{\eta^5\text{-}C_3Ph_3(C_5Ph_5)\}]$ **24**. The molecular structure of **24** was determined by single crystal X-ray diffraction studies and is shown in Figure 1.10.

The $^{13}C\text{-}\{^1H\}$ NMR spectra exhibits a signal at δ 300.8 ppm, which is characteristic of a carbene (W=C) type carbon. To satisfy the 18 electron rule the alkyne must be acting as a four electron donor and this assumption is supported by the presence of two signals at δ 197.4 ppm and 190.0 ppm in the characteristic region for alkynic carbons of a four electron donor alkyne ligand.

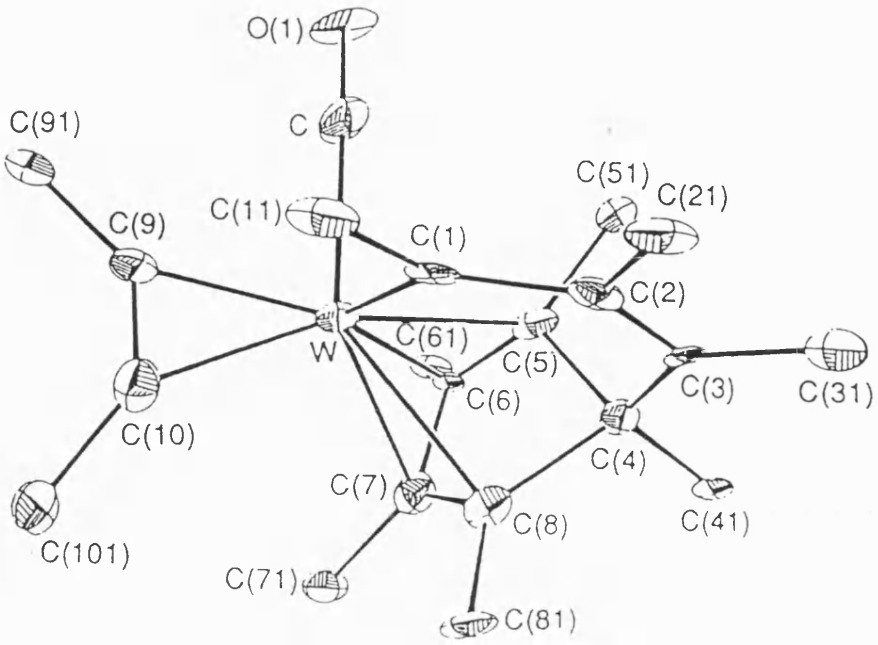

Figure 1.10 molecular structure of **24**.

Treatment of **22** with diphenylacetylene does not produce **24**, hence the two compounds are obviously formed by separate routes. Based upon the molecular structure of **4** in which the three alkyne C≡C axes are parallel to the W-CO group, two pathways can be envisaged for the formation of the product, Scheme 1.13. Presumably, if the C≡C axis of the incoming diphenylacetylene is parallel to the co-ordinated PhC≡CPh ligands, then coupling

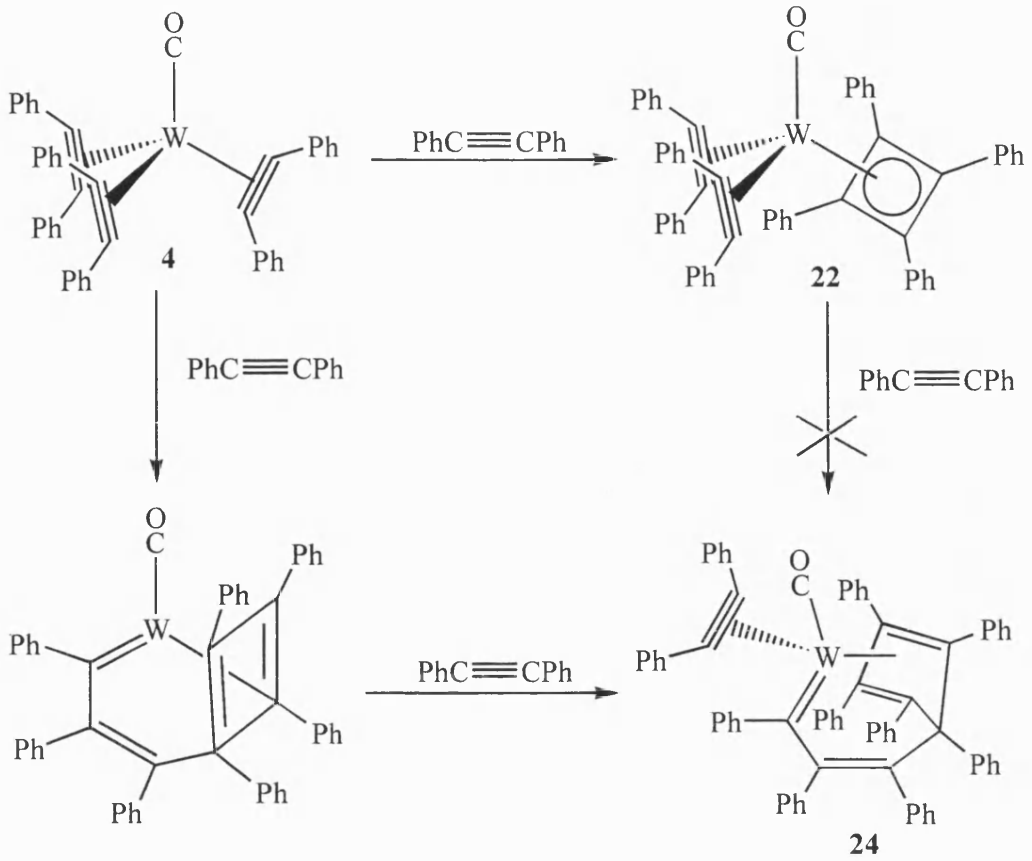

Scheme 1.13.

of the alkynes would give the cyclobutadiene species. If the diphenylacetylene is added in the perpendicular position it could bridge the three co-ordinated alkyne ligands and could then couple to form the cyclopentadiene moiety. However, it remains uncertain whether stepwise coupling occurs after alkyne linkage, or alternatively, completely concerted bond formation proceeds about the metal atom.

Having produced the cyclobutadiene products, **22** and **23**, an investigation was carried out to attempt to promote the coupling of the remaining two alkyne ligands of these complexes. This was achieved by hydrolysis in alkaline solution, producing the desired alkyne/alkyne coupling and hydration of the acetonitrile ligand as well, resulting in orange-yellow crystals of $[W(\eta^2\text{-}CH_3C(O)NH)(\eta^4\text{-}C_4Ph_4)(\eta^4\text{-}C_4Ph_4H)]$ **25**, Scheme 1.14 [26].

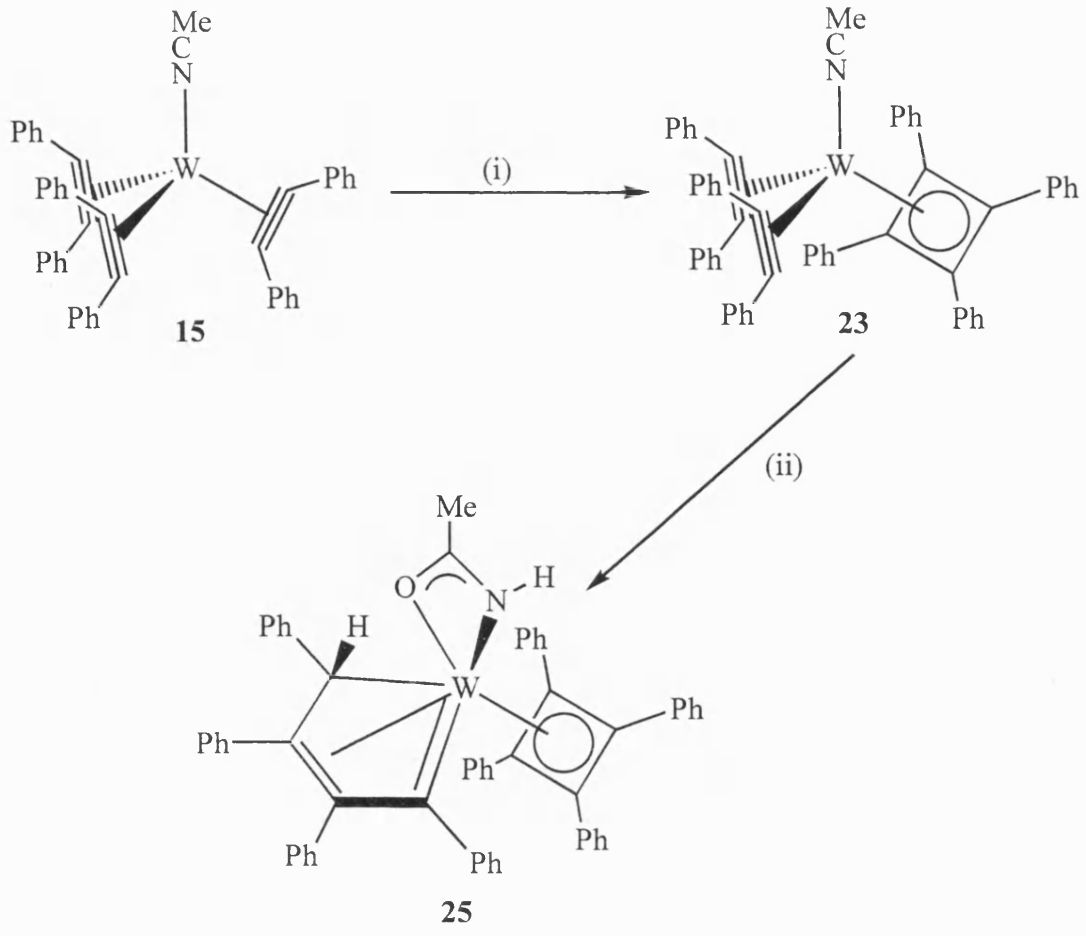

Scheme 1.14 (i) PhC≡CPh; (ii) H_2O, Base.

Again the ^{13}C-{^1H} NMR data supports the formation of a tungsten carbene moiety with a signal at δ 250.2 ppm and in the proton coupled spectrum a doublet at δ 67.7 ppm is attributed to *C*HPh with $^1J(CH) = 143$ Hz and the methyl carbon appearing as a quartet at δ 25.6 ppm. The cyclobutadiene appears as a sharp singlet at δ 88.4 ppm revealing that this ligand is fluxional with facile ring rotation, the carbons of the butadienyl are lost amongst the phenyl signals and the amido carbonyl carbons resonance is at δ 191.2 ppm.

Apparently, alkyne/alkyne coupling is preceded by hydration of the acetonitrile ligand, since hydrolysis of the analogous carbonyl compound **22** gave no reaction. Wen-Yann proposed that the first step of this reaction would be to prepare $[W(\eta^1\text{-}NHC(O)CH_3)(\eta^4\text{-}C_4Ph_4)(\eta^2\text{-}PhC{\equiv}CPh)_2]^-$ and subsequent chelation of the carbonyl oxygen to the tungsten atom would cause alkyne/alkyne coupling followed by abstraction of a proton from water to give the desired product, Scheme 1.15.

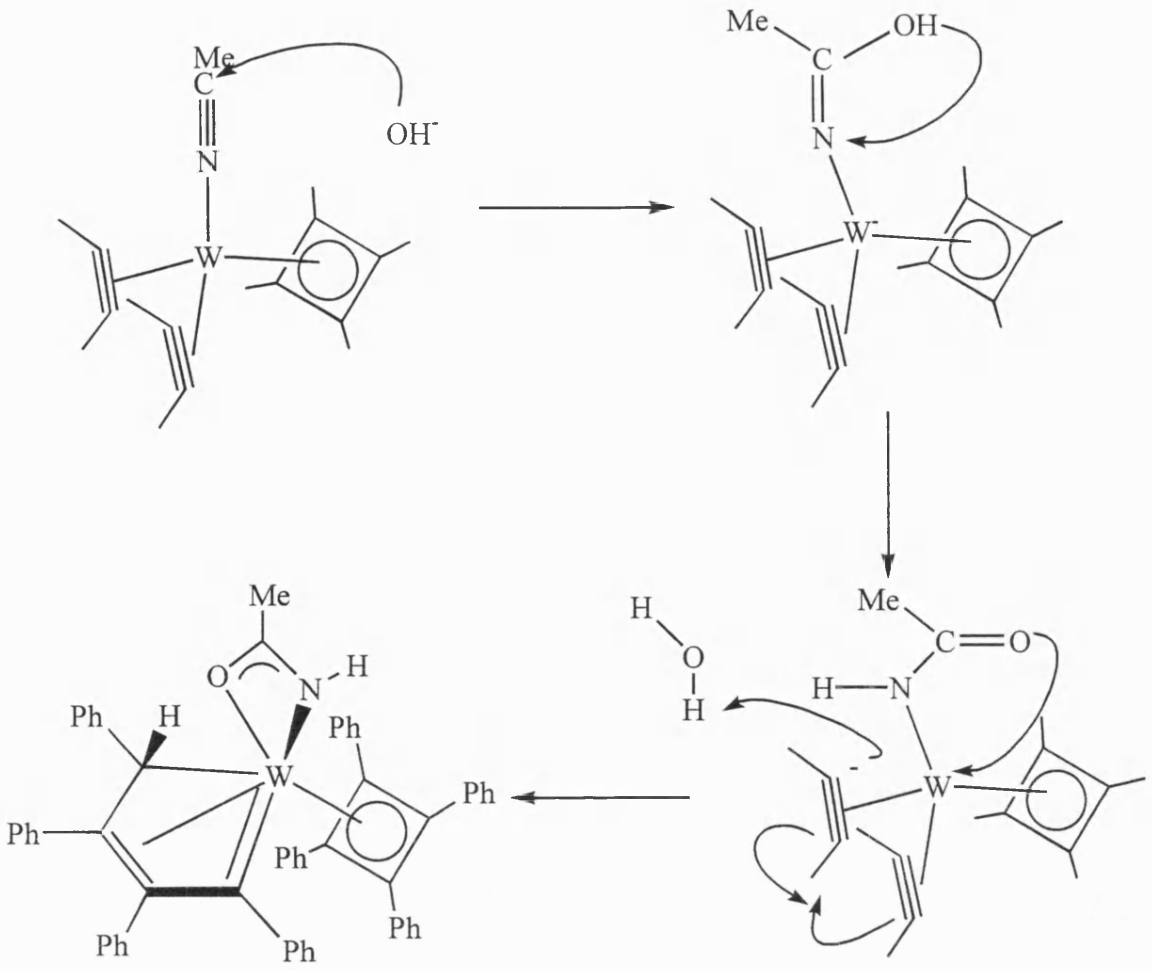

Phenyl groups omitted for clarity

Scheme 1.15.

The η^4-C_4R_4H ligands have been prepared previously by protonation of tungsten and molybdenum bisalkyne complexes [11], elimination of a hydride from a π-butadiene group [27] or coupling of η^2-vinyl and alkyne ligands on a molybdenum centre [27].

CHAPTER 2

Novel Reactions of Alkynes at Transition Metal Centres

2 Discussion.

2.1 Alkyne/Alkene Coupling Reactions.

In exploring the reaction of the chelating ligand *o*-diphenylphosphinostyrene (dpps) [28-31], Figure 2.1, with the bis-but-2-yne complex $[Mo(CO)(\eta^2\text{-MeC}\equiv\text{CMe})_2(\eta\text{-}C_5H_5)][BF_4]$ [32], it was observed that the alkene/alkyne complex $[Mo(\eta^2\text{-MeC}\equiv\text{CMe})(\text{dpps})(\eta\text{-}C_5H_5)][BF_4]$ **26**, was formed, Scheme 2.1; the structure being confirmed by a single crystal X-ray diffraction study.

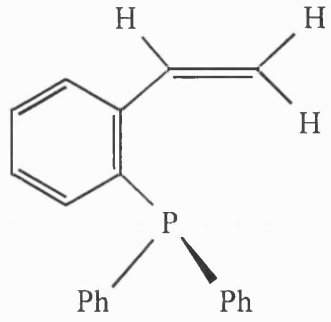

Figure 2.1

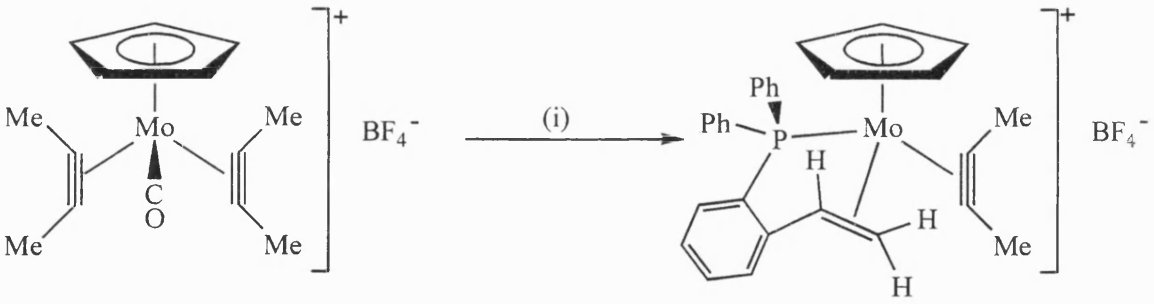

26

Scheme 2.1 (i) dpps, CH_2Cl_2, reflux.

It was found that if complex **26** was heated under reflux in acetonitrile solution, a carbon-carbon coupling reaction occurred [32], resulting in the formation of the complex $[Mo(NCMe)(\eta^4\text{-MeCH}=\text{C(Me)-CH}=\text{CHC}_6H_4PPh_2\text{-}o)(\eta\text{-}C_5H_5)][BF_4]$ **27**, Scheme 2.2, and as is illustrated the cation of **27** consists of a molybdenum atom bound to an $\eta^5\text{-}C_5H_5$ ligand, an N-bonded acetonitrile ligand and a ligand formally derived from coupling of the but-2-yne and the alkene part of the dpps ligand present in **26**. This condensation product is η^4 bound to the molybdenum atom *via* a 1,3-diene moiety, which is the *ortho* substituent on a phenyl ring attached to a diphenylphosphine unit P-bonded to the metal.

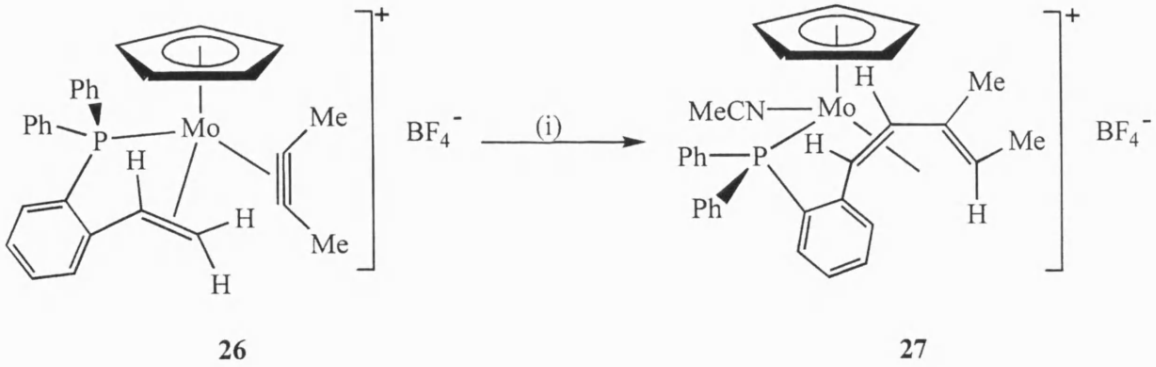

26 **27**

Scheme 2.2 (i) MeCN, reflux.

A rationale for these observations is shown in Scheme 2.3, the reaction proceeds initially with the co-ordination of the sigma donor ligand, MeCN, which is accommodated by a switch in the bonding mode of the but-2-yne from a four electron donor to a two electron donor. This is followed by the formation of a metallacyclopent-2-ene ring in **e**, this oxidative reaction [Mo(II)→Mo(IV)] being facilitated by the donation of electron density to the metal centre by the nitrile. The reaction is completed by a 1,3-hydrogen shift process, which generates the intermediate **f** which then collapses to give **27**. In principle the hydrogen shift process could have occurred *via* a number of routes. An intermolecular elimination sequence involving loss of H^+ from C^4 of the metallocycle **e** followed by protolysis of the Mo-C^2 bond was thought unlikely when it was observed that the reaction still proceeded in high yield in the presence of excess base, that would act as an irreversible proton trap. An α-hydrogen elimination followed by a 1,2-hydrogen shift was also ruled out. Examination of a molecular model of **e** clearly showed that it was impossible for either of the two β-hydrogens bonded to C^4 to interact with the molybdenum, and therefore, unless the chelating phosphine dissociated from the metal, a β-hydrogen elimination process followed by a reductive elimination reaction seemed an unlikely pathway to **f**. Since such an opening of the chelate ring is unlikely a 1,3-hydrogen shift pathway was proposed that does not involve transfer of the migrating hydrogen to the metal. This pathway is a metal assisted suprafacial 1,3-H shift, where the intermediate **e** has a molybdenum substituted allyl fragment encompassing carbon atoms C^2, C^3 and C^4. The suprafacial H-migration from C^4 to C^2 could only take place if it was assumed that the molybdenum donates electrons into the π^* orbital of the vinyl group C^2-C^3, then this could become sufficiently populated to facilitate a suprafacial 1,3-H shift. Once the intermediate **f** is formed it could be captured by collapsing to a 1,3-diene.

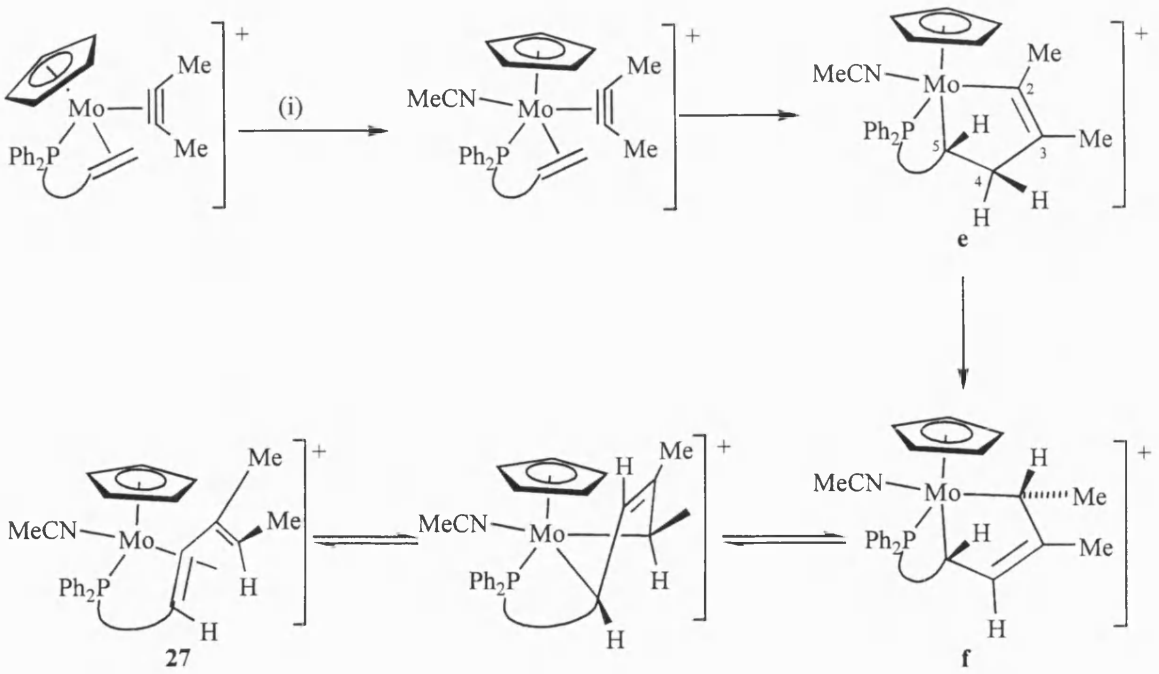

Counter anion is BF_4^- throughout

Scheme 2.3 (i) MeCN.

Further examples of these types of coupling reactions have been reported by Trost [33-36]. The intermediate for these reactions is again thought to be a metallacyclopent-2-ene ring which then needs to undergo a hydrogen migration, as is shown in Scheme 2.4. As previously the hydrogen migration cannot be *via* the metal centre as the β-hydrogens cannot interact with the metal centre, so possibly the migration might also be a metal assisted suprafacial 1,3-H shift.

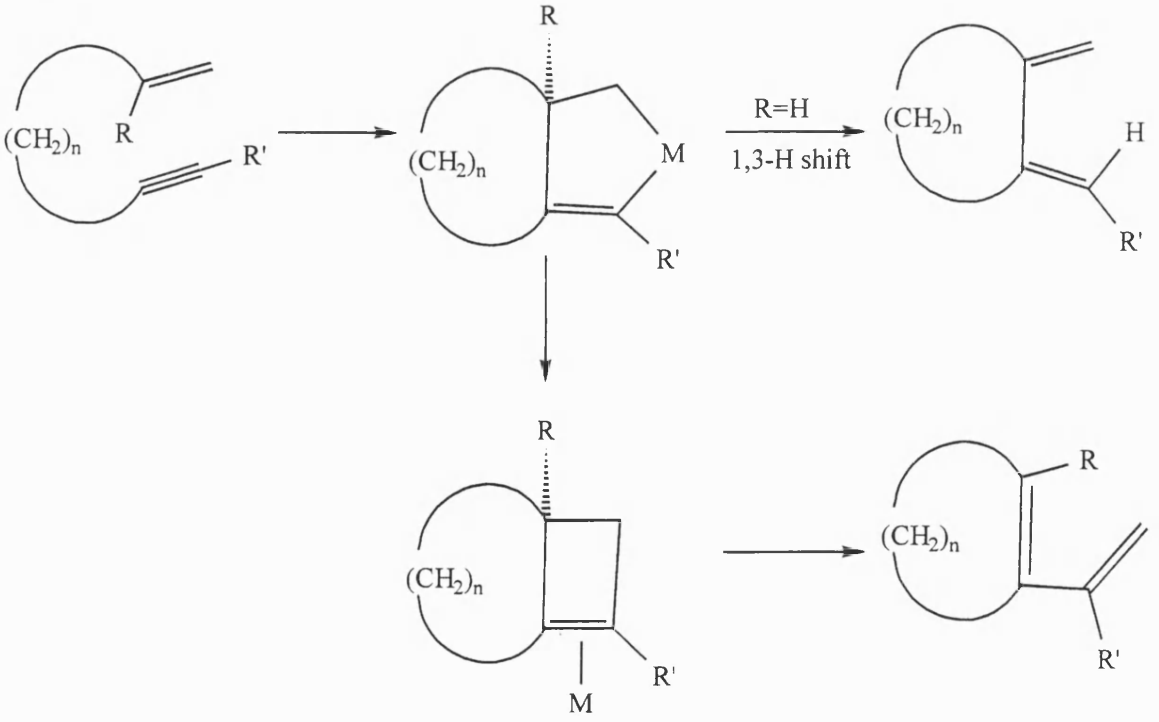

Scheme 2.4

In addition to these studies, Herrmann [37] has explored the reaction of $[ReCl_2(\eta^2\text{-}RC{\equiv}CR')(\eta\text{-}C_5Me_5)]$, where R=R'= Me, Et, Ph, R= Ph, R'= Me, with ethylene and a catalytic amount of tetrafluoroboric acid. This produced as the major product (~85%) a buta-1,3-diene complex and a minor product (~10%) which was characterised as a penta-2,4-dienyl complex. Both products are the result of a carbon-carbon coupling process involving the co-ordinated alkyne and the ethylene, Scheme 2.5.

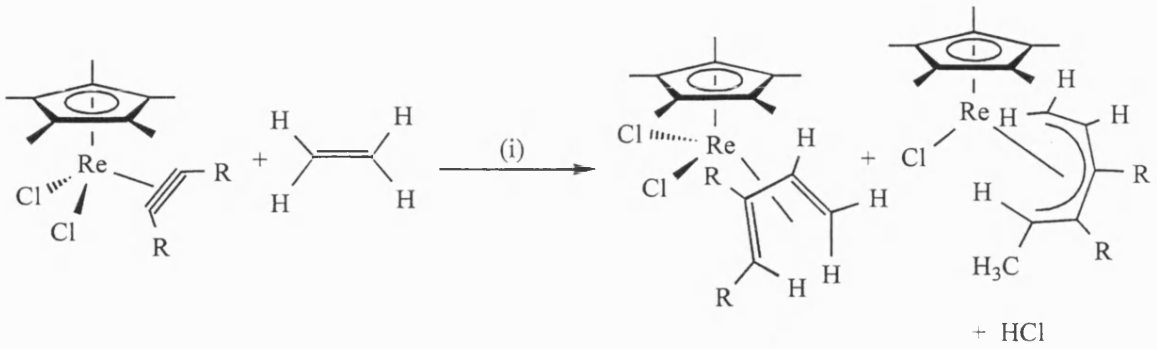

Scheme 2.5 (i) cat. HBF_4.

The buta-1,3-diene is formed by insertion of the alkene into one of the Re-C(alkyne) bonds followed by a rearrangement, the nature of the rearrangement was not initially obvious so labelling experiments were carried out to investigate further. Firstly the reaction was run in deutero solvents and no incorporation of deuterium was observed. Secondly the reaction was attempted using perdeuterated ethylene in toluene and it produced both the major and minor complexes exhibiting total deuterium incorporation. These results suggest that as the coupling reactions take place the rearrangements are occurring intramolecularly and are not reliant upon the solvent or the acid catalyst. The intramolecular rearrangement that is observed is the unusual suprafacial 1,3-hydrogen shift, and must be proceeding in a similar manner to that reported by Green [32], described above. The penta-2,4-dienyl complex is formed by the insertion of an alkene into one of the Re-C(alkyne) bonds followed by a second insertion of alkene into the other Re-C(alkyne) bond, with the subsequent elimination of HCl.

In the study of the reactions between $[ReBr_2(\eta^2\text{-}RC{\equiv}CPh)(\eta\text{-}C_5H_5)]$, where R = Me (**28**) or R = Ph (**29**), and dpps in the presence of two equivalents of $AgBF_4$, butadienylrhenium complexes are surprisingly formed [38], Scheme 2.6.

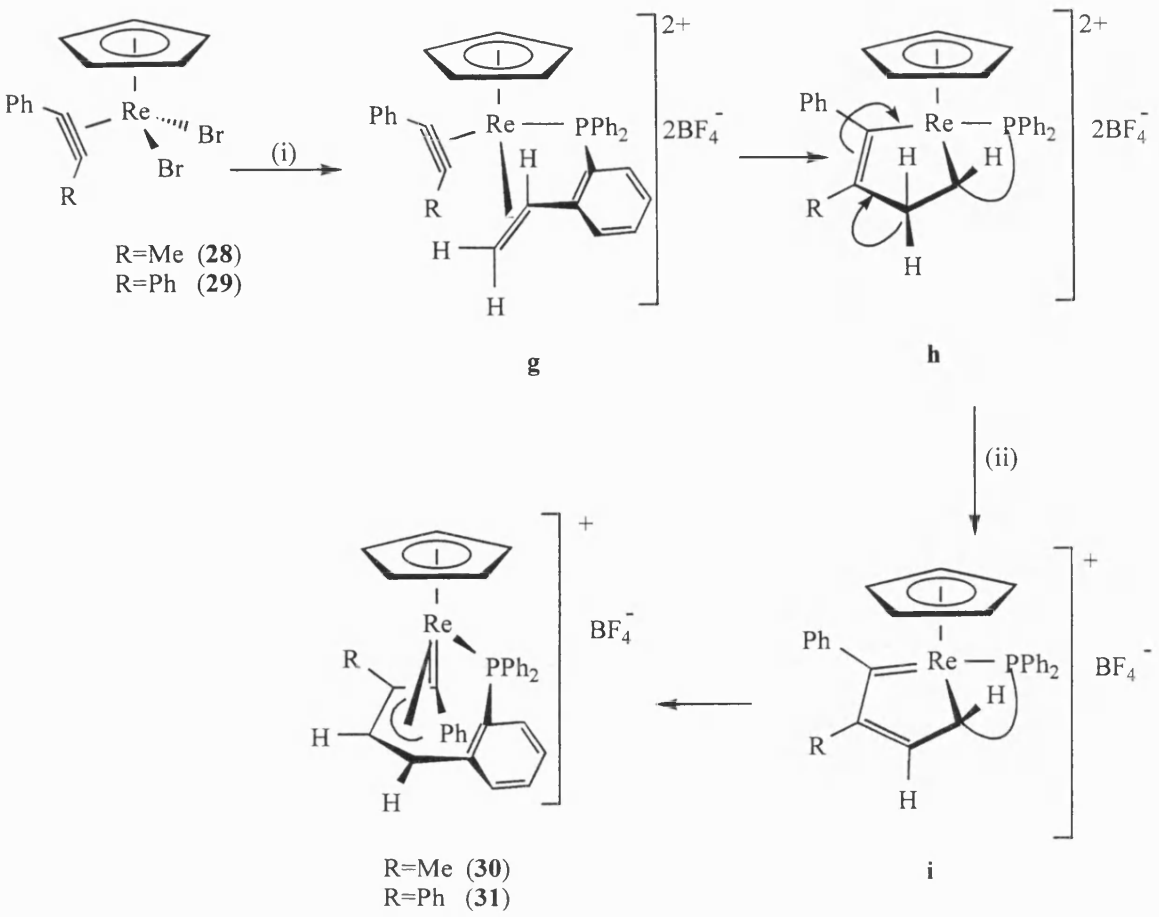

Scheme 2.6 (i) $2AgBF_4$, dpps, thf, room temp.; (ii) - HBF_4

A single crystal X-ray diffraction study showed that complexes **30** and **31** are formed by coupling between the alkyne and alkene moieties, with one carbon atom doubly bonded to the rhenium centre. The products from the reaction were expected to be dicationic species due to the elimination of both the bromide ligands by the silver. Complexes **30** and **31** however, are unusual in as much as they are monocationic, having eliminated a molecule of HBF_4 in the course of the reaction.

It has been suggested, see Scheme 2.6, that the reaction proceeds *via* an intermediate **g**, formed by abstraction of both bromide ligands by the silver tetrafluoroborate and occupation of the subsequent vacant co-ordination sites by the dpps. Oxidative [$Re^{III} \rightarrow Re^{V}$] carbon-carbon coupling provides access to the dicationic rhenacyclopent-2-ene, **h**, similar to the metallacyclopentene seen previously, this then loses a proton, in the form of HBF_4, and forms a strong Re-C double bond, **i**. Clearly, because these complexes carry a positive charge they are protected from attack by the HBF_4 present in solution. If, however, a similar proton loss occurred from the β-carbons of the metallacyclopent-2-enes of Green [32] and Herrmann [37] then the resulting metallacyclopentadienes would be neutral

and liable to attack by a proton on the carbene α-carbon resulting in the formation of the 1,3-diene.

2.2 Reaction of [W(PhC≡CPh)$_3$(NCMe)] with *o*-diphenylphosphinostyrene.

As mentioned earlier the reaction of [W(NCMe)$_3$(CO)$_3$] **1** with diphenylacetylene in refluxing ethanol produces the complex [W(CO)(η^2-PhC≡CPh)$_3$] **4** [5], which can be converted to the labile acetonitrile species by treatment with trimethylamine-N-oxide in acetonitrile [18]. When the resulting complex [W(NCMe)(η^2-PhC≡CPh)$_3$] **15** is then refluxed in toluene in the presence of triphenylphosphine the phosphine species [W(PPh$_3$)(η^2-PhC≡CPh)$_3$] **16** is produced [18]. In view of the earlier work summarised above on alkene/alkyne coupling reactions, this leads to the interesting question, would coupling of diphenylacetylene and the alkene functionality of the dpps ligand occur if the phosphine substituent introduced to **15** was *o*-diphenylphosphinostyrene?

Following the methodology described [W(CO)(η^2-PhC≡CPh)$_3$] **4** was prepared and converted into [W(NCMe)(η^2-PhC≡CPh)$_3$] **15** which was then treated with dpps in refluxing toluene for four hours [39], the reaction mixture turning deep red within the first 30 minutes of reflux. Workup by column chromatography on Al_2O_3 and elution with hexane-dichloromethane (4:1) afforded an orange-red crystalline complex, **I** in 63% yield. Mass spectrometry and elemental analysis indicated that the product of this reaction was a mononuclear complex incorporating a tungsten atom ligated by three alkynes and one dpps ligand. The ^{31}P-{^{1}H} NMR spectra of the crystalline product exhibited two signals at δ 50.0ppm and δ 56.1 ppm, in the ratio of 1.6:1, suggesting the presence of two isomers and intriguingly the ^{13}C-{^{1}H} NMR spectrum of the presumed isomeric mixture showed low field resonances at δ 283.8 ppm [d, J(CP) = 21Hz] and δ 287.1 ppm [d, J(CP) = 18Hz] indicative of the presence of tungsten-carbon multiple bonds in both isomers.

Fractional crystallisation afforded crystals, which were shown by NMR to be of the major product **Ia**, and a suitable crystal was subjected to a single crystal X-ray diffraction study. This showed, Figure 2.2, Table 2.1, that the complex contained a co-ordinated carbyne fragment, W-C(62) 1.799(5) Å, which compares to an average tungsten-carbyne bond length of 1.815 Å [40]. The carbyne has a bond angle of 173.2(4)° between the metal, C(carbyne) C(62) and the bound carbon of the phenyl group C(37), which is as expected

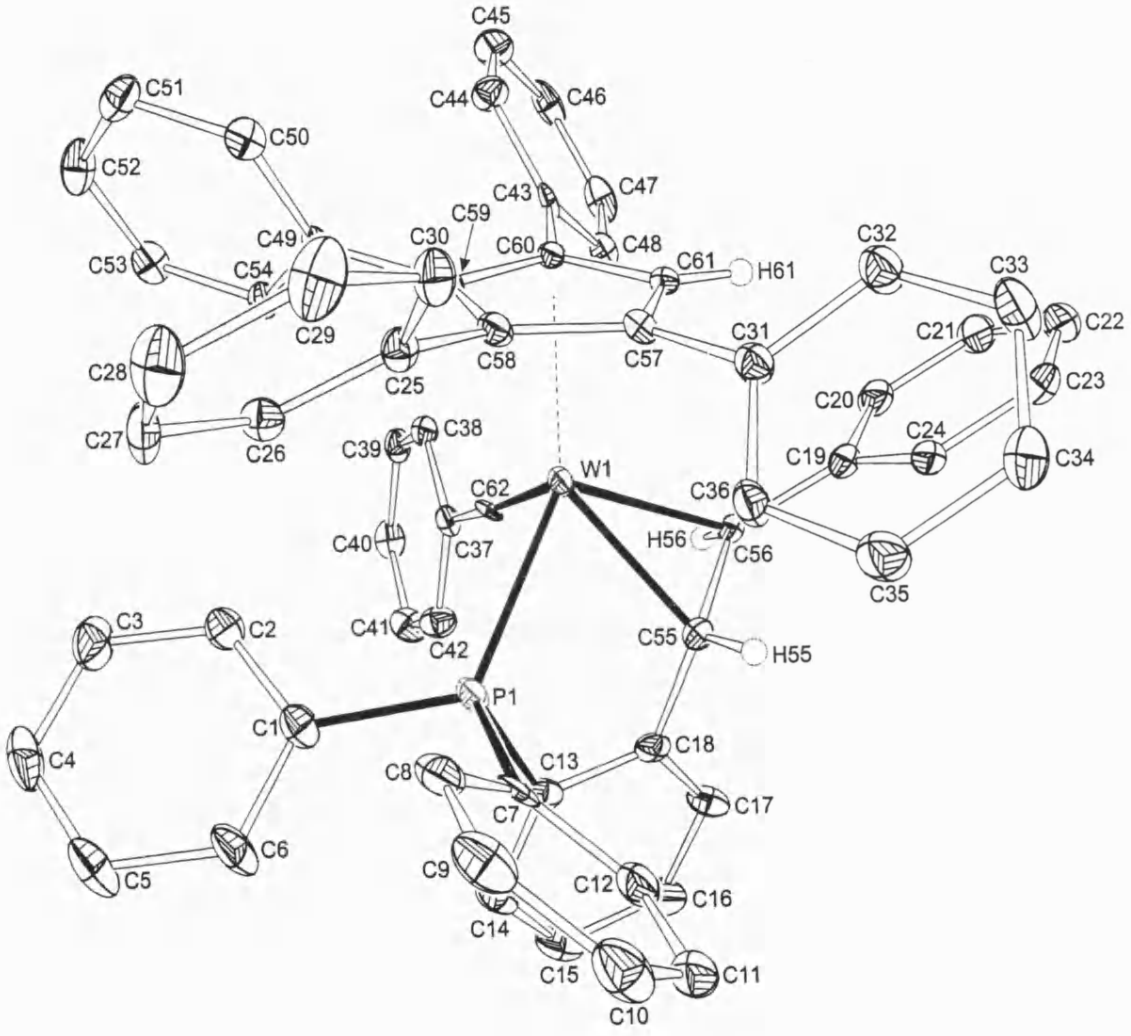

Molecular structure of **Ia**

Figure 2.2

Atoms	Bond Length (Å)	Atoms	Bond Angle (°)
W(1)-P(1)	2.4595(14)	C(37)-C(62)-W(1)	173.2(4)
W(1)-C(62)	1.799(5)	C(13)-P(1)-W(1)	102.5(2)
W(1)-C(55)	2.220(5)	C(1)-P(1)-W(1)	122.3(2)
W(1)-C(56)	2.281(5)	C(7)-P(1)-W(1)	119.7(2)
W(1)-C(57)	2.487(5)	C(31)-C(57)-W(1)	123.6(3)
W(1)-C(58)	2.484(5)	C(25)-C(58)-W(1)	132.0(3)
W(1)-C(59)	2.428(5)	C(25)-C(58)-W(1)	132.0(3)
W(1)-C(60)	2.368(4)	C(25)-C(58)-W(1)	132.0(3)
W(1)-C(61)	2.379(4)	C(19)-C(56)-W(1)	123.9(3)
C(55)-C(56)	1.450(7)	C(18)-C(55)-W(1)	115.9(3)
C(57)-C(61)	1.420(6)	C(56)-C(55)-C(18)	120.7(4)
C(57)-C(58)	1.436(6)	C(55)-C(56)-C(19)	123.6(4)
C(58)-C(59)	1.430(6)		
C(59)-C(60)	1.439(6)		
C(60)-C(61)	1.417(6)		

Table 2.1 Selected Bond lengths and angles for **Ia**.

for an sp hybridised carbon. The complex surprisingly contained a modified dpps ligand, in which the alkene functionality η^2-CH=CH_2 had been replaced by a co-ordinated η^2-(*E*)-CH=CHPh moiety. The tungsten-phosphorus bond length of 2.4595(14) Å is shorter than the average tungsten-phosphorus bond length found in tungsten triphenylphosphine complexes of 2.535 Å [40], which may be due to the chelation of the modified styrene pulling the phosphorus closer to the metal. This chelation effect is also reflected in the bond angles between the metal, the phosphorus and the contact carbons of the phenyl groups. For the two planar phenyl groups this angle, W-P-C, is approximately 120°, but for the styrene, chelation alters this bond angle, W-P-C(13), to 102.5°. The carbon-carbon double bond length of the η^2-(*E*)-CH=CHPh moiety is 1.450(7) Å, which is longer than the average bond length for a π-bonded disubstituted alkene of 1.391 Å [40], but in complexes that contain both *cis* and *trans* stilbene, where one of the phenyl groups of the stilbene is free or when on of the aryl groups is bonded to a co-ordinated PPh_2 moiety, double bond lengths of 1.45Å [30,41] are observed. The lengthening of this double bond is

most probably due to the electron withdrawing nature of the phenyl groups, reducing the electron density in the alkene π system which in turn leads to an increase in the bond length. Both C(56) and C(55) are bound to the tungsten with W-C bond lengths of 2.281(5) Å and 2.220(5) Å respectively which is shorter than the average bond length for disubstituted alkenes of 2.430 Å [40]. The complex also contains a η^5-tetraphenylcyclopentadienyl ligand, which is orientated in such away that the single hydrogen on the ring lies in the face of the η^2-(*E*)-CH=CHPh moiety's phenyl group. The ring exhibits delocalisation around the five carbons that make it up with an average bond length of 1.428 Å and an average distance to the tungsten centre of 2.429 Å. This compares favourably with the average values for a pentamethylcyclopentadienyl ligand, where the bond lengths between the carbons making up the ring average 1.417 Å [40]. Thus in summary the reaction that produces **Ia** is shown in Scheme 2.7.

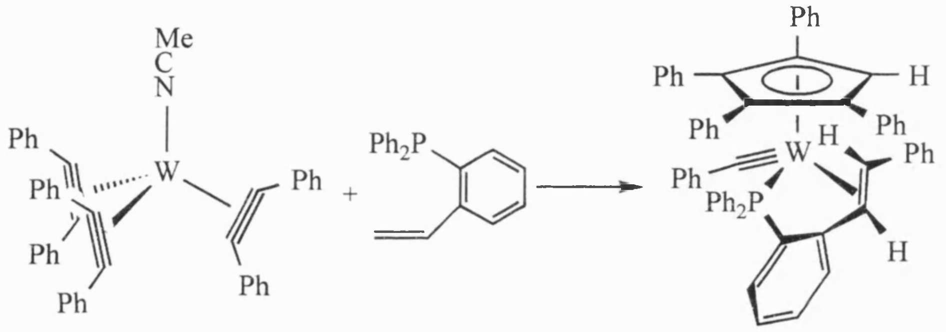

15 **dpps** **Ia**

Scheme 2.7

The formation of **Ia**, a tungsten carbyne alkene complex is highly unusual as only a few complexes of this type have been reported, the partially characterised $[W(\equiv CH)(\eta^2\text{-}C_2H_4)(PMe_3)_3][CF_3SO_3]$ [42], the anionic complexes $[NEt_4][W(\equiv CR)Cl_2(\eta^2\text{-alkene})(py)(CO)]$ [43], where alkene = maleic anhydride or fumaronitrile; R = Me or Ph; py = pyridine, and the X-ray crystallographically identified molecules $[W(\equiv CPh)Cl\{OC(O)CH{=}CHCO\}(py)_2(CO)]$ [43] and $[Mo(\equiv CCH_2Bu^t)\{\eta^2\text{-}C_2(CN)_4\}\{P(OMe)_3\}(\eta^5\text{-}C_5H_5)]$ [44] where the alkene lies orthogonal to the W≡CPh vector as in **Ia**.

As to the structural identity of the other probable isomer, re-examination of the NMR spectra confirmed that the two complexes were isomers. This is because the ^1H and $^{13}C\{^1H\}$ spectra showed exactly similar coupling patterns differing only in their chemical shift. This suggests that the two isomers **Ia, b** differ only with respect to the orientation of the η^5-C_5Ph_4H ligand. Variable temperature studies and nOe experiments demonstrated

that there is a high barrier to rotation for the tetraphenylcyclopentadienyl functionality. This was supported by space filling models of **Ia**, Figure 2.3, these models show the orientation of the η^5-C_5Ph_4H ligand, with respect to the rest of the molecule, and it is plain to see that the hydrogen of the ring is in the centre of the π system of the phenyl group of the new methylene carbon of the modified styrene. This orientation would affect the chemical shift of this hydrogen in the proton NMR spectrum. This reinforces the concept that the differentiating feature between the isomers is the orientation of the tetraphenylcyclopentadienyl ring, Scheme 2.8.

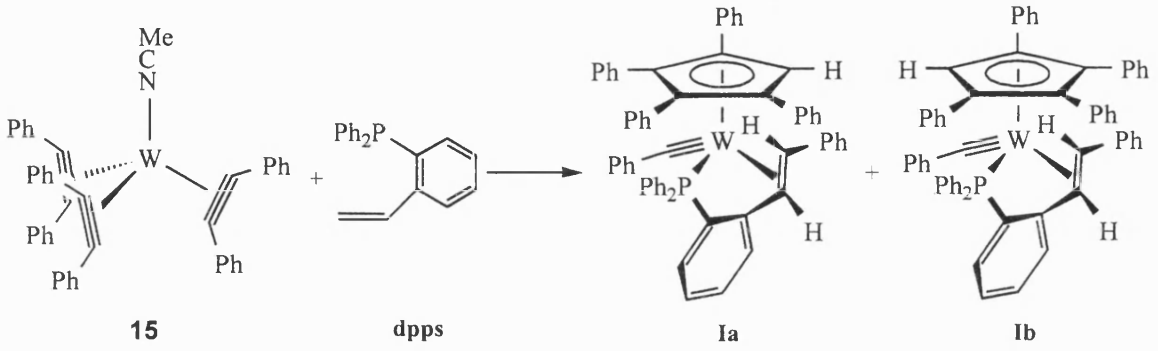

15 **dpps** **Ia** **Ib**

Scheme 2.8.

The formation of a carbyne ligand in a reaction of this type is without precedent [45], moreover, the formation of the η^2-(*E*)-CH=CHPh moiety is difficult to explain and implies the involvement of a possible alkene metathesis reaction.

Since the formation of the isomeric mixture of **Ia, b** is most unusual attempts were made to understand the mechanism of formation by isotopic labelling experiments.

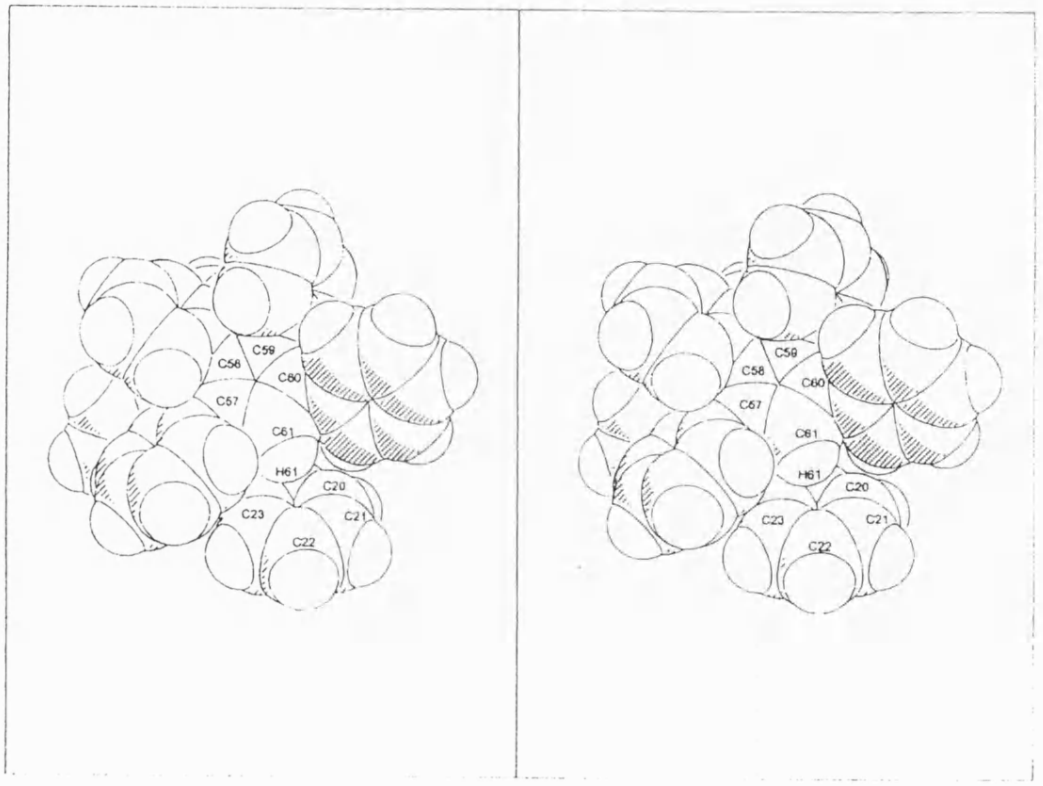

Figure 2.3a Space filling view of **Ia** from above.

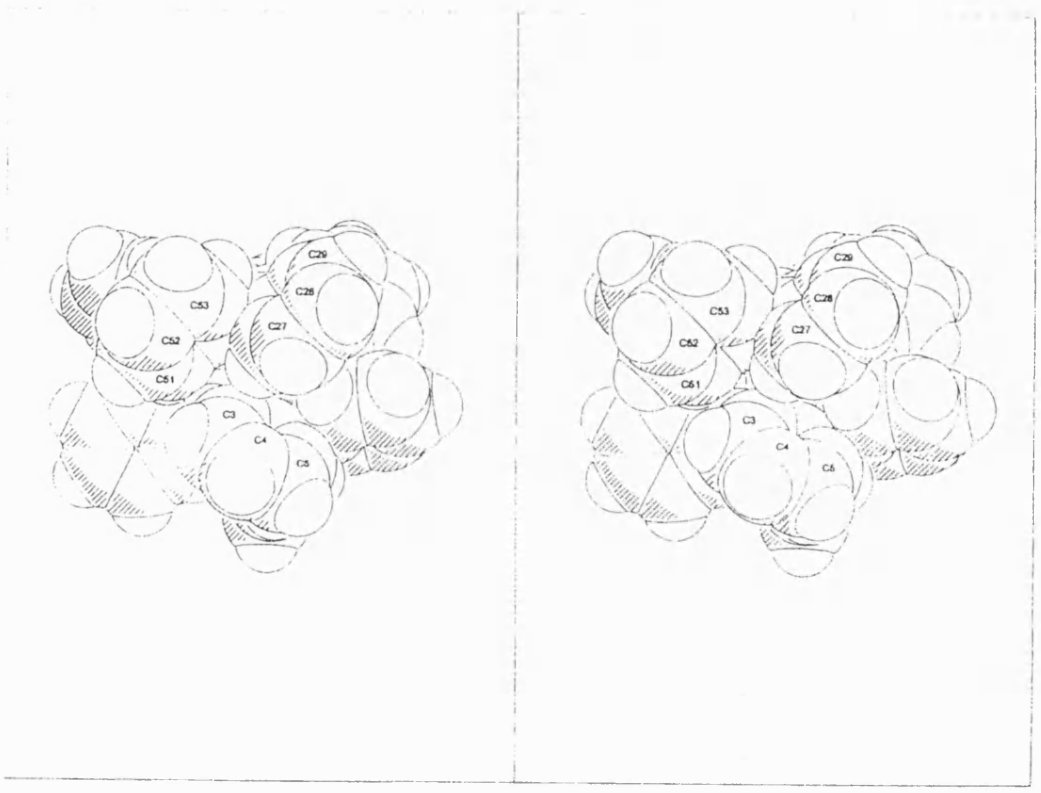

Figure 2.3b Space filling view of **Ia** from the side.

2.3 Isotopic Labelling Experiments.

Labelled diphenylacetylene was prepared from benzoic-*carboxy*-^{13}C-acid ($Ph^{13}COOH$) and chlorodiphenylphosphine *via* a number of known steps. Primarily the chlorodiphenylphosphine was treated with methanol in the presence of triethylamine to produce methyl diphenylphosphinite, $Ph_2P(OMe)$, which underwent an Arbuzov reaction with benzylbromide to form $PhCH_2P(O)Ph_2$. The benzoic-*carboxy*-^{13}C-acid was dissolved in thionyl chloride to yield benzoyl-*carbonyl*-^{13}C chloride ($Ph^{13}COCl$). A proton was then removed from the $PhCH_2P(O)Ph_2$ using butyllithium and the benzoyl-*carbonyl*-^{13}C chloride was added and the diethyl ether solution was brought to reflux. Recrystallisation from ether and water yielded $Ph_2P(O)CHPhC(O)Ph$, which after isolation was heated under vacuum, to 300°C in the presence of potassium *tert*-butoxide and the resulting labelled diphenylacetylene distilled off, Scheme 2.9. After recrystallisation the labelled diphenylacetylene was mixed with some unlabelled diphenylacetylene to give a 5% ^{13}C enrichment by mass.

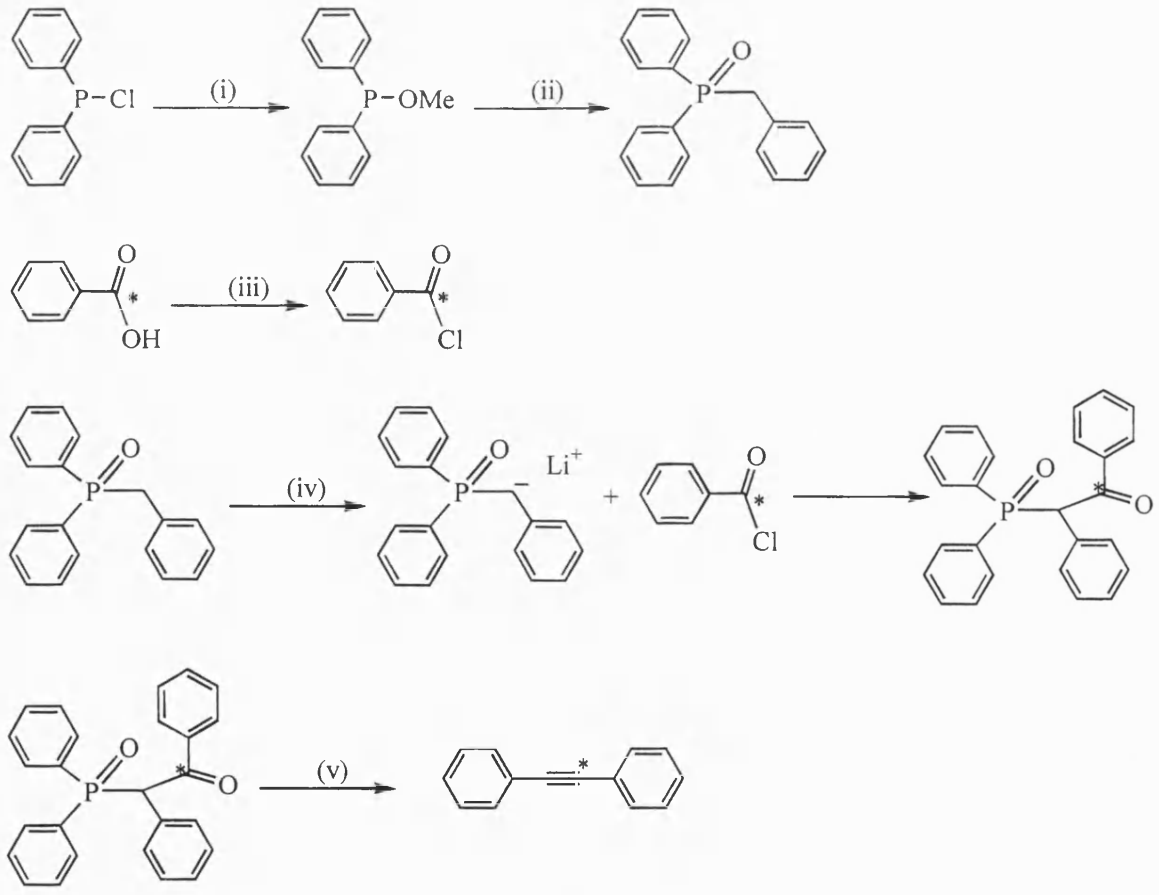

Scheme 2.9 (i) MeOH, Et_3N, (ii) $PhCH_2Br$, (iii) $SOCl_2$, (iv) Bu^nLi, (v) KBu^tO, 300°C.

The enriched diphenylacetylene was reacted with $[W(NCMe)_3(CO)_3]$ **1**, as previously described, to yield $[W(CO)(\eta^2\text{-}PhC{\equiv}{}^{13}CPh)_3]$ **4***. Complex **4*** was then reacted with

trimethylamine-N-oxide in acetonitrile solution to produce [W(NCMe)(η^2-PhC≡^{13}CPh)$_3$] **15***[†] labelled only on the alkyne contact carbons. Reacting this with dpps in refluxing toluene gave **Ia*, b***, which showed enrichment (^{13}C-{^{1}H} NMR) on the four phenyl substituted η^5-cyclopentadienyl contact carbons, the carbyne carbon and the terminal alkene carbon of the modified dpps ligand, as illustrated in Scheme 2.10.

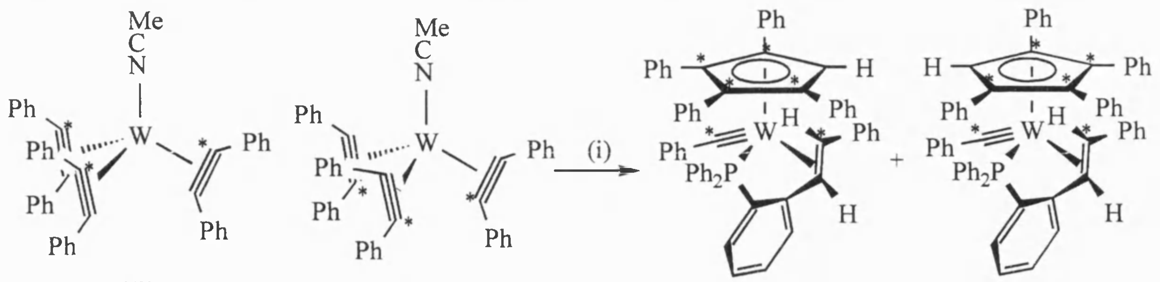

15* **15*** **Ia*** **Ib***

* = ^{13}C

Scheme 2.10 (i) dpps.

The result of the diphenylacetylene labelling experiment showed that one diphenylacetylene molecule has cleaved to produce the carbyne and the terminal CHPh of the modified styrene, whilst the other two molecules of diphenylacetylene have coupled with one other carbon atom to form a tetraphenylcyclopentadienyl ligand.

As a second isotopic labelling experiment ^{13}C labelled *o*-diphenylphosphinostyrene was produced as shown in Scheme 2.11, with a label on the methylene carbon, from *o*-bromobenzaldehyde and iodomethane-^{13}C. The iodomethane-^{13}C was reacted with triphenylphosphine to produce methyl-^{13}C-triphenylphosphonium iodide. This was then mixed with unlabelled methyltriphenylphosphonium iodide to achieve a 25% ^{13}C enrichment by mass. The methyltriphenylphosphonium iodide mixture was then deprotonated using butyllithium and reacted with the 2-bromobenzaldehyde to yield *o*-bromostyrene-^{13}C. The *o*-bromostyrene-^{13}C was then converted to a Grignard reagent by addition to a thf suspension of magnesium turnings. The Grignard was then added dropwise to a thf solution of chlorodiphenylphosphine. Recrystallisation yielded methylene labelled *o*-diphenylphosphinostyrene (dpps*), with enrichment on the methylene carbon ,as a white powder, Scheme 2.11.

[†] The co-ordination of an alkyne to a metal centre to form a tris-alkyne complex as in **15** [18] makes it possible to distinguish between the distal and proximal contact carbons of the alkyne *via* ^{13}C{^{1}H} NMR due to their orientation with respect to, in this case, the acetonitrile ligand. Taking this into account, upon preparing **15*** the labelled contact carbon is observed in both the proximal or distal positions suggesting that **15*** must be represented as a mixture with equivalent amounts of alkyne labelled in the distal position to alkyne labelled in the proximal position.

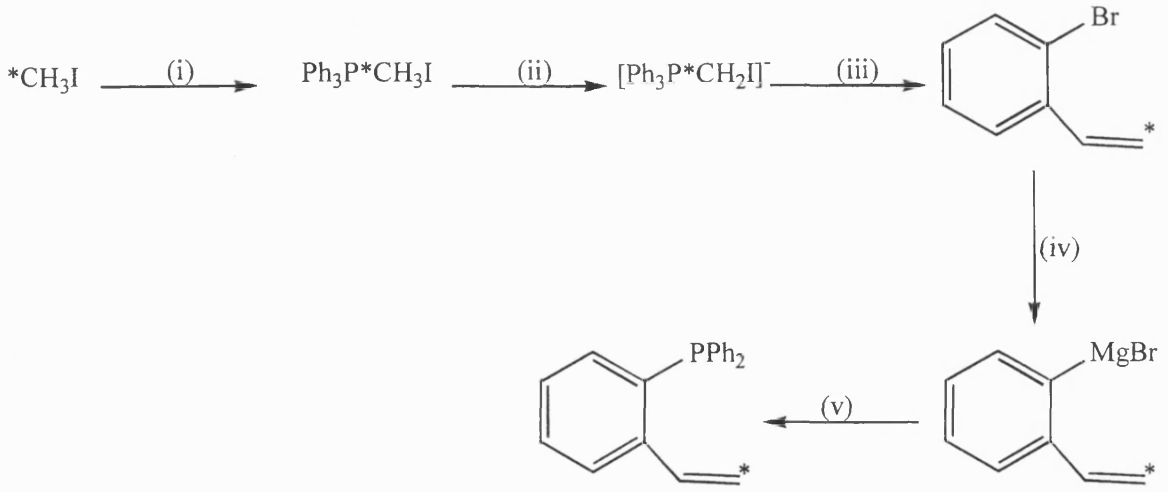

dpps*

Scheme 2.11 (i) PPh_3, (ii) Bu^nLi, (iii) *o*-BrC_6H_4CHO, (iv) Mg, (v) Ph_2PCl.

The dpps* was reacted with [W(NCMe)(η^2-PhC≡CPh)$_3$] **15** in the manner described above and after work up afforded **Ia', b'**, in which ^{13}C enrichment occurred (NMR) only on the hydrogen substituted carbon of the η^5-tetraphenylcyclopentadienyl ligand, Scheme 2.12.

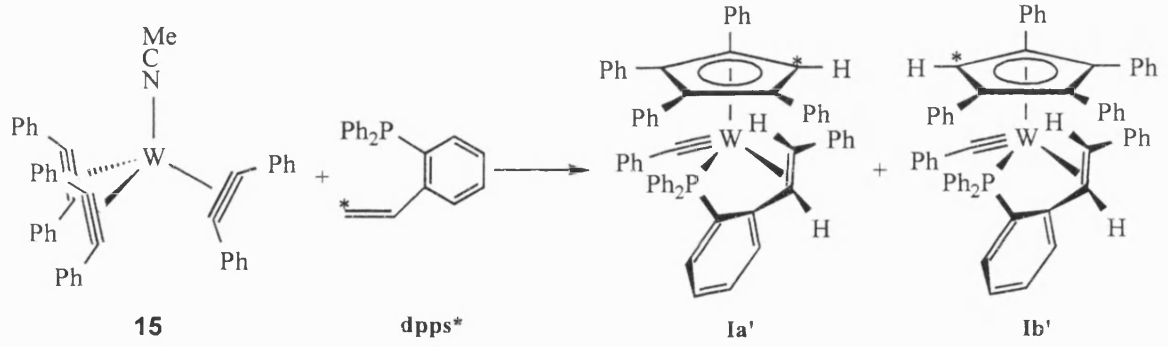

15 **dpps*** **Ia'** **Ib'**

* = ^{13}C

Scheme 2.12.

The appearance of what was the methylene carbon of the styrene in the tetraphenylcyclopentadienyl ring suggests that the alkene double bond of the styrene is cleaved and the methylene carbon couples with two diphenylacetylene ligands to produce the C_5 ring. At the same time the cleaved diphenylacetylene apparently couples with the remnants of the dpps minus its methylene carbon to produce the modified η^2-(*E*)-CH=CHPh moiety observed.

Finally, refluxing a solution of [W(NCCD$_3$)(η^2-PhC≡CPh)$_3$] and dpps in toluene gave **Ia, b**, there being no evidence of deuterium incorporation.

Thus, in summary these experiments confirm that cleavage of both carbon-carbon triple and double bonds has occurred. Having cleaved the fragments these then couple, possibly *via* alkene metathesis to produce the observed molecules **1a, b**.

2.4 Possible Reaction Pathways.

In considering how **Ia, b** might be formed attention has been turned to the possible role of η^2-(3e)-vinyl species. These ligands are one of the more interesting and well known reactions of alkynes, as summarised in Templeton's review [11]. The main synthetic route to an η^2-vinyl is *via* nucleophilic attack upon a cationic alkyne system [46,47,11]. For example nucleophilic attack by $K[BHBu^s_3]$ on $[Mo\{P(OMe)_3\}_2(\eta^2\text{-}PhC{\equiv}CPh)(\eta\text{-}C_5H_5)]^+$ produces the neutral η^2-vinyl complex $[Mo\{C(Ph)CH(Ph)\}\{P(OMe)_3\}_2(\eta\text{-}C_5H_5)]$ **32**, Scheme 2.13.

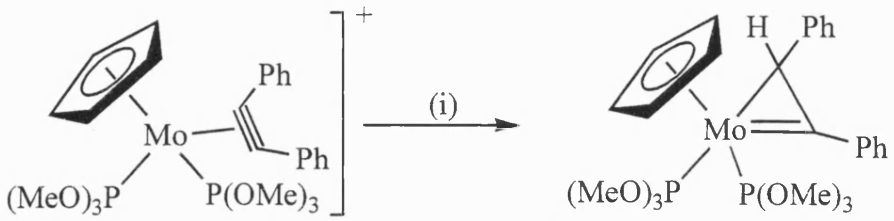

32

Scheme 2.13 (i) $K[BHBu^s_3]$, thf.

Of more relevance to the formation of **Ia, b** is the recently reported case of protonation of a neutral alkyne system [48]. It was suggested that the η^2-vinyl produced, Scheme 2.14, is then trapped by a second alkyne to produce a cationic butadienyl complex [48,49]. For example the reaction of $[MoCl(\eta^2\text{-}MeC{\equiv}CMe)_2(\eta\text{-}C_5H_5)]$ with $HBF_4.Et_2O$ followed by acetonitrile produces an η^4(5e)-butadienyl product $[Mo\{{=}C(Me)\text{-}\eta^3\text{-}[C(Me)C(Me)CHMe]\}Br(NCMe)(\eta\text{-}C_5H_5)][BF_4]$ **33**, with the η^2-vinyl intermediate **j**, playing an important role in the coupling observed.

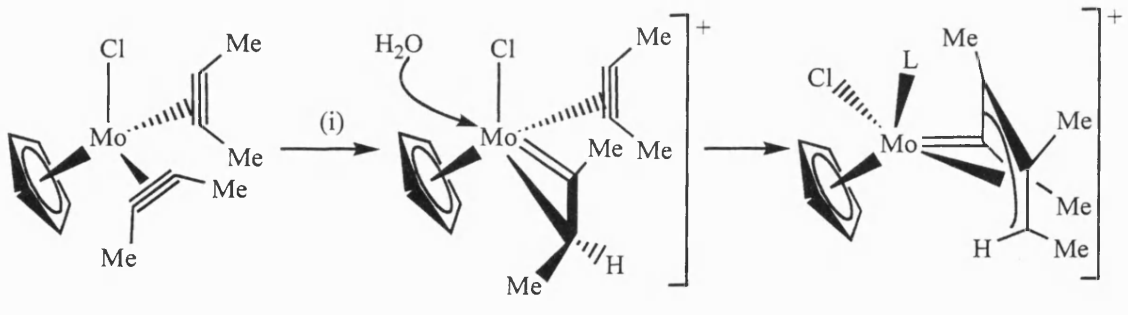

j

Scheme 2.14 (i) $HBF_4.Et_2O$-water, L = H_2O or MeCN (**33**); counter anion BF_4^- throughout.

The formation of a cationic η^2-vinyl ligand by protonation of a η^2-(4e)-alkyne ligand suggested a possible mechanistic rationale for the formation of **Ia, b**. If it is assumed that the first step of the reaction sequence is the formation of the intermediate **A** (Scheme 2.15) then co-ordination of a water molecule (possibly catalytic) could lead to the formation of

the anionic species **B**. The co-ordination of the water is possible because of the oxophilicity of the tungsten and the ability of the alkynes to switch their bonding modes from four electron donors to two electron donors as is the case here for one of the alkynes, implying that the alkyne environment around the tungsten centre consists of one four electron donor alkyne and two two electron donor alkynes to complete the tungsten's noble gas electron configuration. Upon formation of **B** the proton immediately attacks one of the alkyne ligands to form a η^2-vinyl ligand, which cannot be captured by one of the other alkyne ligands, as in the reactions described above, because the phenyl substituents block the approach of the alkyne to the η^2-vinyl, thus, they cannot react. But the η^2-vinyl does undergo a cleavage reaction, producing a carbyne and carbene pair **D** with the expulsion of the hydroxide to become the counter anion. At the same time the styrene becomes co-ordinated to the metal centre **D**, again with a switch in the bonding mode of the final four electron donor alkyne to a two electron donor ligand. The implication of the cleavage of one of the alkynes, *via* the η^2-vinyl intermediate **C** is that this reaction pathway generates the carbyne observed in **Ia, b**.

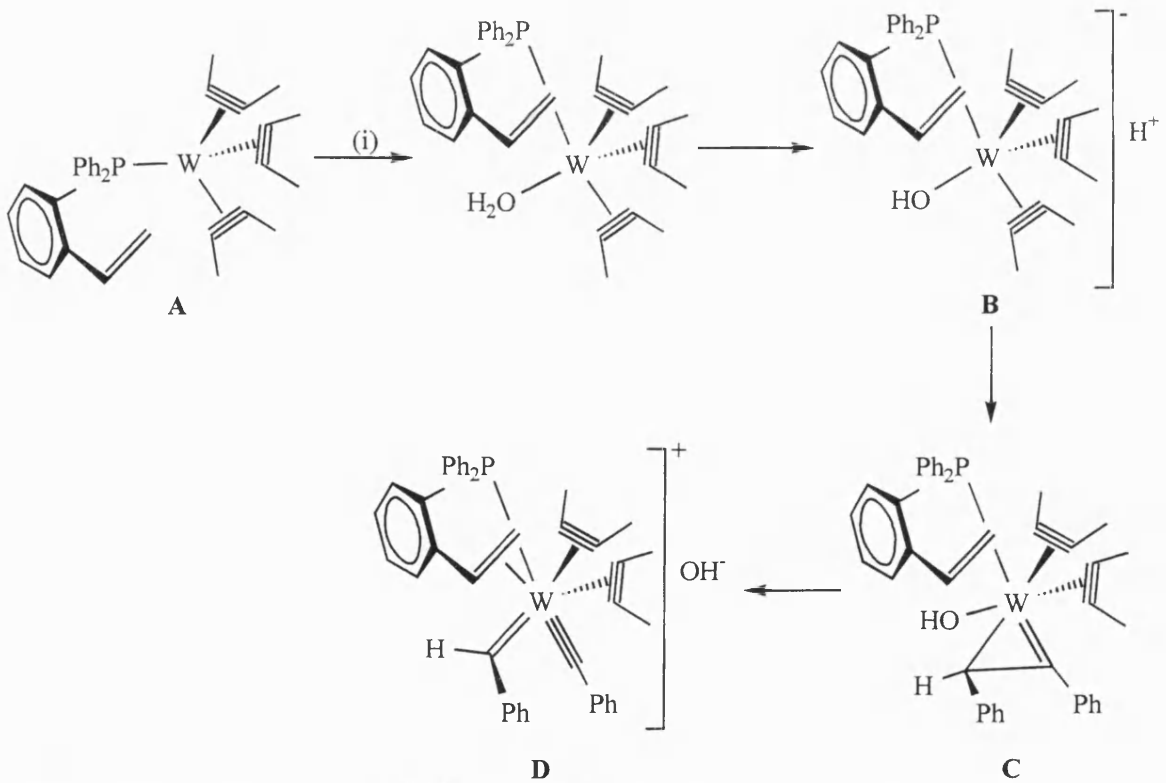

Scheme 2.15 (i) H_2O Cat, ——≡—— = PhC≡CPh, For clarity phenyl groups are omitted.

At first sight it is difficult to rationalise the suggestion that the η^2-vinyl carbon-carbon bond undergoes a cleavage reaction, however, possible support for this idea comes from experiments reported by Mayr, Lippard, Schrock and their respective co-workers on

carbyne/carbyne and carbyne/carbene coupling reactions. There reactions lead to the formation of co-ordinated alkynes and invoking the principle of microscopic reversibility suggests that alkyne should be able to cleave to produce a carbene carbyne pair.

2.4.1 Carbyne and Carbene Coupling Reactions.

In an analysis of the formation of an alkyne by two carbynes coupling on a single transition metal centre based on extended Hückel molecular orbital calculations Hoffmann [50] showed that such a process was possible but would be forbidden for all π electron counts above six (metal d electrons and electrons in the carbyne p orbitals combined).

Stimulated by Hoffmann's conclusions Mayr [51, 52] studied the reaction illustrated in Scheme 2.16. Addition of methyllithium followed by oxalyl bromide formed at low temperature a tungsten carbene intermediate $[W{\equiv}CPh\{{=}C(O)C(O)COBr)Me\}Br(CO)_2(PPh_3)]$ **k**. Warming to ambient temperature, with the addition of triphenylphosphine resulted in a coupling reaction to form the alkyne complex $[WBr_2(CO)(PPh_3)_2(\eta^2\text{-}PhC{\equiv}CMe)]$ **34**.

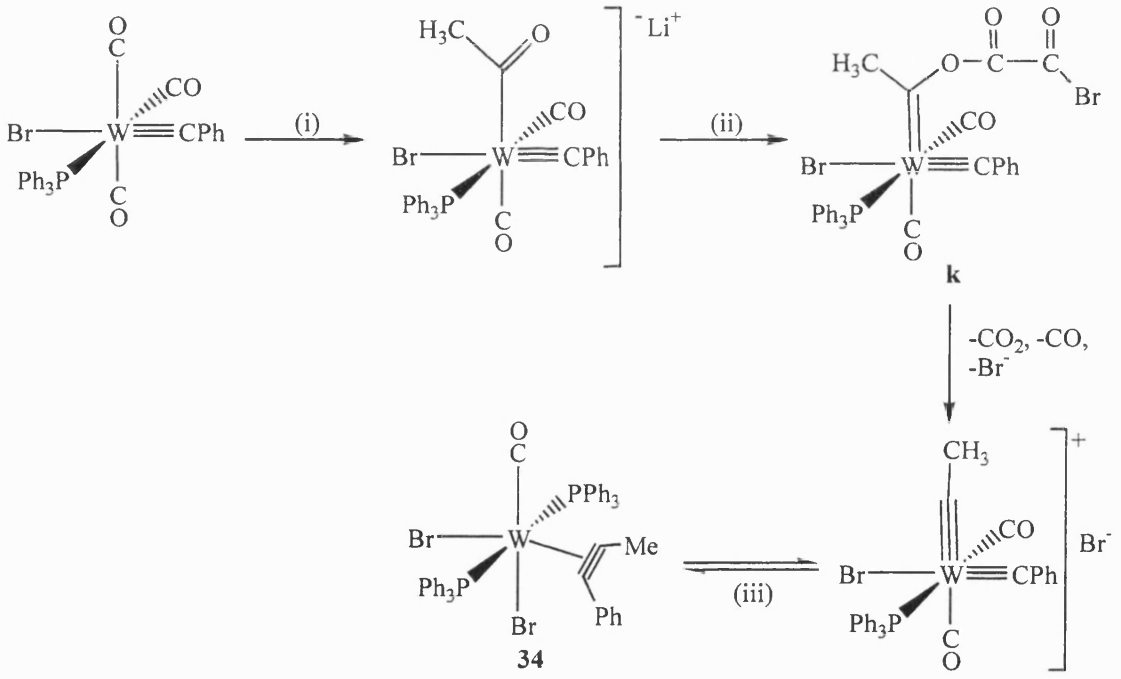

Scheme 2.16 (i) LiMe, thf, -78°C; (ii) $C_2O_2Br_2$, -78°C; (iii) PPh_3, -78°C to room temp.

The mechanism suggested by Mayr for the formation of the alkyne in **34** is illustrated in Scheme 2.16. The proposed intermediate **k** meets the criteria set down by Hoffmann, in as much as the complex has six electrons in its metal-ligand π-orbital system. Mayr suggested that this intermediate then undergoes dissociation of the bromooxalate to produce a cation exhibiting adjacent carbyne ligands which have to share a pair of

electrons in a three centre two electron bond involving two p orbitals of the carbyne carbons and a d orbital of the tungsten atom, as shown in Figure 2.4.

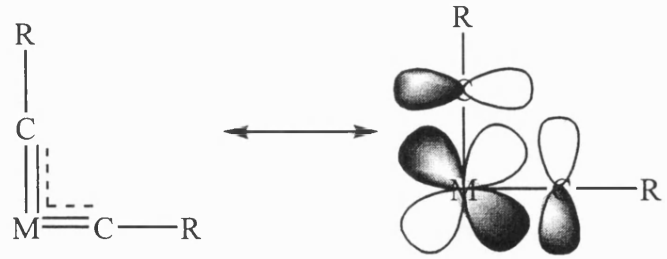

Figure 2.4

It was then proposed that this 'biscarbyne' undergoes coupling to form a phenylmethylacetylene ligand co-ordinated as shown in **34**, with addition of a PPh_3 ligand and displacement of one of the carbonyls by the bromide counter ion to yield the neutral complex observed.

However, an alternative explanation for the formation of **34** is that in the intermediate **k**, Scheme 2.17, coupling between the carbene and the carbyne precedes the dissociation of the bromooxalate, with the result that an η^2-vinyl intermediate is produced, Scheme 2.17. Addition of a further molecule of triphenylphosphine then promotes the formation of the alkyne with dissociation of the bromooxalate.

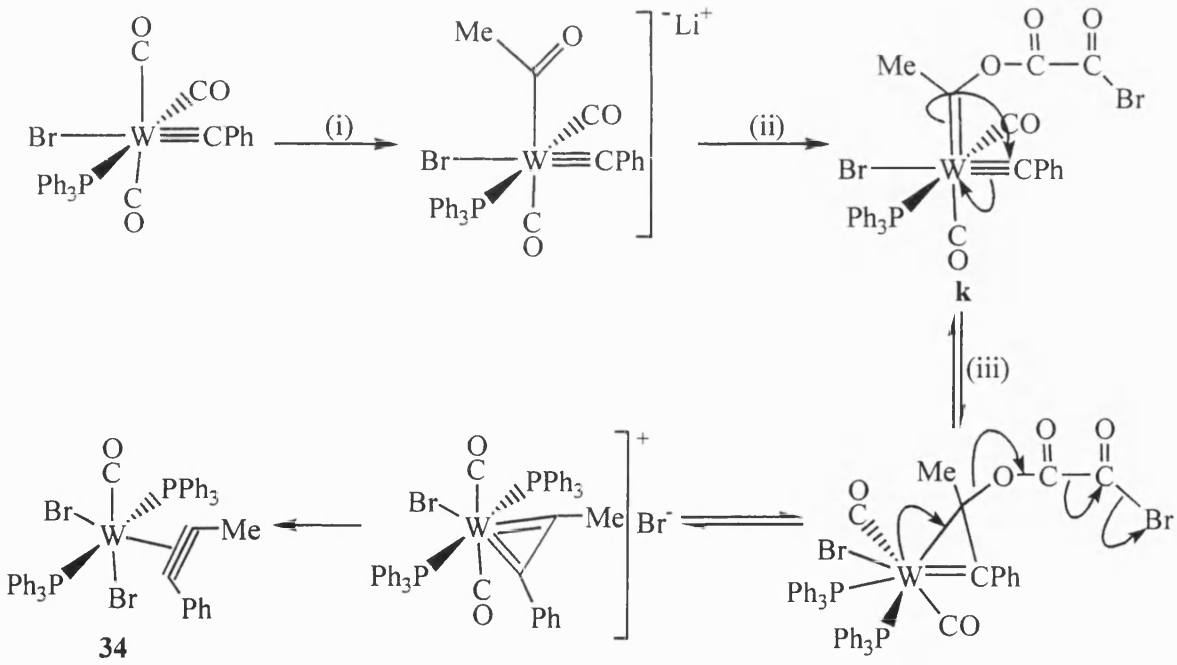

Scheme 2.17 (i) LiMe, thf, -78°C; (ii) $C_2O_2Br_2$, -78°C; (iii) PPh_3, -78°C to room temp.

Interestingly, Lippard and co-workers in a related study have reported that the tantalum carbyne complex $[Ta(\equiv COSiPr^i_3)(CO)(dmpe)_2]$ reacts with Me_3SiCl to form the alkyne complex $[TaCl(\eta^2\text{-}Pr^i_3SiOC\equiv COSiMe_3)(dmpe)_2]$ **35** [53], Scheme 2.18.

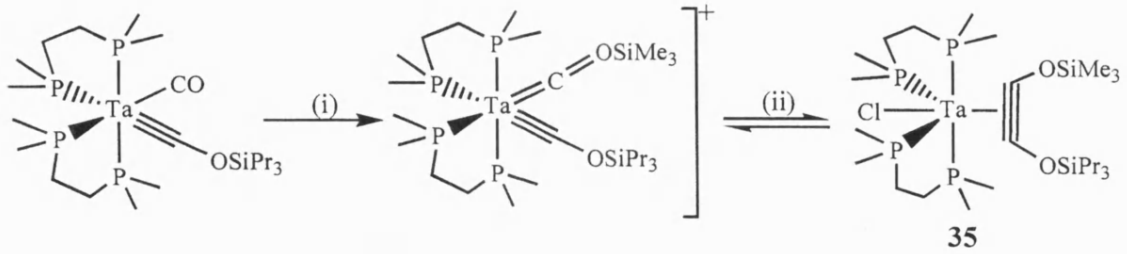

Scheme 2.18 (i) Me_3SiCl; (ii) Cl^-.

Lippard in a footnote [54] to his paper suggested that the intermediate be considered as carbene/carbyne species rather than a bis-carbyne, because d-block transition metal complexes do not have enough orbitals to form two independent metal-carbon triple bonds, and in order to avoid this difficulty proposed that the carbene and the carbyne coupled directly to produce the alkyne.

However, as illustrated in Scheme 2.19 Lippard's chemistry can be rationalised in a similar manner to Mayr's findings by postulating the reversible conversion of the carbene/carbyne species **l** into the η^2-vinyl complex **m**, then nucleophilic attack by the chloride counter ion can lead to the formation of η^2-(4e)-bonded alkyne complex **35**.

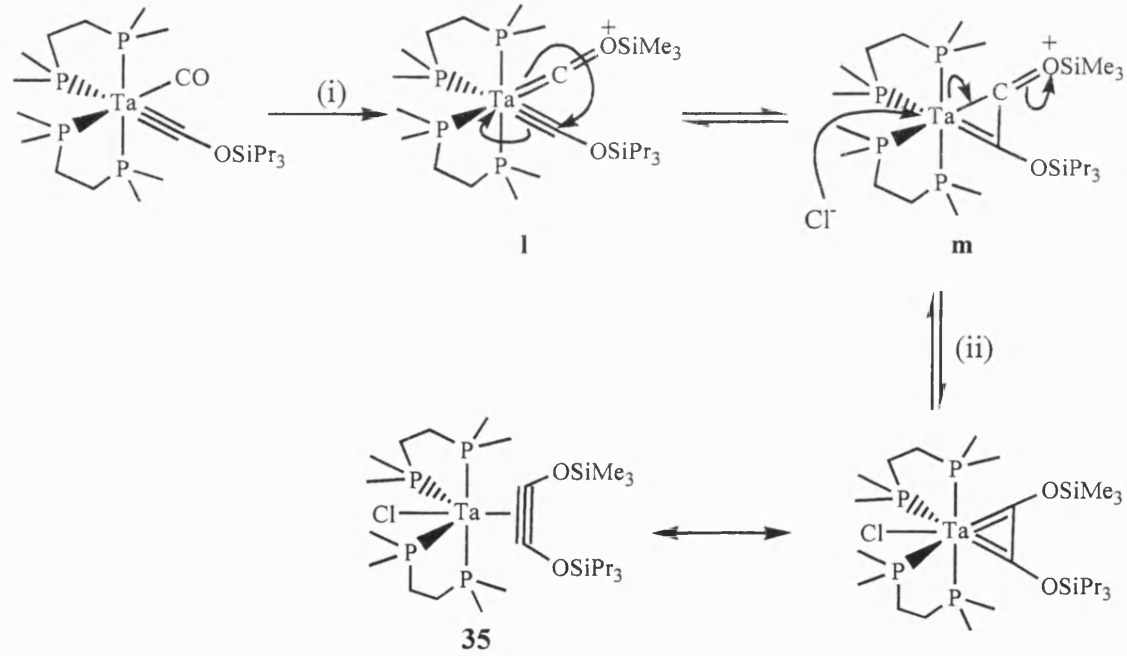

Scheme 2.19 (i) Me_3SiCl; (ii) Cl^-.

Support for the suggested role of an η^2-vinyl intermediate in these reactions comes from a study carried out by Schrock and co-workers [55]. It was found that the bis-carbene complex $[Os(CHBu^t)_2(CH_2Bu^t)_2]$ **36** transformed *via* a C-C bond forming reaction to produce the orange red η^2-(4e)-bonded alkyne complex $[Os(PMe_3)_3(\eta^2\text{-}Bu^tC{\equiv}CBu^t)]$ **37** in 30-40% yield, on treatment with neat trimethylphosphine, Scheme 2.20.

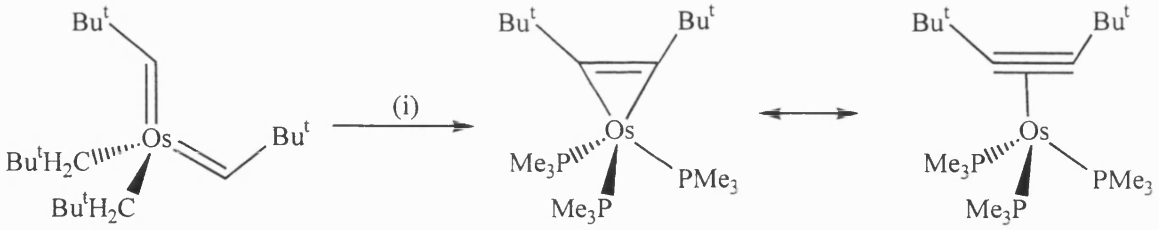

Scheme 2.20 (i) neat PMe_3.

Of the two possible reaction pathways considered by Schrock it was suggested that the steps **n→p→37**, Scheme 2.21 were more likely.

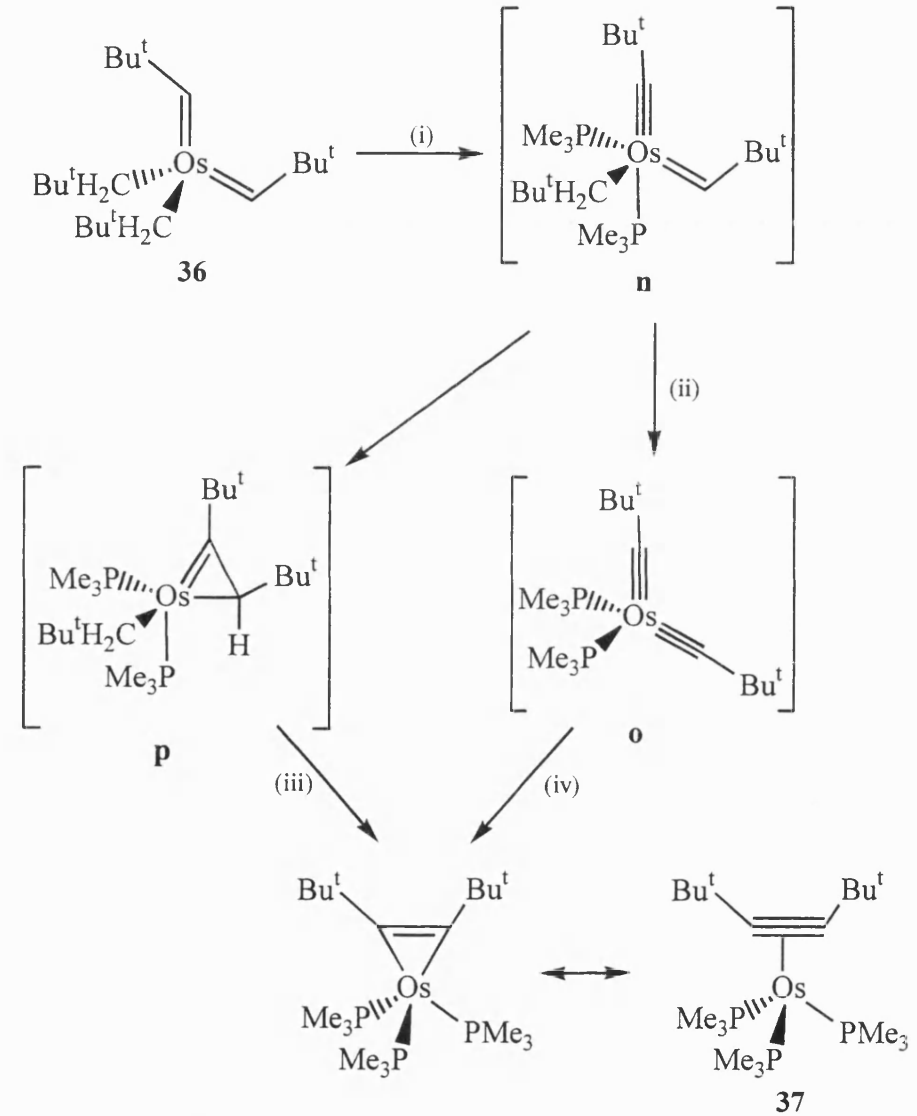

Scheme 2.21 (i) PMe_3, $-CMe_4$, (ii) $-CMe_4$, (iii) PMe_3, $-CMe_4$, (iv) PMe_3.

Thus, in summary Schrock prefers the carbene/carbyne coupling route because of the similarity of this mechanism to those proposed by Lippard [53] and Mayr [51] as discussed above. Though Schrock quotes these systems as examples where an η^2-vinyl plays a pivotal role in the coupling reactions discussed, neither Lippard or Mayr have ever actually suggested the intermediacy of an η^2-vinyl moiety. Therefore, the introduction of an η^2-

vinyl into the mechanism of the coupling observed in this osmium complex supports the postulates made above about the role of the η^2-vinyl in the formation of alkynes from carbenes and carbynes. Moreover, if one invokes the principle of microscopic reversibility the work of Mayr, Lippard and Schrock on the formation of alkynes at mononuclear centres, provides strong support for the suggestion that the cleavage of a carbon-carbon bond in a η^2-vinyl is the initial step in the formation of **Ia, b**. Thus, establishment of a reaction pathway that allows a carbon-carbon triple bond to cleave is the first step in understanding the chemistry taking place in the formation of **Ia, b**.

In order to begin to understand the subtleties of the mechanism a retro synthetic analysis was carried out taking into account the geometry of the final product and the suggested initial step above, Scheme 2.22.

There are three main points to address when considering this analysis.

a) The formation of the tetraphenylcyclopentadienyl ring, which labelling experiments suggest is produced from two of the alkyne ligands and the terminal methylene carbon of the dpps.

b) The modification of the dpps ligand, where the methylene CH_2 is replaced by the CHPh functionality, a substituent which originated as an alkyne in the tris alkyne complex **15**.

c) The cleavage of an alkyne ligand giving rise to a carbyne and carbene which must become the replacement methylene carbon for the styrene.

The final point has already been discussed, however, for the formation of the cyclopentadienyl ring system it has been shown in the literature that the coupling of two diphenylacetylene ligands with a carbene can produce a tetraphenylcyclopentadiene ligand [56] which in turn could be converted into a tetraphenylcyclopentadienyl substituent. The swapping of functionality observed in the styrene may be achieved *via* an alkene metathesis type reaction involving the carbene produced by the cleavage of the η^2-vinyl and the alkene moiety of the dpps.

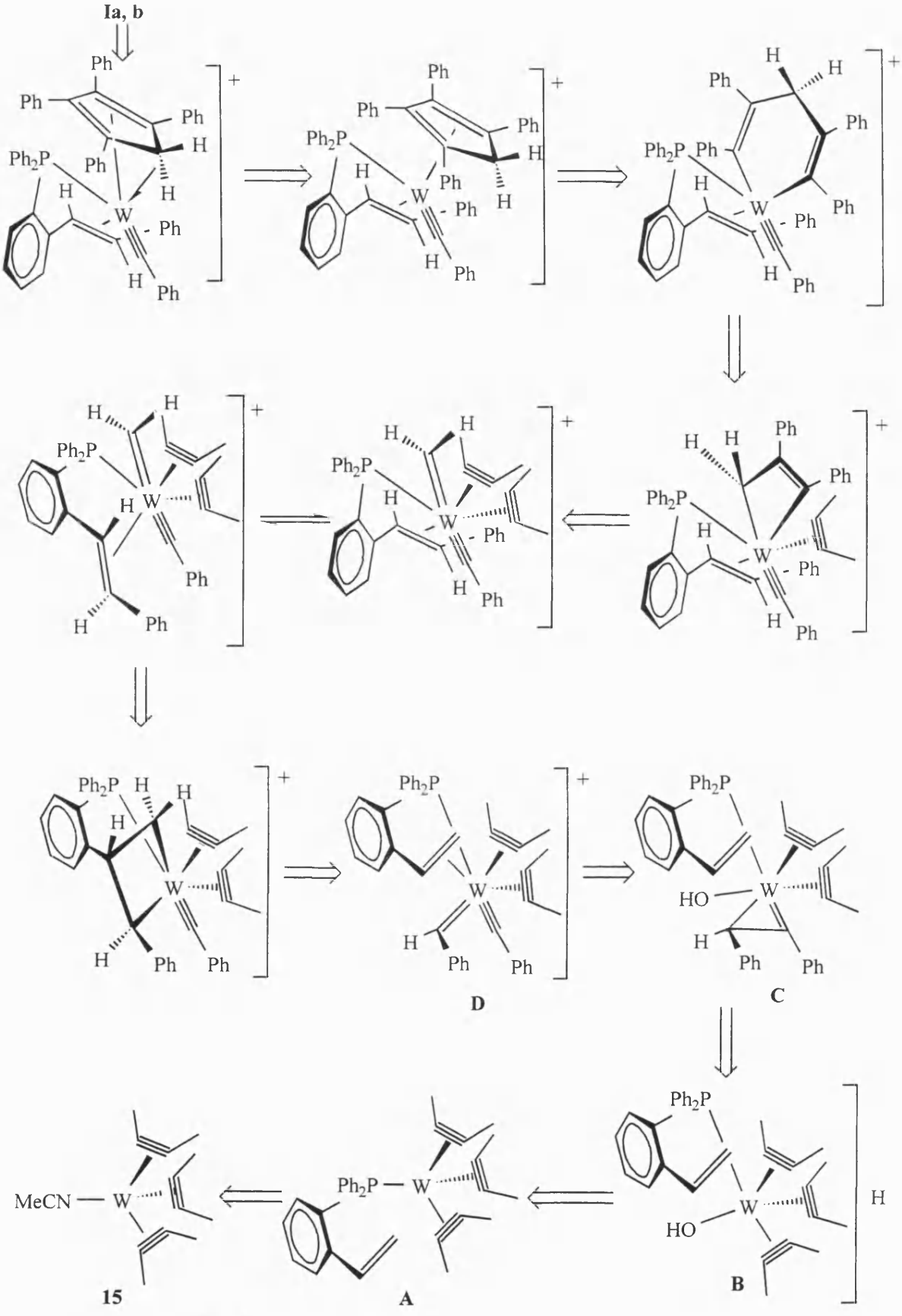

Scheme 2.22 ——≡—— = PhC≡CPh, For clarity phenyl groups are omitted, counter anion OH^- throughout.

2.4.2 Metathesis Reactions.

The Chauvin Mechanism [57] for alkene metathesis, Scheme 2.23, is now generally accepted, and a theoretical study by Hoffmann provided a detailed insight.

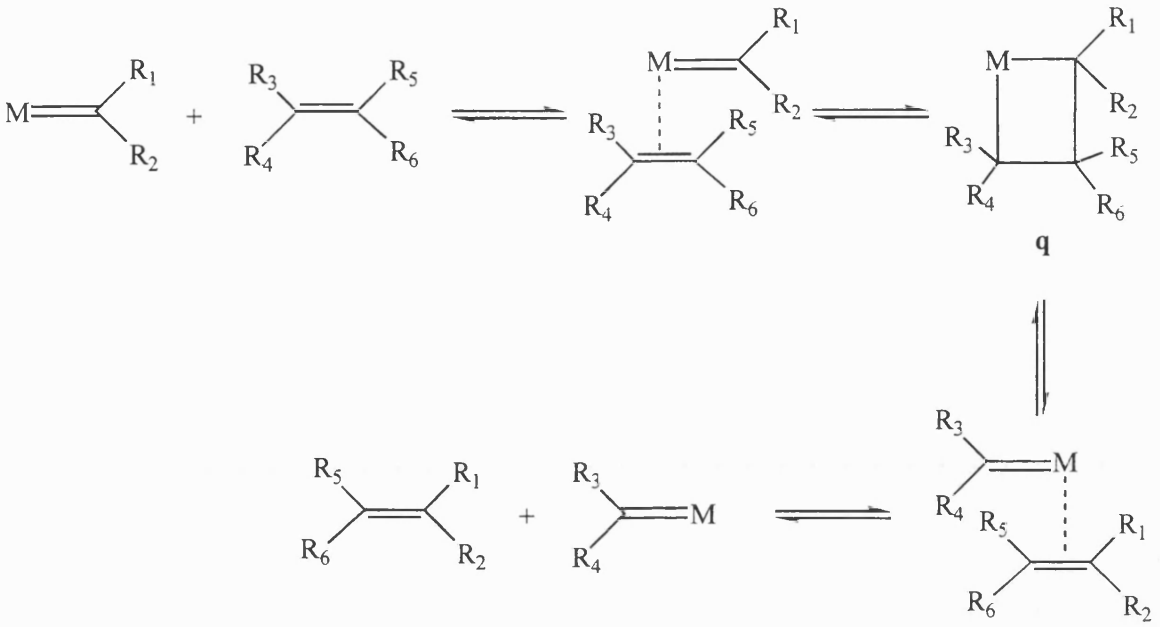

Scheme 2.23.

The stereochemical arrangements that can result during the formation of the metallocyclobutane were investigated by Hoffmann [58]. The suggestion put forward was that the alkene and the carbene can be brought together in four different conformations, and attainment of the proper conformation was crucial for the reaction to take place. These conformations are shown in Figure 2.5.

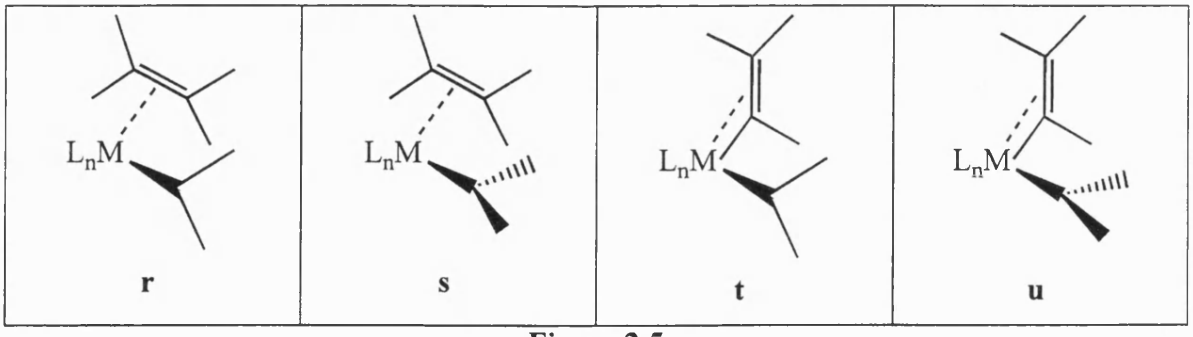

Figure 2.5

Hoffmann proposed that when two single-faced π-acceptor ligands are attached to a d^6 octahedral centre, it is well understood that they will rearrange themselves so as to maximise π bonding [58]. Thus each ligand acceptor orbital will approach a different member of the octahedral t_{2g} set, Figure 2.6, **v** (top view of **u**) rather than both acceptor orbitals compete for the same metal d function **w**.

However, it is the "collinear" conformation **w** = **r** which is required for metathesis according to the Chauvin mechanism. The carbene alkene interaction in **w** (indicated by the arrow) is large, e.g. the relevant CC overlap population is 0.12 in a model undeformed geometry for $H_4W(CH_2)(C_2H_4)^{4-}$. When Hoffmann studied a hypothetical reaction co-ordinate, a linear transit, between the metal-carbene-alkene complex and a

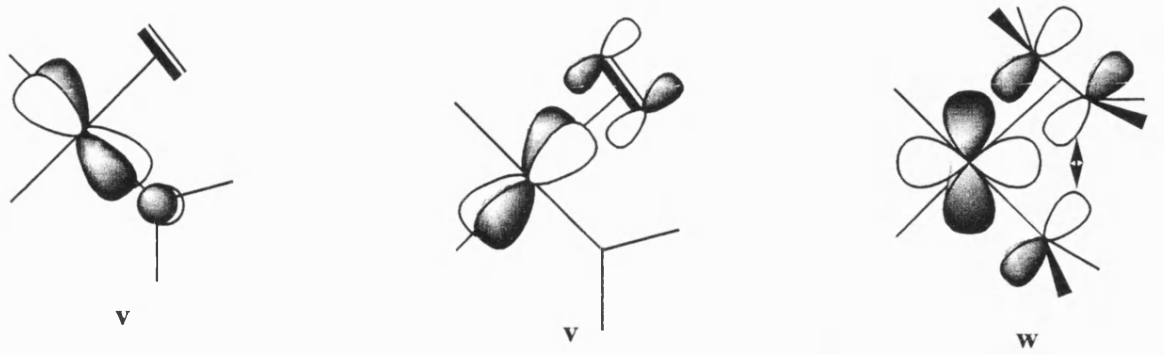

v **v** **w**

Figure 2.6

metallocyclobutane, the energy minimum comes at neither extreme but in the middle, Figure 2.7. This partially bonded metallocycle **x** then allows metathesis to occur producing the observed alkene reorganisations.

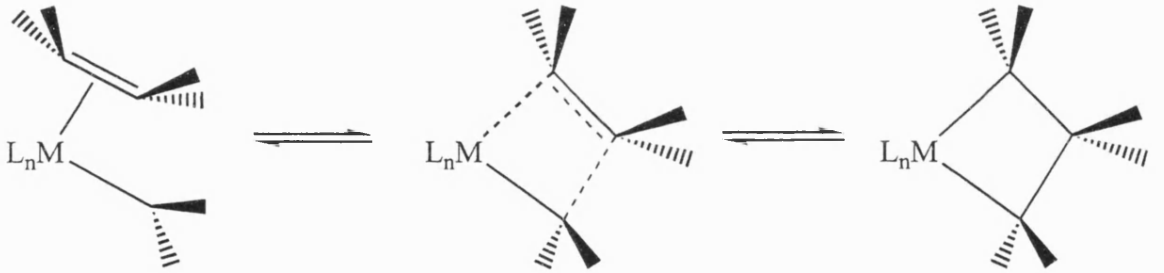

x

Figure 2.7.

If these stereochemical insights are applied to the formation of **Ia, b** where it is clear from the isotopic labelling experiments that metathesis is involved, Scheme 2.24, it is apparent that there are eight possible conformers that can be adopted before coupling commences. These conformers depend upon the orientations of the dpps ligand and the carbene when metathesis occurs, the orientation of the dpps is controlled by rotation about the vinyl-aryl C-C bond. The orientation of the carbene is determined by rotation about the metal-carbon double bond. Carbene ligands have been shown to have a low energy barrier to rotation, *e.g.* it has been calculated that the barrier to rotation for the complex $[Ni(=CH_2)(CO)_3]$ [59] is approximately 0.2 kcal/mol, and for the complex $[Fe(=C_7H_6)(CO)(PBu^n{}_3)(\eta\text{-}C_5H_5)]$ [60] the spectroscopically determined barrier to rotation is 9.6 kcal/mol.

As is shown, in Scheme 2.26, only two of the stereochemical conformers yield the η^2-(*E*)-CH=CHPh moiety and will be discussed later, the other possibilities are described below and are grouped by which face of the carbene the dpps approaches before coupling.

1) Dpps coupling with the carbene from the rear face of the molecule, Scheme 2.24.

Routes **(i)** and **(ii)** produce a co-ordinated carbene as part of a five membered ring, formed between the tungsten, the phosphorus of the dpps, the ortho carbons of the benzene ring and the carbene carbon, Figure 2.8, the other product of the reaction being styrene.

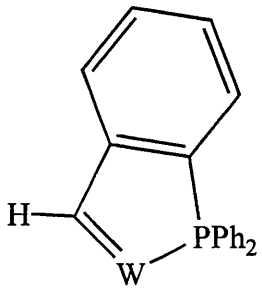

Figure 2.8.

It is possible to suggest that the strain upon this ring is such that in reality it would not form. Route **(iii)**, produces the *cis* form of the modified dpps ligand, we believe this would not form due to steric hindrance between the phenyl substituents of the dpps and of the alkene.

2) Dpps coupling with the carbene from the front face of the molecule, Scheme 2.25.

Similar results are observed as in 1, routes **(iv)** and **(v)** producing the strained five membered ring and route **(vi)** yields the hindered *cis* form of the modified dpps ligand.

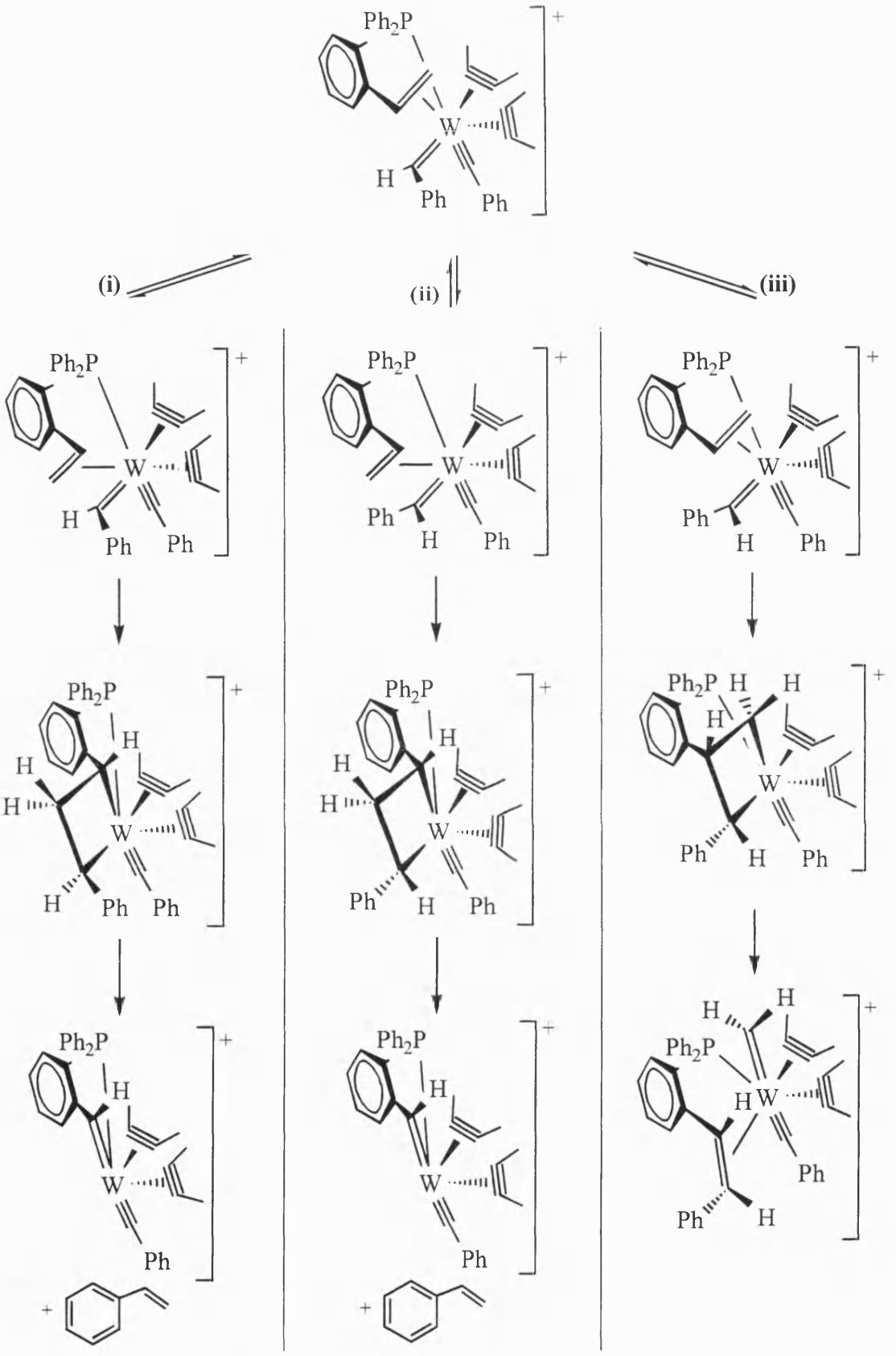

Scheme 2.24 ═══ = PhC≡CPh For clarity phenyl groups are omitted, counter anion OH^- throughout.

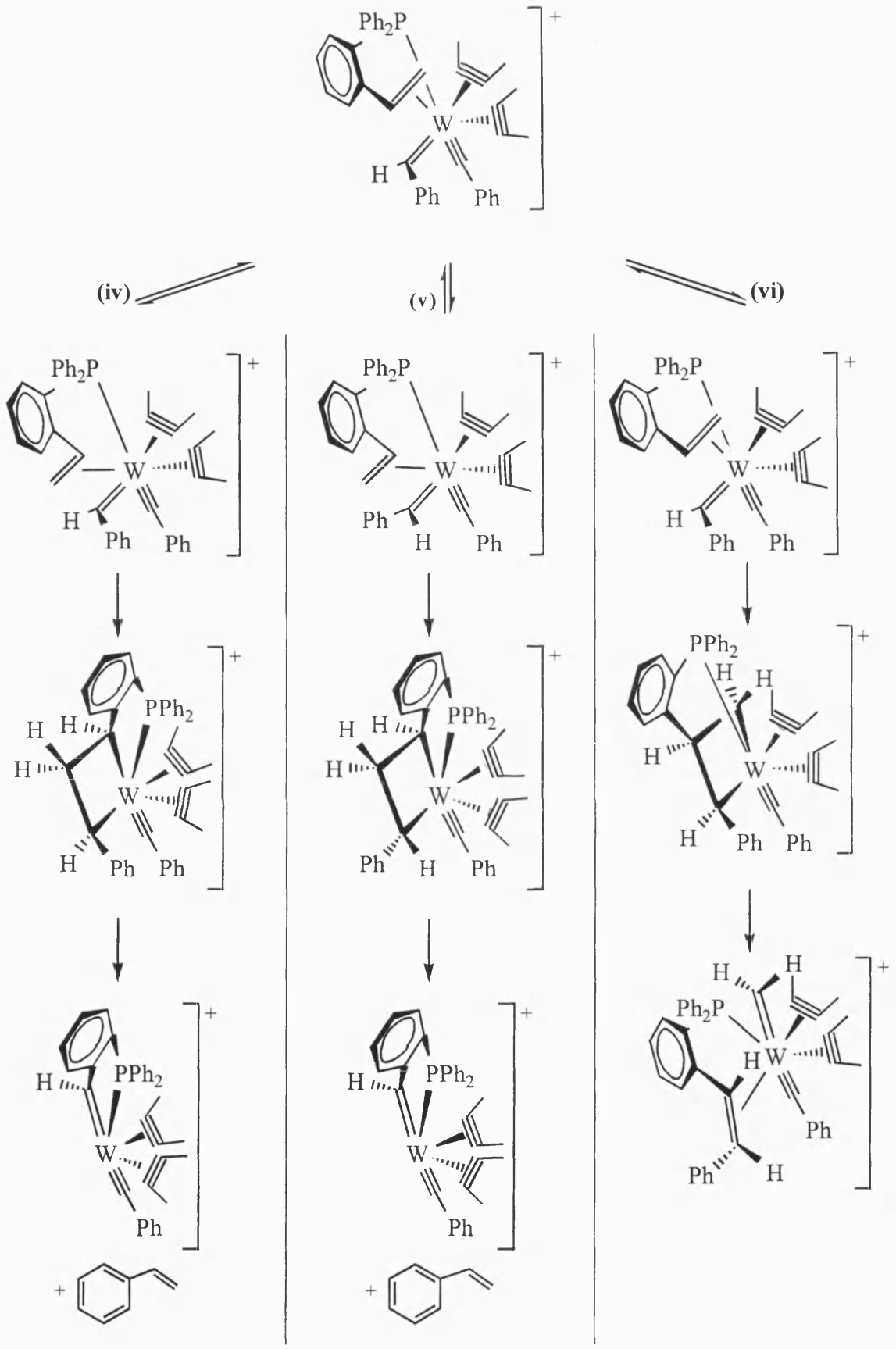

Scheme 2.25 —≡— = PhC≡CPh For clarity phenyl groups are omitted, counter anion OH^- throughout.

Having discounted these pathways the remaining two routes both provide the required *trans* form of the modified dpps **E** observed in **Ia, b**, Scheme 2.26. The intermediate **E** also provides the required stereochemical arrangement around the metal centre for the coupling between the carbene and the remaining two alkynes to take place to produce the tetraphenylcyclopentadienyl moiety of **Ia, b**.

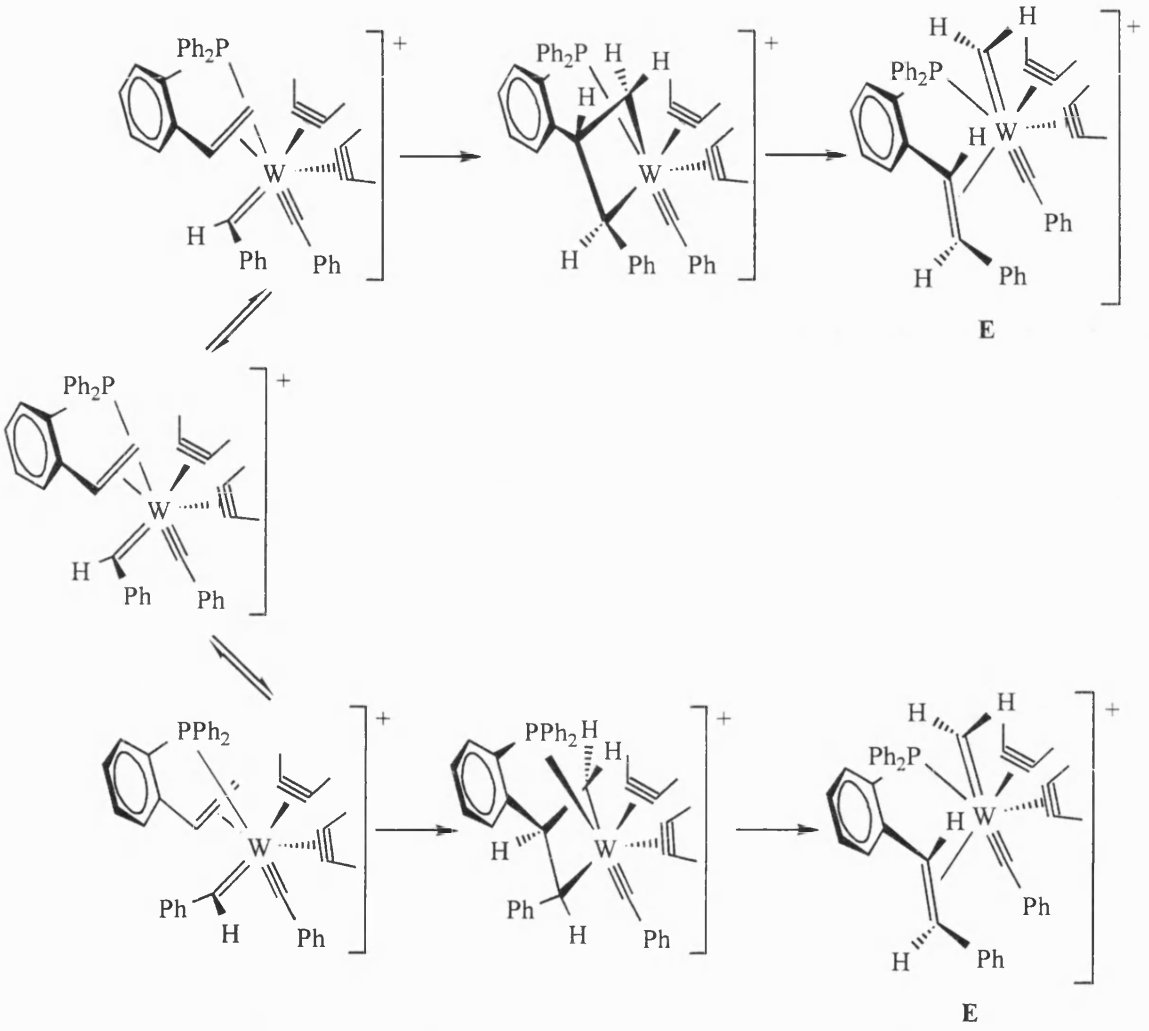

Scheme 2.26 ——≡—— = PhC≡CPh For clarity phenyl groups are omitted, counter anion OH^- throughout.

2.4.3 Production of Tetraphenylcyclopentadienyls.

The coupling of the carbene and the two alkynes to form a tetraphenylcyclopentadienyl is a known reaction following the precedent shown within this group [56] where the methyl substituted complex $[Mo(Me)\{P(OMe)_3\}(\eta^2\text{-PhC}\equiv\text{CPh})(\eta^5\text{-}C_5H_5)]$ was treated with excess diphenylacetylene in benzene and heated *in vacuo* at 78°C in a sealed tube. This was

carried out under the assumption that the alkyne would capture the intermediate carbene complex. After 12 hours a change was observed in the reaction mixture from green to yellow which after work up gave the yellow crystalline complex $[Mo(H)\{P(OMe)_3\}(\eta^5\text{-}C_5H_5)(\eta^4\text{-}C_5H_2Ph_4)]$ **38**, which has a geometry similar to that of a familiar sandwich $ML_2(\eta^5\text{-}C_5H_5)_2$ species, Scheme 2.27. Complex **38** then undergoes a dissociative loss of phosphite followed by rapid transfer of the allylic *endo*-hydrogen onto the molybdenum centre to produce the complex $[MoH_2(\eta^5\text{-}C_5H_5)(\eta^5\text{-}C_5Ph_4H)]$.

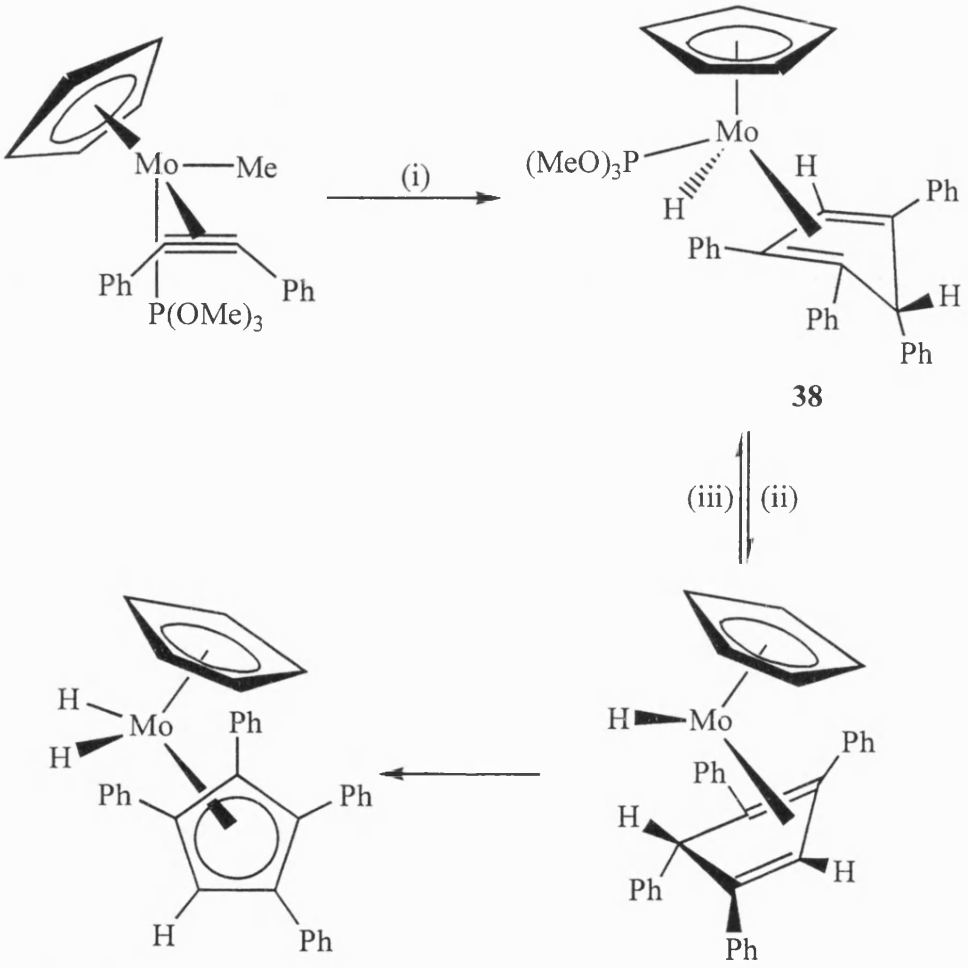

Scheme 2.27 i) excess PhC≡CPh in benzene heated to 78°C *in vacuo*, ii) - $P(OMe)_3$, iii) + $P(OMe)_3$.

Extending these ideas to the carbene complex formed after the metathesis step, the stereochemical arrangement of the ligands around the tungsten brings the carbene into a perpendicular arrangement with respect to two diphenylacetylene ligands, which allows coupling to occur in a similar manner to the way described above, Scheme 2.28.

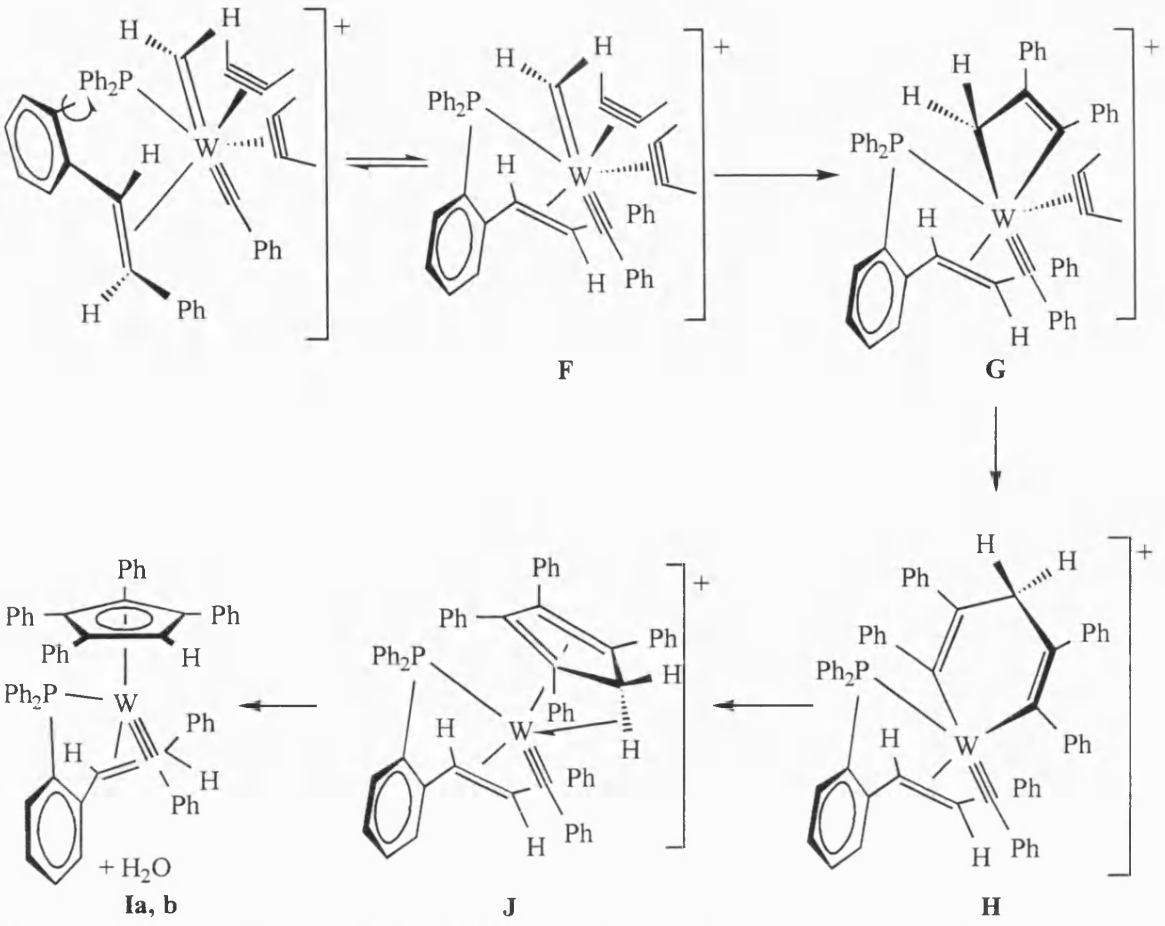

Scheme 2.28 ═══ = PhC≡CPh For clarity phenyl groups are omitted, counter anion OH^- throughout.

Initially rotation around the P-aryl bond moves the modified styrene into the position observed in the x-ray diffraction study of **Ia**, **F**. The carbene initially couples with one of the diphenylacetylene ligands to form the metallocyclobutene ring **G**, which immediately couples with the second diphenylacetylene ligand to produce the fourteen electron metallocyclohexadiene species **H**. In order to become an eighteen electron species the metallocyclohexadiene species collapses into a η^4-cyclopentadienyl ring which brings one of the hydrogens into the co-ordination sphere of the metal where an agostic M-H bond is formed to produce an eighteen electron species **J**. The formation of the agostic hydrogen interaction increases the acidity of the hydrogen involved and it is a simple matter for the hydroxide anion to attack it generating the neutral species **Ia, b** and the catalytic molecule of water which initiated the reaction pathway.

2.4.4 Overall Reaction Pathway.

Combining the ideas discussed above we can produce a proposed reaction pathway for the formation of [W(≡CPh){η^2-(E)-CHPh=CHC$_6$H$_4$PPh$_2$-o}(η^5-C$_5$Ph$_4$H)] **Ia, b** from [W(NCMe)(η^2-PhC≡CPh)$_3$] **15**, Scheme 2.29.

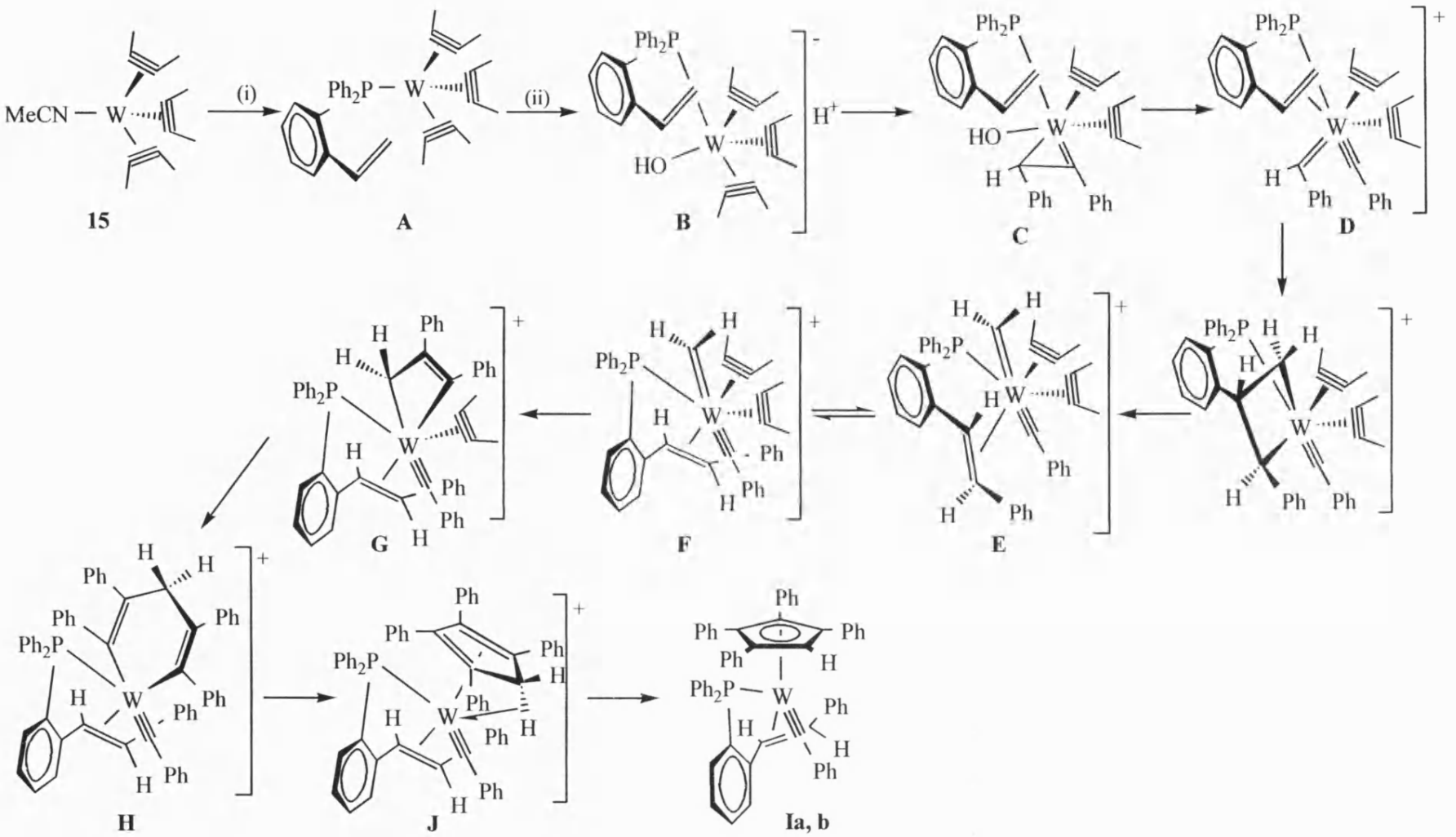

Scheme 2.29 i) dpps, refluxing toluene ii) cat. H_2O ——≡—— = PhC≡CPh For clarity phenyl groups are omitted, counter anion OH^- throughout.

2.5 Reaction of [W(NCMe)(η^2-PhC$_2$Ph)$_3$] 15 with *o*-diphenylphosphinoallylbenzene.

In seeking to expand our understanding of the above reorganisation reaction the *o*-diphenylphosphinoallylbenzene (dppa) equivalent of dpps was prepared [61], Figure 2.9.

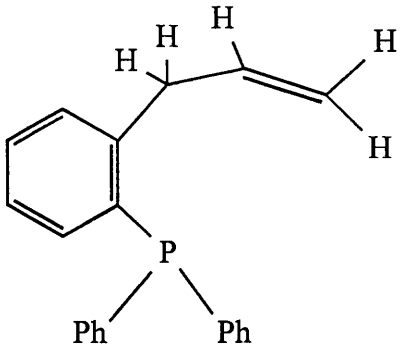

Figure 2.9.

It was thought it would be interesting to see if the dppa reacted in a similar manner to the dpps, although of course there would be extra flexibility of the allyl subsistent as a result of the additional CH_2. To investigate this idea, [W(NCMe)(η^2-PhC$_2$Ph)$_3$] **15** was treated with dppa in refluxing toluene, the pale yellow solution turning initially light red and after four hours into a deep red/orange. Work-up by column chromatography on Al_2O_3 and elution with hexane-dichloromethane (4:1) gave an orange powder in 52% yield, which upon crystallisation afforded orange crystals of **II**. As with the previous dpps reaction the elemental analysis and mass spectrum indicated the incorporation of three diphenylacetylene molecules and one dppa ligand. Examination of the $^{13}C\{^1H\}$ NMR spectra showed a peak at δ 289.4ppm characteristic of a tungsten-carbon multiple bond. A single peak in the ^{31}P NMR spectrum at δ 36.44ppm suggested that a single novel complex had been formed. The ^1H spectrum clearly showed that a different type of reaction from that found with dpps had occurred. However, the spectra were too complex to be able to assign unequivocally a structure for the orange complex **II**. In order to clarify the structural identity of **II** a single crystal was prepared for an X-ray diffraction study, which established the molecular structure shown in Figure 2.10, Table 2.2.

The molecular structure of **II** shows that it is surprisingly a tungsten carbene complex with a W-C bond length of 2.000(11) Å, which is considerably shorter than the average W-C bond length for a carbene of 2.298 Å [40], the bond angle around the carbene shows that it is a slightly distorted sp^2 carbon, the distortion being due to its substituents. The other

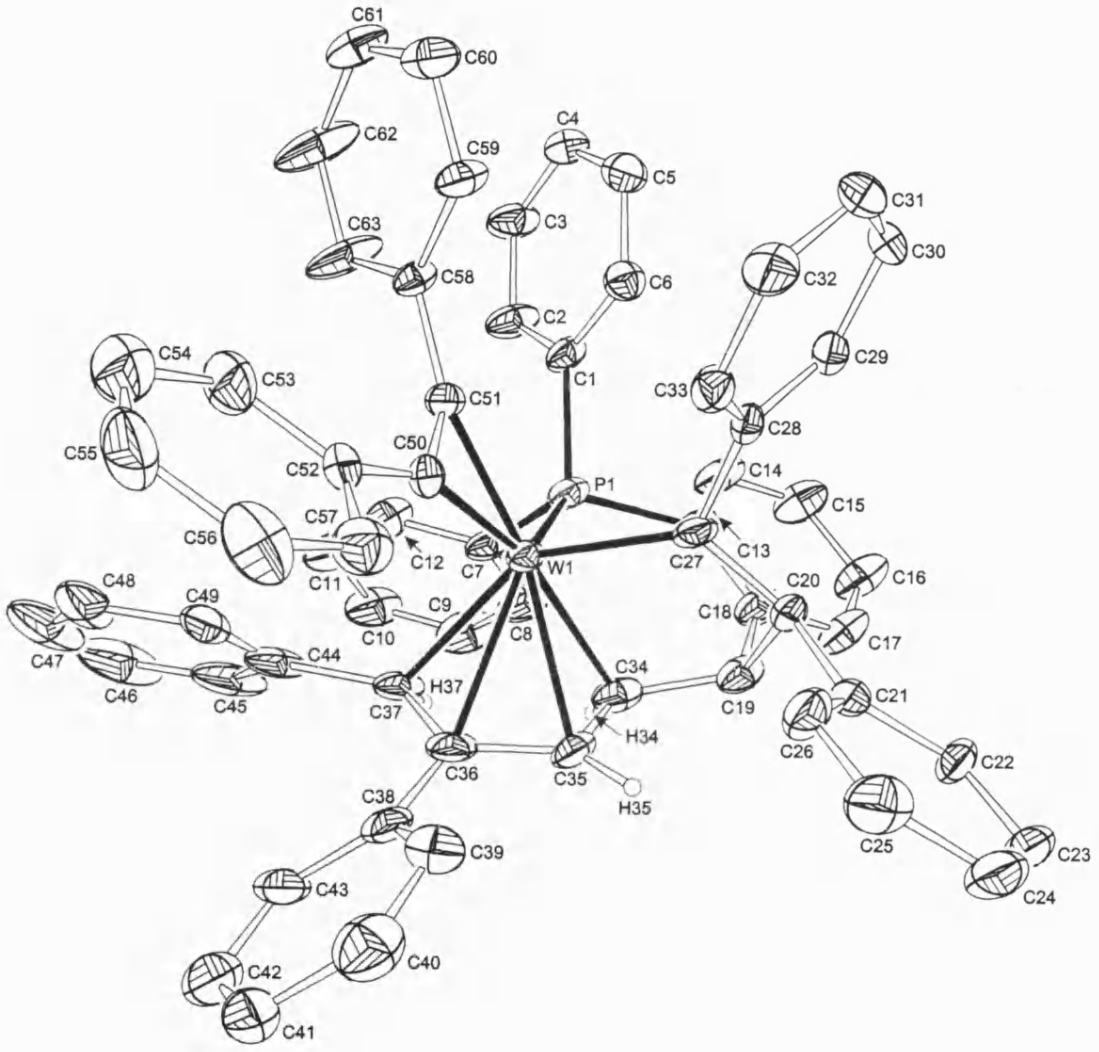

Molecular structure of **II**

Figure 2.10.

Atoms	Bond Length (Å)	Atoms	Bond Angle (°)
W(1)-P(1)	2.454(4)	C(28)-C(27)-W(1)	123.7(7)
W(1)-C(27)	2.000(11)	C(20)-C(27)-W(1)	123.1(7)
W(1)-C(34)	2.302(12)	C(20)-C(27)-C(28)	113.2(8)
W(1)-C(35)	2.306(11)	C(1)-P(1)-W(1)	117.5(3)
W(1)-C(36)	2.349(12)	C(7)-P(1)-W(1)	115.3(3)
W(1)-C(37)	2.331(11)	C(13)-P(1)-W(1)	116.4(3)
W(1)-C(50)	2.044(10)	C(35)-C(34)-C(19)	119.2(11)
W(1)-C(51)	2.018(13)	C(36)-C(35)-C(34)	118.4(12)
C(50)-C(51)	1.32(2)	C(35)-C(36)-C(37)	113.8(14)
C(34)-C(35)	1.42(2)	C(35)-C(36)-W(1)	70.9(7)
C(35)-C(36)	1.40(2)	C(37)-C(36)-W(1)	71.6(7)
C(36)-C(37)	1.43(2)	C(36)-C(35)-W(1)	74.2(6)
C(19)-C(20)	1.551(13)	C(34)-C(35)-W(1)	72.0(7)
C(20)-C(27)	1.500(14)		

Table 2.2 Selected bond lengths and angles for **II**.

moieties around the tungsten consist of a diphenylacetylene ligand, where the W-C bond length averages 2.031 Å, which compares favourably with an average value for a W-C bond length of 2.025 Å in a four electron donor alkyne at a tungsten centre [40]. The C-C bond length of the alkyne *i.e.* C(50)-C(51) is 1.32(2) Å, and a comparison between this value and the average value for a four electron donor alkyne of 1.304 Å[40] suggests that the alkyne is acting as a four electron donor. The number of electrons donated by the diphenylacetylene is confirmed by its alkyne contact ^{13}C chemical shift (δ 220.0ppm) which is in the region expected for four electron donor alkynes [11]. Coupling had also occurred between the alkene of the dppa and a diphenylacetylene ligand to produce an η^4-bonded 1,3-diene where the bond lengths C(34)-C(35) and C(36)-C(37) are 1.42(2) and 1.43(2) Å respectively, which compares to a reported average value of 1.420 Å, and the C(35)-C(36) bond length is 1.40(2) Å, compared to a value of 1.405Å [40]. The diene tilts slightly away from the metal centre with shorter bond lengths for W-C(34) and W-C(35), 2.302(12) and 2.306(11) Å, than for W-C(36) and W-C(37), 2.349(12) and 2.331(11) Å. The phosphino functionality of the dppa is bound to the tungsten with a bond length of

2.454(4) Å, which is shorter than the average tungsten phosphorus bond length in a tungsten triphenylphosphine complex, but this is most probably due to the chelation and coupling of the alkene end of the allylic group. The phosphino group does not seem to be under any strain as the arrangement of the phenyl groups about the phosphorus is uniform as is shown by their near matching bond angles, Table 2.2. The most surprising structural feature is the two carbon unit C(20), C(27), which links the tungsten and the carbon atom C(19), this atom has its origin in the allylic CH_2 carbon of the dppa ligand. The formation of this bridge W-C(27)-C(20)-C(19) is highly unusual and is most likely to be responsible for the observed shortening of the tungsten-carbene bond.

Having established the structure of compound **II** by crystallography, assignment of the complex NMR spectra was much simplified and selective two dimensional NMR techniques, correlation spectroscopy (COSY) and CH correlation, were used to establish the couplings and assignments listed in the experimental section.

Thus, the reaction to produce **II** is summarised in Scheme 2.30, and in an attempt to further

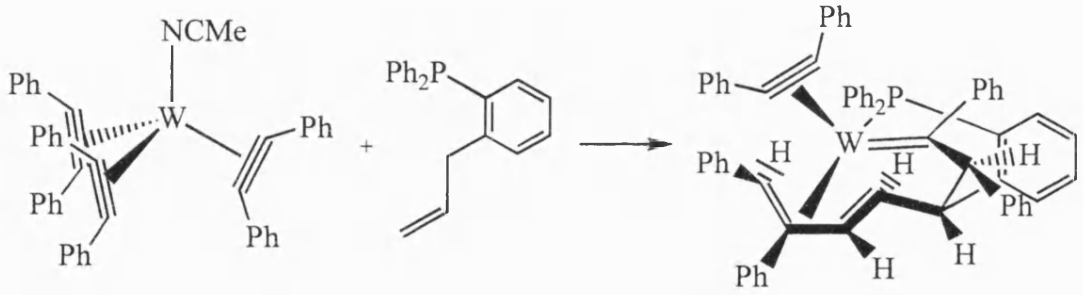

15 **dppa** **II**

Scheme 2.30.

understand the nature of this unusual reaction ^{13}C-labelling experiments were carried out. Reaction of ^{13}C-labelled **15*** with dppa in refluxing toluene gave according to the NMR complex **II** with carbon-13 enrichment in the positions shown in Figure 2.11.

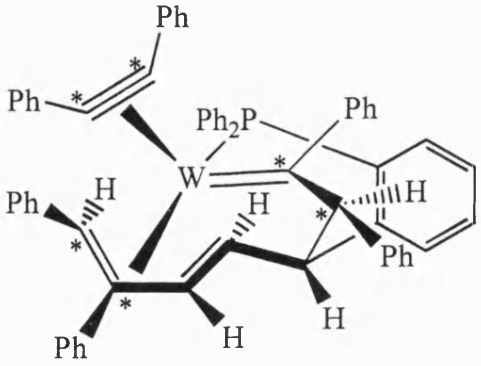

II

* = ^{13}C

Figure 2.11.

As expected enrichment is observed in the co-ordinated alkyne, and the phenyl substituted carbons of the diene. Most importantly enrichment is observed in the carbons that make up the metal-carbene and the bridge to the allylic carbon of the dppa, C(27) and C(20), implying that the bridge has formed from a diphenylacetylene ligand.

2.6 Possible Reaction Pathways.

As in the case of the formation of **Ia, b** it was thought that a retro synthetic analysis based upon the geometry of the isolated product **II** and the result of the isotopic labelling experiment would provide mechanistic insight, Scheme 2.31. This analysis breaks the reaction pathway down into a series of known reaction steps after the co-ordination and the chelation of the dppa moiety. Primarily, it is necessary to understand the origin of an η^3-allylic system, then to consider alkyne insertions into transition metal hydrogen sigma bonds and finally a Faller-Rosan 'envelope shift'. These concepts are reviewed below with literature examples of the reaction type given where possible.

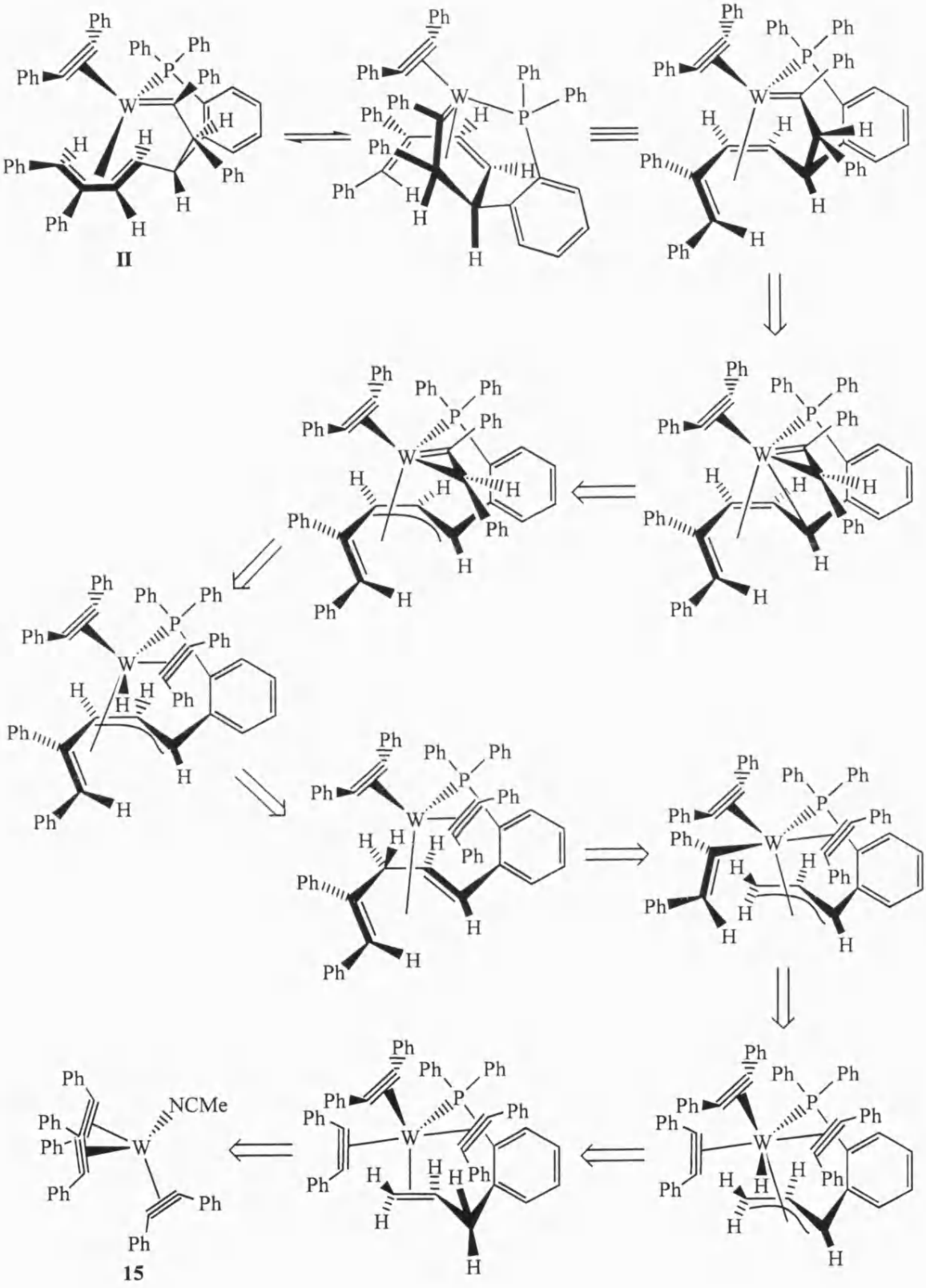

Scheme 2.31.

2.6.1 Allyl Complexes.

The retro synthetic analysis highlights the possible important role played by the conversion of an alkene into an allyl complex. This is one of the most commonly used synthetic routes to the π-allyl ligand, and this reaction usually involves the transfer of an allylic hydrogen from the alkene to the transition metal to which it was bound. It was initially suggested that this proceeds by direct metal insertion into an allylic C-H bond [62], but most probably involves the formation of an agostic hydrogen intermediate, as shown in Scheme 2.32.

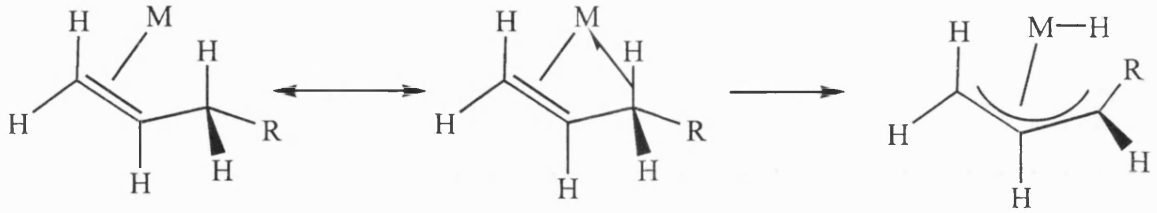

Scheme 2.32.

Thus it is reasonable to suggest that in the initial reaction between the [W(NCMe)(η^2-PhC≡CPh)$_3$] **15** and dppa, the phosphine displaces the acetonitrile leading to co-ordination of the alkene substrate of the diphenylphosphinoallylbenzene to the metal centre. The dppa co-ordinates in the correct orientation that an agostic bond can form between a hydrogen atom of the CH_2 bridge and the tungsten, as illustrated in species **K**. The tungsten then inserts into this C-H bond as described above producing a tungsten tris-alkyne π-allyl complex **L**, Scheme 2.33.

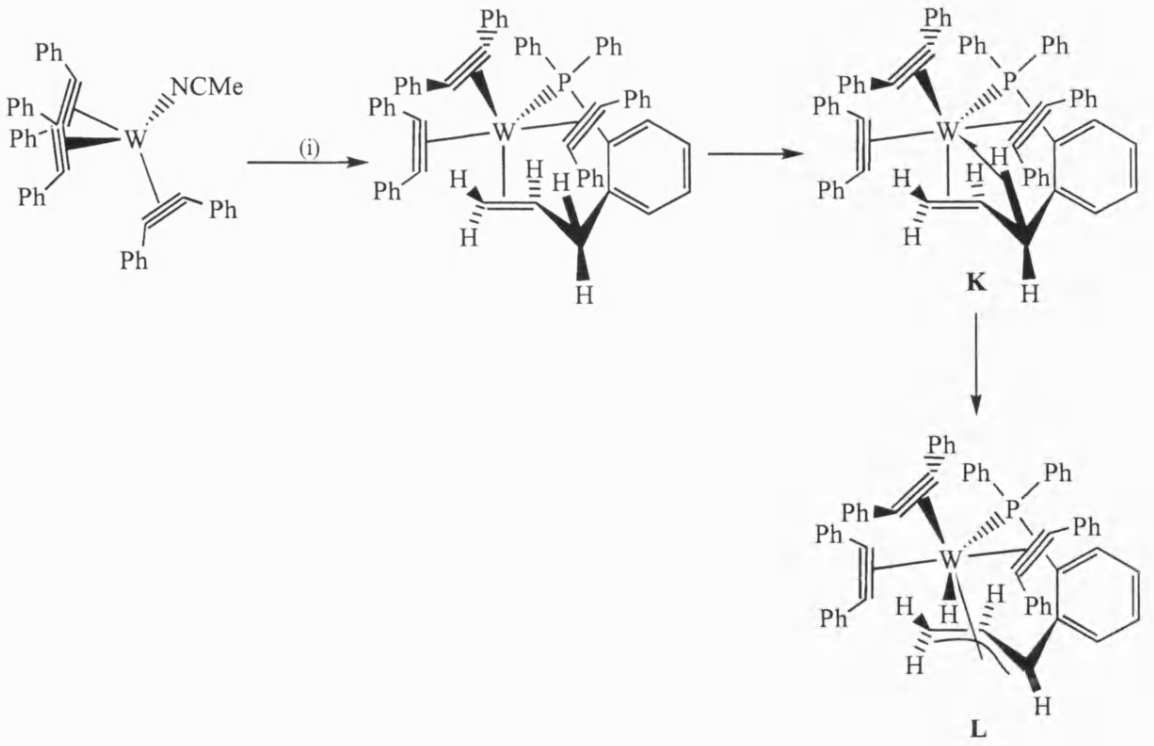

Scheme 2.33 (i) dppa, refluxing toluene.

2.6.2 Alkyne Insertions into Transition Metal-Hydrogen σ Bonds.

The conversion of the chelating dppa ligand into a π-allyl metal hydride intermediate **L** then allows one of the co-ordinated alkynes to insert into the metal-hydrogen bond. This is a common organometallic reaction that yields as its product alkenyl complexes [63,64]. For example, the reaction of phenylacetylene with a monohydrido rhodium complex yields a mixture of the alkenyl and acetylide complexes in a ratio of 1:1, Scheme 2.34. If the above reaction is carried out with an excess of phenylacetylene it still affords the same ratio of products suggesting that they proceed *via* a common intermediate **y** where the alkyne is co-ordinated to the rhodium centre *cis* to the hydride. Insertion of the alkyne into the rhodium-hydrogen bond of **y** yields the alkenyl whilst loss of H_2 *via* C(alkyne)-H oxidative addition to the rhodium produces the acetylide.

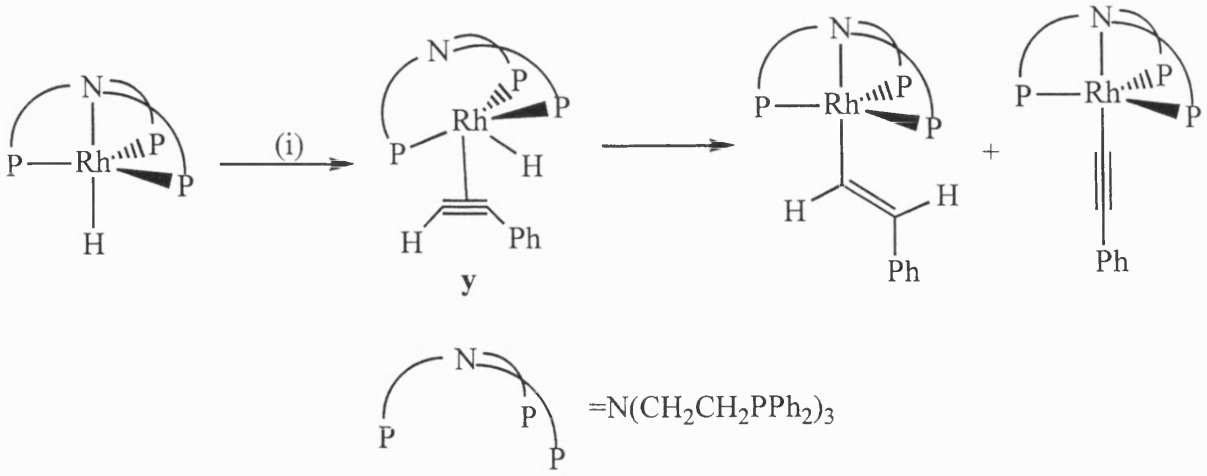

Scheme 2.34 i) PhC≡CH, thf.

The *cis* geometry of the hydride to one of the alkynes in **L** suggests that a reaction of the type described above could occur, the diphenylacetylene ligand inserting into the tungsten hydrogen bond resulting in the formation of an alkenyl intermediate, which can then undergo a reductive elimination reaction [65] between the resulting σ-vinyl and a σ/π allyl to form the 1,4 diene moiety present in **M**, Scheme 2.35.

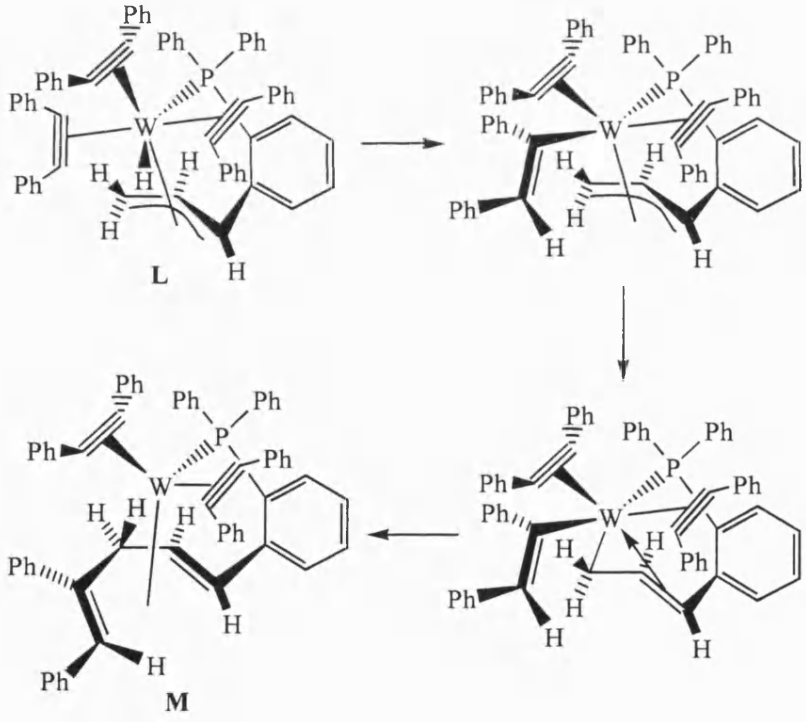

Scheme 2.35.

The reaction can then proceed, as illustrated in Scheme 2.36, *via* conversion of the 1,4-diene into an allylic system **N** after hydrogen transfer to the tungsten. This then provides a possible pathway for the formation of the unusual bridge observed in **II**. If one of the

diphenylacetylene ligands inserts into the metal-hydrogen σ bond present in **N**, the η^2-vinyl containing species **O** is formed.

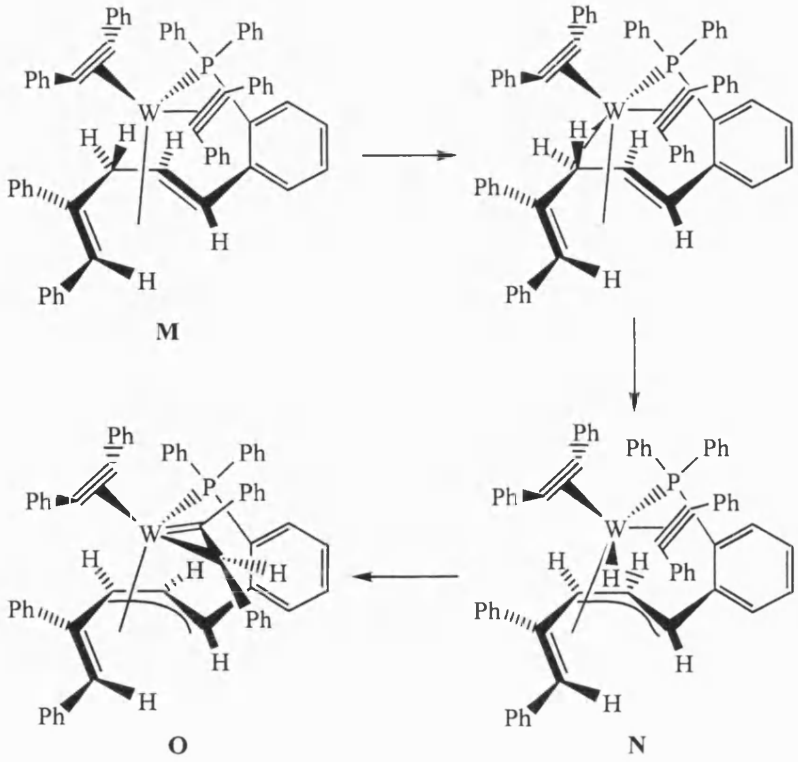

Scheme 2.36.

The intermediate **O** then undergoes an allylic rearrangement from a η^3-π-allyl to a σ-π donating species **P**, Scheme 2.37, which in doing so forms the 1,3-butadiene ligand observed in **II**. This rearrangement brings the η^2-vinyl into a *cis* configuration with the tungsten-carbon bond and these react *via* an unprecedented reductive elimination to form the bridging carbene functionality seen in **II** , illustrated in intermediate **Q** Scheme 2.37. This occurs with a switching of the bonding mode of the remaining alkyne from a two electron donor to a four electron donor to complete the tungsten's 18 electron count.

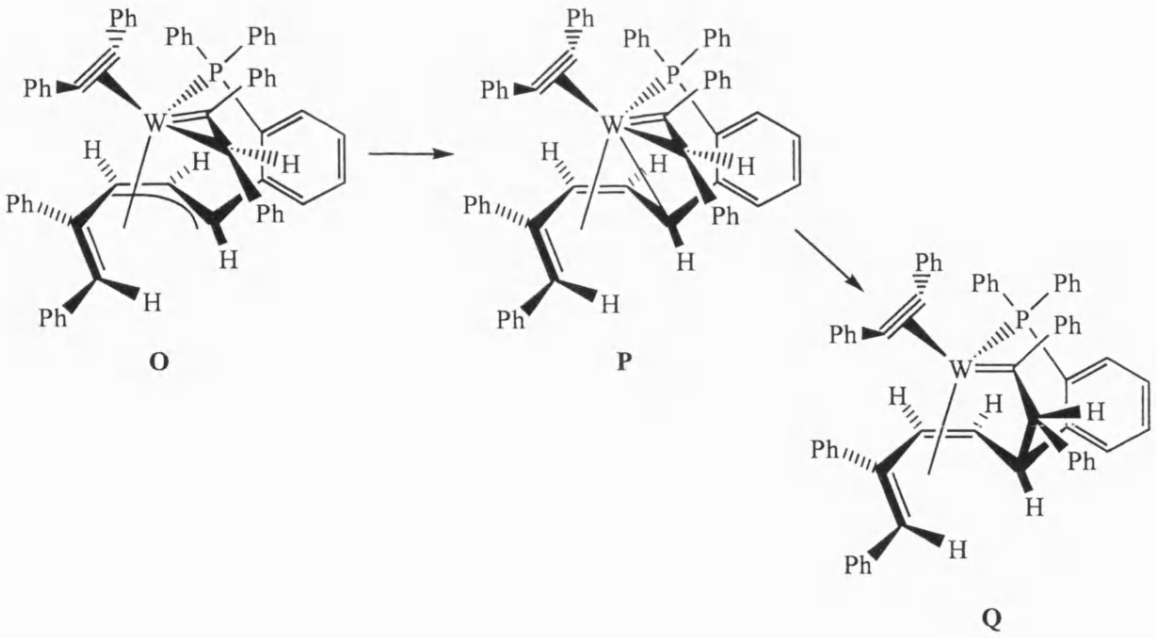

Scheme 2.37.

2.6.3 Faller-Rosan 'envelope shift'.

With the formation of the 1,3-butadiene and the novel carbene bridge, as shown in **Q**, the butadiene undergoes one final rearrangement to achieve the stereochemistry observed in the molecular structure of **II**. This rearrangement is known as a Faller-Rosan envelope shift [66], it has the effect of exchanging the anti and syn substituents on the 1,3-butadiene *via* a metallacyclopentene intermediate, Figure 2.12.

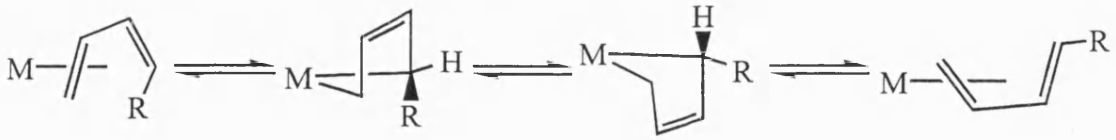

Figure 2.12.

Thus, it is proposed the intermediate **Q** undergoes this envelope shift converting to the observed product **II**. For the ease of drawing, in Scheme 2.38, **Q** is drawn looking down the tungsten-carbene bond so when the envelope shift is illustrated the product is displayed in the format used for complex **II** throughout this thesis.

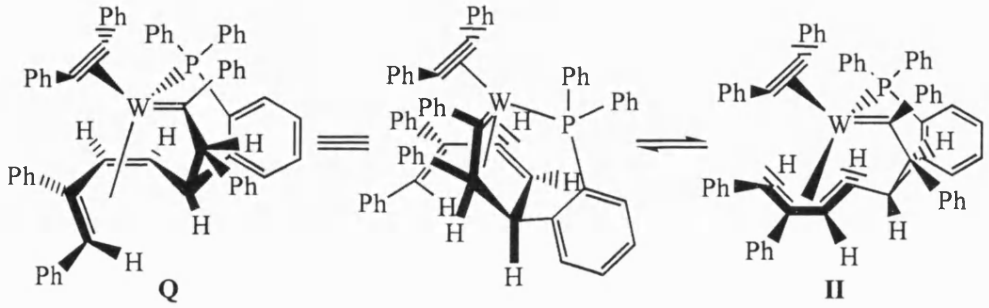

Scheme 2.38.

2.6.4 Overall Reaction Pathway.

By combining the concepts outlined above it is possible to suggest a reaction pathway for the formation of **II** from [W(NCMe)(η^2-PhC≡CPh)$_3$] **15** as is summarised in Scheme 2.39.

2.7 Summary.

In summary, new and unexpected reactions of alkynes and alkenes have been observed with tris-alkyne transition metal complexes upon the introduction of either *o*-diphenylphosphinostyrene or *o*-diphenylphosphinoallylbenzene. We have observed cleavage of both carbon-carbon triple and double bonds, novel rearrangements, a unique role for η^2-(3e)-vinyls, and couplings that could not have been predicted at the outset of this study.

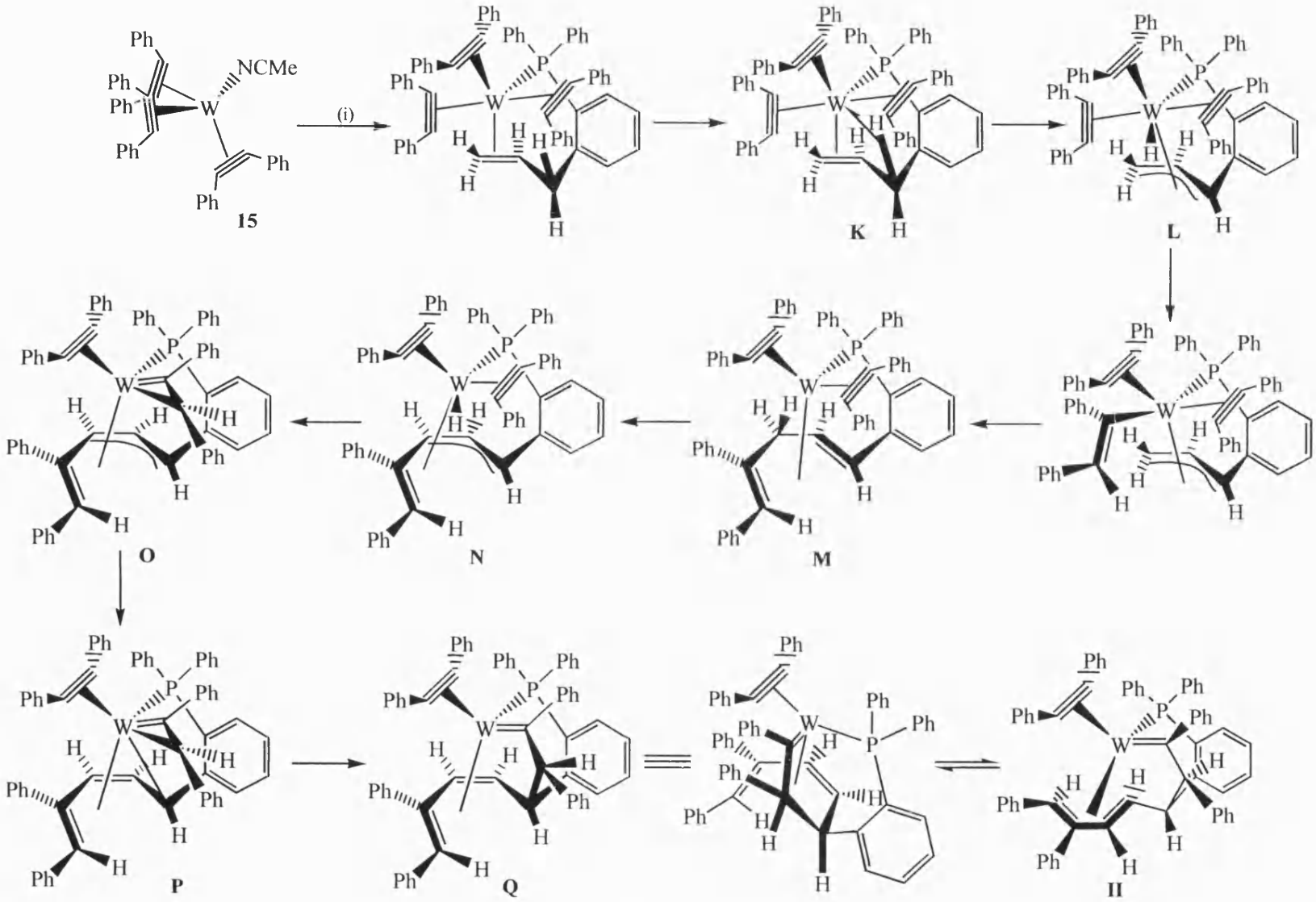

Scheme 2.39 (i) dppa.

2.8 Reaction of $[ReBr_2(\eta^2\text{-}PhC{\equiv}CPh)(\eta\text{-}C_5H_5)]$ with *o*-diphenylphosphino-allylbenzene.

The observation that a different type of coupling reaction occurs between a tris-alkyne complex and dpps than a tris-alkyne complex and dppa prompted the question: Would the same be true in the rhenium system where reaction with dpps yielded butadienylrhenium complexes? [38], shown previously in Scheme 2.6. The analogous reaction of $[ReBr_2(\eta^2\text{-}PhC{\equiv}CPh)(\eta\text{-}C_5H_5)]$ **29** with 2 equivalents of $AgBF_4$ in the presence of dppa was attempted. The solution showed an initial change from orange to green with the formation of a precipitate, which upon work up gave a green powder. Unfortunately analysis of this powder by NMR showed no discernible products which was initially intriguing. In order to address this an attempt was made to prepare the phosphorus bound dppa, mono bromide rhenium complex by only reacting in the presence of a single equivalent of $AgBF_4$. The reaction mixture changed colour from orange to light green with the production of a precipitate, after work up elemental analysis and NMR suggested the formation of the phosphorus bound mono bromide rhenium complex, $[Re(Br)(PPh_2C_6H_4CH_2CH{=}CH_2)(\eta^2\text{-}PhC{\equiv}CPh)(\eta\text{-}C_5H_5)][BF_4]$ **III**, Scheme 2.40.

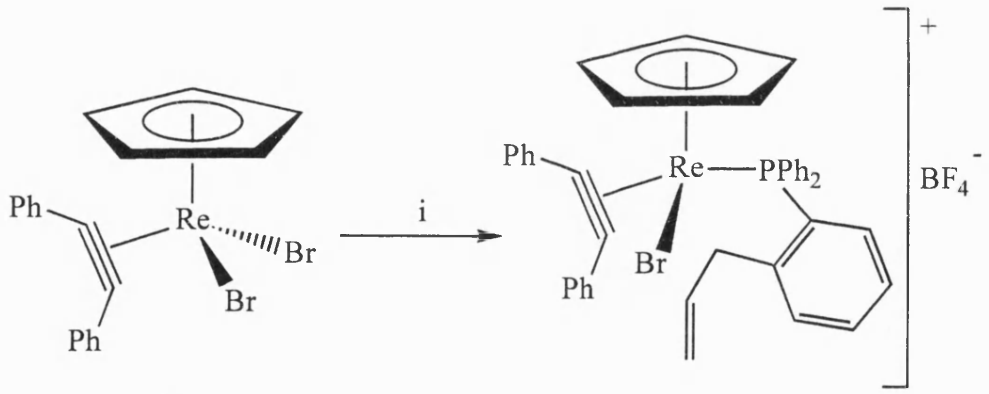

29 **III**

Scheme 2.40 i) $AgBF_4$, dppa.

The structure of **III** above is supported by the NMR data, primarily in the $^{31}P\{^1H\}$ NMR spectra where a single peak is observed at -5.62ppm which indicates a phosphorus bound dppa ligand, compared to -15.37ppm for free dppa. The main features of the $^{13}C\{^1H\}$ NMR indicate a 4 electron donor alkyne with a chemical shift of 222.9ppm and a cyclopentadienyl moiety at 97.6ppm. The presence of the bromide ligand is confirmed by the mass spectrum where the parent ion peak at 811m/z shows the expected isotope peaks

for both the bromide and the rhenium and matches the expected mass of the cation $[Re(Br)(PPh_2C_6H_4CH_2CH{=}CH_2)(\eta^2\text{-}PhC{\equiv}CPh)(\eta\text{-}C_5H_5)]^+$ exactly.

The production of **III** suggested that the next step was to see if the addition of a further equivalent of $AgBF_4$ would strip the remaining bromide causing the dppa to chelate with the possible coupling observed in the scenario above. Upon work up of the resulting dark green product, no discernible products were observed in the NMR spectra. It was puzzling that chelation of the co-ordinated dppa complex was not taking place. In an attempt to force the production of this product, $[ReBr_2(\eta^2\text{-}PhC{\equiv}CPh)(\eta\text{-}C_5H_5)]$ **29**, dppa and two equivalents of $AgBF_4$ were heated to reflux in thf for 1.5 hours and a colour change from orange to light brown was noted, but again no products were discernible in the NMR spectra.

In order to determine if the $AgBF_4$ was responsible for the decomposition of the rhenium complex the *bis*-acetonitrile rhenium complex was prepared by treating $[Re(Br)_2(\eta^2\text{-}PhC{\equiv}CPh)(\eta\text{-}C_5H_5)]$ **29** with two equivalents of $TlPF_6$ in acetonitrile solution to form the salmon pink solution of $[Re(MeCN)_2(\eta^2\text{-}PhC{\equiv}CPh)(\eta\text{-}C_5H_5)][(PF_6)_2]$ **39**. Dppa was added to this solution and an immediate colour change was noted to red brown, which gave an oily brown powder after work up. Elemental analysis and ^1H, $^{13}C\{^1H\}$, $^{31}P\{^1H\}$ NMR spectra confirm the formation of $[Re(MeCN)(PPh_2C_6H_4CH_2CH{=}CH_2\text{-}o)(\eta^2\text{-}PhC{\equiv}CPh)(\eta\text{-}C_5H_5)][(PF_6)_2]$ **IV**, Scheme 2.41.

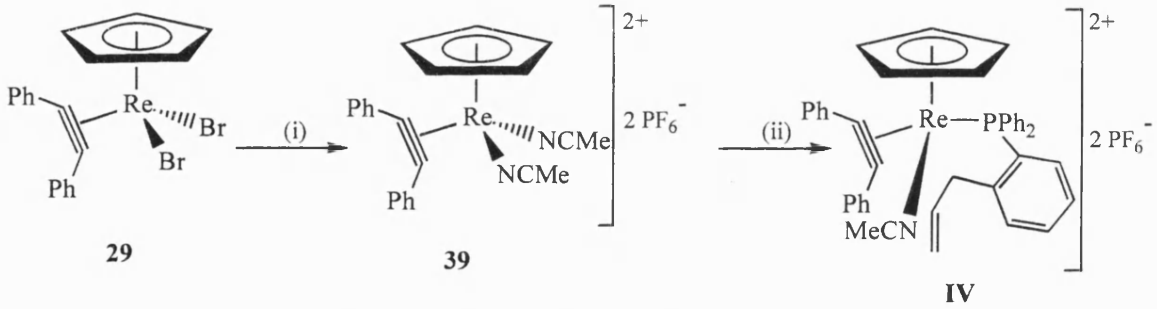

Scheme 2.41 i) $TlPF_6$, MeCN; ii) dppa.

The alkyne is confirmed as a four electron donor as it displays a chemical shift of 218.0ppm in the $^{13}C\{^1H\}$ NMR spectrum, the other major features of this spectrum being the singlet at 98.8ppm corresponding to the cyclopentadienyl ligand and another singlet at 14.2ppm which is due to the methyl carbon of the acetonitrile. The allyl group shows three singlet resonances at 117.4, 91.0 and 38.6ppm. In the $^{31}P\{^1H\}$ NMR spectrum a singlet is observed at -3.69ppm for the co-ordinated phosphine ligand and the expected septet at -144.48ppm for the hexafluorophosphate, due to the coupling between the phosphorus and the six fluorines {J(PF) = 711.8Hz.). The proton spectrum shows the expected couplings

for the allyl moiety in a series of ABC and ABX type patterns at 4.76ppm, 4.67ppm, 4.49ppm, 2.55ppm and 2.27ppm, in order to attempt to prove that the allyl group is not co-ordinated to the metal centre we shall compare it to a free allyl group in the precursor material *o*-$C_6H_4ClCH_2CH{=}CH_2$, Figure 2.13.

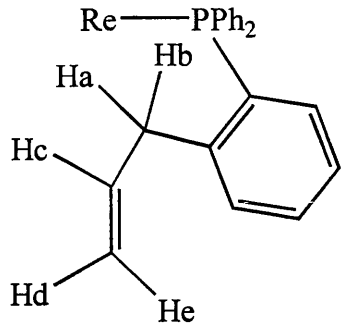

z

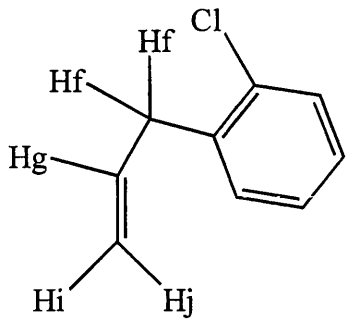

aa

Figure 2.13.

Firstly it is important to note that **z** differs slightly from **aa** in as much as Ha and Hb are in different environments due to the lack of a plane of symmetry through the complex **IV** and the two hydrogens labelled Hf can be in the same environment. In order to prove that the allyl group in **z** is not bound to the metal, the couplings between the protons of the allyl groups should be fairly similar to that of **aa**, this is shown in Table 2.3.

Fragment **z**	Coupling Constant	Compound **aa**	Coupling Constant
Ha-Hc	6.7 Hz	Hf-Hg	6.4 Hz
Hb-Hc	6.7 Hz	Hf-Hg	6.4 Hz
Hc-Hd	9.1 Hz	Hg-Hi	10.3 Hz
Hc-He	16.8 Hz	Hg-Hj	16.9 Hz

Table 2.3.

As is apparent, the coupling constants have fairly similar values, thus, implying that the allyl of **IV**, represented by fragment **z** is not co-ordinated to the rhenium centre. Completing the ^1H NMR there is a singlet at 3.15ppm is observed for the methyl group of the acetonitrile, with another singlet at 6.14ppm for the cyclopentadienyl and a multiplet between 7.81ppm and 6.22ppm for the phenyl groups. Heating **IV** and allowing it to stir in dichloromethane did not displace the acetonitrile from the rhenium allowing the allyl to co-ordinate.

It is surprising that the dppa does not chelate to the rhenium, considering the results of the reaction between dppa and the tungsten tris-alkyne system. A possible reason for this failure could be that the metallacycle formed upon reaction, even if just as an intermediate before coupling occurs, may be unstable. In the reaction between **29** and dpps, a six

membered metallacycle would be formed which would be thermodynamically favoured, Figure 2.14, but in the dppa reaction chelation would yield a seven membered ring and this may be thermodynamically unfavoured, Figure 2.14.

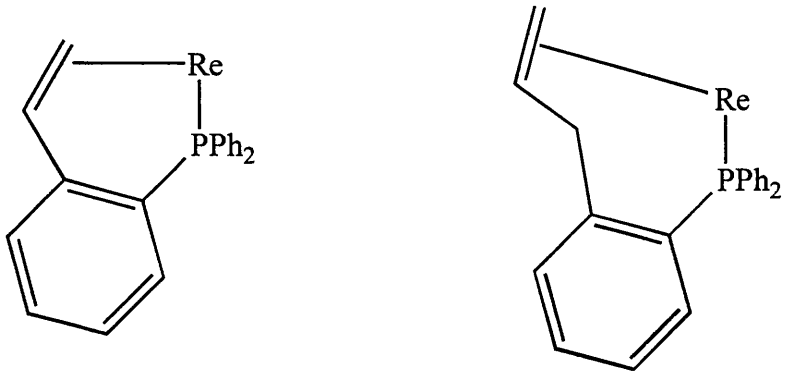

Figure 2.14.

CHAPTER 3

Carborane and Cycloheptatrienyl Chemistry

3 Introduction.

A second theme within this thesis is work directed to the formation of a labile 16 electron molybdocarborane complex which would possibly provide a synthetic route into a bis-alkyne molybdocarborane species. The aim was to synthesise the mixed sandwich complex $[NEt_4][closo\text{-}3\text{-}(\eta^7\text{-}C_7H_7)\text{-}3,1,2\text{-}MoC_2B_9H_{11}]$ which upon protonation would yield the labile 16 electron complex $[closo\text{-}3\text{-}(\eta^6\text{-}C_7H_8)\text{-}3,1,2\text{-}MoC_2B_9H_{11}]$. Loss of the cycloheptatriene ligand would produce vacant co-ordination sites which could be filled with two alkynes to produce the complex $[closo\text{-}3,3\text{-}(\eta^2\text{-}RC{\equiv}CR)_2\text{-}3,1,2\text{-}MoC_2B_9H_{11}]$. To provide an understanding of what we are trying to achieve a brief overview of the literature on both carborane and cycloheptatrienyl chemistry is presented below.

3.1 Carborane Chemistry.

Carboranes, or more correctly carbaboranes, are compounds having as the basic structural unit a number of carbon and boron atoms arranged on the vertices of a triangulated polyhedron. Their structures are closely related to those of the isoelectronic boranes and these structures can be rationalised by a series of rules devised by Wade [67]. Wade's rules relate the polyhedral structure to the electronic configuration of the borane or carborane which is possible because of the isolobility of BH, B^- and C and of BH_2, BH^- and CH, and can be summarised as follows [68].

Carboranes have the general formula $[(CH)_a(BH)_mH_b]^{c-}$, with *a* CH units and *m* BH units at the polyhedral vertices, plus *b* extra H atoms which are either bridging or *endo* (*i.e.* tangential to the surface of the polyhedron as part of a BH_2 group). The number of electrons available for skeletal bonding is 3 electrons from each CH, 2 electrons from each BH, 1 electron from each bridging or *endo* H and *c* electrons from the anionic charge. Hence the total number of skeletal bonding electron pairs = $\frac{1}{2}(3a + 2m + b + c) = n + \frac{1}{2}(a + b + c)$, where *n* is the number of occupied vertices of the polyhedron, *i.e.* $n = a + m$. In the case of boranes, *a* is obviously equal to zero when calculating the number of skeletal bonding electron pairs.

Having determined the total number of skeletal bonding electron pairs it is possible to decided which structure the carborane will assume. *Closo*-structures have $n + 1$ pairs of skeletal bonding electrons *i.e.* $(a + b + c) = 2$, *nido*-structures have $n + 2$ pairs of skeletal

bonding electrons *i.e.* $(a + b + c) = 4$, and *arachno*-structures have $n + 3$ pairs of skeletal bonding electrons *i.e.* $(a + b + c) = 6$, for examples of each type of structure see figure 3.1. To confirm that the structures shown have the correct number of skeletal bonding electron pairs the calculations are shown in table 3.1.

Carborane	n	Number of Skeletal Bonding Electron Pairs	Structure Inferred
$C_2B_{10}H_{12}$	12	$12 + ½ (2) = 13$	$(n + 1) \Rightarrow$ *Closo*
$C_2B_9H_{12}^-$	11	$11 + ½ (2 + 1 + 1) = 13$	$(n + 2) \Rightarrow$ *Nido*
$C_2B_8H_{12}^{2-}$	10	$10 + ½ (2 + 2 + 2) = 13$	$(n + 3) \Rightarrow$ *Arachno*

Table 3.1.

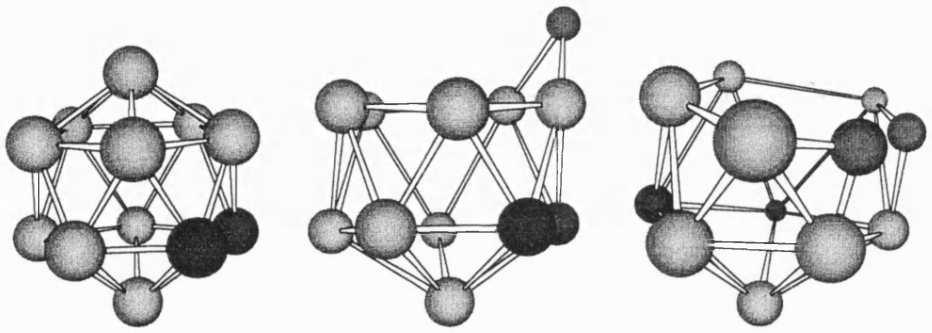

Figure 3.1.

Of main interest to us were the icosahedral carboranes and from this point on when the term carborane is used it means that an icosahedral carborane is being referred to. It is important to clarify the nomenclature used in describing these systems [69]. Numbering begins with the apex atom of lowest co-ordination and successive rings or belts of polyhedral vertex atoms are numbered in a clockwise direction with the carbon atoms being given the lowest possible number within these rules, Figure 3.2.

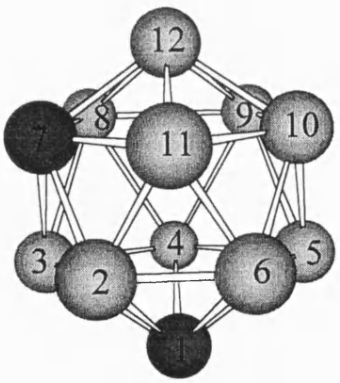

● =BH ● =CH

meta-carborane, 1,7-$C_2B_{10}H_{12}$

Figure 3.2.

The *ortho*-carborane **40** is best prepared from the reaction of ethyne with decaborane in the presence of a Lewis base, preferably Et_2S, Scheme 3.1.

$$\textit{nido}\text{-}B_{10}H_{14} + 2\ SEt_2 \longrightarrow B_{10}H_{12}(SEt)_2 + H_2$$

$$B_{10}H_{12}(SEt)_2 + HC{\equiv}CH \longrightarrow \underset{\mathbf{40}}{\textit{closo}\text{-}1,2\text{-}C_2B_{10}H_{12}} + 2\ SEt_2 + H_2$$

Scheme 3.1.

It is then reasonably easy to convert the 1,2-isomer **40** into the 1,7-isomer **41** in 90% yield by heating in the gas phase at 470°C for several hours. The 1,12-isomer **42** can then be prepared by heating the 1,7-isomer for a few seconds at 700°C, the yield for this transformation being only 20%.

It is apparent from the above transformations that these carboranes are stable to high temperatures, they are also unreactive with most common reagents. They can however, be specifically degraded to *nido*-carborane anions by the reaction of strong bases in the presence of protonic solvents [70], Scheme 3.2.

$$\underset{\mathbf{40}}{1,2\text{-}C_2B_{10}H_{12}} + EtO^- + 2\ EtOH \xrightarrow{85^oC} \underset{\mathbf{43}}{7,8\text{-}C_2B_9H_{12}^-} + B(OEt)_3 + H_2$$

$$\underset{\mathbf{41}}{1,7\text{-}C_2B_{10}H_{12}} + EtO^- + 2\ EtOH \longrightarrow \underset{\mathbf{44}}{7,9\text{-}C_2B_9H_{12}^-} + B(OEt)_3 + H_2$$

Scheme 3.2.

The BH vertex that is removed is the one adjacent to the two CH vertices, since the carbon atoms tend to remove electronic charge preferentially from the contiguous boron atoms, the

reaction can be described as nucleophilic attack on the most electron deficient boron atom in the cluster, Scheme 3.3.

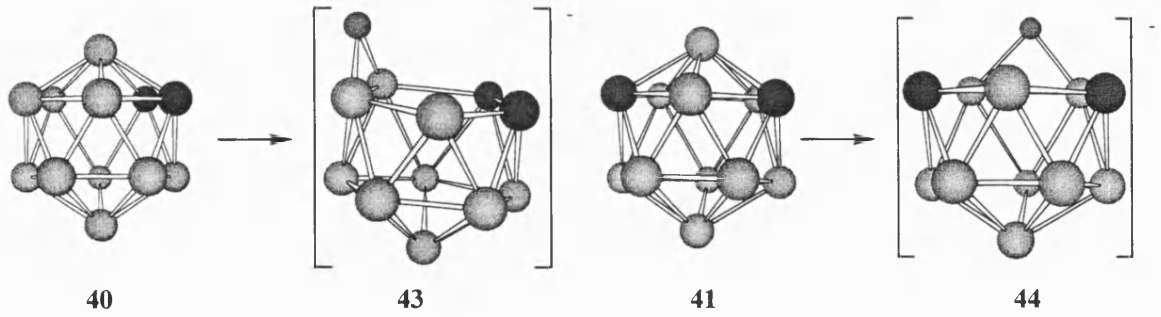

40 **43** **41** **44**

=BH ● =CH ● = H

Scheme 3.3.

Deprotonation of the *nido*-anions **43** and **44** by sodium hydride removes the bridging proton to produce the dianions $7,8\text{-}C_2B_9H_{11}^{2-}$ **45** and $7,9\text{-}C_2B_9H_{11}^{2-}$ **46** [71]. It was the recognition that the open pentagonal faces of these dianions were structurally and electronically equivalent to the cyclopentadienyl ligand that lead to the discovery of metallocarboranes. This isolability with cyclopentadienyl can be illustrated if we consider the orbitals available for the bonding of $7,8\text{-}C_2B_9H_{11}^{2-}$ **45** and $7,9\text{-}C_2B_9H_{11}^{2-}$ **46** and $\eta^5\text{-}C_5H_5$, Figure 3.3. Further studies have suggested that due to the bulkiness of the *nido*-carborane anion a better comparison would be with pentamethylcyclopentadienyl [72].

45 **C_5H_5** **46**

=BH ● =CH

Figure 3.3.

3.2 Metallocarboranes Synthesis.

There are a number of synthetic routes to metallocarboranes [73] but the route of major importance utilises the *nido*-carborane anion described above. The first reaction of this type was the reaction of $7,8\text{-}C_2B_9H_{11}^{2-}$ **45** with iron(II) chloride yielding the metallacarborane in a manner analogous to the synthesis of ferrocene [74], Scheme 3.4.

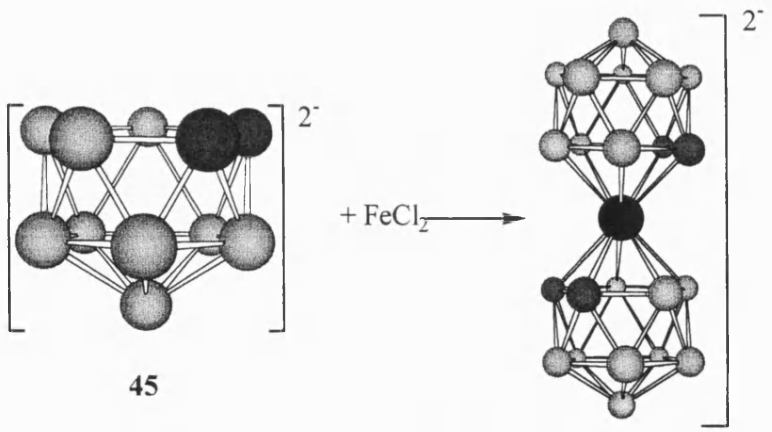

Scheme 3.4.

It is also possible to produce mono-substituted systems, for example the photolysis of molybdenum hexacarbonyl with **45** produced the complex [*closo*-3,3,3-$(CO)_3$-3,1,2,-$MoC_2B_9H_{11}]^{2-}$ [74] which upon reaction with methyl iodide formed the complex [*closo*-3-(CH_3)-3,3,3-(CO)-3,2,1-$MoC_2B_9H_{11}]^-$, both of these compounds can be isolated as the tetraethylammonium salt, Scheme 3.5.

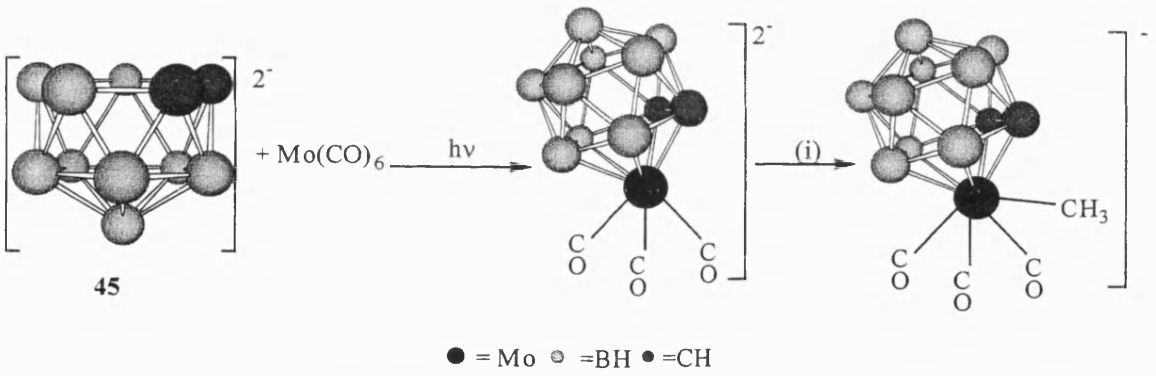

Scheme 3.5 (i) MeI, NEt_4 counter ion throughout.

The chemistry of the molybdenum and tungsten half-sandwich compounds has been extended recently with the formation of an allylic system which upon protonation will allow access to a number of novel carborane complexes. The allyl complex can be produced by two methods [75].

Firstly the reaction of $[Mo(CO)_3(NCMe)_3]$ and Tl[*closo*-3,1,2-$TlC_2B_9H_9Me_2$] followed by addition of allyl bromide and $[N(PPh_3)_2]Cl$ produces the salt $[N(PPh_3)_2]$[*closo*-1,2-$(CH_3)_2$-3,3-$(CO)_2$-3-(η^3-C_3H_5)-3,1,2-$MoC_2B_9H_9$] **47** in approximately 40% yield, Scheme 3.6. The yields are poor due to the difficulties experienced in purification associated with the formation of $[N(PPh_3)_2]$[7,8-$C_2B_9H_9Me_2$] as a side product.

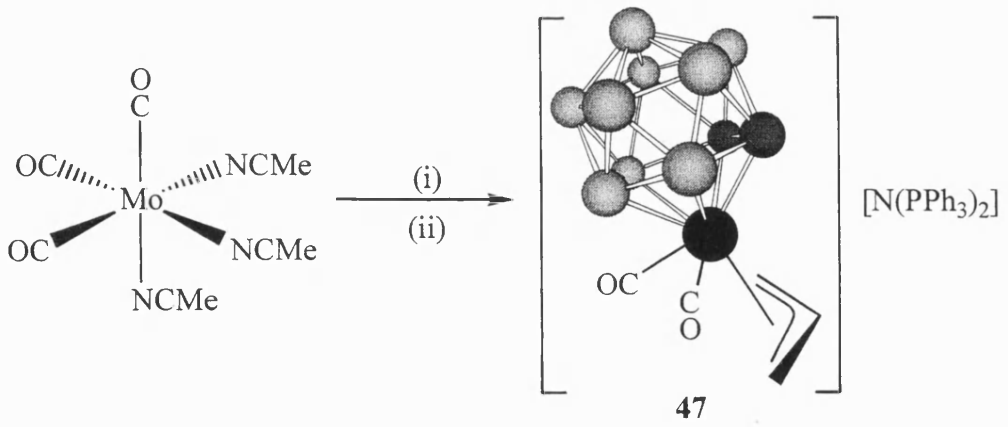

47

● = Mo ◎ =BH ● =CMe

Scheme 3.6 (i) Tl[*closo*-3,1,2-$TlC_2B_9H_9Me_2$], (ii) C_3H_5Br, $[N(PPh_3)_2]Cl$.

The poor yields above led to the development of an alternative, high yield synthesis involving the reaction between the allylmetal complexes $[MBr(CO)_2(NCMe)_2(\eta^3\text{-}C_3H_5)]$ (M = Mo or W) and $Na_2[C_2B_9H_9Me_2]$ followed by the addition of $[N(PPh_3)_2]Cl$. Similar methodology, employing $Na_2[C_2B_9H_{11}]$, $[MoBr(CO)_2(NCMe)_2(\eta^3\text{-}C_3H_5)]$ and $[NEt_4]Cl$ afforded $[NEt_4][closo\text{-}3,3\text{-}(CO)_2\text{-}3\text{-}(\eta^3\text{-}C_3H_5)\text{-}3,1,2\text{-}MoC_2B_9H_{11}]$ **48** in 75% yield, Scheme 3.7.

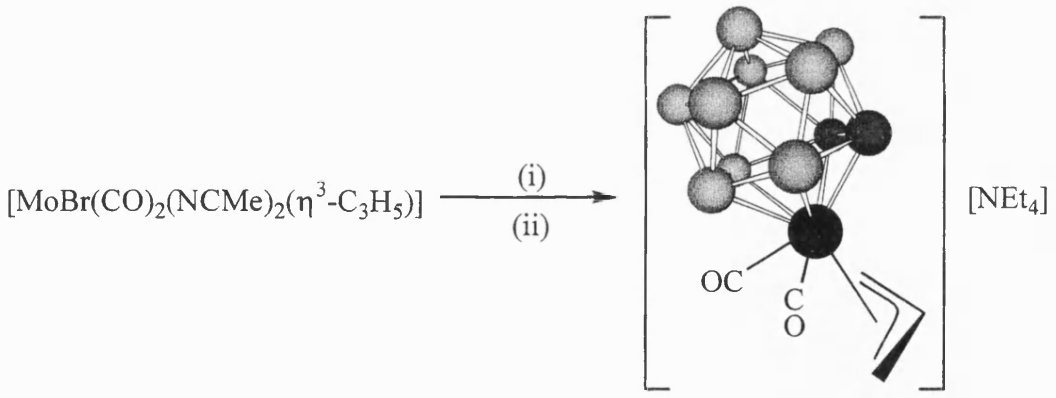

48

● = Mo ◎ =BH ● =CH

Scheme 3.7 (i) $Na_2[C_2B_9H_{11}]$, (ii) $[NEt_4]Cl$.

The formation of the allylmetal complex opened a synthetic route into a number of varied complexes [75,76]. After protonation of the allyl group with $HBF_4.Et_2O$ the introduction of phosphines, alkynes and buta-1,3-dienes is possible thus producing the range of complexes as shown in Scheme 3.8.

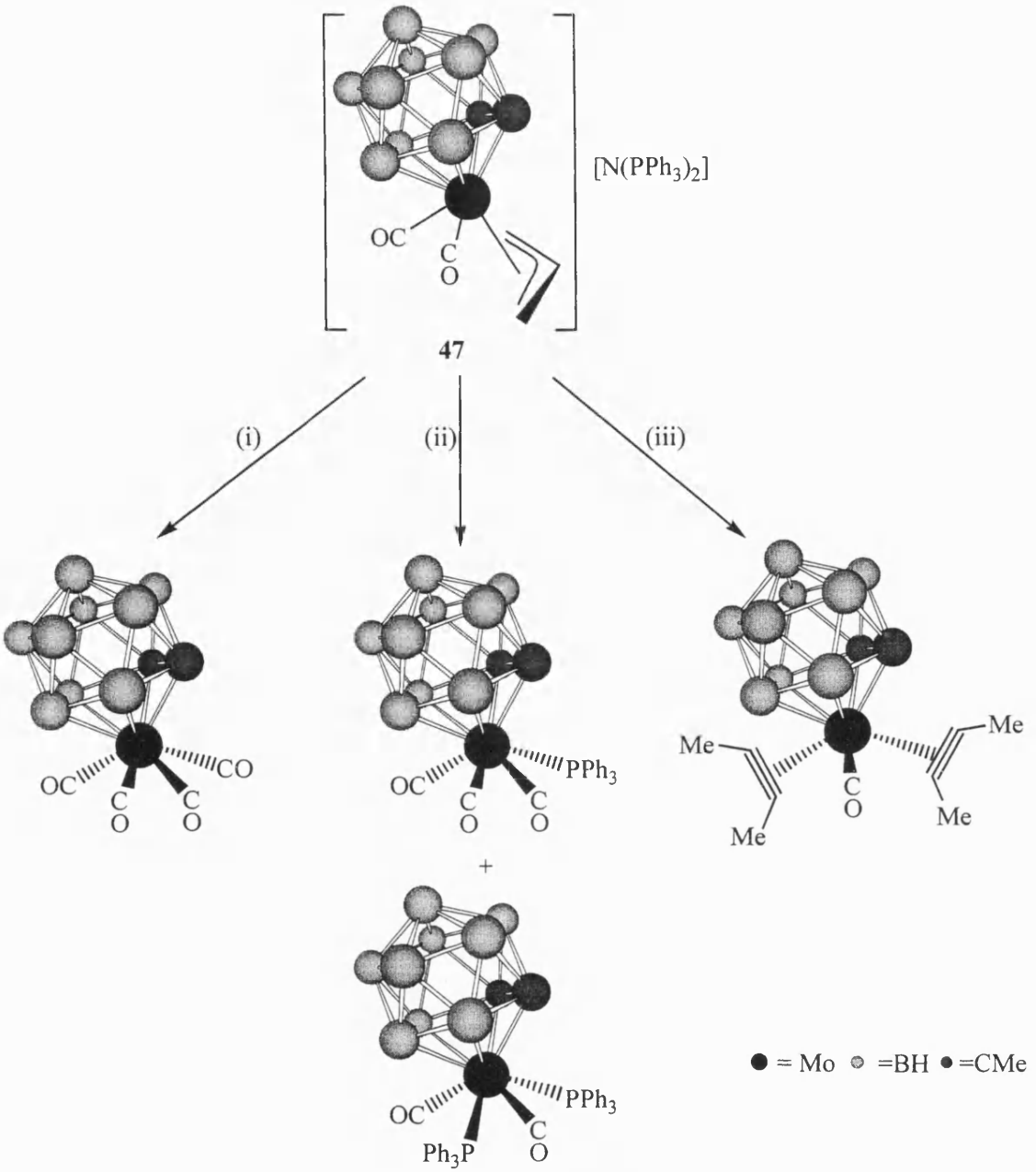

Scheme 3.8 (i) $HBF_4.Et_2O$ in CO saturated CH_2Cl_2, (ii) $HBF_4.Et_2O$, PPh_3, (iii) $HBF_4.Et_2O$, MeC≡CMe.

It is interesting to note that the reaction of the protonated allyl complex with triphenylphosphine produces a mixture of products, that are chromatographically inseparable. However, crystallisation yielded pure [*closo*-1,2-$(CH_3)_2$-3,3-$(CO)_2$-3,3-$(PPh_3)_2$-3,1,2-$MoC_2B_9H_9$]. In contrast, the analogous tungsten reaction affords the complex [*closo*-1,2-$(CH_3)_2$-3,3-$(CO)_2$-3,3-$(PPh_3)_2$-3,1,2-$WC_2B_9H_9$] as the only product.

The protonation of $[N(PPh_3)_2]$[*closo*-1,2-$(CH_3)_2$-3,3-$(CO)_2$-3-(η^3-C_3H_5)-3,1,2-$MoC_2B_9H_9$] **47** in the presence of diphenylacetylene [76], does not produce the expected bis-alkyne complex, and no stable complex could be isolated from the reaction mixture. However, if this mixture was treated with triphenylphosphine then a green complex was isolated in high

yield. This complex is [*closo*-1,2-(CH_3)-3-(CO)-3-(PPh_3)-3-(η^2-PhC≡CPh)-3,1,2-$MoC_2B_9H_9$], and if this compound is left in dichloromethane solution for 24 hours rearrangement occurs to give a mixture of the previously prepared species [*closo*-1,2-$(CH_3)_2$-3,3,3-$(CO)_3$-3-(PPh_3)-3,1,2-$MoC_2B_9H_9$] and the new compound [*closo*-1,2-$(CH)_3$-3,3-$(CO)_2$-3-(PPh_3)-8,3-{σ:η^2-C(Ph)=C(H)Ph}-3,1,2-$MoC_2B_9H_9$], Scheme 3.9.

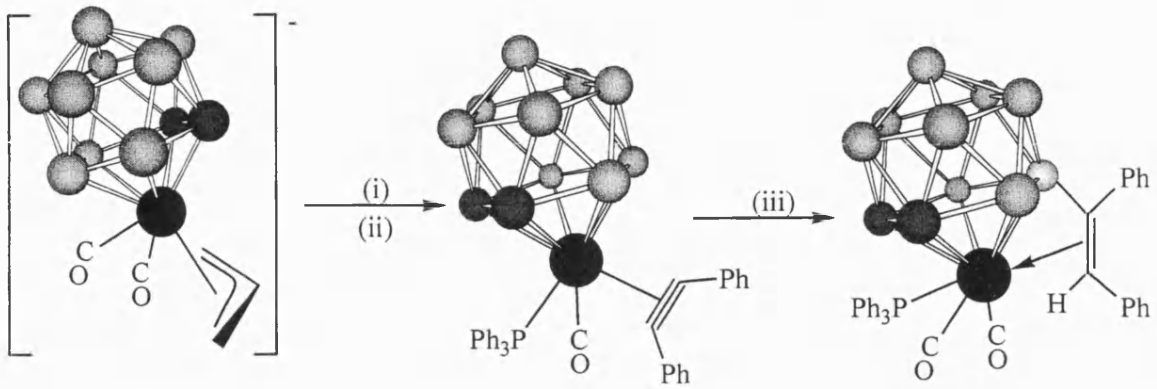

47

● = Mo ◎ =BH ● =CMe ○ = B

Scheme 3.9 (i) $HBF_4.Et_2O$, PhC≡CPh, (ii) PPh_3, (iii) stand in CH_2Cl_2 for 24h.

Though the new compound could not be isolated pure, NMR implies that the ligated PhC≡CPh molecule in the precursor has inserted into a cage B-H vertex. A second example of this type of insertion reaction was observed when the protonation of **48** in the presence of $Me_3SiC{\equiv}CSiMe_3$ was found to yield the complex [*closo*-3,3,3-$(CO)_3$-8,3-{σ:η^2-C(H)=C(H)$SiMe_3$}-3,1,2,-$MoC_2B_9H_{10}$]. The structure of this complex was confirmed by single crystal x-ray diffraction study, the results of which are shown in Figure 3.4.

Recently further examples of this type of insertion have been observed [77] in the chemistry of the complex [*closo*-3-(CO)-3,3-(η^2-PhC≡CPh)$_2$-3,1,2-$MoC_2B_9H_{11}$] **49**. This complex is formed by the protonation of [NEt_4][*closo*-3,3-$(CO)_2$-3-(η^3-C_3H_5)-3,1,2-$MoC_2B_9H_{11}$] **48** in the presence of diphenylacetylene. If **49** is heated in toluene in the presence of trimethyl phosphite an alkyne insertion is observed to give the minor product [*closo*-3,3-{$P(OMe)_3$}$_2$-3-(η^2-PhC≡CPh)-8-{σ-trans-C(Ph)=C(H)Ph}-3,1,2-$MoC_2B_9H_{11}$] **50**. The major product is [*closo*-3,3-{$P(OMe)_3$}$_2$-3-(η^2-PhC≡CPh)-3,1,2-$MoC_2B_9H_{11}$] **51**.

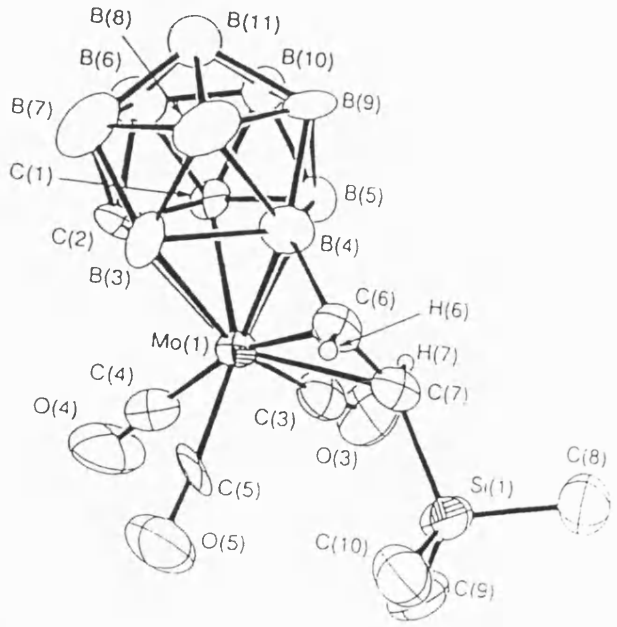

Figure 3.4 Molecular Structure of [*closo*-3,3,3-$(CO)_3$-8,3-{σ:η^2-C(H)=C(H)$SiMe_3$}-3,1,2,-$MoC_2B_9H_{10}$].

An increased yield of **50** can be achieved if complex **51** is heated to 100°C in toluene in the presence of diphenylacetylene and from the products of this reaction a single crystal was obtained which after a diffraction study confirmed the structure of **50**. Refluxing **49** in acetonitrile with excess diphenylacetylene also leads to an insertion reaction and the formation of [*closo*-3-(NCMe)-3,3-(η^2-PhC≡CPh)$_2$-8-{σ-trans-C(Ph)=C(H)Ph}-3,1,2-$MoC_2B_9H_{11}$] **52**, Scheme 3.10, and the structure of **52** was again confirmed by a single crystal X-ray diffraction study.

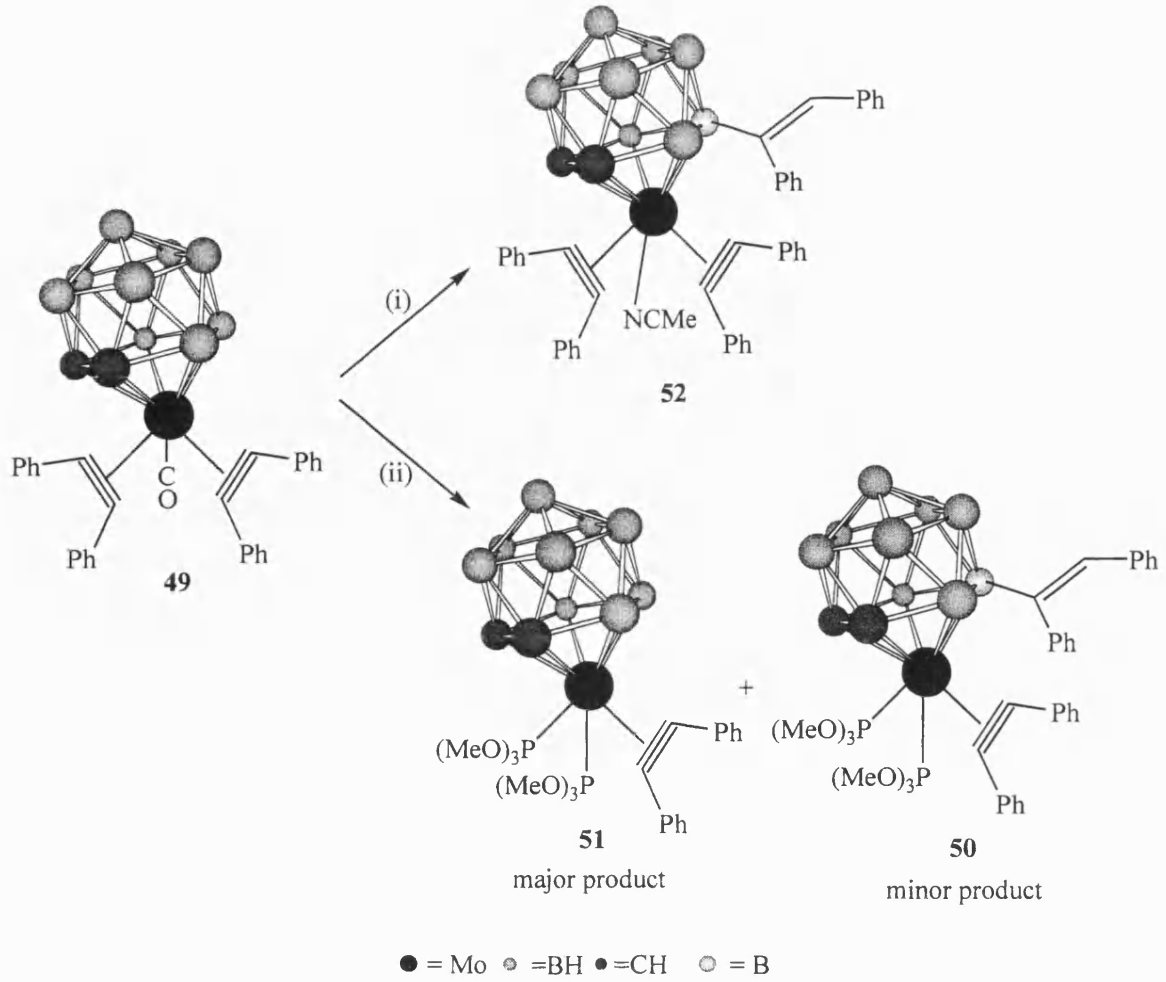

Scheme 3.10 (i) PhC≡CPh, refluxing NCMe, (ii) $P(OMe)_3$, heated in toluene.

3.3 Cycloheptatrienyl Chemistry.

The use of cycloheptatrienyl as a ligand in organometallic chemistry was first addressed forty years ago [78], when the complex $[Mo(CO)_3(\eta^7\text{-}C_7H_7)][BF_4]$ **53** was synthesised. The production of **53** involved the preparation of $[Mo(CO)_3(\eta^6\text{-}C_7H_8)]$ **54** from molybdenum hexacarbonyl and cycloheptatriene in refluxing *n*-octane [79], followed by treatment with triphenylmethyl tetrafluoroborate, Scheme 3.11.

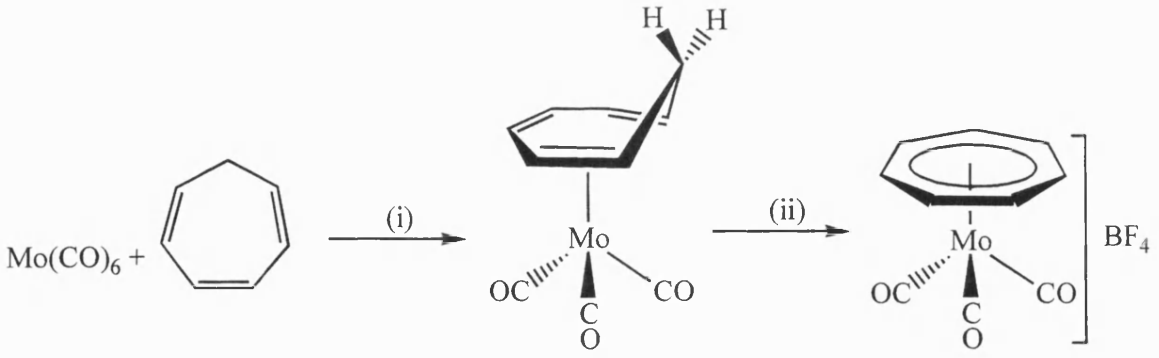

54 **53**

Scheme 3.11 (i) reflux in *n*-octane, (ii) $[Ph_3C][BF_4]$, CH_2Cl_2.

Having produced the cycloheptatrienyl species **53**, a further reaction with sodium iodide in acetone converts **53** into $[MoI(CO)_2(\eta^7\text{-}C_7H_7)]$ **55**, [79], a colour change was observed from tan to deep green with vigorous gas evolution producing a 75% yield of **55**, Scheme 3.12.

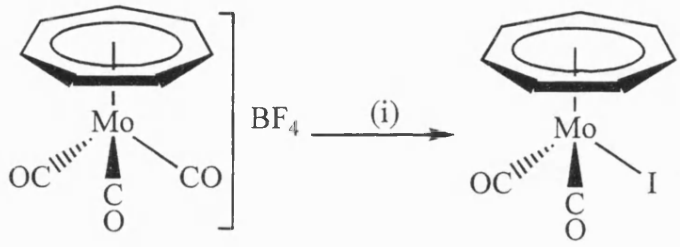

53 **55**

Scheme 3.12 (i) NaI.

Further reaction of **53** includes the formation of the mixed sandwich complex $[Mo(\eta^6\text{-}C_6H_5CH_3)(\eta^7\text{-}C_7H_7)][BF_4]$ **56** [80], Scheme 3.13, *via* reflux in toluene. Complex **56** is a widely used precursor for the synthesis of other $Mo(\eta^7\text{-}C_7H_7)$ derivatives, Scheme 3.14. Its synthetic versatility is due to the lability of the arene group, that will undergo displacement reactions with a number of potential ligands.

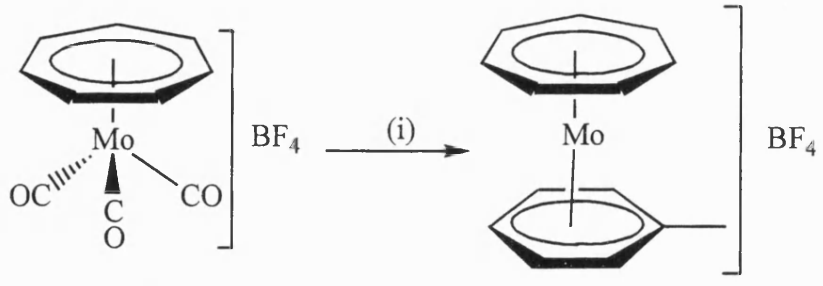

53 **56**

Scheme 3.13 (i) toluene, reflux.

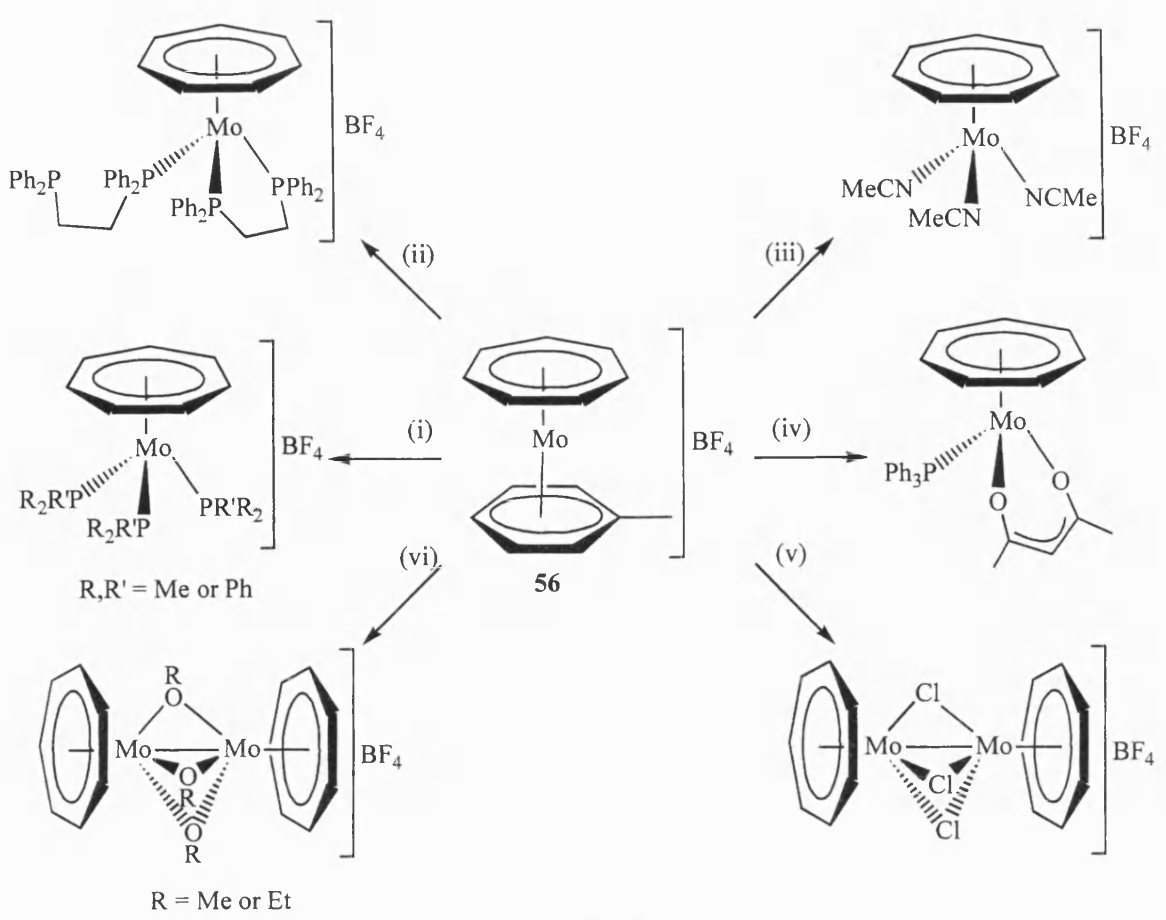

Scheme 3.14 (i) PR_2R', R,R'=Me or Ph, (ii) dppe, (iii) MeCN, (iv) Na(acac), PPh_3, (v) HCl, HBF_4, (vi) ROH, R=Me or Et.

Reactions to produce a cyclopentadienyl/cycloheptatrienyl sandwich complex did not result in the expected product. The reaction of $[MoI(CO)_2(\eta^7\text{-}C_7H_7)]$ **55** with sodium cyclopentadienyl [81] produced $[Mo(CO)_2(\eta^3\text{-}C_7H_7)(\eta\text{-}C_5H_5)]$ **57**, Scheme 3.15.

Infra red spectra of **57** confirmed that a mixed sandwich complex was not the isolated product, because two peaks were visible at 1933cm^{-1} and 1893cm^{-1} indicative of metal carbonyl stretching modes. The proton NMR exhibited only two sharp resonances,

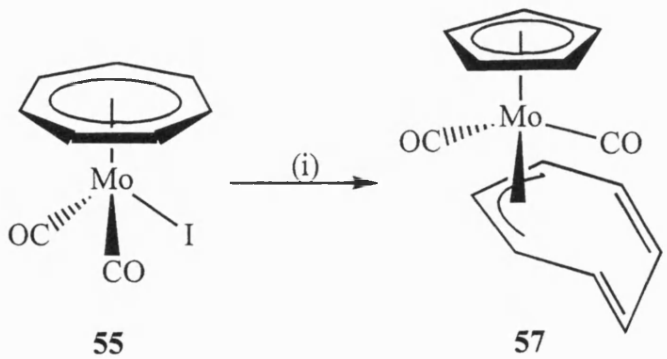

55 **57**

Scheme 3.15 (i) NaC_5H_5.

one at 5.07ppm due to the cyclopentadienyl ring and the other at 4.79ppm due to the cycloheptatrienyl ring; these signals being in the ratio of 5:7. If the structure of **57** was as suggested above *i.e.* $[Mo(CO)_2(\eta^3\text{-}C_7H_7)(\eta\text{-}C_5H_5)]$, then the only way the proton NMR described can be observed is if there is fluxional rotation of the C_7H_7 ring. Variable temperature NMR studies of **57** were carried out. At -40°C, a broadening of the signal assigned to the cycloheptatrienyl was observed [82]. It was assumed that this broadening was due to hindrance of the position equalising rotation of the allylic cycloheptatrienyl ring. Lowering of the temperature further to -110°C slows the rotation to the stage where peak positions and multiplicities for the four different proton environments can be observed [83], Figure 3.5.

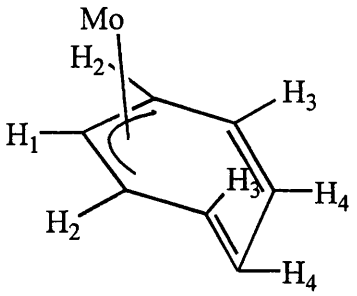

H_1 δ 2.1ppm, t, $J(H_1H_2)$ = 6.7Hz.

H_2 δ 4.27ppm, t, $J(H_2H_1)$ = 6.7Hz.

H_3 δ 6.00ppm, t.

H_4 δ 5.00ppm, d.

Figure 3.5.

These low temperature NMR studies support the postulation of an allylic bonded cycloheptatrienyl ring, which is hinged as shown in Figure 3.5.

3.4 Summary.

The chemistry reported above concerning the formation of metallocarboranes and the novel reactions they undergo, including the insertion of alkynes into cage B-H bonds, suggests, that preparation of a molybdocarborane bis alkyne complex could display unexpected reactivity. As proposed at the start of this chapter, the production of a carborane/cycloheptatriene molybdenum sandwich complex may provide a preparative synthesis of the desired bis alkyne species. Reviewing the known reactions of cycloheptatrienyl complexes yielded potential routes to the target complex that are explored in the next chapter.

CHAPTER 4

Novel Carborane Complexes and an η^2-(4e)-phosphaalkyne Complex

4 Discussion.

Two attempts were made to produce the target complex $[NEt_4][closo\text{-}3\text{-}(\eta^7\text{-}C_7H_7)\text{-}3,1,2\text{-}MoC_2B_9H_{11}]$. Firstly the reaction was studied between complex $[Mo(\eta^6\text{-}C_6H_5CH_3)(\eta^7\text{-}C_7H_7)][BF_4]$ **56** and $Tl[closo\text{-}3,1,2\text{-}TlC_2B_9H_{11}]$, under varying reaction conditions, no discernible products were observed after work up of these reactions. The second attempt to form the target compound was *via* the reaction between $[MoI(CO)_2(\eta^7\text{-}C_7H_7)]$ **55** and $Tl[closo\text{-}3,1,2\text{-}TlC_2B_9H_{11}]$, the results of this study are discussed below.

4.1 Reaction of $[MoI(CO)_2(\eta^7\text{-}C_7H_7)]$ 55 with $Tl[closo\text{-}3,1,2\text{-}TlC_2B_9H_{11}]$.

The addition of $Tl[closo\text{-}3,1,2\text{-}TlC_2B_9H_{11}]$ to a solution of **55** in thf with overnight stirring produced an observed change from dark green to orange with the formation of a precipitate. This suggested that reaction had taken place with the formation of thallium iodide. Counter cation exchange was carried out with the addition of a slight excess tetraethylammonium chloride. Chromatographic work up of this reaction followed by recrystallisation from dicholromethane:hexane produced an orange powder, **V**, in 85% yield.

If the reaction had occurred in a similar manner to that of the sodium cyclopentadienyl system described above then infra red spectroscopy should clearly show the presence of two metal carbonyl stretches. The infra red spectrum of **V** displays two metal carbonyl stretching modes at $1930cm^{-1}$ and $1853cm^{-1}$, also observed in this spectrum was a broad signal at $2509cm^{-1}$ which is assigned to the B-H stretches of the carborane cage. This suggests that the reaction between **55** and $Tl[closo\text{-}3,1,2\text{-}TlC_2B_9H_{11}]$ proceeds in a similar manner to the cyclopentadienyl reaction, producing $[NEt_4][closo\text{-}3,3\text{-}(CO)_2\text{-}3\text{-}(\eta^3\text{-}C_7H_7)\text{-}3,1,2\text{-}MoC_2B_9H_{11}]$ **V**, Scheme 4.1.

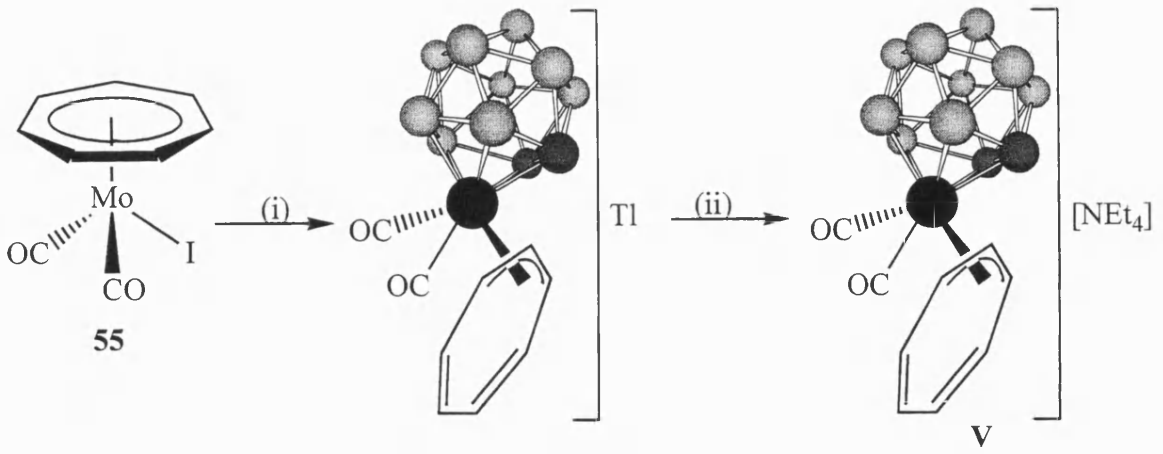

● = Mo ◎ =BH ● =CH

Scheme 4.1 (i) Tl[*closo*-3,1,2-$TlC_2B_9H_{11}$], (ii) $Et_4NCl.H_2O$.

The proton NMR of **V** at ambient temperature exhibits a singlet at δ 4.76ppm for the cycloheptatrienyl ligand indicating that if the ring is η^3-bonded then it is in a fluxional state allowing the protons on the ring to be chemically equivalent. The fluxional nature of the cycloheptatrienyl ring was proven by a low temperature proton NMR study where the resonances relating to the tetraethylammonium and the CHs of the cage remain in the same positions whilst the singlet of the cycloheptatrienyl ring collapses into a series of signals shown in Table 4.1. The cycloheptatrienyl hydrogens utilise the same labelling scheme as in Figure 3.5.

The proton at H_1 is a triplet as expected due to coupling to the two equivalent H_2 protons. Although in the NMR spectrum H_2 appears as a doublet of doublets where the centre signals overlap. H_4 shows couplings to both H_3 and H_4 to produce the observed doublet of doublets and H_3 is an unresolved multiplet due to coupling

to H_2 and to H_4 as well as secondary couplings to the other protons of the ring.

Signal (ppm)	Assignment
6.41	2H, unresolved multiplet, H_3.
5.24	2H, dd, $^3J(H_3H_4)$ = 8.8 Hz, $^3J(H_4H_4)$ = 3.4 Hz, H_4.
4.59	2H, dd, $^3J(H_2H_1)$ = 7.0 Hz, $^3J(H_2H_3)$ = 7.0 Hz, H_2.
3.20	8H, q, $^3J(HH)$ = 7.27 Hz, $(CH_3\mathit{CH_2})_4N$.
1.87	2H, s, br, cage CH.
1.68	1H, t, $^3J(H_1H_2)$ = 7.0 Hz, H_1.
1.33	12H, tt, $^3J(HH)$ = 7.27 Hz, $^4J(HN)$ = 2.01 Hz, $(\mathit{CH_3}CH_2)_4N$.

Table 4.1.

The low temperature NMR spectra support the assumption that **V** is $[NEt_4][closo\text{-}3,3\text{-}(CO)_2\text{-}3\text{-}(\eta^3\text{-}C_7H_7)\text{-}3,1,2\text{-}MoC_2B_9H_{11}]$ as it is possible to freeze out the position equalising rotation of the allylic cycloheptatrienyl ring. A possible mechanism for this rotation at ambient temperature has been suggested by Faller [84]. He studied the NMR of $[Mo(CO)_2(\eta^3\text{-}C_7H_7)(\eta\text{-}C_5H_5)]$ **57** at a range of temperatures between -118°C and -23°C and by noting the way the signals changed upon warming he concluded that the rotation of the cycloheptatrienyl ring occurs *via* a 1,2 shift. Faller also noted that if the infra red spectrum of **57** was run in cyclohexane four carbonyl stretching modes were observed, due to the exo and endo conformers of the cycloheptatrienyl ring, Figure 4.1.

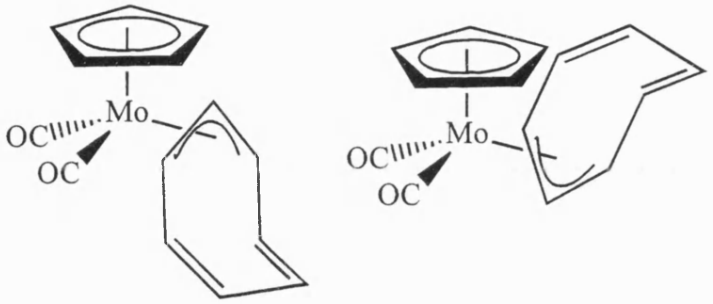

endo exo

Figure 4.1.

In the case of **V** only two signals are observed this suggests that the steric bulk of the metallocarborane cluster aligns the cycloheptatrienyl ring in the endo configuration.

The fluxional rotation of the C_7H_7 ring of **V** is confirmed by the carbon-13 NMR spectrum where the cycloheptatrienyl appears as a broad signal at δ 99.2 ppm. The other main features being the carbonyls at 240.2ppm, the tetraethylammonium cation at 52.8 and 7.6ppm and a further broad signal for the carborane carbons at 44.4ppm. The $^{11}B\{^1H\}$ NMR confirms the presence of 9 boron atoms in the cage and the molecular formula of **V** was confirmed by elemental analysis and with a parent ion in the FAB- mass spectrum with a mass of 376.

Having prepared $[NEt_4][closo\text{-}3,3\text{-}(CO)_2\text{-}3\text{-}(\eta^3\text{-}C_7H_7)\text{-}3,1,2\text{-}MoC_2B_9H_{11}]$ **V** an obvious comparison can be made between this complex and the allyl complexes $[N(PPh_3)_2][closo\text{-}1,2\text{-}(CH_3)_2\text{-}3,3\text{-}(CO)_2\text{-}3\text{-}(\eta^3\text{-}C_3H_5)\text{-}3,1,2\text{-}MoC_2B_9H_9]$ **47** and $[NEt_4][closo\text{-}3,3\text{-}(CO)_2\text{-}3\text{-}(\eta^3\text{-}C_3H_5)\text{-}3,1,2\text{-}MoC_2B_9H_{11}]$ **48** prepared by Stone [75], which were utilised as a route into further molybdocarborane chemistry. Protonation of **47** afforded a labile leaving group which was easily displaced by numerous substituents as described in Chapter 3. Would protonation of **V** offer the same synthetic utility?

4.2 Protonation of $[NEt_4][closo\text{-}3,3\text{-}(CO)_2\text{-}3\text{-}(\eta^3\text{-}C_7H_7)\text{-}3,1,2\text{-}MoC_2B_9H_{11}]$ V with $HBF_4.Et_2O$.

A dichloromethane solution of **V** was cooled to -78°C in a slush bath, to this was added $HBF_4.Et_2O$ and the mixture was allowed to warm to ambient temperature. A change was observed from orange to red and infra red spectroscopy showed a shift in the carbonyl stretching bands to 2017cm^{-1} and 1958cm^{-1}. Work up on a florisil column, followed by recrystallisation produced highly air sensitive orange microcrystals of **VI** in 83% yield.
The unstable nature of this complex unfortunately made it impossible to complete any NMR studies on it. The reaction that is assumed to take place is summarised in Scheme 4.2.

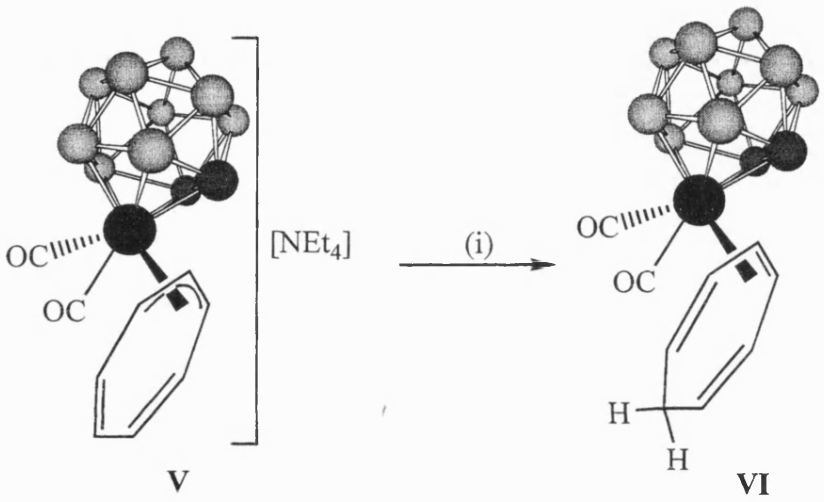

Scheme 4.2 (i) $HBF_4.Et_2O$, CH_2Cl_2, -78°C.

4.3 A New Preparative Route to $[closo\text{-}3\text{-}(CO)\text{-}3,3\text{-}(\eta^2\text{-}PhC{\equiv}CPh)_2\text{-}3,1,2\text{-}MoC_2B_9H_{11}]$ 49.

The protonation of **48** in the presence of diphenylacetylene leads to the formation of the complex $[closo\text{-}3\text{-}(CO)\text{-}3,3\text{-}(\eta^2\text{-}PhC{\equiv}CPh)_2\text{-}3,1,2\text{-}MoC_2B_9H_{11}]$ **49** [85]. It was suggested that if $[NEt_4][closo\text{-}3,3\text{-}(CO)_2\text{-}3\text{-}(\eta^3\text{-}C_7H_7)\text{-}3,1,2\text{-}MoC_2B_9H_{11}]$ **V** was protonated in the presence of diphenylacetylene and the product was **49** then the synthetic utility of **V** would be proven. After protonation, at -78°C, with $HBF_4.Et_2O$ diphenylacetylene was added to the solution and the mixture was allowed to stir overnight. A lightening was observed from orange to yellow and a yellow powder was isolated after work up. This powder

exhibited a similar infra-red spectrum to **49** with a peak corresponding to carbonyl stretching mode at 2062cm^{-1}, suggesting the formation of the same complex, Scheme 4.3.

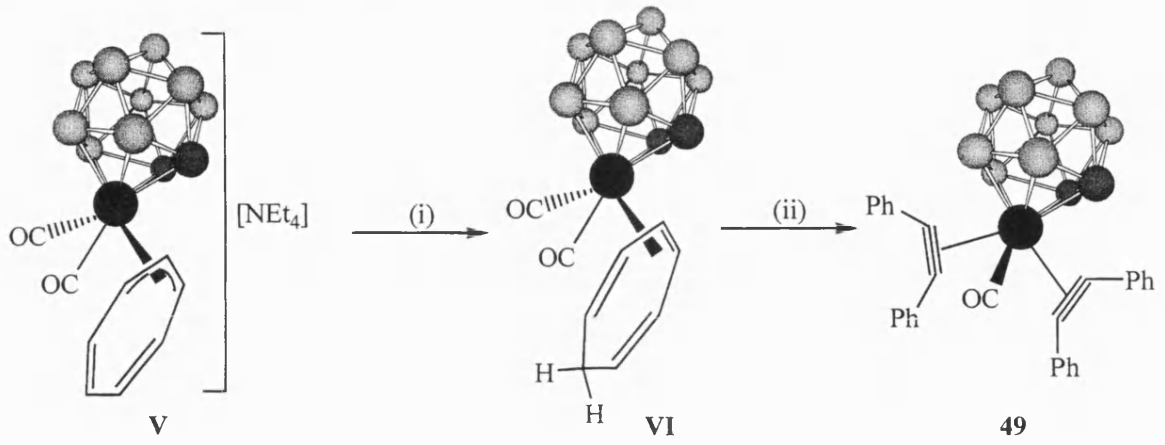

V **VI** **49**

● = Mo ● =BH ● =CH

Scheme 4.3 (i) $HBF_4.Et_2O$, CH_2Cl_2, -78°C, (ii) PhC≡CPh.

The new method of preparing **49** is confirmed when the proton, carbon and boron NMRs are compared and prove to be identical, Table 4.2. This experiment indicates that complex **V** does, upon protonation to complex **VI**, provide a route into the preparation of further molybdocarborane complexes. This is shown in the next series of reactions where after protonation a variety of potential ligands are introduced into the co-ordination sphere of the molybdenum.

49 prepared from **48**	**49** prepared from **V**
^{1}H NMR (CD_2Cl_2): δ 7.60-7.29, m, 20H, Ph; 3.31, s, br, 2H, cage CH.	^{1}H NMR (CD_2Cl_2): δ 7.62-7.31, m, 20H, Ph; 3.31, s, br, 2H, cage CH.
^{13}C{^{1}H} NMR (CD_2Cl_2): δ 222.1, *C*O; 168.8, PhC≡*C*Ph; 152.9, Ph*C*≡CPh; 134.9-127.4, Ph; 51.6, br, cage *C*H.	^{13}C{^{1}H} NMR (CD_2Cl_2): 222.1, *C*O; 168.8, PhC≡*C*Ph; 152.9, Ph*C*≡CPh; 134.9-127.4, Ph; 51.6, br, cage *C*H.
^{11}B{^{1}H) NMR (CD_2Cl_2): δ -3.5, 1B; -5.8, 1B; -6.9, 1B; -11.5, 2B; -16.2, 3B.	^{11}B{^{1}H) NMR (CD_2Cl_2): δ -3.5, 1B; -5.8, 1B; -6.9, 1B; -11.5, 2B; -16.2, 3B.

Table 4.2.

4.4 Reaction of [*closo*-3,3-$(CO)_2$-3-(η^4-C_7H_8)-3,1,2-$MoC_2B_9H_{11}$] VI with triphenylphosphine.

A dichloromethane solution of [*closo*-3,3-$(CO)_2$-3-(η^4-C_7H_8)-3,1,2-$MoC_2B_9H_{11}$] **VI** was prepared in situ from **V** and upon warming to near ambient temperature triphenylphosphine

was added. After overnight stirring a yellow precipitate was observed and a yellow solution was isolated after filtration. The product of this reaction after chromatographic work up was a yellow solid which exhibited two bands in the infra red spectrum, at 1950 and 1865cm^{-1}, indicative of two carbonyl stretching modes. The phosphorus NMR spectrum displayed a single peak at δ 63.32ppm, which is characteristic of triphenylphosphine ligands. The appearance of only a single peak in this spectrum indicates that the molecule exhibits a plane of symmetry which places both phosphines in similar chemical environments. The equivalence of the phosphines is confirmed by the appearance in the $^{13}C\{^{1}H\}$ NMR of a low field triplet for the carbonyl carbons, the coupling to phosphorus being 30Hz. This coupled with the elemental analysis suggests that the complex formed exhibits *trans* phosphines, which are made equivalent by rotation of the metallocarborane cluster, Scheme 4.4.

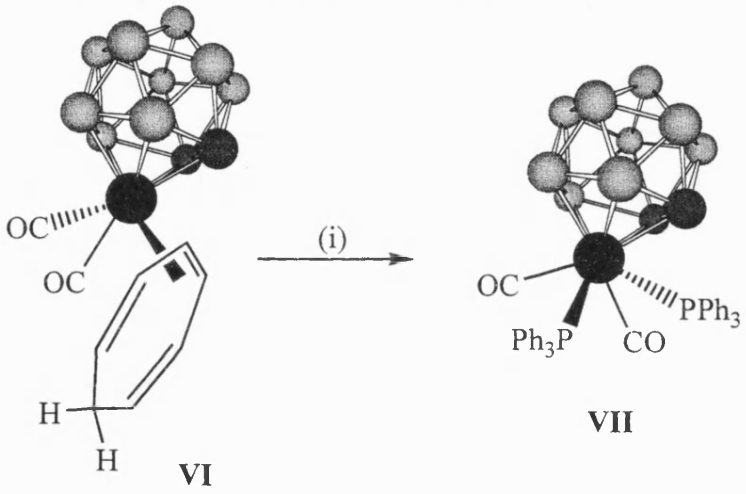

VI **VII**

● = Mo ● =BH ● =CH

Scheme 4.4 (i) PPh_3.

The stereochemical arrangement around the metal centre can be confirmed by the work of Stone and co-workers [86]. He reported that protonation of the species $[NEt_4][closo\text{-}1,2\text{-}(CH_3)_2\text{-}3,3\text{-}(CO)_2\text{-}3\text{-}(\equiv CC_6H_4CH_3\text{-}p)\text{-}3,1,2\text{-}WC_2B_9H_9]$ **58** in the presence of triphenylphosphine at low temperature, yielded the complex $[closo\text{-}1,2\text{-}(CH_3)_2\text{-}3,3\text{-}(CO)_2\text{-}3\text{-}(PPh_3)\text{-}7\text{-}(CH_2C_6H_4CH_3\text{-}p)\text{-}3,1,2\text{-}WC_2B_9H_9]$ **59**, Scheme 4.5. When they attempted to grow crystals of **59** for a single crystal X-ray diffraction study, decomposition of the solution occurred and the crystals obtained were of the complex $[closo\text{-}1,2\text{-}(CH_3)_2\text{-}3,3\text{-}(CO)_2\text{-}3,3\text{-}(PPh_3)_2\text{-}7\text{-}(CH_2C_6H_4CH_3\text{-}p)\text{-}3,1,2\text{-}WC_2B_9H_9]$ **60** Scheme 4.5. The molecular structure of **60** shows that the triphenylphosphines are trans to one another and the

orientation of the ($CH_2C_6H_4CH_3$-*p*) seems to have no steric involvement

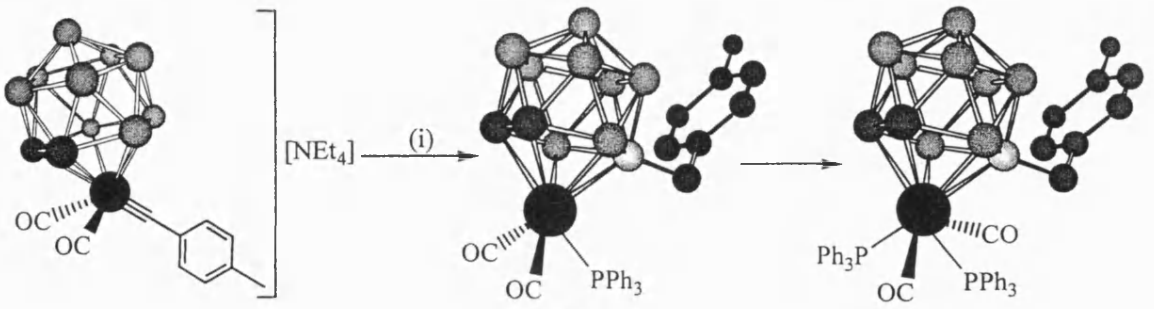

● = W ◎ = BH ● = CMe ○ = B

Scheme 4.5 (i) $HBF_4.Et_2O$.

in the arrangement of the ligands around the metal centre, Figure 4.2.

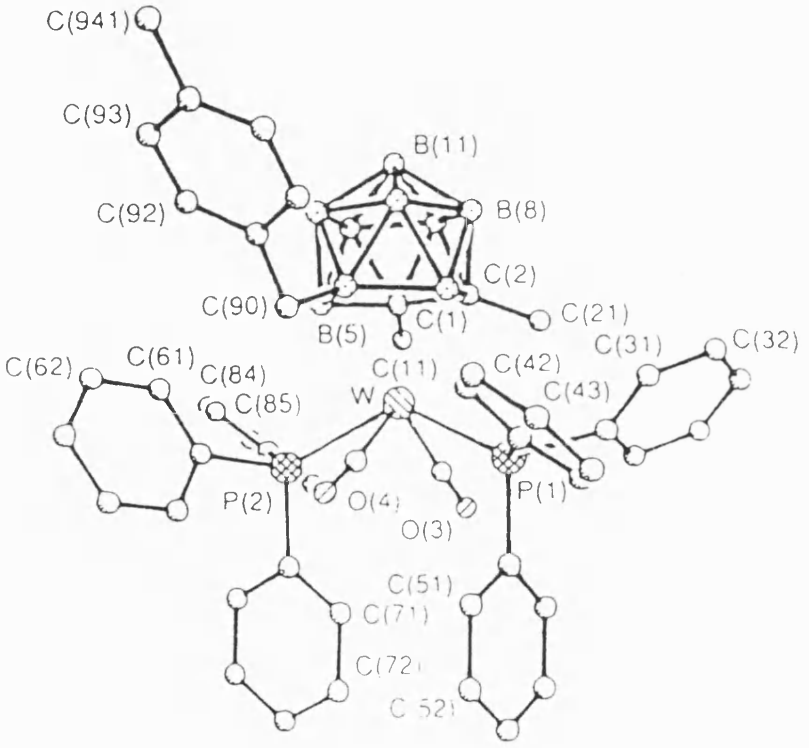

Molecular Structure of **60**

Figure 4.2.

4.5 Reaction of [*closo*-3,3-$(CO)_2$-3,3-$(PPh_3)_2$-3,1,2-$MoC_2B_9H_{11}$] VII with diphenylacetylene.

To a yellow solution of [*closo*-3,3-$(CO)_2$-3,3-$(PPh_3)_2$-3,1,2-$MoC_2B_9H_{11}$] **VII** was added diphenylacetylene and the mixture was allowed to stir. After 24 hours the solution became dark purple but infra red spectroscopy indicted that the reaction had not gone to completion. The reaction was completed after five and a half days stirring and

chromatographic work up yielded a green powder. The infra red spectrum indicated the presence of a single carbonyl ligand with a stretching frequency of 1968cm^{-1}. Elemental analysis confirmed the presence of triphenylphosphine, diphenylacetylene, carbonyl and molybdocarborane moieties, Scheme 4.6.

The formation of [*closo*-3-(CO)-3-(PPh_3)-3-(η^2-PhC≡CPh)-3,1,2-$MoC_2B_9H_{11}$] **VIII** was confirmed by the NMR spectra, with a single peak observed in the phosphorus NMR at 54.1ppm. The proton NMR exhibits the expected multiplet at δ 7.48 - 7.24ppm for the phenyl groups and two singlets for the cage CH's at δ 3.50ppm and 2.17ppm respectively. Two signals are observed because of the lack of a plane of symmetry through the molecule and so the resonances are for non-equivalent CH's.

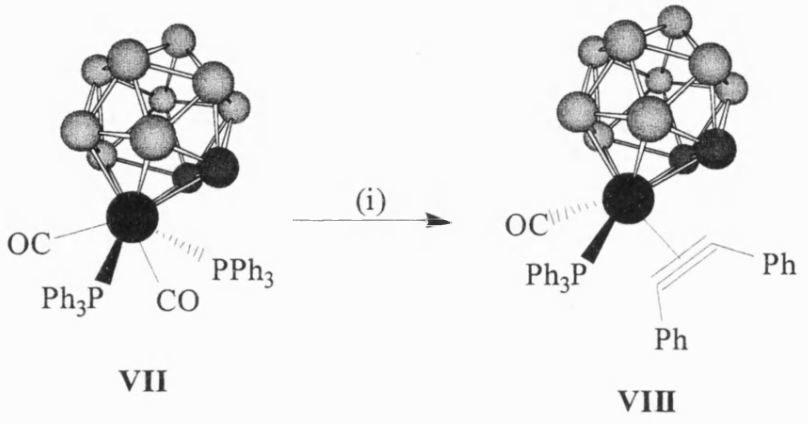

VII **VIII**

● = Mo ● =BH ●=CH

Scheme 4.6 (i) PhC≡CPh, -CO. -PPh_3.

This observation is reflected in the $^{13}C\{^1H\}$ NMR where the two carbons of the cage exhibit separate signals at 50.5 and 46.3ppm respectively. The other features of the carbon NMR spectrum are a low field doublet at 236.1ppm for the carbonyl carbon, a broad signal at 208.4ppm for the contact carbons of the alkyne, indicative of a four electron donor alkyne and a multiplet between 133.2 and 129.1ppm for the phenyl groups. The appearance of the separate signals for the metallocarborane cluster carbons indicates that in this case the barrier of rotation for the cluster must be fairly high. The difference between the barrier of rotation in complex **VIII** when compared to complex **VII** must be due to the different ligands at the metal. This implies that the increased electron donation to the metal of an alkyne compared to both a phosphine and a carbonyl alters the electronic configuration of the metallocarborane cluster making it require more energy to rotate.

4.6 Reaction of [*closo*-3,3-$(CO)_2$-3-(η^4-C_7H_8)-3,1,2-$MoC_2B_9H_{11}$] VI with 1,2-bis-(diphenylphosphino)ethane (dppe).

[*closo*-3,3-$(CO)_2$-3-(η^4-C_7H_8)-3,1,2-$MoC_2B_9H_{11}$] **VI** was prepared from **V** and upon warming to room temperature 1,2-bis-(diphenylphosphino)ethane (dppe) was added and the mixture was allowed to stir overnight. A reaction was deemed to have taken place as a change in the carbonyl stretching modes was observed in the infra red. The solution now exhibited carbonyl stretches at 1972 and 1904cm^{-1}. After work up a yellow microcrystalline solid was obtained in 64% yield. The infra red spectrum suggests the formation of [*closo*-3,3-$(CO)_2$-3-(η^2-$Ph_2PCH_2CH_2PPh_2$)-3,1,2-$MoC_2B_9H_{11}$] **IX**, Scheme 4.7, which is confirmed by the NMR data.

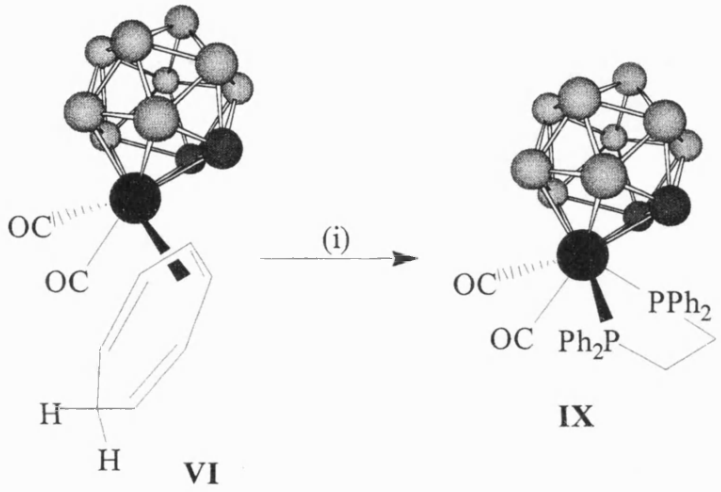

Scheme 4.7 (i) dppe.

The $^{31}P\{^1H\}$ NMR spectrum displays a single peak at 78.4ppm consistent with an η^2 bound dppe ligand where the two phosphorus atoms are chemically equivalent. The proton NMR shows three different sets of multiplets, the first at 7.58 to 7.31ppm due to the phenyl substituents of the dppe and the other two sets at 2.72 to 2.64ppm and 2.32 to 2.23ppm due to the couplings of the bridging ethane CH_2's. The carbons of the ethane bridge appear in the $^{13}C\{^1H\}$ NMR as a triplet at 27.9ppm where the coupling to phosphorus is 21.7Hz. This implies that there is a plane of symmetry through the molecule running perpendicularly to the C-C bond of the bridge, directly through its centre. If in the proton spectrum only one signal was observed for the CH_2's of the bridging ethane then there would be a second plane of symmetry running parallel to the C-C bond of the bridge. These multiplets can be assigned to the two hydrogens nearest the cage Ha and the two

hydrogens furthest away from the cage Hb, as shown in the fragment depicted in Figure 4.3.

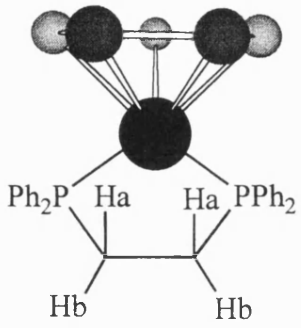

● = Mo ◎ =BH ● =CH

Figure 4.3.

It is the perpendicular plane of symmetry which brings the phosphorus's into equivalence resulting in the singlet observed in the ^{31}P NMR as reported above. The cage CH's appear as a singlet in both the proton and carbon NMRs at 1.80ppm and 47.3ppm respectively. This implies that the two carbons are equivalent, this equivalence could be achieved in two ways, either by rapid rotation of the cluster producing a time averaged picture of the two CH's, or the cluster is static with the plane of symmetry described above running between the two carbons, Figure 4.4. From all of the previous NMR evidence the latter seems to be the more probable reasoning.

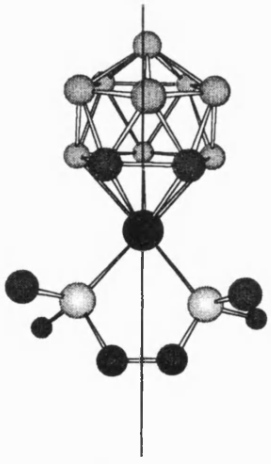

plane of symmetry

● = Mo ◎ =BH ● =CH ○ =P

Figure 4.4.

The only other feature of the carbon NMR is the multiplet assigned to the phenyl groups of the dppe, between 133.2 - 128.9ppm.

4.7 Reaction of [*closo*-3,3-$(CO)_2$-3-(η^4-C_7H_8)-3,1,2-$MoC_2B_9H_{11}$] VI with *o*-diphenylphosphinostyrene.

O-diphenylphosphinostyrene was added to a dichloromethane solution of freshly prepared [*closo*-3,3-$(CO)_2$-3-(η^4-C_7H_8)-3,1,2-$MoC_2B_9H_{11}$] **VI** and allowed to stir overnight. A lightening of the solution's initial orange colour was observed the following morning and infra red spectroscopy indicated a change in the carbonyl stretching frequencies to 2019 and 1956cm^{-1}. Chromatographic work up on alumina, eluting with dichloromethane hexane 2:1 produced a yellow band, which yielded a yellow powder **X** after recrystallisation. Elemental analysis confirmed the presence of a molybdocarborane unit, two carbonyls and a dpps ligand suggesting that the product formed was [*closo*-3,3-$(CO)_2$-3-(σ:η^2-$PPh_2C_6H_4CH_2$=CH-o)-3,1,2-$MoC_2B_9H_{11}$] **X**, Scheme 4.8.

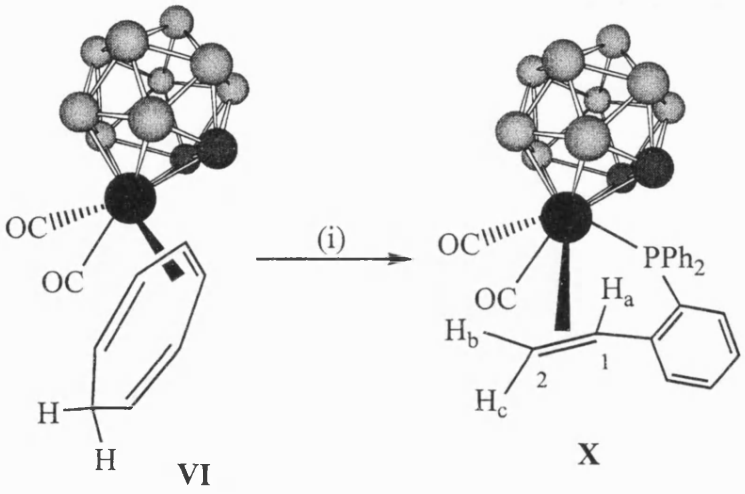

● = Mo ◎ =BH • =CH

Scheme 4.8 (i) dpps.

The molecule formed **X** displayed two separate signals in the proton NMR for the cage CH's at 3.26ppm and 3.11ppm indicating that there is no plane of symmetry through the molecule. The lack of a plane of symmetry is induced by the chelation of the styrene, which must occur, otherwise the complex would be an electron deficient 16e$^-$ species. The coupling patterns of the alkene functionality are a doublet of doublet of doublets at 5.29ppm for Ha with coupling to Hb, Hc and P, where the coupling constants are $^3J(H_aP)$ = 3.9Hz, $^3J(H_aH_b)$ = 13.3Hz, $^3J(H_aH_c)$ = 9.5Hz. Hc exhibits an apparent triplet, with a chemical shift of 3.69ppm, due to the overlap of a pair of doublets produced by the couplings to Ha and Hb where the coupling constant for both is 9.5Hz. The final hydrogen (Hb) on the styrene displays a doublet of doublets pattern at high field, 2.82ppm, which shows coupling to Ha and Hc with coupling constants of $^3J(H_bH_a)$ = 13.3Hz, $^2J(H_bH_c)$ =

9.52Hz. The remainder of the proton spectrum is the multiplet for the phenyl hydrogens between 7.69ppm and 7.07ppm. The lack of a plane of symmetry is reflected in the carbon-13 NMR where two individual doublets are observed for the carbonyl carbons with chemical shifts of 228.4ppm and 227.4ppm, with couplings to the phosphorus of 18Hz and 10Hz respectively. These couplings are indicative of one carbonyl being cis to the phosphorus, thus showing the smaller coupling, whilst the other is trans, exhibiting the larger coupling. The cage CH's are also observed as unique resonances due to the unsymmetrical nature of **X** at 50.0 and 49.7ppm The alkene functionality of the dpps displays two signals one a doublet at 152.9 for C_1 with a coupling to phosphorus of 26.5Hz and for C_2 a singlet at 82.4ppm. The phosphorus NMR is a single peak with a chemical shift of 49.8ppm, confirming the co-ordination of the phosphorus atom of the dpps.

4.8 Summary.

The attempt to produce cycloheptatrienyl/carborane mixed sandwich complex, as a precursor to a possible bis alkyne system, yielded an η^3-bonded cycloheptatrienyl molybdocarborane dicarbonyl species, which upon protonation produced a labile leaving group, in the form of cycloheptatriene, allowing a number of potential ligands to fill the vacant co-ordination site yielding complexes of the general formula [*closo*-3-$(CO)_x$-3-$(L)_y$-3,1,2-$MoC_2B_9H_{11}$], where if L = PhC≡CPh, y = 2, x = 1; if L = PPh_3, y = 2, x = 2; if L = $Ph_2PCH_2CH_2PPh_2$, y = 1, x = 2; if L = dpps, y = 1, x = 2. It was also possible to produce the complex [*closo*-3-(CO)-3-(η^2-PhC≡CPh)-3-(PPh_3)-3,1,2-$MoC_2B_9H_{11}$]

4.9 Production of A Four Electron Donor Phosphaalkyne Ligand.

4.9.1 Phosphaalkyne Chemistry.

The first report of the formation of a phosphaalkyne was published in 1950 [87] but it was not for another decade that the synthesis of phosphaalkynes could be achieved experimentally and a further twenty years before a kinetically stable phosphaalkyne was isolated. The major derivative produced in high yields today is the easily handled stable liquid *tert*-butylphosphaalkyne.

The reactions of *tert*-butylphosphaalkyne with transition metals give rise to two main types of complex, one where the phosphaalkyne is η^2-bonded to the metal centre the other where the phosphaalkyne acts as a bridging molecule, Figure 4.5.

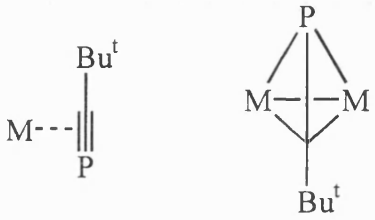

Figure 4.5.

In almost all cases reported to date the η^2-P≡CBu^t acts as only a two electron donor and attempts to react with it systems where alkynes produce four electron donor ligands have produced η^4-diphosphacyclobutadiene ligands. For example Green [88] and co-workers have reported the reaction between $[Mo(CO)_2(NCMe)_2(\eta^5\text{-}C_9H_7)][BF_4]$ and *tert*-butylphosphaalkyne to produce $[Mo(CO)_2(\eta^4\text{-}Bu^tCP)_2(\eta^5\text{-}C_9H_7)][BF_4]$ **61**, Scheme 4.9.

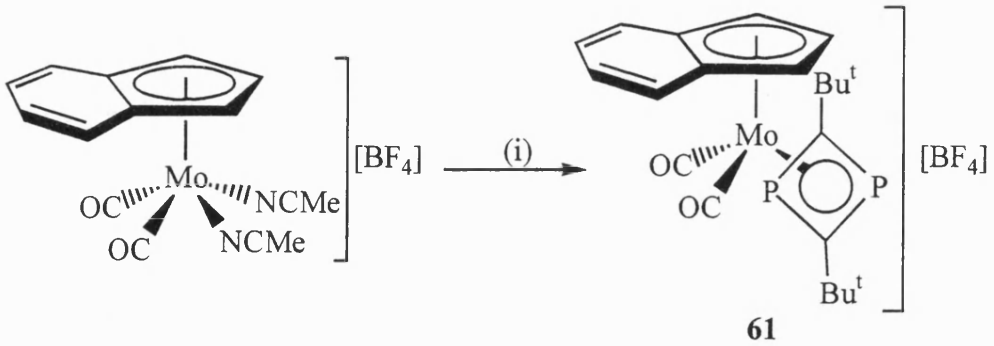

Scheme 4.9 (i) P≡CBu^t.

The formation of **61** was confirmed by a single crystal X-ray diffraction study, there was a slight difference between the NMR's of the solution and the molecular structure of the solid state. The molecular structure of **61** shows an interaction between one of the phosphorus

atoms and one of the fluorine atoms of the tetrafluoroborate anion, with a switch in the bonding mode of the diphosphacyclobutadiene from η^4 to η^3, Figure 4.6.

The synthesis of the first mononuclear η^2-(4e)-phosphaalkyne complex was reported by Green and Nixon [89], who having taken account of the formation of **61** in the reaction above considered the implications of reacting *tert*-butylphosphaalkyne with a molybdenum η^2-vinyl complex.

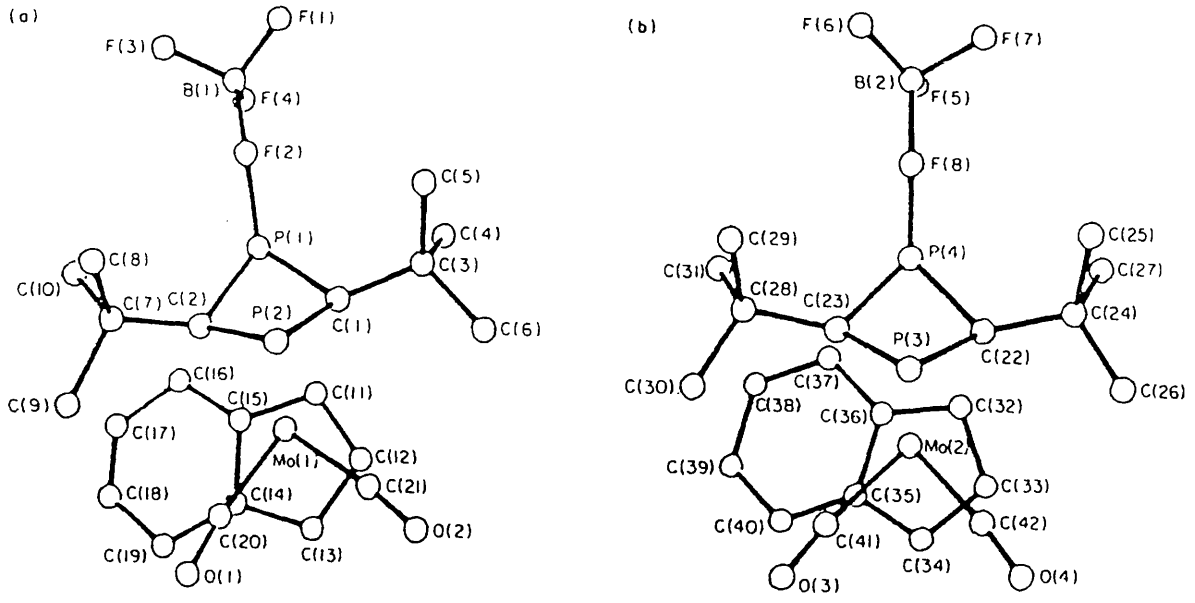

Molecular Structure of **61**.

Figure 4.6.

The η^2-vinyl complex utilised was $[Mo(=CPhC(H)Ph)\{\eta^2\text{-}(MeO)_2POBF_2OP(OMe)_2\}(\eta^5\text{-}C_5H_5)]$ **62** produced *via* the reaction of $[Mo\{P(OMe)_3\}_2(\eta^2\text{-}PhC{\equiv}CPh)(\eta^5\text{-}C_5H_5)][BF_4]$ with the di-Grignard $CH_2(MgI)_2$ followed by $K[BHBu^s_3]$, Scheme 4.10.

The reasoning for reacting **62** with *tert*-butylphosphaalkyne was that a previous experiment had shown that if **62** was protonated with $HBF_4.Et_2O$ in the presence of diphenylacetylene, a molecule of trans-stilbene was formed with the regeneration of **ab**. The suggestion was that, replacement of diphenylacetylene in the protonation step, with *tert*-butylphosphaalkyne could possibly provide access to an η^2-(4e)-phosphaalkyne complex.

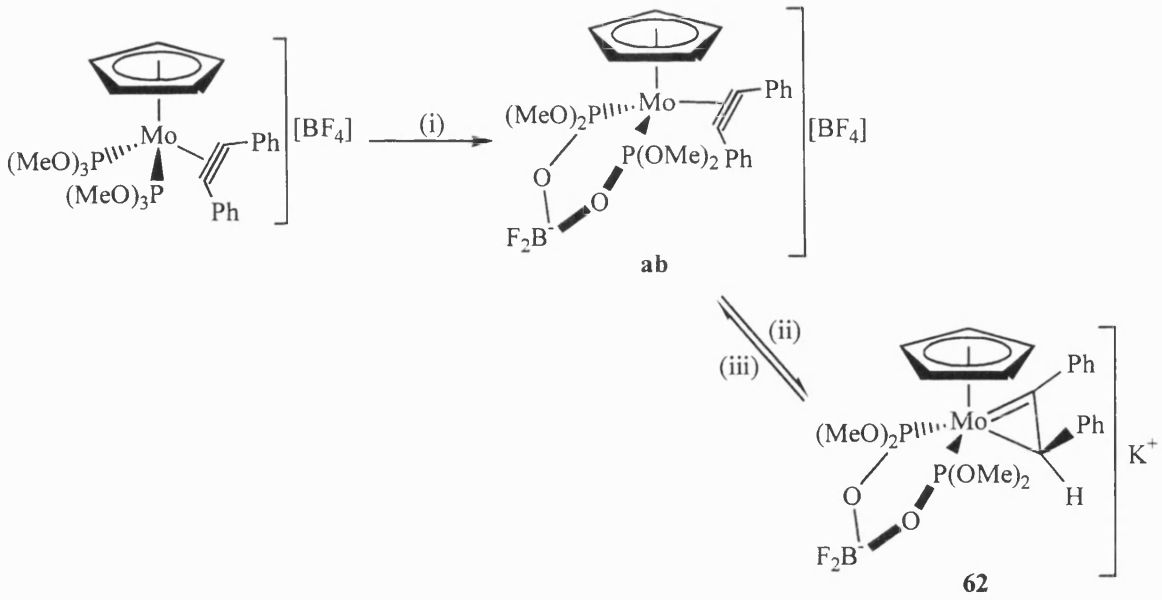

Scheme 4.10 (i) $CH_2(MgI)_2$, (ii) $K[BHBu^s_3]$ (iii) $HBF_4.Et_2O$, PhC≡CPh.

Protonation of **62** at -78°C with $HBF_4.Et_2O$ led to a colour change from green to yellow upon warming to ambient temperature. The yellow solution was then recooled to -78°C and a single equivalent of P≡CBu^t was added, with an immediate colour change to deep green. Workup by evaporation of the solvent followed by an extraction with toluene, followed by addition of hexane and cooling to -20°C afforded a low melting green complex **63** in 65% yield, Scheme 4.11.

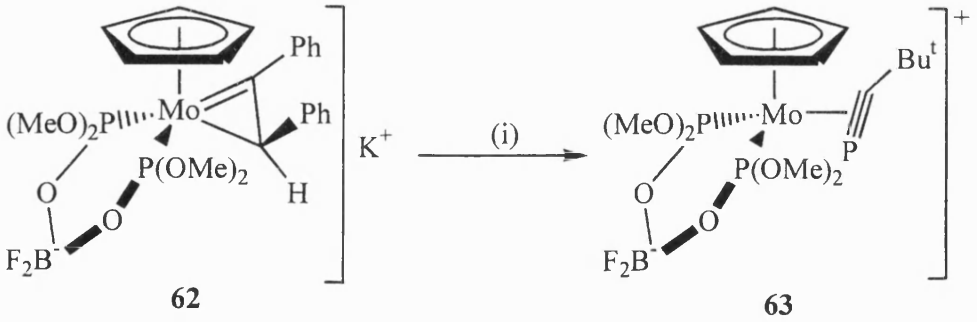

Scheme 4.11 (i) $HBF_4.Et_2O$, P≡CBu^t.

The proton NMR of **63** showed the expected features for a complex containing only one phosphaalkyne co-ordinated to a $[Mo\{\eta^2\text{-}(MeO)_2POBF_2OP(OMe)_2\}(\eta^5\text{-}C_5H_5)]$ fragment. The $^{31}P\{^1H\}$ NMR spectrum consisted of two singlet resonances, which showed no change over the temperature range 25°C to -80°C, one at 157.3ppm owing to the bidentate ligand $[(MeO)_2POBF_2OP(OMe)_2]^-$ and the other at 467.8ppm. This low field signal was assigned to the phosphorus of an η^2-(4e)-phosphaalkyne ligand, and is very deshielded compared with the resonances of the η^2-(2e)-bonded P≡CBu^t ligands present in the platinum complexes $[Pt(\eta^2\text{-}P{\equiv}CBu^t)(PPh_3)_2]$, 84.1ppm [90], $[Pt(\eta^2\text{-}P{\equiv}CBu^t)(dppe)]$, 87.7ppm [91] and $[Pt(\eta^2\text{-}P{\equiv}CBu^t)(\eta^2\text{-}Ph_2PCH_2CMe(CH_2PPh_2)CH_2PPh_2]$, 82.3ppm [92]. Support for the

assignment was found in a report that the $^{31}P\{^{1}H\}$ NMR spectrum of the aromatic phosphirenylium cation $[PhCC(Bu^t)P][B(OSO_2CF_3)_4]$ shows a resonance at 309.7ppm deshielded by 313ppm from $PhC{=}C(Bu^t)POSO_2CF_3$ [93]. Thus because of the isolobal relationship between $MoL_2(\eta^5\text{-}C_5H_5)$ and CR, Figure 4.7 a similar low field resonance would be expected in the $^{31}P\{^{1}H\}$ NMR spectrum of **63**.

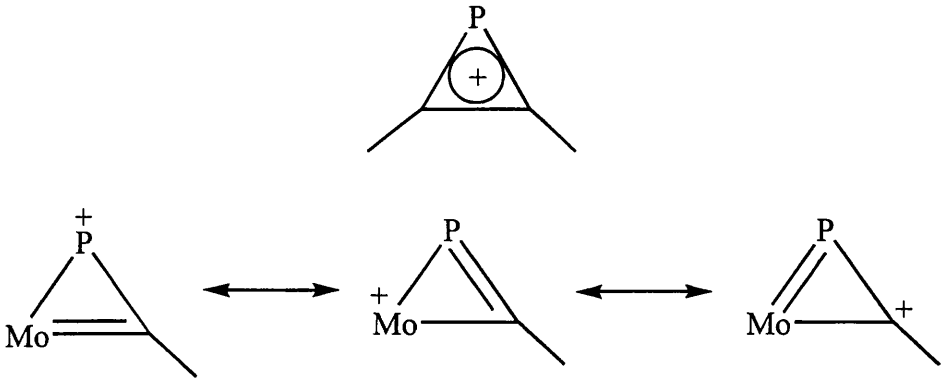

Figure 4.7.

Green then went on to propose that the signature of an η^2-(4e)-phosphaalkyne is a ^{31}P resonance in the region of 450ppm.

The carbon NMR of **63** also provided an insight into the bonding mode of the phosphaalkyne. It is well known that the ^{13}C chemical shift of an alkyne contact carbon can give an insight into the number of electrons being donated by that alkyne [11], and it was proposed that the same can be implied for a phosphaalkyne. The spectrum of **63** shows a low field doublet of triplets at 328.5ppm (J(PC) = 114.4Hz and J(PC) = 6.6Hz), which upon comparison to the ^{13}C shift for uncoordinated $P{\equiv}CBu^t$, a doublet at 184.3ppm (J(PC) = 38.6Hz) and for the η^2-(2e)-bonded $[Pt(\eta^2\text{-}P{\equiv}CBu^t)(PPh_3)_2]$, a multiplet at 242.0 - 239.5ppm [90] suggests that a correlation between number of electrons donated and ^{13}C NMR chemical shift does exist. However, it has been reported that the complex $[Ti(\eta^2\text{-}P{\equiv}CBu^t)(PMe_3)(\eta^5\text{-}C_5H_5)_2]$ [94] shows the phosphaalkyne contact carbon with a chemical shift of 298.6ppm and a phosphorus resonance of 122.7ppm, suggesting that although the ^{13}C shift observed for **63** is consistent for an η^2-(4e)-bonding mode, the distinction between η^2-(4e)- and η^2-(2e)-bonding for a phosphaalkyne as observed by contact carbons shifts, is less pronounced than with alkynes.

Treatment of **63** with a further equivalent of *tert*-butylphosphaalkyne leads to the formation of a diphosphacyclobutadiene ring as with the work of Green previously, Scheme 4.12.

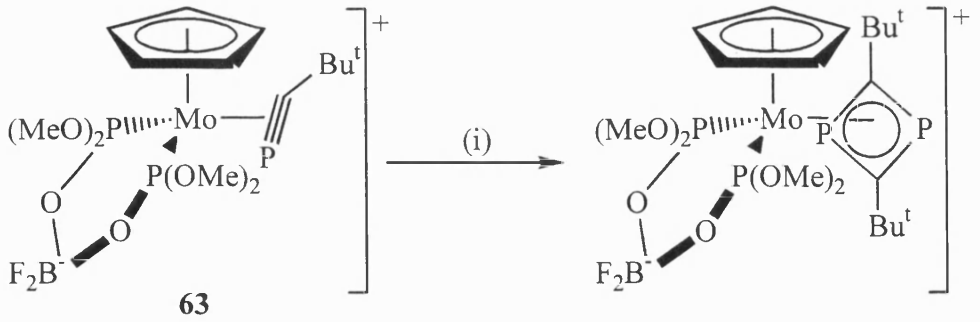

63

Scheme 4.12 (i) $P{\equiv}CBu^t$.

A second η^2-(4e)-phosphaalkyne complex has been reported recently [95] from the reaction of $[W(CO)_3F(C_6H_4CH_2NMeCH_2CH_2NMe_2)]$ with *tert*-butylphosphaalkyne, stirring in toluene for three hours. The product of the reaction was impossible to isolate in crystalline form but the NMR's suggested it to be $[W(CO)_2F(\eta^2\text{-}P{\equiv}CBu^t)(C_6H_4CH_2NMeCH_2CH_2NMe_2)]$, Scheme 4.13. The complex exhibited a low field peak in the phosphorus NMR at 452.4ppm, the carbon spectrum exhibited a doublet at 315.2ppm with a coupling to phosphorus of 117.7Hz. This complex will again react further with an excess of $P{\equiv}CBu^t$ in toluene at 90°C to produce $[W(CO)F(C_6H_4CH_2NMeCH_2CH_2NMe_2)(\eta^4\text{-}PCBu^t(CO)CBu^tP)]$.

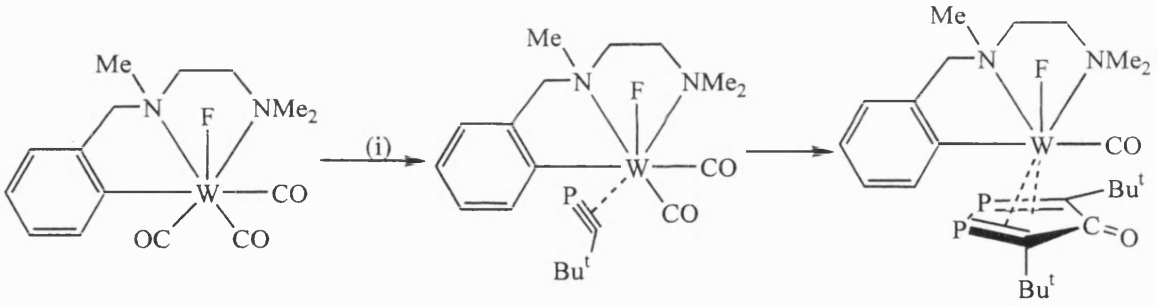

Scheme 4.13 (i) $P{\equiv}CBu^t$.

Thus, the examples of η^2-(4e)-phosphaalkynes discussed are not of great synthetic utility and are proving difficult to isolate in a crystalline form and hence, be able to confirm their structures by single crystal X-ray diffraction study. To this end recent work in the synthesis of tantalum alkyne complexes may provide a simple synthetic route to a more accessible and useful four electron donor phosphaalkyne system.

4.9.2 Pentamethylcyclopentadienyltantalum Alkyne Chemistry.

The formation of cyclopentadienyl alkyne complexes of tantalum were initially studied in the 1960s [96] and were typically prepared by photolysis of $[Ta(CO)_4(\eta^5\text{-}C_5H_5)]$ in the presence of an alkyne. The majority of these complexes though have the general form

$[TaX(\eta^2\text{-}RC{\equiv}CR)(\eta^5\text{-}C_5R_5)]$ or $[TaX_2(\eta^2\text{-}RC{\equiv}CR)(\eta^5\text{-}C_5R_5)]$ where the ligand X in these very stable complexes may be halide, alkyl, vinyl, hydride or alkoxide. One of the most important routes into complex of this type is the displacement of an alkene, typically styrene or cyclooctene, from $[TaX_2(\eta^2\text{-alkene})(\eta^5\text{-}C_5Me_5)]$, where X= Cl or Br, with an alkyne [97] to produce $[TaCl_2(\eta^2\text{-}RC{\equiv}CR)(\eta^5\text{-}C_5Me_5)]$ where RC≡CR = PhC≡CPh **64**, PhC≡CH, MeC≡CMe, EtC≡CEt or HC≡CH, Scheme 4.14.

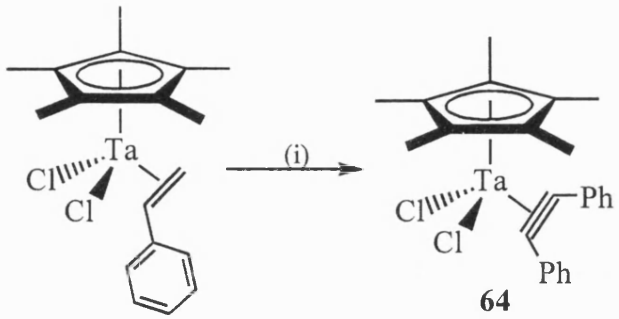

64

Scheme 4.14 (i) PhC≡CPh.

It is interesting to note that none of these complexes reacts with excess alkyne to form metallocyclopentadienes or cyclobutadiene derivatives.

Recently a new synthetic route into pentamethylcyclopentadienyl tantalum complexes has been reported [98] by Curtis. Taking the easily prepared complex $[TaCl_4(\eta^5\text{-}C_5Me_5)]$ **65** [99] and treating it with aluminium and mercury(II) chloride under a carbon monoxide atmosphere overnight produced $[TaCl_2(CO)_2(thf)(\eta^5\text{-}C_5Me_5)]$ **66** in 85% yield, Scheme 4.15.

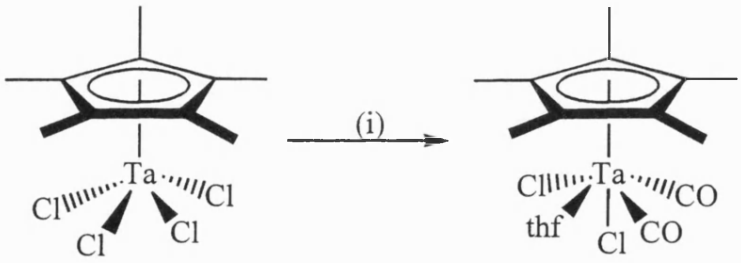

65 **66**

Scheme 4.15 (i) Al, $HgCl_2$, CO, thf.

Interestingly, complex **66** is highly reactive, readily undergoing displacement reactions with loss of thf and either one or two of its carbonyl ligands to form a series of new complexes [98], Scheme 4.16. The most important of these, with respect to the formation of a η^2-(4e)-phosphaalkyne compound is, the reaction of **66** with diphenylacetylene which yields, after stirring overnight, the complex $[TaCl_2(\eta^2\text{-PhC}{\equiv}CPh)(\eta^5\text{-}C_5Me_5)]$ **64** in 90% yield.

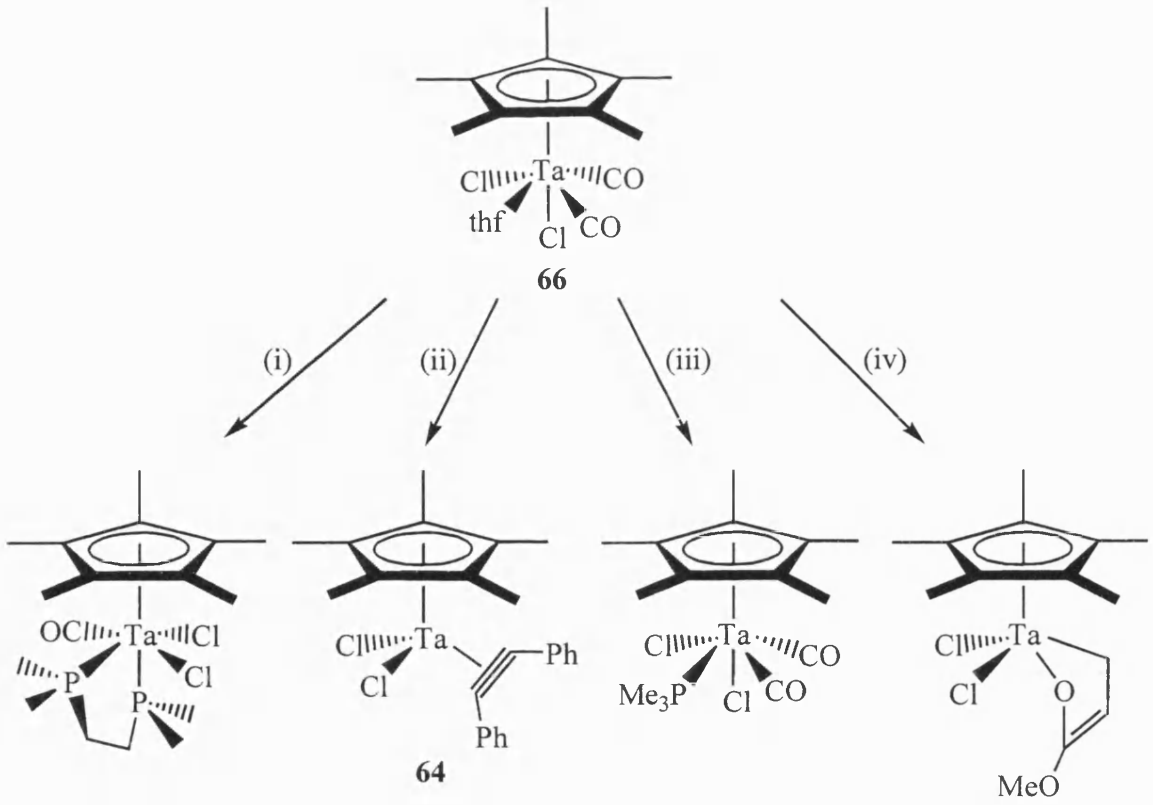

Scheme 4.16 (i) dmpe, (ii) PhC≡CPh, (iii) PMe_3, (iv) methyl acrylate.

The ease of formation of an η^2-(4e)-alkyne complex, such as **64** should provide an simple synthetic route to an η^2-(4e)-phosphaalkyne ligated tantalum species. It is also important to note that once formed the alkyne species does not couple with any further molecules of diphenylacetylene, suggesting it may be possible to isolate the η^2-(4e)-phosphaalkyne species without formation of the diphosphacyclobutadiene observed in the previous reactions.

4.9.3 Reaction of $[TaCl_2(CO)_2(thf)(\eta^5\text{-}C_5Me_5)]$ 66 with *Tert*-butylphosphaalkyne.

To a thf solution of $[TaCl_2(CO)_2(thf)(\eta^5\text{-}C_5Me_5)]$ **66** at -78°C *tert*-butylphosphaalkyne was added dropwise. The solution was allowed to warm to ambient temperature turning dark red in the process, stirring continued at room temperature for approximately 30 minutes. Infra red spectroscopy confirms that reaction has taken place as the signals assigned to the metal carbonyl stretching modes are no longer observed. The solvent was removed *in vacuo* and the residue was extracted with hexane, the resultant purple solution was filtered over celite and yielded upon evaporation of the solvent a purple powder **XI** in 29% yield. Low temperature recrystallisation of **XI**, -40°C for three days, yielded crystals of **XI** which were submitted for elemental analysis and a single crystal X-ray diffraction study. Unfortunately, the crystal lost solvent whilst being prepared for the diffractometer,

subsequent crystals have been prepared, but none were of sufficient quality for a diffraction study.

Elemental analysis confirmed the presence of a pentamethylcyclopentadienyltantalum species ligated by two chloride molecules and a single molecule of phosphaalkyne, supporting the formation of $[TaCl_2(\eta^2\text{-}P{\equiv}CBu^t)(\eta^5\text{-}C_5Me_5)]$ **XI**, Scheme 4.17.

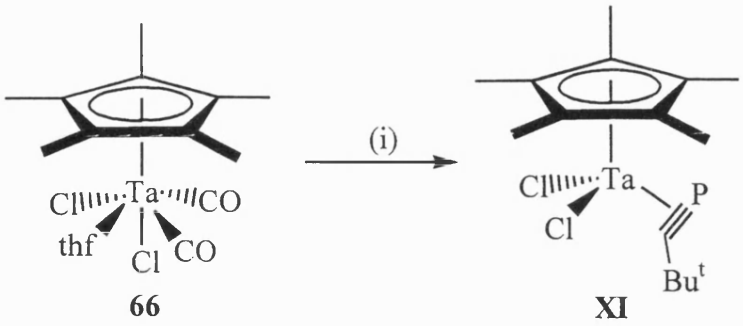

66 **XI**

Scheme 4.17 (i) $P{\equiv}CBu^t$.

The phosphorus NMR of **XI** shows a low field signal for the phosphorus of the phosphaalkyne with a chemical shift of 509.0ppm, suggesting that the phosphorus atom is deshielded. The proton spectrum exhibits the expected two singlets, one at 1.89ppm for the methyl protons of the pentamethylcyclopentadienyl ligand and the other at 1.71ppm for the *tert*-butyl groups. The carbon NMR reveals a doublet at low field with a chemical shift of 337.2ppm and a coupling to phosphorus of 113Hz, this is the contact carbon of the four electron donor phosphaalkyne. It is in the expected region from the work of Green and Nixon described above. The remainder of the carbon spectrum consists of four singlets at 122.2ppm cyclopentadienyl carbons, 52.5ppm central carbons of the *tert*-butyl groups, 34.6ppm methyl groups of the pentamethylcyclopentadienyl ring and 13.0ppm methyl groups of the *tert*-butyl.

The low field chemical shift of the phosphorus of the phosphaalkyne in the $^{31}P\{^1H\}$ NMR can tentatively be explained using the principle of isolobal relationships. It is possible to prepare complexes of the general formula $[TaCl(\equiv CR)(P)_2(\eta\text{-}C_5H_5)]$ where P is a phosphine. The isolobal principle suggests that for these complexes $TaCl(\eta\text{-}C_5H_5)$ can be considered to be isolobal to CR, which implies that $[TaCl(\eta\text{-}C_5H_5)]^+$ is isolobal to CR^+ and it may be possible to postulate that $TaCl_2(\eta\text{-}C_5H_5)$ is isolobal to CR^+. Thus it is suggested that the tantalum phosphaalkyne complex **XI** can be considered to be isolobal to delocalised phosphacyclopropene species shown in Figure 4.8.

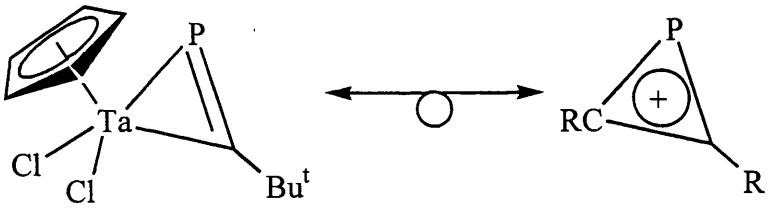

Figure 4.8.

This relationship is similar to that described above for the molybdenum phosphaalkyne species described above and the comparisons can be drawn with the aromatic phosphirenylium cation $[PhCC(Bu^t)P][B(OSO_2CF_3)_4]$ [93] in which a deshielding of the phosphorus atom leads to a shift to lower field in the phosphorus NMR of 313ppm. If a comparison can be made between **XI** and the phosphirenylium cation then it is fair to assume that a similar shifting to lower field, of the phosphorus signal of the phosphaalkyne, may occur. It is impossible to quantify the size of this shift, but the appearance of the signal for **XI** in the area predicted for a four electron donor phosphaalkyne by Green and Nixon [89] further supports the formation of a η^2-(4e)-phosphaalkyne tantalum complex.

The evidence presented above confirms the preparation and isolation of the $[TaCl_2(\eta^2\text{-}(4e)\text{-}P{\equiv}CBu^t)(\eta^5\text{-}C_5Me_5)]$ complex as an air sensitive crystalline solid that should show a diverse synthetic utility as its reactivity is compared to that of alkynes.

CHAPTER 5

Experimental

5 Experimental.

5.1 General Experimental Procedures.

All reactions were carried out under an atmosphere of dry, oxygen-free nitrogen, using standard Schlenk techniques. All solvents used were deoxygenated and dried by standard literature methods [100].

NMR spectra were recorded on Jeol JNM GX270 (270MHz) or Jeol EX400 (400MHz) Fourier transform spectrometers. NMR spectra are referenced to the solvent for ^{1}H and ^{13}C nuclei and to the following standards for each nuclei respectively; ^{31}P: $85\%H_3PO_4$; ^{11}B: $BF_3.Et_2O$.

Infrared spectra were recorded on a Nicolet 510P FT-IR spectrometer. The samples were dissolved in the stated solvents and the absorption recorded using sodium chloride cells.

Microanalysis were determined in the School of Chemistry, University of Bath.

5.2 Preparation of Starting Materials.

The following compounds were prepared according to the published literature methods:-

$[W(NCMe)(PhC{\equiv}CPh)_3]$ **15** [18].

o-diphenylphosphinostyrene (dpps) [28].

o-diphenylphosphinoallylbenzene (dppa) [61].

$[ReBr_2(\eta^2\text{-}PhC{\equiv}CPh)(\eta\text{-}C_5H_5)]$ **29** [41].

$[Mo(CO)_2I(\eta^7\text{-}C_7H_7)]$ **55** [79].

$Tl[closo\text{-}3,1,2\text{-}TlC_2B_9H_{11}]$ [75].

$[TaCl_2(CO)_2(thf)(\eta^5\text{-}C_5Me_5)]$ **66** [98].

All other compounds and reagents were obtained from commercial sources and were used as received unless otherwise indicated.

5.3 Alkyne/Alkene Coupling Reactions.

5.3.1 Reaction of [W(NCMe)(η^2-PhC≡CPh)$_3$] 15 with *o*-diphenylphosphinostyrene.

To a toluene solution (50ml) of [W(NCMe)(η^2-PhC$_2$Ph)$_3$] **15** (0.698g, 0.919mmol) was added o-diphenylphosphinostyrene (dpps) (0.265g, 0.919mmol) and this mixture was brought to reflux. After approximately 30 minutes, the pale yellow solution turns red/orange, the reflux was continued for another 3.5 hours then. The reaction mixture was cooled to room temperature and dried *in vacuo*. The reaction products were then preabsorbed onto alumina and chromatographed on alumina/hexane, eluting with hexane/dichloromethane 4:1. An orange/yellow band was collected which produced a brown powder upon drying *in vacuo*. This yields 0.6g of [W(≡CPh){η^2-(E)-CHPh=CHC$_6$H$_4$PPh$_2$-o}(η^5-C$_5$Ph$_4$H)] **Ia, b** (0.596mmol, 65% yield).

Initial NMR studies show a mixture of isomers in a 1.6:1 ratio, layered recrystallisation gave a single crystal for an X-ray determination of the major isomer.

Major Isomer

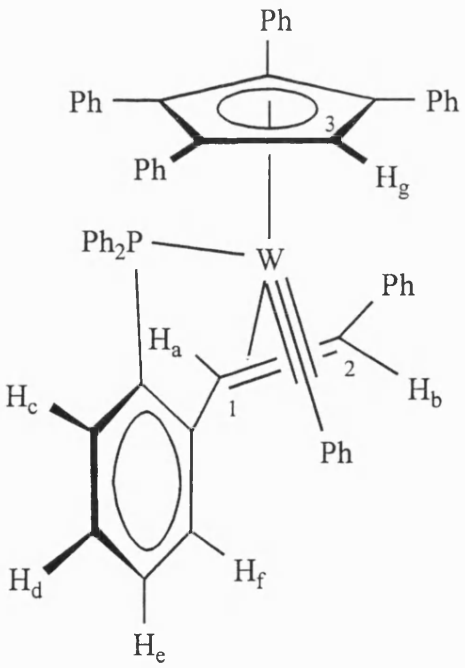

$[W(\equiv CPh)\{\eta^2\text{-}(E)\text{-}CHPh{=}CHC_6H_4PPh_2\text{-}o\}(\eta^5\text{-}C_5Ph_4H)].0.25CH_2Cl_2$	calculated	%C	72.7	%H	4.65
	found	%C	72.3	%H	4.47

^{1}H NMR (CD_2Cl_2)

δ 8.16 - 6.67, m, 40H, Ph; 6.02 & 5.77, $[AB]_2$, 4H, H_c H_d H_e H_f, J(AB)= 7.0Hz; 4.77, s, 1H, H_g; 4.12 & 3.99, [AB], 2H, H_a H_b, $^3J(H_aH_b)$ = 10.4Hz; $^3J(H_aP)$ = 5.5Hz.

$^{13}C\{^1H\}$ NMR (CD_2Cl_2)

δ 283.8, d, ≡*C*Ph, $^2J(CP)$ = 21Hz; 159.6 - 120.4, m, Ph; 116.6, 112.3, 111.8, 110.3, *C*$_4$Ph$_4$CH; 112.5, C_3; 60.1, d, C_1, $^2J(C_1P)$ = 6Hz; 38.0, C_2.

$^{31}P\{^1H\}$ NMR (CD_2Cl_2)

δ 50.0, *P*$Ph_2C_6H_4C_2H_3$, $^1J(PW)$= 347Hz.

Mass Spectrum

Parent ion 1006.1

Minor Isomer

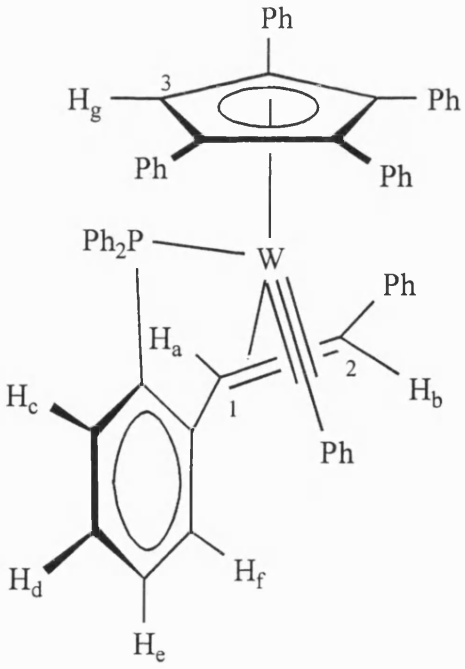

^{1}H NMR (CD_2Cl_2)

δ 8.20 - 6.65, m, 40H, Ph; 6.41 & 6.09, $[AB]_2$, 4H, H_c H_d H_e H_f, J(AB) = 7.0Hz; 6.05, d, 1H, H_g, ^{3}J(H_gP) = 5.8Hz; 3.11 & 2.91, [AB], 2H, H_a H_b, J(H_aH_b) = 12.8Hz; J(H_aP) = 5.5Hz.

^{13}C{^{1}H} NMR (CD_2Cl_2)

δ 287.1, d, ≡*C*Ph, ^{2}J(CP) = 18Hz; 159.3 - 123.0, m, Ph; 119.8, 116.5, 108.0, 107.2, *C*$_4$$Ph_4CH$; 96.18, C_3; 65.6, d, C_1, ^{2}J(C_1P) = 4Hz; 45.8, C_2.

^{31}P{^{1}H} NMR (CD_2Cl_2)

δ 56.1, *P*$Ph_2C_6H_4C_2H_3$, ^{1}J(PW)= 350Hz.

All assignments assisted by CH & HH 2D cosy experiments.

5.3.2 Reaction of [W(NCMe)(η^2-PhC≡CPh)$_3$] 15 with *o*-diphenylphosphinoallyl-benzene.

[W(NCMe)(η^2-PhC_2Ph)] **15** (0.370g, 0.487mmol) was dissolved in toluene (20ml), to this was added o-diphenylphosphinoallylbenzene (dppa) (0.15g, 0.496mmol) and the reaction mixture was brought to reflux. After 30 minutes the solution was observed to turn red/orange from pale yellow, the reflux was continued for a further 3.5 hours and then allowed to cool and dried *in vacuo*. The reaction mixture was then preabsorbed onto alumina and columned on alumina/hexane, eluting with 4:1 hexane/dichloromethane. A single orange band was collected that was dried *in vacuo* and recrystallised from dichloromethane/hexane to yield an orange powder **II** that was washed once with hexane and dried *in vacuo* (0.258g, 0.253mmol, 52% yield)

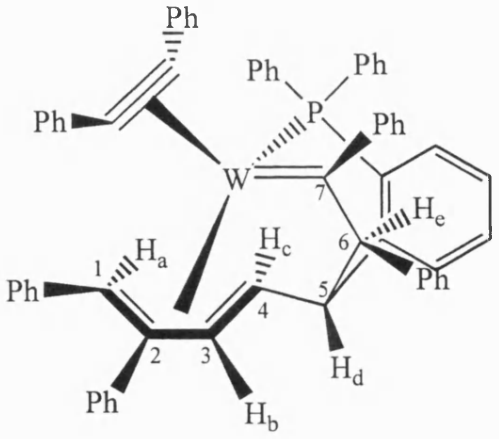

II . $0.5CH_2Cl_2$ calculated %C 71.8 %H 4.74

found %C 71.2 %H 4.67

^{1}H NMR (CD_2Cl_2)

δ 7.75 - 5.64, m, 44H, Ph; 6.47, d, 1H, H_b, $^3J(H_bH_c)$ = 12.9Hz; 5.11, d, 1H, H_d, $^4J(H_dP)$ = 2.4Hz; 4.17, d, 1H, H_e, $^4J(H_eP)$ = 3.4Hz; 1.59, dd, 1H, Hc, $^3J(H_cH_b)$ = 12.9Hz, $^3J(H_cP)$ = 4.9Hz; 0.49, d, 1H, H_a, $^3J(H_aP)$ = 5.1Hz.

$^{13}C\{^1H\}$ NMR (CD_2Cl_2)

δ 289.4, C_7; 220.0, C_8, C_9; 155.6 - 123.0, m, Ph; 111.1, C_2; 99.8, C_3; 75.2, C_6; 65.9, d, C_1, $^2J(C_1P)$ = 4Hz; 63.0, d, C_4, $^2J(C_4P)$ = 12 Hz; 57.0, C_5.

$^{31}P\{^1H\}$ NMR (CD_2Cl_2)

δ 36.44, $^1J(PW)$= 276Hz.

5.3.3 Reaction of [$ReBr_2(\eta^2$-PhC≡CPh)(η^5-C_5H_5)] 29 with *o*-diphenylphosphinoallylbenzene.

To a thf solution (20ml) of [$ReBr_2(\eta^2$-PhC≡CPh)(η^5-C_5H_5)] **29** (0.25g, 0.424mmol) was added o-diphenylphosphinoallylbenzene (0.141g, 0.466mmol) and $AgBF_4$ (0.083g, 0.424mmol) and allowed to stir for four hours. A colour change from orange to green was observed with the formation of a precipitate. Upon completion of the reaction the volatiles

were removed in vacuo. Extraction with dichloromethane and filtering over celite, gave a green solution that was dried *in vacuo* and recrystallised from dichloromethane/ether to yield a light green powder, $[ReBr(PPh_2C_6H_4CH_2CH{=}CH_2)(\eta^2\text{-}PhC{\equiv}CPh)(\eta\text{-}C_5H_5)][BF_4]$ **III** (0.171g, 0.191mmol, 45%)

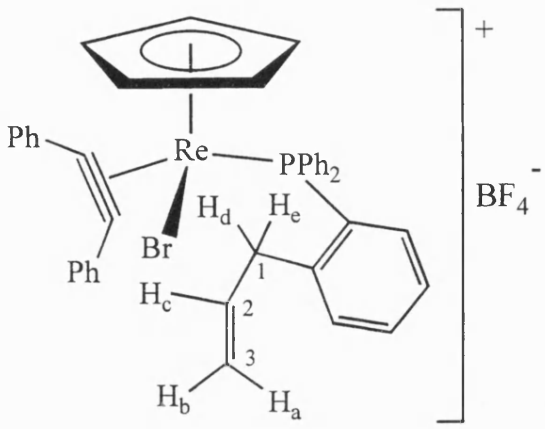

$[ReBr(PPh_2C_6H_4CH_2CH{=}CH_2)(\eta^2\text{-}PhC{\equiv}CPh)(\eta\text{-}C_5H_5)][BF_4]$	calculated	%C 53.47	%H 3.81
	found	%C 53.68	%H 3.85

^1H NMR (CD_2Cl_2)

δ 8.07-7.00, m, 24H, Ph; 5.81, s, 5H, C_5H_5; 4.70, m, 1H, H_c; 4.62,[ABC], 1H, H_b, $^3J(H_bH_c)$ = 10.0Hz, $^2J(H_bH_a)$ = 2.0Hz; 4.48 [ABC], 1H, H_a, $^3J(H_aH_c)$ = 16.4Hz, $^2J(H_aH_b)$ = 2.0Hz; 2.51, [ABX], 1H, H_d, $^2J(H_dH_e)$ = 16.2Hz, $^3J(H_dH_c)$ = 6.7Hz; 2.27 , [ABX], 1H, H_e, $^2J(H_eH_d)$ = 16.2Hz, $^3J(H_eH_c)$ = 6.7Hz.

$^{13}C\{^1H\}$ NMR (CD_2Cl_2)

δ 222.9 Ph*C*≡*C*Ph; 145.0-123.8, m, Ph; 117.1, C_3; 97.6, C_5H_5; 95.8, C_2; 38.9, C_1.

$^{31}P\{^1H\}$ NMR (CD_2Cl_2)

δ -5.62, $PPh_2C_6H_4C_3H_5$.

5.3.4 Reaction of $[ReBr_2(\eta^2\text{-}PhC{\equiv}CPh)(\eta^5\text{-}C_5H_5)]$ 29 with acetonitrile followed by *o*-diphenylphosphinoallylbenzene.

$[ReBr_2(\eta^2\text{-}PhC{\equiv}CPh)(\eta^5\text{-}C_5H_5)]$ **29** (0.25g, 0.424mmol) was dissolved in 20ml of acetonitrile and to this was added $TlPF_6$ (0.37g, 1.059mmol) the solution immediately changed colour from orange to pink. After 30 minutes of stirring o-diphenylphosphinoallylbenzene (0.141g, 0.466mmol) was added and this mixture was allowed to stir for a further two hours. A further colour change to red brown was observed with the formation of a precipitate. The mixture was then dried *in* vacuo and extracted with dichloromethane, after filtration over celite, the brown solution was dried *in vacuo* and then recrystallised from dichloromethane/hexane to yield an oily brown powder, $[Re(NCMe)(PPh_2C_6H_4CH_2CH{=}CH_2)(\eta^2\text{-}PhC{\equiv}CPh)(\eta^5\text{-}C_5H_5)][PF_6]_2$ **IV** (0.283g, 0.267mmol, 63%).

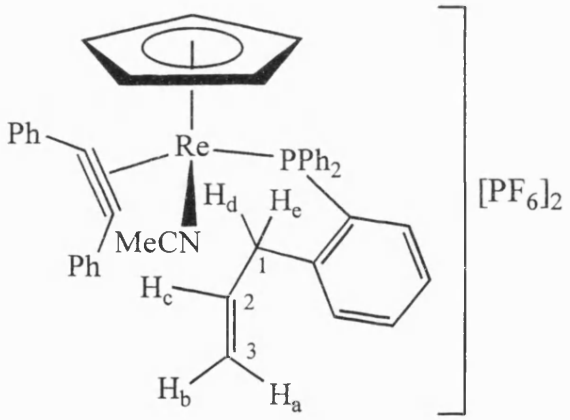

$[Re(NCMe)(PPh_2C_6H_4CH_2CH{=}CH_2)(\eta^2\text{-}PhC{\equiv}CPh)(\eta^5\text{-}C_5H_5)][PF_6]_2$	calculated	%C 47.46	%H 3.51	%N 1.32
	found	%C 47.53	%H 3.54	%N 1.41

^1H NMR (CD_2Cl_2)

δ 7.81-6.22, m, 24H, Ph; 6.14, s, 5H, C_5H_5; 4.76, [ABC], 1H, H_c, $^3J(H_cH_{d,e})$ = 6.7Hz (x2), $^3J(H_cH_a)$ = 16.8Hz, $^3J(H_cH_b)$ = 9.1Hz; 4.67, [ABC], 1H, H_b, $^2J(H_bH_a)$ = 1.7Hz, $^3J(H_bH_c)$ = 9.1Hz; 4.49, [ABC], 1H, H_a, $^2J(H_aH_b)$ = 1.7Hz, $^3J(H_aH_c)$ = 16.8Hz; 3.15, s, 3H, NC*CH3*; 2.55, [ABX], 1H, H_d, $^2J(H_dH_e)$ = 16.2Hz, $^3J(H_dH_c)$ = 6.7Hz; 2.27, [ABX], 1H, H_e, $^2J(H_eH_d)$ = 16.2Hz, $^3J(H_eH_c)$ = 6.7Hz.

$^{13}C\{^1H\}$ NMR (CD_2Cl_2)

δ 218.0, Ph*C*≡*C*Ph; 145.0-122.7, m, Ph and N*C*CH_3; 117.4, C_3; 98.8, C_5H_5; 91.0, C_2; 38.6, C_1; 14.2, NC*C*H_3.

$^{31}P\{^1H\}$ NMR (CD_2Cl_2)

δ -3.69, s, $PPh_2C_6H_4C_3H_5$; -144.48, hept, PF_6, $^1J(PF) = 711.8Hz$.

5.4 Carborane Reactions.

5.4.1 Reaction of $[Mo(CO)_2I(\eta^7\text{-}C_7H_7)]$ 54 with $Tl[closo\text{-}3,1,2\text{-}TlC_2B_9H_{11}]$.

To a solution of $[Mo(CO)_2I(\eta^7\text{-}C_7H_7)]$ **54** (0.2g, 0.54mmol)in thf (20ml) was added $Tl[closo\text{-}3,1,2\text{-}TlC_2B_9H_{11}]$ (0.292g, 0.54mmol) and allowed to stir overnight. Counter cation exchange was carried out with the addition of $Et_4NCl.H_2O$ (0.134g, 0.81mmol) and stirring for 30 min. This mixture was filtered over a Celite plug and the resultant orange solution dried *in vacuo* to yield an orange oil. This oil was columned on alumina/dichloromethane and eluted with dichloromethane, the single orange/yellow band was collected, dried *in vacuo* and the product recrystallised from dichloromethane and hexane. The orange powder produced was washed three times with hexane and dried *in vacuo*. 0.232g (0.459mmol) of $[NEt_4][closo\text{-}3,3\text{-}(CO)_2\text{-}3\text{-}(\eta^3\text{-}C_7H_7)\text{-}3,1,2\text{-}MoC_2B_9H_{11}]$ **V** was produced giving a yield of 85%.

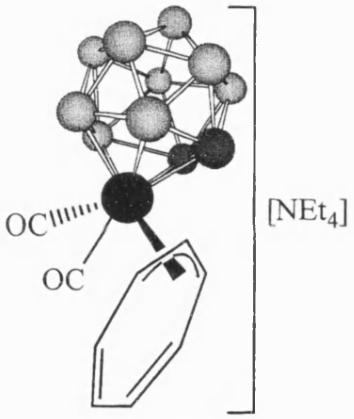

V

● = Mo ◎ =BH ● =CH

$[NEt_4][closo\text{-}3,3\text{-}(CO)_2\text{-}3\text{-}(\eta^3\text{-}C_7H_7)\text{-}3,1,2\text{-}MoC_2B_9H_{11}]$	calculated	%C 45.12	%H 7.67	%N 2.77
	found	%C 45.20	%H 8.11	%N 2.95

^1H NMR (CD_2Cl_2)

δ 4.76, s, br, 7H, C_7H_7; 3.20, q, 8H, $(CH_3CH_2)N$, $^3J(HH)$ = 7.27Hz; 1.69, s, br, 2H, cage CH; 1.33, tt, 12H, $(CH_3CH_2)N$, $^3J(HH)$ = 7.27Hz, $^3J(HN)$ = 2.01Hz.

$^{13}C\{^1H\}$NMR (CD_2Cl_2)

δ 240.2, *C*O; 99.2, br, C_7H_7; 52.8, $(CH_3CH_2)N$; 44.4, br, cage CH; 7.6, $(CH_3CH_2)N$.

$^{11}B\{^{1}H\}NMR$ (CD_2Cl_2)

δ -6.66, 1B; -8.95, 2B; -13.80, 2B; -15.37, 1B; -21.32, 3B.

IR. Spectra (CH_2Cl_2)

ν CO 1930cm^{-1}, 1853cm^{-1}, ν cage 2509cm^{-1}.

5.4.2 Reaction of [NEt_4][*closo*-3,3-$(CO)_2$-3-(η^3-C_7H_7)-3,1,2-$MoC_2B_9H_{11}$] V with $HBF_4.Et_2O$.

A dichloromethane solution (20ml) of [NEt_4][*closo*-3,3-$(CO)_2$-3-(η^3-C_7H_7)-3,1,2-$MoC_2B_9H_{11}$] **V** (0.15g, 0.3mmol) was cooled to -78°C. To this was added 56μl of an 85% solution of $HBF_4.Et_2O$ (0.35mmol), and the mixture was allowed to warm to ambient temperature a colour change from orange to red was observed. Infra red suggested that the reaction proceeds in quantitative yields and this solution was used, without further workup, in subsequent reactions. Analytically pure material was prepared by chromatography on a fluorasil/hexane column, eluted with 2:1 dichloromethane/hexane. An orange red band was collected, and this was dried under vacuum and recrystallised from dichloromethane/hexane to produce unstable orange microcrystals, wash with hexane and dry *in vacuo*. Yield 0.111g of [*closo*-3,3-$(CO)_2$-3-(η^4-C_7H_8)-3,1,2-$MoC_2B_9H_{11}$] **VI** (0.094g, 0.25mmol, 83%). Unfortunately this complex proved too unstable to record any NMR spectra.

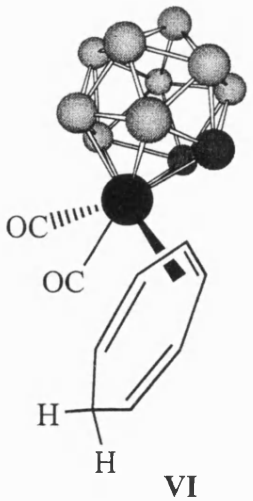

VI

● = Mo ◎ =BH ● =CH

Infra Red Spectra (CH_2Cl_2)

νCO 2017cm^{-1}, 1958cm^{-1}, ν Cage 2545cm^{-1}.

5.4.3 Reaction of [*closo*-3,3-(CO)$_2$-3-(η^4-C_7H_8)-3,1,2-$MoC_2B_9H_{11}$] VI with diphenylacetylene.

A solution of [*closo*-3,3-(CO)$_2$-3-(η^4-C_7H_8)-3,1,2-$MoC_2B_9H_{11}$] **VI** (0.089g, 0.20mmol) was freshly prepared in dichloromethane (20ml) to this was added diphenylacetylene (0.085g, 0.47mmol) and allowed to stir overnight. The volatiles were removed *in vacuo* and the resultant yellow oil was loaded onto a silica gel/pentane column and eluted with pentane/ether 1:1 collecting a yellow band which upon drying *in vacuo* gave a yellow powder, [*closo*-3-(CO)-3,3-(η^2-PhC≡CPh)$_2$-3,1,2-$MoC_2B_9H_{11}$] **48**.

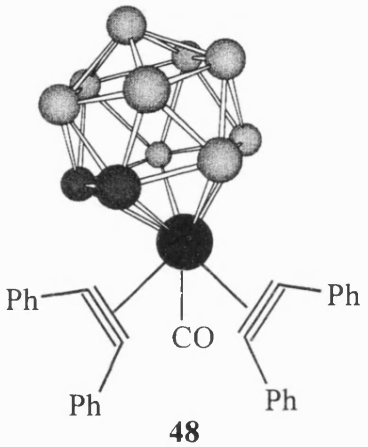

48

● = Mo ◎ =BH ● =CH

[*closo*-3-(CO)-3,3-(η^2-PhC≡CPh)$_2$-3,1,2-$MoC_2B_9H_{11}$]	calculated	%C 60.8	%H 5.1
	found	%C 60.7	%H 5.1

^{1}H NMR (CD_2Cl_2)

δ 7.62-7.31, m, 20H, Ph; 3.31, s, br, 2H, cage CH.

^{13}C{^{1}H} NMR (CD_2Cl_2)

δ 222.1, *C*O; 168.8, PhC≡*C*Ph; 152.9, Ph*C*≡CPh; 134.9-127.4, Ph; 51.6, br, cage *C*H.

^{11}B{^{1}H} NMR (CD_2Cl_2)

δ -3.5, 1B; -5.8, 1B; -6.9, 1B; -11.5, 2B; -16.2, 3B.

Infra Red Spectra (CH_2Cl_2)

νCO 2062cm^{-1}; νCage 2571cm^{-1}.

5.4.4 Reaction of [*closo*-3,3-$(CO)_2$-3-(η^4-C_7H_8)-3,1,2-$MoC_2B_9H_{11}$] VI with triphenylphosphine.

To a freshly prepared dichloromethane solution (20ml) of [*closo*-3,3-$(CO)_2$-3-(η^4-C_7H_8)-3,1,2-$MoC_2B_9H_{11}$] **VI** (0.113g, 0.3mmol) was added triphenylphosphine (0.314g, 1.2mmol) and this solution was allowed to stir overnight. A yellow precipitate was observed to form, and the supernatant liquid was filtered off over Celite and dried *in vacuo*. The yellow solid produced was dissolved in a minimum volume of dichloromethane and loaded onto an alumina/hexane column, that was eluted with 1:1 dichloromethane/hexane. A yellow band was collected which was dried in vacuo and recrystallised from dichloromethane/hexane to give a yellow powder, [*closo*-3,3-$(CO)_2$-3,3-$(PPh_3)_2$-3,1,2-$MoC_2B_9H_{11}$] **VII** (0.177g, 0.219mmol, 73% yield).

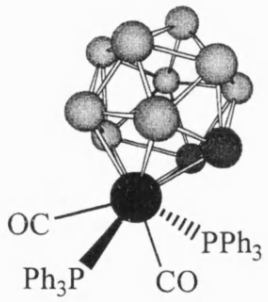

VII

● = Mo ◎ =BH ● =CH

[*closo*-3,3-$(CO)_2$-3,3-$(PPh_3)_2$-3,1,2-$MoC_2B_9H_{11}$]	calculated	%C 59.39	%H 5.11
	found	%C 58.50	%H 5.08

^{1}H NMR (CD_2Cl_2)

δ 7.67 - 7.23, m, 30H, Ph; 2.14, s, br, 2H, cage CH.

^{13}C{^{1}H} NMR (CD_2Cl_2)

δ 240.5, t, *C*O, ^{2}J(CP) = 30Hz; 135.1 - 128.5, m, Ph; 48.1, cage CH.

^{31}P{^{1}H} NMR (CD_2Cl_2)

δ 63.32, $P\text{Ph}_3$

$^{11}B\{^1H\}$ NMR (CD_2Cl_2)

δ -1.86, 1B; -4.43, 2B; -9.18, 2B; -13.42, 1B; -17.61, 2B; -23.79, 1B.

Infra Red Spectra (CH_2Cl_2)

νCO 1950cm^{-1}, 1865cm^{-1}; νCage 2558 cm^{-1}.

5.4.5 Reaction of [*closo*-3,3-$(CO)_2$-3,3-$(PPh_3)_2$-3,1,2-$MoC_2B_9H_{11}$] VII with diphenylacetylene.

Diphenylacetylene (0.15g, 0.57mmol) was added to a solution of [*closo*-3,3-$(CO)_2$-3,3-$(PPh_3)_2$-3,1,2-$MoC_2B_9H_{11}$] **VII** (0.15g, 0.18mmol) in dichloromethane (20ml). The reaction was monitored by infra red, which showed completion after 5.5 days, whence the volatiles were removed *in vacuo* leaving a purple oil. This oil was chromatographed on a silica gel/hexane column, which was eluted with dichloromethane/hexane with an increasing dichloromethane concentration. A green band was collected that after drying, *in vacuo* was recrystallised from dichloromethane/hexane to give a green powder which was washed three times with hexane and dried under vacuum. Yield of [*closo*-3-(CO)-3-(PPh_3)-3-(η^2-PhC≡CPh)-3,1,2-$MoC_2B_9H_{11}$] **VIII** 0.228g (0.314mmol, 55%).

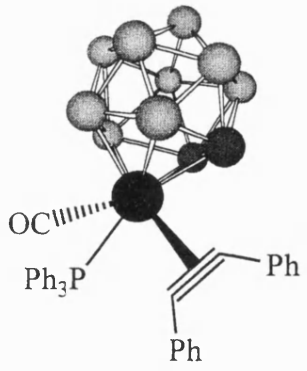

VIII

● = Mo ◎ =BH ● =CH

[*closo*-3-(CO)-3-(PPh_3)-3-(η^2-PhC≡CPh)-3,1,2-$MoC_2B_9H_{11}$]	calculated	%C 60.32	%H 5.21
	found	%C 60.40	%H 5.51

^{1}H NMR (CD_2Cl_2)

δ 7.48 - 7.24, m, 25H, Ph; 3.50, s, br, 1H, cage CH; 2.17, s, br, 1H, cage CH.

$^{13}C\{^{1}H\}$ NMR (CD_2Cl_2)

δ 236.1, d, *C*O, $^{2}J(CP)$ = 12.2Hz; 208.4, br, Ph*C*≡*C*Ph; 133.2 - 129.1, m, Ph; 50.5 & 46.3, cage CH.

$^{31}P\{^{1}H\}$ NMR (CD_2Cl_2)

δ 54.12, PPH_3.

$^{11}B\{^{1}H\}$ NMR (CD_2Cl_2)

δ -1.48, 1B; -5.85, 1B; -7.85, 2B; -11.42, 2B; -18.37, 3B.

Infra Red Spectra (CH_2Cl_2)

νCO 1968cm^{-1}; νCage 2567 cm^{-1}.

5.4.6 Reaction of [*closo*-3,3-$(CO)_2$-3-(η^4-C_7H_8)-3,1,2-$MoC_2B_9H_{11}$] VI with 1,2-bis-(diphenylphosphino)ethane.

A solution of [*closo*-3,3-$(CO)_2$-3-(η^4-C_7H_8)-3,1,2-$MoC_2B_9H_{11}$] **VI** (0.113g, 0.3mmol) in dichloromethane was prepared in situ, to this was added 1,2-bis-(diphenylphosphino)ethane (dppe) (0.238g, 0.58mmol) and this mixture was stirred overnight. The resultant yellow/orange solution was dried under vacuum and the yellow oil was loaded onto a silica gel/hexane column and eluted with dichloromethane/hexane 1:1, a single yellow band was collected which was dried *in vacuo* then recrystallised from dichloromethane/hexane to give yellow microcrystals, [*closo*-3,3-$(CO)_2$-3-(η^2-$Ph_2PCH_2CH_2PPh_2$)-3,1,2-$MoC_2B_9H_{11}$] **IX** in a 64% yield (0.113g, 0.192mmol).

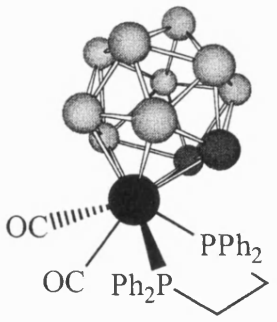

IX

● = Mo ◎ =BH ● =CH

^{1}H NMR (CD_2Cl_2)

δ 7.58 - 7.31, m, 20H, Ph; 2.72 - 2.64, m, 2H and 2.32 - 2.23, m 2H, $Ph_2PCH_2CH_2PPh_2$; 1.80, s, br, cage CH's.

^{13}C{^{1}H} NMR (CD_2Cl_2)

δ241.5, CO; 133.2 - 128.9, m , Ph; 47.3, cage CH's; 27.9, t, $Ph_2PCH_2CH_2PPh_2$, ^{1}J(CP)= 21.7Hz.

^{31}P{^{1}H} NMR (CD_2Cl_2)

δ 78.47, $Ph_2PCH_2CH_2PPh_2$.

^{11}B{^{1}H} NMR (CD_2Cl_2)

δ -0.43,2B; -4.85, 1B; -6.66, 2B; -14.75, 2B; -16.80, 1B; -21.46, 1B.

Infra Red Spectrum (CH_2Cl_2)

νCO 1972cm^{-1}, 1904cm $^{-1}$; νCage 2560cm^{-1}.

5.4.7 Reaction of [*closo*-3,3-(CO)$_2$-3-(η^4-C$_7$H$_8$)-3,1,2-MoC$_2$B$_9$H$_{11}$] VI with *o*-diphenylphosphinostyrene.

[*closo*-3,3-(CO)$_2$-3-(η^4-C$_7$H$_8$)-3,1,2-MoC$_2$B$_9$H$_{11}$] **VI** (0.186g, 0.494mmol) was prepared in situ as a dichloromethane solution (20ml) to this was added o-diphenylphosphinostyrene (0.143g, 0.496mmol) and stirred overnight then dried *in vacuo*. The reaction mixture was then preabsorbed onto alumina and chromatographed on alumina/hexane, eluting with hexane/dichloromethane 2:1. A single yellow band was collected that was recrystallised

from dichloromethane/ hexane to yield a yellow powder, [*closo*-3,3-$(CO)_2$-3-(σ:η^2-$PPh_2C_6H_4CH_2$=CH-o)-3,1,2-$MoC_2B_9H_{11}$] **X** (0.235g, 0.410mmol, 83% yield).

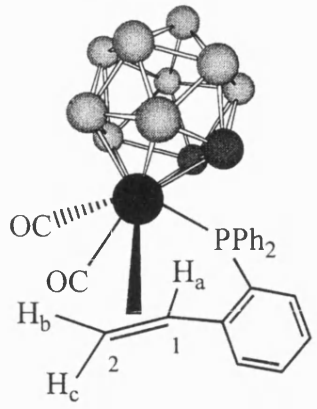

X

● = Mo ◎ =BH ● =CH

[*closo*-3,3-$(CO)_2$-3-(σ:η^2-$PPh_2C_6H_4CH_2$=CH-o)-3,1,2-$MoC_2B_9H_{11}$]	calculated	%C 50.33	%H 4.93
	found	%C 50.1	%H 4.98

^{1}H NMR (CD_2Cl_2)

δ 7.69 - 7.07, m, 14H, Ph; 5.29, ddd, 1H, Ha, $^3J(H_aP)$ = 3.9Hz, $^3J(H_aH_b)$ = 13.3Hz, $^3J(H_aH_c)$ = 9.5Hz; 3.69, at, 1H, Hc, $^3J(H_cH_a)$ = 9.5Hz, $^2J(H_cH_b)$ = 13.3Hz; 3.26, s, br, 1H, cage CH; 3.11, s, br, 1H, cage Ch; 2.82, dd, 1H, Hb, $^3J(H_bH_a)$ = 13.3Hz, $^2J(H_bH_c)$ = 9.52Hz.

^{13}C{^{1}H} NMR (CD_2Cl_2)

δ 228.4, d, *C*O, $^2J(CP)$ = 18Hz; 227.4, d, *C*O, $^2J(CP)$ = 10Hz; 152.9, d, C_1, $^2J(C_2P)$ = 26.5Hz; 135.6-127.5, m, Ph; 82.4, C_2; 50.0, cage CH; 49.7, cage CH.

^{31}P{^{1}H} NMR (CD_2Cl_2)

δ 49.8, $Ph_2PC_6H_4C_2H_3$-*o*.

^{11}B{^{1}H} NMR (CD_2Cl_2)

δ -0.86, 1B; -1.95, 1B; -3.52, 1B; -8.57, 1B; -11.04, 1B; -13.37, 1B; -18.08, 1B; -19.56, 2B.

Infra Red Spectrum (CH_2Cl_2)

νCO 2019cm^{-1}, 1956cm $^{-1}$; νCage 2548cm^{-1}.

5.5 Phosphaalkyne Chemistry.

5.5.1 Reaction of $[TaCl_2(CO)_2(thf)(\eta^5\text{-}C_5Me_5)]$ and $P{\equiv}CBu^t$.

$[TaCl_2(CO)_2(thf)(\eta^5\text{-}C_5Me_5)]$ **66** (0.1g, 0.23mmol) was dissolved in thf (20ml) and $P{\equiv}CBu^t$ (0.037ml, 0.23mmol) was added. The resulting dark red coloured solution was stirred at ambient temperature for 30 min, then dried *in vacuo*. This dark red oil was extracted with hexane and the resultant deep red solution was filtered and dried *in vacuo* to yield a purple powder of $[TaCl_2(\eta^2\text{-}P{\equiv}CBu^t)(\eta^5\text{-}C_5Me_5)]$ **XI** (0.032g, 29%).

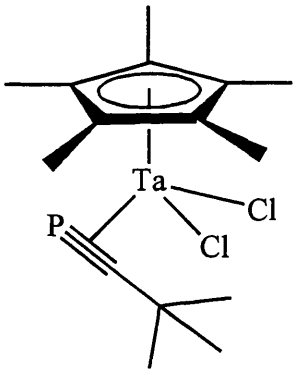

XI

$[TaCl_2(\eta^2\text{-}P{\equiv}CBu^t)(\eta^5\text{-}C_5Me_5)]$	calculated	%C	36.98	%H	4.97
	found	%C	36.7	%H	5.03

^1H NMR (CD_2Cl_2)

δ 1.89, s, 15H, $C_5(CH_3)_5$; 1.71, s, 9H, $P{\equiv}CC(CH_3)_3$.

$^{13}C\{^1H\}$ NMR (CD_2Cl_2)

δ 337.2, d, $P{\equiv}CC(CH_3)_3$, $^1J(CP) = 113Hz$; 122.2, $C_5(CH_3)_5$; 52.5, $P{\equiv}CC(CH_3)_3$; 34.6, $C_5(CH_3)_5$; 13.0, $P{\equiv}CC(CH_3)_3$.

$^{31}P\{^1H\}$ NMR (CD_2Cl_2)

δ 509.0, $P{\equiv}CC(CH_3)_3$.

CHAPTER 6

References

6 References.

1 Elschenbroich Ch., Salzer A., *Organometallics*, VCH, 2nd edition, 1992.

2 Bochmann M., *Organometallics 2*, OUP, 1st edition, 1994.

3 Tate D.P., Augl J.M., *J. Am. Chem. Soc.*, **85**, 1963, 2174.

4 Chatt J., Rowe G.A., Williams A.A., *Proc. Chem. Soc.*, 1957, 208.

5 Tate D.P., Augl J.M., Ritchey W.M., Ross B.L., Grasselli J.G., *J. Am. Chem. Soc.*, **86**, 1964, 3261.

6 King R.B., Fronzaglia A., *Inorg. Chem.*, **5**, 1966, 1837.

7 King R.B., *J. Organomet. Chem.*, **8**, 1967, 139.

8 King R.B., *Inorg. Chem*, **7**, 1968, 1044.

9 Laine R.M., Moriarty R.E., Bau R., *J. Am. Chem. Soc.*, **94**, 1972, 1402.

10 Bowerbank R., Green M., Kirsch H.P., Mortreux A., Smart L.E., Stone F.G.A., *J. Chem. Soc. Chem. Commun.*, 1977, 245.

11 Templeton J.L., *Adv. Organom. Chem.*, **29**, 1989, 1.

12 Templeton J.L., Ward B.C., *J. Am. Chem. Soc.*, **102**, 1980, 3290.

13 Odell K.J., Hyde E.M., Shaw B.L., Shepherd I., *J. Organomet. Chem.*, **168**, 1979, 103.

14 Connor J.A., Hudson G.A., *J. Organomet. Chem.*, **185**, 1980, 385.

15 Connor J.A., Hudson G.A., *J. Organomet. Chem.*, **160**, 1978, 159.

16 Chiu K.W., Lyons D., Wilkinson G., Thornton-Pett, M., Hursthouse M.B., *Polyhedron.*, **2**, 1983, 803.

17 Sharp P.R., Schrock R.R., *J. Am. Chem. Soc.*, **102**, 1980, 1430.

18 Wen-Yann Y., Che-Sheng T., Chu-fang C., *J. Organomet. Chem.*, **427**, 1991, 257.

19 Manion A.B., Erickson T.K.G., Spaltenstein E., Mayer J.M., *Organometallics.*, **8**, 1989, 1871

20 Conry R.R., Mayer J.M., *Organometallics.*, **12**, 1993, 3179.

21 Maher J.M., Fox J.R., Foxman B.M., Cooper N.J., *J. Am. Chem. Soc.*, **106**, 1984, 2347.

22 Wink D.J., Cooper N.J., *Organometallics.*, **10**, 1991, 494.

23 Ellis J.E., Hentges S.G., Kalina D.G., Hagen G.P., *J. Organomet. Chem.*, **97**, 1975, 79.

24 Wen-Yann Y., Ling-Kang L., *J. Am. Chem. Soc.*, **114**, 1992, 2267.

25 Wen-Yann Y., Shie-Ming P., Gene-Hsiang L., *J. Chem. Soc., Chem. Commun.*, 1993, 1056.

26 Wen-Yann Y., Shie-Ming P., Ling-Kang L., *Inorg. Chem.*, **32**, 1993, 2965.

27 Green M., Mahon M.F., Molloy K.C., Nation C.B.M., Woolhouse C.M., *J. Chem. Soc., Chem. Commun.*, 1991, 1587.

28 Bennett M.A., Nyholm R.S., Saxby J.D., *J. Organomet. Chem.*, **10**, 1967, 301.

29 Bennett M.A., Chiraratvatana C., *J. Organomet. Chem.*, **296**, 1985, 255.

30 Bennett M.A., Kapoor P.N., *J. Organomet. Chem.*, **336**, 1987, 257.

31 Bennett M.A., Chiraratvatana C., Robertson G.B., Tooptakong U., *Organometallics.*,**7**, 1988, 1394.

32 Allen S.R., Green M., Moran G., Orpen A.G., Taylor G.E., *J. Chem. Soc., Dalton Trans.*, 1984, 441.

33 Trost B.M., Lautens M., *J. Am. Chem. Soc.*, **107**, 1985, 1781.

34 Trost B.M., Shyh-Fong C., *J. Am. Chem. Soc.*, **108**, 1986, 6053.

35 Trost B.M., Tour J.M., *J. Am. Chem. Soc.*, **109**, 1987, 5268.

36 Trost B.M., Trost M.K., *J. Am. Chem. Soc.*, **113**, 1991, 1850.

37 Herrmann W.A., Fischer R.A., Herdtweck E., *Organometallics.*, **8**, 1989, 2821.

38 Dossett S.J., Green M.,Mahon M.F., McInnes J.M., *J. Chem. Soc., Chem. Commun.*, 1995, 767.

39 Cairns G.A., Carr N., Green M., Mahon M.F., *J. Chem. Soc., Chem. Commun.*, 1996, 2431.

40 Orpen A.G., Brammer L., Allen F.H., Kennard O., Watson D.G., Taylor R., *J. Chem. Soc., Dalton Trans.*, 1989, S1.

41 Carfagna C., Carr N., Deeth R.J., Dossett S.J., Green M., Mahon M.F., Vaughan C., *J. Chem. Soc., Dalton Trans.*, 1996, 415.

42 Holmes S.J., Schrock R.R., Churchill M.R., Wasserman H.J., *Organometallics.*, **3**, 1984, 476.

43 Mayr A., Dorries A.M., McDermott G.A., Geib S.J., Rheingold A.L., *J. Am. Chem. Soc.*, **107**, 1985, 7775.

44 Bottrill M., Green M., Orpen A.G., Saunders D.R., Williams I.D., *J. Chem. Soc., Dalton Trans.*, 1989, 511.

45 Fischer H., Hofmann P., Kreissl F. R., Schrock R.R., Schubert U., Weiss K., *Carbyne Complexes*, VCH, 1st Edition, 1988.

46 Green M., Norman N.C., Orpen A.G., *J. Am. Chem. Soc.*, **103**, 1981, 1267.

47 Allen S.R., Beevor R.G., Green M., Norman N.C., Orpen A.G., Williams I.D., *J. Chem. Soc., Dalton Trans.*, 1985, 435.

48 Fries A., Green M., Mahon M.F., McGrath T.D., Nation C.B.M., Walker A.P., Woolhouse C.M., *J. Chem. Soc., Dalton Trans.*, 1996, 4517.

49 Morrow J.R., Tonker T.L., Templeton J.L., *J. Am. Chem. Soc.*, **107**, 1985, 5004.

50 Hoffmann R., Wilker C.N., Eisenstein O., *J. Am. Chem. Soc.*, **104**, 1982, 632.

51 McDermott G.A., Mayr A., *J. Am. Chem. Soc.*, **109**, 1987, 580.

52 Mayr A., Bastos C.M., Daubenspeck N., McDermott G.A., *Chem. Ber.*, **125**, 1992,1583.

53 Carnahan E.M., Protasiewicz J.D., Lippard S.J., *Acc. Chem. Res.*, **26**, 1993, 90.

54 Protasiewicz J.D., Masschelein A., Lippard S.J., *J. Am. Chem. Soc.*, **115**, 1993, 808

55 LaPointe A.M., Schrock R.R., Davis W.M., *J. Am. Chem. Soc.*, **117**, 1995, 4802.

56 Brauers G., Feher F.J., Green M., Hogg J.K., Orpen A.G., *J. Chem. Soc., Dalton Trans*, 1996, 3387.

57 Herrison J.-L., Chauvin Y., *Makromol. Chem.*, **141**, 1970, 161.

58 Eisenstein O., Hoffmann R., *J. Am. Chem. Soc.*, **103**, 1981, 5582 and references therein.

59 Spangler D., Wendoloski J.J., Dupuis M., Chen M.M.L., Schaefer H.F, *J. Am. Chem. Soc.*, **103**, 1981, 3985.

60 Manganiello F.J., Radcliffe M.D., Jones W.M., *J. Organomet. Chem.*, **228**, 1982, 273.

61 Interrante L.V., Bennett M.A., Nyholm R.S., *Inorg. Chem.*, **5**, 1966, 2213.

62 Green M., Hughes R.P., *J. Chem. Soc., Dalton Trans.*, 1976, 1907.

63 Bianchini C., Meli A., Peruzzini M., Vizza F., Frediani P., *Organometallics.*, **9**, 1990, 1146.

64 Bianchini C., Innocenti P., Meli A., Peruzzini M., Zanobini F., Zanello P., *Organometallics.*, **9**, 1990, 2514.

65 Collmann J.P., Hegedes L.S., Norton T.R., Finke R.G., *Principles and Applications of Organotrasition Metal Chemistry*, University Science Books, 1987, 714.

66 Faller J.W., Rosan A.M., *J. Am. Chem. Soc.*, **99**, 1977, 4858.

67 Wade K., *Adv. Inorg. Chem. Radiochem.*, **18**, 1976, 1

68 Greenwood N.N., Earnshaw A., *Chemistry of the Elements*, Butterworth and Heinemann, 2nd Edition, 1997.

69 Leigh G.J. (ed.), *Nomenclature of Inorganic Chemistry: Recommendations 1990*, Blackwell, 1990, 207.

70 Hawthorne M.F., Weisboeck R.A., *J. Am. Chem. Soc.*, **86**, 1964, 1642.

71 Hawthorne M.F., Young D.C., Garrett P.M., Owen D.A., Schwerin S.G., Tebbe F.N., Wegner P.A., *J. Am. Chem. Soc.*, **90**, 1968, 862.

72 Hanusa T.P., *Polyhedron*, **1**, 1982, 663.

73 Callahan K.P., Hawthorne M.F., *Adv. Organom. Chem.*, **14**, 1976, 145.

74 Hawthorne M.F., Young D.C., Wenger P.A., *J. Am. Chem. Soc.*, **87**, 1965, 1818.

75 Dossett S.J., Li S., Stone F.G.A., *J. Chem. Soc., Dalton Trans.*, 1993, 1585.

76 Dossett S.J., Li S., Mullica D.F., Sappenfield E.L., Stone F.G.A., *J. Chem. Soc., Dalton Trans.*, 1993, 3551.

77 Brauers G., Dossett S.J., Green M., Mahon M.F., *J. Chem. Soc., Chem. Commun.*, 1995, 985.

78 Dauben H.J., Honnen L.R., *J. Am. Chem. Soc.*, **80**, 1958, 5570.

79 Eisch J.J., King R.B., *Organometallic Syntheses*, **1**, 1965, 122.

80 Bochmann M., Cooke M., Green M., Kirsh H.P., Stone F.G.A., Welch A.J., *J. Chem. Soc., Chem. Commun.*, 1976, 381.

81 King R.B., Bisnette M.B., *Inorg. Chem.*, **3**, 1964, 785.

82 King R.B., Fronzaglia A., *J. Am. Chem. Soc.*, **88**, 1966, 709.

83 Bennett M.A., Bramley R., Watt R., *J. Am. Chem. Soc.*, **91**, 1969, 3089.

84 Faller J.W., *Inorg. Chem.*, **8**, 1969, 767.

85 Brauers G., *Ph. D. Thesis*, University of Bath, 1996.

86 Brew S.A., Devore D.D., Jenkins P.D., Pilotti M.U., Stone F.G.A., *J. Chem. Soc., Dalton Trans.*, 1992, 393.

87 Regitz M., Scherer O.J., *Multiple Bonds and Low Co-ordination in Phosphorus Chemistry.*, Thieme, 1990, 58.

88 Hitchcock P.B., Maah M.J., Nixon J.F., Green M., *J. Organomet. Chem.*, **466**, 1994, 153.

89 Brauers G., Green M., Jones C., Nixon J.F., *J. Chem. Soc., Chem. Commun.*, 1995, 1125.

90 Burckett-St. Laurent J.C.T.R., Hitchcock P.B., Meidine M.F., Nixon J.F., *J. Chem. Soc., Chem. Commun.*, 1981, 1141.

91 Al-Resayes S.I., Hitchcock P.B., Meidine M.F., Nixon J.F., *J. Chem. Soc., Chem. Commun.*, 1984, 1080.

92 Al-Resayes S.I., Klein S.I., Kroto H.W., Meidine M.F., Nixon J.F., *J. Chem. Soc., Chem. Commun.*, 1983, 930.

93 Laali K.K., Geissler B., Wagner O., Hofman J., Armburst R., Eisfeld W., Regitz M., *J. Am. Chem. Soc.*, **116**, 1994, 9407.

94 Binger P., Biedenbach B., Herrmann A.T., Langhauser F., Betz P., Goddard R., Krüger C., *Chem. Ber.*, **123**, 1990, 1617.

95 Benvenutti M.H.A., Hitchcock P.B., Kiplinger J.L., Nixon J.F., Richmond T.G., *J. Chem. Soc., Chem. Commun.*, 1997, 1539.

96 Abel E.W., Stone F.G.A., Wilkinson G., *Comprehensive Organometallics 2*, Pergamon Press, **5**, 1995, 92.

97 Smith G., Schrock R.R., Churchill M.R., Youngs W.J., *Inorg. Chem.*, **20**, 1981, 387.

98 Kwon D., Curtis M.D., *Organometallics.*, **9**, 1990, 1.

99 King R.B., Eisch J.J., *Organometallic Syntheses.*, Elsevier, **4**, ,22.

100 Perrin D.D., Armavego W.L.F., Perrin D.R., *Purification of Laboratory Chemicals*, Pergamon Press, 2nd Edition.

101 Sheldrick G.M., *Acta Cryst.*, **A46**, 1990, 467.

102 Sheldrick G.M., *J.Appl.Cryst.*, 1995 (In preparation.).

103 McArdle P., *J.Appl.Cryst.*, **27**, 1994, 438.

CHAPTER 7

Appendix

7 Appendix.

7.1 Notes on Crystal Structure of [W(≡CPh){η^2-(E)-CHPh=CHC$_6$H$_4$PPh$_2$-o}(η^5-C$_5$Ph$_4$H)] Ia.

A crystal of approximate dimensions 0.2 x 0.2 x 0.2 mm was used for data collection.
Crystal data: $C_{63}H_{49}Cl_2PW$, M = 1091.74, Monoclinic , a = 12.785(3), b = 21.982(4), c = 17.830(4) Å , β = 99.20(2)°, U = 4946.5(18) Å^3, space group $P2_1/n$, Z = 4, D_C = 1.466 gcm^{-3}, (μMo-K_α) = 2.517 mm^{-1}, F(000) = 2200. Crystallographic measurements were made at 170(2)° K on a CAD4 automatic four-circle diffractometer in the range 2.05<θ<23.93°. Data (8136 reflections) were corrected for Lorentz and polarization but not for absorption.
In the final least squares cycles all atoms were allowed to vibrate anisotropically. Hydrogen atoms were included at calculated positions where relevant except for H55, H56 and H61 (attached to C55, C56 and C61 respectively), which were located in the penultimate difference Fourier and refined at a fixed distance from the relevant parent atoms.
The asymmetric unit was also seen to contain one solvent molecule of recrystallization (CH_2Cl_2).
The solution of the structure (SHELX86) [101] and refinement (SHELX93) [102] converged to a conventional [i.e. based on 5874 with $Fo>4\sigma(Fo)$] $R1$ = 0.0293 and $wR2$ = 0.0608. Goodness of fit = 1.107. The max. and min. residual densities were 1.485 and -0.678 eÅ^{-3} respectively. The asymmetric unit, Figure 7.1, along with the labelling scheme used was produced using ORTEX. [103] Final fractional atomic co-ordinates and isotropic thermal parameters, bond distances and angles are given in Tables 7.1, 7.2, 7.3, 7.4 and 7.5 respectively.

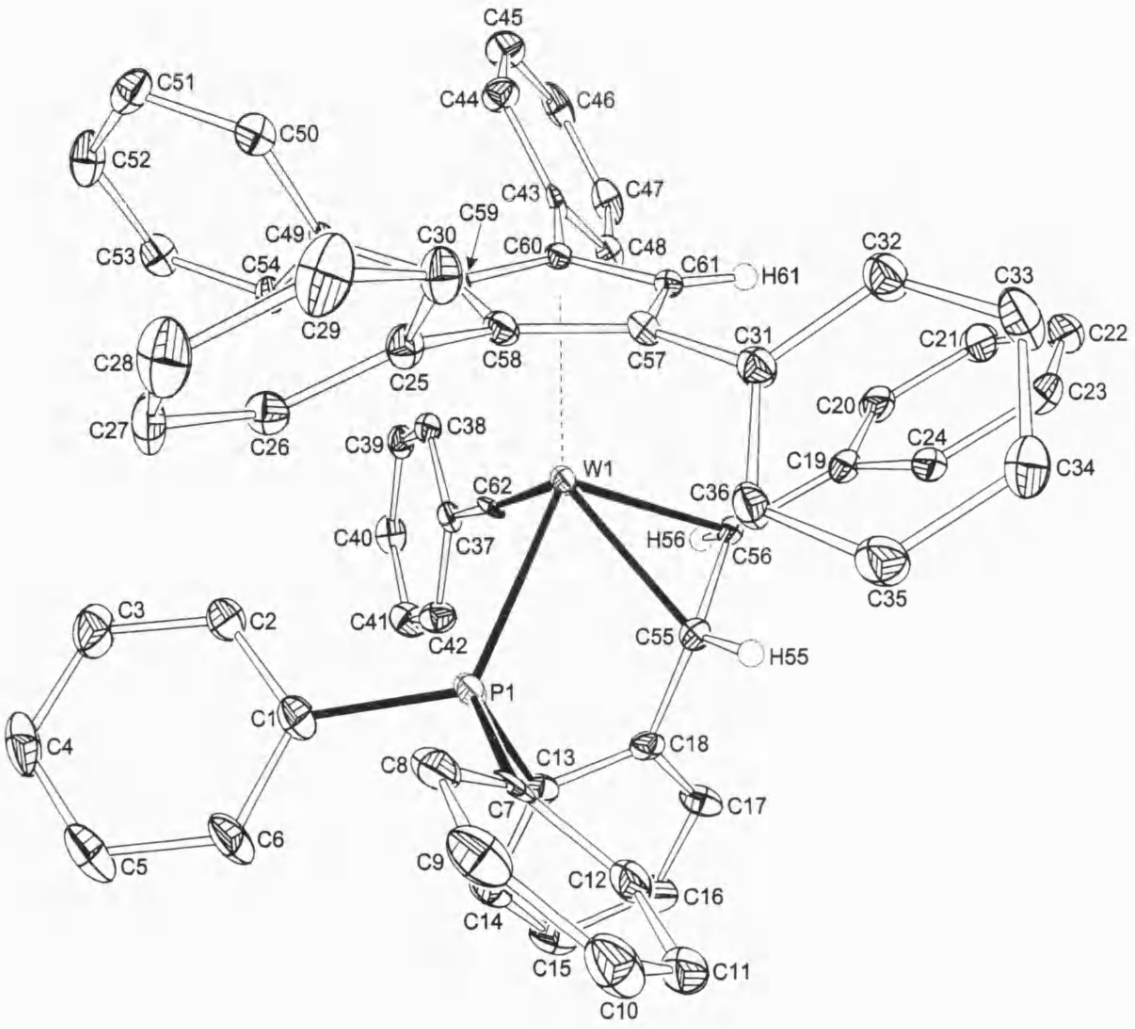
C45
C51
C44
C46
C50
C52
C43
C47
C59
C49
C30
C60
C48
C61
H61
C32
C33
C53
C54
C29
C31
C21
C22
C28
C58
C57
C25
C23
C20
C27
C26
C39
C38
C24
C19
C34
W1
C62
C36
C40
C37
H56
C56
C35
C3
C2
C41
C42
C55
H55
P1
C1
C4
C8
C13
C18
C7
C17
C6
C5
C9
C12
C16
C14
C15
C11
C10

Figure 7.1

Identification code	95MG8
Empirical formula	$C_{63}H_{49}Cl_2PW$
Formula weight	1091.74
Temperature	170(2)°K
Wavelength	0.70930 Å
Crystal system	Monoclinic
Space group	$P2_1/n$
Unit cell dimensions	a = 12.785(3)Å
	b = 21.982(4)Å β= 99.20(2)°
	c = 17.830(4)Å
Volume	4947(2) $Å^3$
Z	4
Density (calculated)	1.466 Mg/m^3
Absorption coefficient	2.517 mm^{-1}
F(000)	2200
Crystal size	0.2 x 0.2 x 0.2 mm
Theta range for data collection	2.05 to 23.93°
Index ranges	-14<=h<=0; 0<=k<=25; -20<=l<=20
Reflections collected	8136
Independent reflections	7749 [R(int) = 0.0340]
Refinement method	Full-matrix least-squares on F^2
Data / restraints / parameters	7741 / 3 / 617
Goodness-of-fit on F^2	1.107
Final R indices [I>2sigma(I)]	R1 = 0.0293 wR2 = 0.0608
R indices (all data)	R1 = 0.0603 wR2 = 0.0736
Largest diff. peak and hole	1.485 and -0.678 $eÅ^{-3}$
Weighting scheme	calc $w=1/[\sigma^2(Fo^2)+(0.0278P)^2+12.1483P]$
	where $P=(Fo^2+2Fc^2)/3$
Extinction coefficient	0.00009(5)
Extinction expression	$Fc^*=kFc[1+0.001xFc^2\lambda^3/\sin(2\theta)]^{-1/4}$

Table 7.1 Crystal data and structure refinement for **Ia**.

Atom	x	y	z	U(eq)
W(1)	1826(1)	848(1)	2424(1)	13(1)
P(1)	3372(1)	621(1)	3392(1)	18(1)
Cl(1)	1389(1)	1192(1)	6556(1)	45(1)
Cl(2)	2166(1)	2043(1)	7777(1)	45(1)
C(1)	4337(4)	1200(2)	3764(3)	23(1)
C(2)	4140(4)	1808(2)	3565(3)	25(1)
C(3)	4911(5)	2249(3)	3765(3)	34(1)
C(4)	5873(4)	2090(3)	4180(3)	36(2)
C(5)	6063(4)	1498(3)	4412(3)	37(2)
C(6)	5304(4)	1052(3)	4202(3)	31(1)
C(7)	4256(4)	-16(2)	3244(3)	18(1)
C(8)	5114(4)	69(2)	2869(3)	24(1)
C(9)	5747(4)	-421(3)	2726(3)	30(1)
C(10)	5523(4)	-998(3)	2959(3)	32(1)
C(11)	4678(4)	-1087(3)	3338(3)	31(1)
C(12)	4044(4)	-607(2)	3479(3)	24(1)
C(13)	2764(4)	344(2)	4182(3)	21(1)
C(14)	3130(4)	387(2)	4958(3)	25(1)
C(15)	2512(4)	150(3)	5457(3)	31(1)
C(16)	1564(4)	-134(3)	5195(3)	32(1)
C(17)	1209(4)	-184(2)	4417(3)	24(1)
C(18)	1810(4)	50(2)	3909(3)	18(1)
C(19)	-190(4)	-137(2)	2090(3)	22(1)
C(20)	-1275(4)	5(2)	1920(3)	28(1)
C(21)	-1954(4)	-313(3)	1368(3)	32(1)
C(22)	-1579(4)	-779(3)	969(3)	34(1)
C(23)	-514(4)	-931(2)	1122(3)	31(1)
C(24)	174(4)	-618(2)	1682(3)	23(1)
C(25)	3926(4)	999(2)	1265(3)	17(1)
C(26)	4638(4)	1357(2)	1749(3)	19(1)
C(27)	5683(4)	1401(2)	1642(3)	24(1)
C(28)	6041(4)	1101(2)	1053(3)	30(1)
C(29)	5333(4)	753(2)	563(3)	31(1)
C(30)	4289(4)	702(2)	664(3)	22(1)
C(31)	2286(4)	-147(2)	965(3)	18(1)
C(32)	1663(4)	-451(2)	365(3)	23(1)
C(33)	1826(4)	-1059(2)	224(3)	29(1)
C(34)	2623(4)	-1381(2)	675(3)	27(1)
C(35)	3263(4)	-1084(2)	1255(3)	26(1)
C(36)	3103(4)	-477(2)	1403(3)	19(1)
C(37)	1028(4)	1827(2)	3561(3)	18(1)
C(38)	408(4)	2327(2)	3265(3)	20(1)
C(39)	-48(4)	2718(2)	3730(3)	22(1)
C(40)	124(4)	2634(2)	4508(3)	26(1)

C(41)	735(4)	2149(3)	4816(3)	29(1)
C(42)	1182(4)	1749(2)	4354(3)	25(1)
C(43)	146(4)	1768(2)	1235(3)	15(1)
C(44)	72(4)	2262(2)	742(3)	22(1)
C(45)	-820(4)	2635(2)	636(3)	29(1)
C(46)	-1627(4)	2521(3)	1034(3)	30(1)
C(47)	-1571(4)	2034(3)	1529(3)	28(1)
C(48)	-684(4)	1660(2)	1630(3)	21(1)
C(49)	2577(3)	2158(2)	1455(3)	14(1)
C(50)	2457(3)	2557(2)	2047(3)	16(1)
C(51)	2837(4)	3145(2)	2050(3)	22(1)
C(52)	3335(4)	3351(2)	1468(3)	26(1)
C(53)	3447(4)	2967(2)	871(3)	24(1)
C(54)	3070(4)	2375(2)	870(3)	20(1)
C(55)	1526(4)	14(2)	3059(3)	18(1)
C(56)	503(4)	223(2)	2678(3)	16(1)
C(57)	2057(4)	488(2)	1138(3)	16(1)
C(58)	2774(4)	988(2)	1324(3)	16(1)
C(59)	2175(4)	1524(2)	1416(3)	14(1)
C(60)	1072(3)	1357(2)	1295(3)	14(1)
C(61)	1023(4)	726(2)	1134(3)	14(1)
C(62)	1452(3)	1395(2)	3083(3)	15(1)
C(63)	1044(5)	1709(3)	7231(4)	48(2)

Table 7.2 Atomic coordinates (x 10^4) and equivalent isotropic displacement parameters ($Å^2$ x 10^3) for **Ia**. U(eq) is defined as one third of the trace of the orthogonalized Uij tensor.

W(1)-C(62)	1.799(5)	C(25)-C(30)	1.395(7)
W(1)-C(55)	2.220(5)	C(25)-C(58)	1.493(6)
W(1)-C(56)	2.281(5)	C(26)-C(27)	1.383(7)
W(1)-C(60)	2.368(4)	C(27)-C(28)	1.379(7)
W(1)-C(61)	2.379(4)	C(28)-C(29)	1.385(8)
W(1)-C(59)	2.428(5)	C(29)-C(30)	1.379(7)
W(1)-P(1)	2.4595(14)	C(31)-C(32)	1.397(7)
W(1)-C(58)	2.484(5)	C(31)-C(36)	1.403(7)
W(1)-C(57)	2.487(5)	C(31)-C(57)	1.468(7)
P(1)-C(13)	1.818(5)	C(32)-C(33)	1.381(7)
P(1)-C(1)	1.822(5)	C(33)-C(34)	1.387(7)
P(1)-C(7)	1.843(5)	C(34)-C(35)	1.378(7)
Cl(1)-C(63)	1.763(7)	C(35)-C(36)	1.382(7)
Cl(2)-C(63)	1.760(6)	C(37)-C(38)	1.406(7)
C(1)-C(6)	1.392(7)	C(37)-C(42)	1.407(7)
C(1)-C(2)	1.397(7)	C(37)-C(62)	1.438(7)
C(2)-C(3)	1.388(7)	C(38)-C(39)	1.387(7)
C(3)-C(4)	1.375(8)	C(39)-C(40)	1.382(7)
C(4)-C(5)	1.374(9)	C(40)-C(41)	1.382(7)
C(5)-C(6)	1.388(8)	C(41)-C(42)	1.390(7)
C(7)-C(8)	1.387(7)	C(43)-C(48)	1.385(7)
C(7)-C(12)	1.404(7)	C(43)-C(44)	1.392(7)
C(8)-C(9)	1.394(7)	C(43)-C(60)	1.479(6)
C(9)-C(10)	1.378(8)	C(44)-C(45)	1.392(7)
C(10)-C(11)	1.376(8)	C(45)-C(46)	1.366(8)
C(11)-C(12)	1.378(7)	C(46)-C(47)	1.383(8)
C(13)-C(14)	1.392(7)	C(47)-C(48)	1.388(7)
C(13)-C(18)	1.397(7)	C(49)-C(54)	1.386(7)
C(14)-C(15)	1.383(8)	C(49)-C(50)	1.399(6)
C(15)-C(16)	1.377(8)	C(49)-C(59)	1.483(7)
C(16)-C(17)	1.393(7)	C(50)-C(51)	1.379(7)
C(17)-C(18)	1.379(7)	C(51)-C(52)	1.378(7)
C(18)-C(55)	1.502(7)	C(52)-C(53)	1.383(7)
C(19)-C(24)	1.403(7)	C(53)-C(54)	1.388(7)
C(19)-C(20)	1.407(7)	C(55)-C(56)	1.450(7)
C(19)-C(56)	1.488(7)	C(57)-C(61)	1.420(6)
C(20)-C(21)	1.392(7)	C(57)-C(58)	1.436(6)
C(21)-C(22)	1.377(8)	C(58)-C(59)	1.430(6)
C(22)-C(23)	1.386(8)	C(59)-C(60)	1.439(6)
C(23)-C(24)	1.402(7)	C(60)-C(61)	1.417(6)
C(25)-C(26)	1.394(7)		

C(62)-W(1)-C(55)	97.6(2)	C(26)-C(25)-C(30)	118.3(4)
C(62)-W(1)-C(56)	89.4(2)	C(26)-C(25)-C(58)	121.3(4)
C(55)-W(1)-C(56)	37.5(2)	C(30)-C(25)-C(58)	120.0(4)
C(62)-W(1)-C(60)	97.2(2)	C(27)-C(26)-C(25)	120.3(5)

C(55)-W(1)-C(60)	138.1(2)	C(28)-C(27)-C(26)	121.2(5)
C(56)-W(1)-C(60)	103.9(2)	C(27)-C(28)-C(29)	118.8(5)
C(62)-W(1)-C(61)	126.1(2)	C(30)-C(29)-C(28)	120.7(5)
C(55)-W(1)-C(61)	108.5(2)	C(29)-C(30)-C(25)	120.7(5)
C(56)-W(1)-C(61)	84.5(2)	C(32)-C(31)-C(36)	117.5(5)
C(60)-W(1)-C(61)	34.7(2)	C(32)-C(31)-C(57)	120.5(4)
C(62)-W(1)-C(59)	100.0(2)	C(36)-C(31)-C(57)	121.9(4)
C(55)-W(1)-C(59)	161.9(2)	C(33)-C(32)-C(31)	121.2(5)
C(56)-W(1)-C(59)	138.2(2)	C(32)-C(33)-C(34)	120.5(5)
C(60)-W(1)-C(59)	34.9(2)	C(35)-C(34)-C(33)	119.1(5)
C(61)-W(1)-C(59)	57.0(2)	C(34)-C(35)-C(36)	120.9(5)
C(62)-W(1)-P(1)	86.82(14)	C(35)-C(36)-C(31)	120.8(5)
C(55)-W(1)-P(1)	70.04(13)	C(38)-C(37)-C(42)	116.8(4)
C(56)-W(1)-P(1)	106.06(12)	C(38)-C(37)-C(62)	122.5(4)
C(60)-W(1)-P(1)	149.86(11)	C(42)-C(37)-C(62)	120.6(4)
C(61)-W(1)-P(1)	146.10(12)	C(39)-C(38)-C(37)	121.7(5)
C(59)-W(1)-P(1)	114.96(11)	C(40)-C(39)-C(38)	120.2(5)
C(62)-W(1)-C(58)	130.4(2)	C(39)-C(40)-C(41)	119.4(5)
C(55)-W(1)-C(58)	130.6(2)	C(40)-C(41)-C(42)	120.8(5)
C(56)-W(1)-C(58)	134.6(2)	C(41)-C(42)-C(37)	121.0(5)
C(60)-W(1)-C(58)	56.9(2)	C(48)-C(43)-C(44)	118.4(4)
C(61)-W(1)-C(58)	56.0(2)	C(48)-C(43)-C(60)	121.9(4)
C(59)-W(1)-C(58)	33.8(2)	C(44)-C(43)-C(60)	119.6(4)
P(1)-W(1)-C(58)	98.09(11)	C(45)-C(44)-C(43)	121.1(5)
C(62)-W(1)-C(57)	154.0(2)	C(46)-C(45)-C(44)	119.5(5)
C(55)-W(1)-C(57)	105.2(2)	C(45)-C(46)-C(47)	120.4(5)
C(56)-W(1)-C(57)	101.1(2)	C(46)-C(47)-C(48)	120.0(5)
C(60)-W(1)-C(57)	57.3(2)	C(43)-C(48)-C(47)	120.6(5)
C(61)-W(1)-C(57)	33.8(2)	C(54)-C(49)-C(50)	118.0(4)
C(59)-W(1)-C(57)	56.6(2)	C(54)-C(49)-C(59)	118.9(4)
P(1)-W(1)-C(57)	112.46(11)	C(50)-C(49)-C(59)	123.1(4)
C(58)-W(1)-C(57)	33.6(2)	C(51)-C(50)-C(49)	120.6(4)
C(13)-P(1)-C(1)	107.5(2)	C(52)-C(51)-C(50)	120.7(5)
C(13)-P(1)-C(7)	101.8(2)	C(51)-C(52)-C(53)	119.8(5)
C(1)-P(1)-C(7)	100.8(2)	C(52)-C(53)-C(54)	119.5(5)
C(13)-P(1)-W(1)	102.5(2)	C(49)-C(54)-C(53)	121.5(5)
C(1)-P(1)-W(1)	122.3(2)	C(56)-C(55)-C(18)	120.7(4)
C(7)-P(1)-W(1)	119.7(2)	C(56)-C(55)-W(1)	73.5(3)
C(6)-C(1)-C(2)	118.3(5)	C(18)-C(55)-W(1)	115.9(3)
C(6)-C(1)-P(1)	122.0(4)	C(55)-C(56)-C(19)	123.6(4)
C(2)-C(1)-P(1)	119.5(4)	C(55)-C(56)-W(1)	69.0(3)
C(3)-C(2)-C(1)	120.8(5)	C(19)-C(56)-W(1)	123.9(3)
C(4)-C(3)-C(2)	119.8(6)	C(61)-C(57)-C(58)	106.2(4)
C(5)-C(4)-C(3)	120.2(5)	C(61)-C(57)-C(31)	124.4(4)
C(4)-C(5)-C(6)	120.3(5)	C(58)-C(57)-C(31)	129.4(4)
C(5)-C(6)-C(1)	120.4(5)	C(61)-C(57)-W(1)	68.9(3)
C(8)-C(7)-C(12)	118.2(5)	C(58)-C(57)-W(1)	73.1(3)

C(8)-C(7)-P(1)	121.2(4)	C(31)-C(57)-W(1)	123.6(3)
C(12)-C(7)-P(1)	120.5(4)	C(59)-C(58)-C(57)	108.9(4)
C(7)-C(8)-C(9)	120.7(5)	C(59)-C(58)-C(25)	123.2(4)
C(10)-C(9)-C(8)	120.1(5)	C(57)-C(58)-C(25)	126.6(4)
C(11)-C(10)-C(9)	119.7(5)	C(59)-C(58)-W(1)	70.9(3)
C(10)-C(11)-C(12)	120.7(5)	C(57)-C(58)-W(1)	73.3(3)
C(11)-C(12)-C(7)	120.5(5)	C(25)-C(58)-W(1)	132.0(3)
C(14)-C(13)-C(18)	120.9(5)	C(58)-C(59)-C(60)	107.6(4)
C(14)-C(13)-P(1)	129.1(4)	C(58)-C(59)-C(49)	126.4(4)
C(18)-C(13)-P(1)	110.1(4)	C(60)-C(59)-C(49)	124.8(4)
C(15)-C(14)-C(13)	118.7(5)	C(58)-C(59)-W(1)	75.2(3)
C(16)-C(15)-C(14)	120.9(5)	C(60)-C(59)-W(1)	70.3(3)
C(15)-C(16)-C(17)	120.3(5)	C(49)-C(59)-W(1)	130.0(3)
C(18)-C(17)-C(16)	119.8(5)	C(61)-C(60)-C(59)	106.9(4)
C(17)-C(18)-C(13)	119.5(4)	C(61)-C(60)-C(43)	125.0(4)
C(17)-C(18)-C(55)	125.0(5)	C(59)-C(60)-C(43)	127.5(4)
C(13)-C(18)-C(55)	115.6(4)	C(61)-C(60)-W(1)	73.0(3)
C(24)-C(19)-C(20)	116.9(5)	C(59)-C(60)-W(1)	74.8(3)
C(24)-C(19)-C(56)	123.8(5)	C(25)-C(58)-W(1)	132.0(3)
C(20)-C(19)-C(56)	119.3(5)	C(60)-C(61)-C(57)	110.4(4)
C(21)-C(20)-C(19)	121.6(5)	C(60)-C(61)-W(1)	72.2(3)
C(22)-C(21)-C(20)	120.6(5)	C(57)-C(61)-W(1)	77.2(3)
C(21)-C(22)-C(23)	119.3(5)	C(37)-C(62)-W(1)	173.2(4)
C(22)-C(23)-C(24)	120.5(5)	Cl(2)-C(63)-Cl(1)	112.0(3)
C(23)-C(24)-C(19)	121.1(5)		

Table 7.3 Bond lengths [Å] and angles [°] for **Ia**.

Atom	U11	U22	U33	U23	U13	U12
W(1)	12(1)	11(1)	14(1)	-1(1)	-3(1)	0(1)
P(1)	15(1)	16(1)	19(1)	-2(1)	-5(1)	1(1)
Cl(1)	45(1)	42(1)	46(1)	8(1)	5(1)	-7(1)
Cl(2)	40(1)	47(1)	51(1)	2(1)	11(1)	-11(1)
C(1)	21(3)	25(3)	22(3)	-7(2)	0(2)	-1(2)
C(2)	31(3)	24(3)	19(3)	-6(2)	0(2)	-5(2)
C(3)	45(4)	27(3)	30(3)	-9(3)	4(3)	-13(3)
C(4)	31(3)	45(4)	30(3)	-18(3)	4(3)	-21(3)
C(5)	22(3)	48(4)	36(3)	-16(3)	-9(3)	-2(3)
C(6)	25(3)	31(3)	32(3)	-15(3)	-11(2)	1(2)
C(7)	13(2)	24(3)	15(2)	-5(2)	-11(2)	5(2)
C(8)	23(3)	27(3)	19(3)	-1(2)	-6(2)	1(2)
C(9)	19(3)	43(4)	27(3)	-6(3)	-1(2)	6(3)
C(10)	23(3)	33(4)	36(3)	-13(3)	-6(2)	9(2)
C(11)	29(3)	20(3)	38(3)	-1(2)	-13(3)	4(2)
C(12)	16(3)	24(3)	28(3)	-2(2)	-5(2)	2(2)
C(13)	22(3)	21(3)	20(3)	0(2)	1(2)	10(2)
C(14)	22(3)	26(3)	25(3)	-6(2)	-8(2)	10(2)
C(15)	32(3)	39(3)	18(3)	-2(2)	-2(2)	12(3)
C(16)	27(3)	45(4)	26(3)	6(3)	9(2)	12(3)
C(17)	19(3)	32(3)	19(3)	1(2)	-1(2)	8(2)
C(18)	22(3)	13(3)	19(3)	0(2)	0(2)	8(2)
C(19)	24(3)	19(3)	22(3)	6(2)	0(2)	-8(2)
C(20)	25(3)	25(3)	31(3)	8(2)	-1(2)	-8(2)
C(21)	24(3)	33(3)	35(3)	9(3)	-8(3)	-11(3)
C(22)	35(3)	32(3)	29(3)	5(3)	-13(2)	-14(3)
C(23)	46(3)	19(3)	25(3)	5(2)	1(3)	-13(3)
C(24)	25(3)	19(3)	22(3)	5(2)	-6(2)	-5(2)
C(25)	16(2)	14(3)	21(3)	-1(2)	2(2)	1(2)
C(26)	17(3)	20(3)	19(3)	0(2)	3(2)	2(2)
C(27)	17(3)	18(3)	37(3)	-2(2)	1(2)	-7(2)
C(28)	14(3)	30(3)	47(4)	-3(3)	12(3)	1(2)
C(29)	28(3)	25(3)	45(3)	-5(3)	21(3)	-1(2)
C(30)	25(3)	16(3)	26(3)	-4(2)	3(2)	-3(2)
C(31)	16(3)	19(3)	18(3)	-1(2)	0(2)	0(2)
C(32)	21(3)	23(3)	23(3)	-2(2)	-3(2)	1(2)
C(33)	27(3)	29(3)	28(3)	-12(2)	-5(2)	-2(2)
C(34)	34(3)	18(3)	29(3)	-6(2)	4(3)	-1(2)
C(35)	25(3)	24(3)	26(3)	0(2)	-3(2)	6(2)
C(36)	18(3)	16(3)	21(3)	-5(2)	-4(2)	1(2)
C(37)	17(3)	18(3)	17(3)	-3(2)	-1(2)	-5(2)
C(38)	21(3)	16(3)	20(3)	0(2)	0(2)	-1(2)
C(39)	18(3)	16(3)	32(3)	-2(2)	0(2)	0(2)
C(40)	20(3)	28(3)	32(3)	-8(2)	10(2)	0(2)

C(41)	26(3)	42(3)	19(3)	-2(3)	6(2)	0(3)
C(42)	22(3)	27(3)	26(3)	5(2)	3(2)	5(2)
C(43)	13(2)	14(2)	16(2)	-8(2)	-3(2)	-3(2)
C(44)	20(3)	21(3)	24(3)	6(2)	1(2)	4(2)
C(45)	33(3)	19(3)	31(3)	6(2)	-6(3)	9(2)
C(46)	19(3)	28(3)	38(3)	-16(3)	-10(2)	9(2)
C(47)	14(3)	35(3)	34(3)	-13(3)	4(2)	-1(2)
C(48)	18(3)	21(3)	21(3)	-4(2)	-1(2)	-2(2)
C(49)	4(2)	17(3)	21(3)	-1(2)	-3(2)	3(2)
C(50)	9(2)	19(3)	20(2)	-1(2)	2(2)	1(2)
C(51)	21(3)	18(3)	26(3)	-5(2)	2(2)	4(2)
C(52)	22(3)	12(3)	46(4)	-3(2)	8(3)	0(2)
C(53)	17(3)	22(3)	34(3)	12(2)	8(2)	2(2)
C(54)	21(3)	18(3)	21(3)	-2(2)	4(2)	3(2)
C(55)	20(3)	12(3)	20(3)	0(2)	-1(2)	1(2)
C(56)	17(2)	14(3)	17(3)	4(2)	0(2)	-3(2)
C(57)	16(2)	18(3)	12(2)	-1(2)	-2(2)	-1(2)
C(58)	17(2)	15(3)	15(2)	0(2)	-3(2)	1(2)
C(59)	15(2)	16(3)	11(2)	-4(2)	1(2)	0(2)
C(60)	14(2)	13(2)	12(2)	0(2)	-1(2)	2(2)
C(61)	15(2)	12(3)	13(2)	1(2)	-3(2)	-1(2)
C(62)	13(2)	18(3)	12(2)	2(2)	-9(2)	-1(2)
C(63)	27(3)	75(5)	44(4)	-2(4)	11(3)	-10(3)

Table 7.4 Anisotropic displacement parameters ($Å^2$ x 10^3) for **Ia**.
The anisotropic displacement factor exponent takes the form:
$-2\ pi^2\ [\ h^2\ a^*\ 2\ U11 + ... + 2\ h\ k\ a^*\ b^*\ U12\ ]$

Atom	x	y	z	U(eq)
H(2)	3484(4)	1919(2)	3295(3)	30
H(3)	4777(5)	2652(3)	3619(3)	41
H(4)	6396(4)	2383(3)	4304(3)	43
H(5)	6703(4)	1396(3)	4711(3)	44
H(6)	5443(4)	652(3)	4355(3)	37
H(8)	5270(4)	457(2)	2710(3)	29
H(9)	6321(4)	-358(3)	2474(3)	36
H(10)	5940(4)	-1325(3)	2859(3)	38
H(11)	4534(4)	-1475(3)	3501(3)	37
H(12)	3472(4)	-674(2)	3731(3)	28
H(14)	3776(4)	571(2)	5137(3)	30
H(15)	2740(4)	184(3)	5978(3)	37
H(16)	1160(4)	-293(3)	5538(3)	38
H(17)	568(4)	-376(2)	4241(3)	29
H(20)	-1545(4)	318(2)	2182(3)	33
H(21)	-2668(4)	-209(3)	1268(3)	38
H(22)	-2036(4)	-991(3)	601(3)	40
H(23)	-254(4)	-1242(2)	850(3)	37
H(24)	884(4)	-731(2)	1786(3)	28
H(26)	4410(4)	1567(2)	2146(3)	22
H(27)	6153(4)	1637(2)	1973(3)	29
H(28)	6746(4)	1131(2)	986(3)	36
H(29)	5563(4)	551(2)	160(3)	37
H(30)	3823(4)	468(2)	329(3)	27
H(32)	1129(4)	-241(2)	55(3)	28
H(33)	1399(4)	-1254(2)	-176(3)	35
H(34)	2723(4)	-1793(2)	587(3)	32
H(35)	3811(4)	-1294(2)	1551(3)	31
H(36)	3542(4)	-284(2)	1799(3)	23
H(38)	301(4)	2396(2)	2744(3)	23
H(39)	-470(4)	3038(2)	3518(3)	27
H(40)	-168(4)	2902(2)	4822(3)	31
H(41)	848(4)	2090(3)	5340(3)	34
H(42)	1589(4)	1425(2)	4572(3)	30
H(44)	628(4)	2345(2)	479(3)	26
H(45)	-866(4)	2958(2)	296(3)	34
H(46)	-2219(4)	2773(3)	971(3)	36
H(47)	-2127(4)	1957(3)	1794(3)	33
H(48)	-648(4)	1335(2)	1966(3)	25
H(50)	2118(3)	2426(2)	2442(3)	19
H(51)	2757(4)	3404(2)	2449(3)	26
H(52)	3594(4)	3746(2)	1476(3)	32
H(53)	3773(4)	3105(2)	472(3)	29
H(54)	3149(4)	2118(2)	469(3)	24

H(55)	1763(32)	-334(15)	2858(23)	8(11)
H(56)	129(34)	453(20)	2993(23)	18(13)
H(61)	421(27)	513(20)	1049(26)	15(13)
H(63A)	599(5)	2027(3)	6971(4)	58
H(63B)	638(5)	1498(3)	7566(4)	58

Table 7.5 Hydrogen coordinates (x 10^4) and isotropic displacement parameters ($Å^2$ x 10^3) for 1.

7.2 Notes on Crystal Structure of II.

A crystal of approximate dimensions 0.17 x 0.17 x 0.2 mm was used for data collection. *Crystal data:* C_{63} H_{49} P W, M = 1020.84, Monoclinic , a = 12.060, b = 18.020, c = 21.755 Å , β = 90.16°, U = 4727.8 $Å^3$, space group $P2_1/n$, Z = 4, D_C = 1.434 gcm^{-3}, (μMo-K_α) = 2.518 mm^{-1}, $F(000)$ = 2064. Crystallographic measurements were made at 293(2)° K on a CAD4 automatic four-circle diffractometer in the range $2.03<\theta<22.00°$. Data (6162 reflections) were corrected for Lorentz and polarization but not for absorption.

In the final least squares cycles all atoms were allowed to vibrate anisotropically. Hydrogen atoms were included at calculated positions where relevant except in the cases of H34, H35 and H37 which were located in the penultimate difference Fourier map and refined at a fixed distance of 0.96 Å from the relevant parent atoms.

Anisotropic thermal parameters of the phenyl carbon atoms are generally larger than might be expected in this structure, as a consequence of a fall off in the intensity of diffraction data at higher Bragg angles. Application of an empirical absorption correction, which would have inevitably reduced the contribution of weak high-angle data to the structure factor calculations thereby shrinking the thermal parameters artificially, was not applied to this data set due to the small crystal size. (A trial run which *did* include an empirical absorption correction afforded little improvement in R factors and only a minor reduction of residual peak heights in the electron density map.)

The solution of the structure (SHELX86) [101] and refinement (SHELX93) [102] converged to a conventional [i.e. based on 3345 with $Fo>4\sigma(Fo)$] $R1$ = 0.0497 and $wR2$ = 0.0969. Goodness of fit = 1.062. The max. and min. residual densities were 0.855 and -1.587e$Å^{-3}$ respectively. The asymmetric unit, Figure 7.2, along with the labelling scheme used was produced using ORTEX. [103] Final fractional atomic co-ordinates and isotropic thermal parameters, bond distances and angles are given in Tables 7.6, 7.7, 7.8, 7.9 and 7.10 respectively.

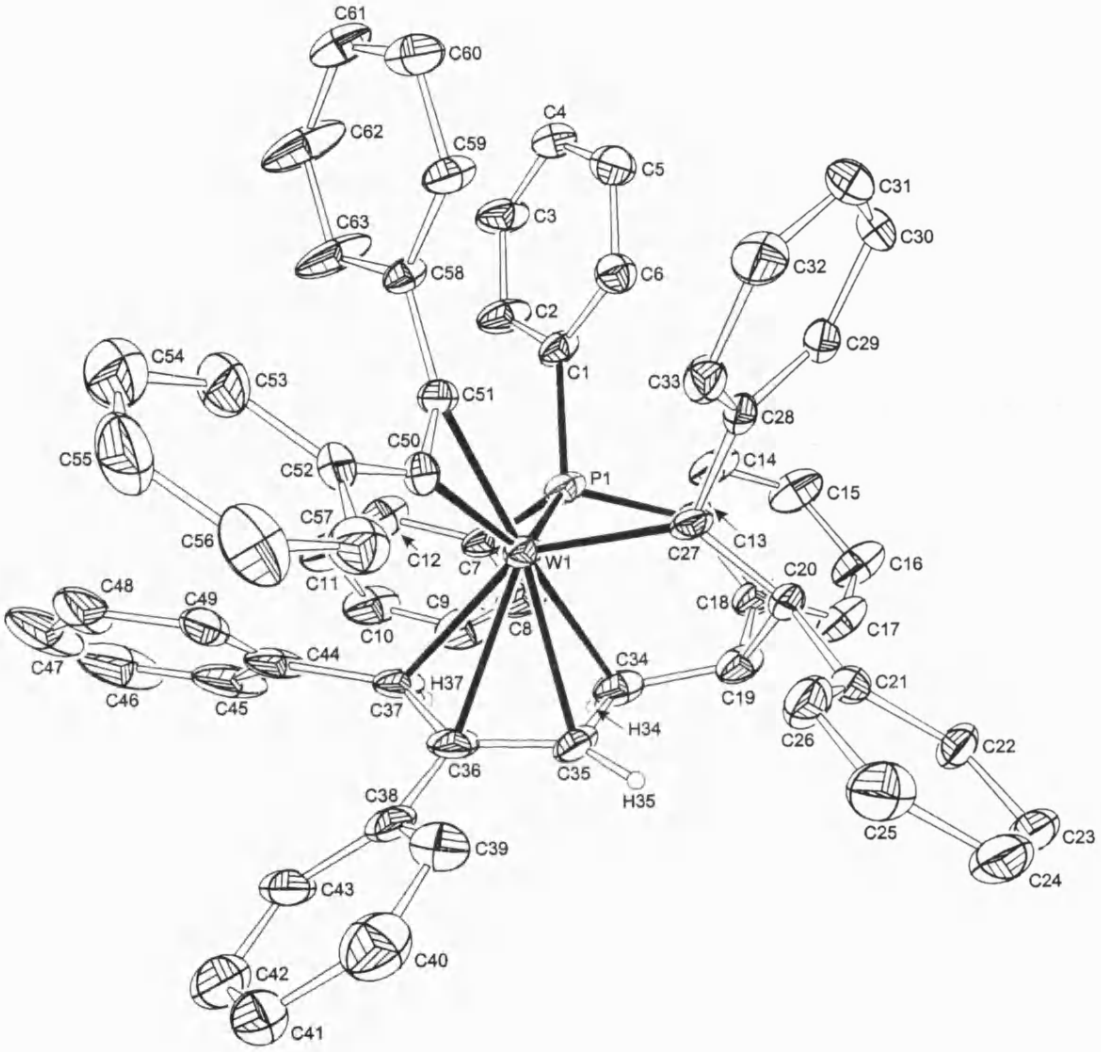
C61
C60
C62
C59
C4
C5
C63
C3
C31
C30
C58
C6
C32
C2
C29
C1
C54
C53
C51
C33
C28
C55
C50
C52
P1
C14
C15
C57
C56
C12
C7
W1
C27
C13
C16
C11
C20
C48
C49
C9
C18
C10
C8
C17
C44
C47
H37
C34
C21
C46
C45
C37
C19
H34
C26
C22
C36
C35
C38
H35
C25
C23
C39
C43
C24
C40
C42
C41

Figure 7.2.

Identification code	96MG1
Empirical formula	$C_{63}H_{49}PW$
Formula weight	1020.84
Temperature	293(2)° K
Wavelength	0.70930 Å
Crystal system	Monoclinic
Space group	$P2_1/n$
Unit cell dimensions	a = 12.060Å
	b = 18.020Å β= 90.16°
	c = 21.755Å
Volume	4727.8 $Å^3$
Z	4
Density (calculated)	1.434 Mg/m^3
Absorption coefficient	2.518 mm^{-1}
F(000)	2064
Crystal size	0.17 x 0.17 x 0.2 mm
Theta range for data collection	2.03 to 22.00°
Index ranges	-13<=h<=0; 0<=k<=20; -24<=l<=24
Reflections collected	6162
Independent reflections	5832 [R(int) = 0.0441]
Refinement method	Full-matrix least-squares on F^2
Data / restraints / parameters	5638 / 3 / 488
Goodness-of-fit on F^2	1.062
Final R indices [I>2σ(I)]	R1 = 0.0497 wR2 = 0.0969
R indices (all data)	R1 = 0.1351 wR2 = 0.1304
Largest diff. peak and hole	0.855 and -1.587 $eÅ^{-3}$
Weighting scheme	calc $w=1/[\sigma^2(Fo^2)+(0.0438P)^2+20.9168P]$
	where $P=(Fo^2+2Fc^2)/3$
Extinction coefficient	0.00050(9)

Table 7.6 Crystal data and structure refinement for **II**.

Atom	x	y	z	U(eq)
W(1)	3359(1)	2148(1)	484(1)	55(1)
P(1)	4692(3)	2496(2)	1288(2)	65(1)
C(1)	4199(6)	3105(4)	1905(3)	61(3)
C(2)	4767(5)	3746(4)	2072(4)	91(5)
C(3)	4366(7)	4191(4)	2543(4)	99(5)
C(4)	3398(8)	3995(5)	2849(3)	86(4)
C(5)	2831(5)	3354(5)	2682(3)	77(4)
C(6)	3231(6)	2909(4)	2210(4)	66(3)
C(7)	5949(5)	2964(4)	1017(4)	72(4)
C(8)	7001(7)	2658(4)	1075(4)	97(5)
C(9)	7921(5)	3046(6)	865(5)	125(6)
C(10)	7789(7)	3740(6)	596(5)	129(7)
C(11)	6736(9)	4046(4)	537(5)	130(7)
C(12)	5816(6)	3659(4)	747(4)	99(5)
C(13)	5285(7)	1734(4)	1738(5)	73(4)
C(14)	5817(8)	1929(4)	2282(5)	96(5)
C(16)	6382(8)	1394(6)	2620(4)	106(5)
C(16)	6414(7)	664(5)	2415(5)	106(5)
C(17)	5882(7)	469(3)	1871(5)	87(5)
C(18)	5317(6)	1004(5)	1532(4)	72(4)
C(19)	4713(8)	738(6)	964(6)	67(4)
C(20)	3468(8)	610(5)	1105(5)	52(3)
C(21)	2970(7)	-51(3)	768(4)	56(3)
C(22)	3375(6)	-753(4)	909(4)	74(4)
C(23)	2922(8)	-1375(3)	627(5)	94(5)
C(24)	2063(9)	-1296(5)	205(4)	108(6)
C(25)	1657(7)	-594(6)	64(4)	96(5)
C(26)	2111(7)	29(4)	346(4)	77(4)
C(27)	2824(9)	1313(5)	1011(5)	55(3)
C(28)	1757(5)	1334(4)	1368(3)	50(3)
C(29)	1821(5)	1239(4)	2002(3)	61(3)
C(30)	861(8)	1249(4)	2353(3)	76(4)
C(31)	-164(6)	1353(4)	2072(4)	87(5)
C(32)	-228(5)	1448(4)	1439(4)	73(4)
C(33)	732(6)	1438(4)	1087(3)	59(3)
C(34)	4792(10)	1305(7)	455(7)	68(4)
C(35)	4148(11)	1207(6)	-84(7)	70(4)
C(36)	4034(11)	1807(7)	-487(7)	77(4)
C(37)	4603(11)	2460(7)	-292(6)	81(5)
C(38)	3514(9)	1696(5)	-1100(4)	93(5)

C(39)	2600(9)	1234(5)	-1174(5)	90(4)
C(40)	2179(7)	1097(5)	-1759(7)	110(5)
C(41)	2673(11)	1422(7)	-2269(4)	105(5)
C(42)	3586(11)	1884(6)	-2194(4)	123(7)
C(43)	4007(8)	2021(5)	-1610(6)	115(6)
C(44)	4463(11)	3171(4)	-627(4)	132(9)
C(45)	5423(10)	3582(7)	-723(5)	168(10)
C(46)	5370(14)	4251(6)	-1039(5)	246(20)
C(47)	4357(17)	4510(4)	-1258(4)	239(20)
C(48)	3398(13)	4100(6)	-1161(5)	187(13)
C(49)	3451(10)	3430(6)	-846(5)	149(10)
C(50)	2306(9)	3001(5)	692(6)	56(3)
C(51)	1951(11)	2648(6)	198(6)	65(4)
C(52)	1022(7)	2804(7)	-230(4)	81(4)
C(53)	690(11)	3540(6)	-286(5)	117(6)
C(54)	-133(11)	3731(6)	-706(6)	147(8)
C(55)	-624(8)	3187(10)	-1068(5)	129(7)
C(56)	-293(9)	2452(8)	-1012(5)	108(5)
C(57)	530(10)	2260(5)	-592(5)	79(4)
C(58)	1889(6)	3604(3)	1064(3)	48(3)
C(59)	889(5)	3520(4)	1373(4)	68(3)
C(60)	474(6)	4099(5)	1726(4)	97(5)
C(61)	1059(8)	4761(4)	1772(4)	93(5)
C(62)	2059(8)	4845(4)	1464(5)	141(8)
C(63)	2475(6)	4266(4)	1110(5)	125(7)

Table 7.7 Atomic coordinates (x 10^4) and equivalent isotropic displacement parameters ($Å^2$ x 10^3) for 1. U(eq) is defined as one third of the trace of the orthogonalized Uij tensor.

W(1)-C(27)	2.000(11)	C(13)-P(1)-C(7)	101.3(4)
W(1)-C(51)	2.018(13)	C(1)-P(1)-C(7)	103.3(4)
W(1)-C(50)	2.044(10)	C(13)-P(1)-W(1)	116.4(3)
W(1)-C(34)	2.302(12)	C(1)-P(1)-W(1)	117.5(3)
W(1)-C(35)	2.306(11)	C(7)-P(1)-W(1)	115.3(3)
W(1)-C(37)	2.331(11)	C(2)-C(1)-C(6)	120.0
W(1)-C(36)	2.349(12)	C(2)-C(1)-P(1)	121.9(4)
W(1)-P(1)	2.454(4)	C(6)-C(1)-P(1)	118.1(4)
P(1)-C(13)	1.830(8)	C(1)-C(2)-C(3)	120.0
P(1)-C(1)	1.834(6)	C(4)-C(3)-C(2)	120.0
P(1)-C(7)	1.834(6)	C(3)-C(4)-C(5)	120.0
C(1)-C(2)	1.39	C(6)-C(5)-C(4)	120.0
C(1)-C(6)	1.39	C(5)-C(6)-C(1)	120.0
C(2)-C(3)	1.39	C(8)-C(7)-C(12)	120.0
C(3)-C(4)	1.39	C(8)-C(7)-P(1)	122.9(5)
C(4)-C(5)	1.39	C(12)-C(7)-P(1)	117.1(5)
C(5)-C(6)	1.39	C(9)-C(8)-C(7)	120.0
C(7)-C(8)	1.39	C(10)-C(9)-C(8)	120.0
C(7)-C(12)	1.39	C(9)-C(10)-C(11)	120.0
C(8)-C(9)	1.39	C(10)-C(11)-C(12)	120.0
C(9)-C(10)	1.39	C(11)-C(12)-C(7)	120.0
C(10)-C(11)	1.39	C(14)-C(13)-C(18)	120.0
C(11)-C(12)	1.39	C(14)-C(13)-P(1)	116.4(6)
C(13)-C(14)	1.39	C(18)-C(13)-P(1)	123.3(6)
C(13)-C(18)	1.39	C(16)-C(14)-C(13)	120.0
C(14)-C(16)	1.39	C(14)-C(16)-C(16)	120.0
C(16)-C(16)	1.39	C(16)-C(16)-C(17)	120.0
C(16)-C(17)	1.39	C(18)-C(17)-C(16)	120.0
C(17)-C(18)	1.39	C(17)-C(18)-C(13)	120.0
C(18)-C(19)	1.511(14)	C(17)-C(18)-C(19)	116.6(8)
C(19)-C(34)	1.51(2)	C(13)-C(18)-C(19)	123.3(8)
C(19)-C(20)	1.551(13)	C(34)-C(19)-C(18)	110.8(10)
C(20)-C(27)	1.500(14)	C(34)-C(19)-C(20)	108.0(10)
C(20)-C(21)	1.520(11)	C(18)-C(19)-C(20)	110.5(9)
C(21)-C(22)	1.39	C(27)-C(20)-C(21)	113.1(9)
C(21)-C(26)	1.39	C(27)-C(20)-C(19)	110.4(8)
C(22)-C(23)	1.39	C(21)-C(20)-C(19)	113.8(8)
C(23)-C(24)	1.39	C(22)-C(21)-C(26)	120.0
C(24)-C(25)	1.39	C(22)-C(21)-C(20)	117.9(7)
C(25)-C(26)	1.39	C(26)-C(21)-C(20)	122.0(7)
C(27)-C(28)	1.506(11)	C(23)-C(22)-C(21)	120.0
C(28)-C(29)	1.39	C(22)-C(23)-C(24)	120.0

C(28)-C(33)	1.39	C(23)-C(24)-C(25)	120.0
C(29)-C(30)	1.39	C(26)-C(25)-C(24)	120.0
C(30)-C(31)	1.39	C(25)-C(26)-C(21)	120.0
C(31)-C(32)	1.39	C(20)-C(27)-C(28)	113.2(8)
C(32)-C(33)	1.39	C(20)-C(27)-W(1)	123.1(7)
C(34)-C(35)	1.42(2)	C(28)-C(27)-W(1)	123.7(7)
C(35)-C(36)	1.40(2)	C(29)-C(28)-C(33)	120.0
C(36)-C(37)	1.43(2)	C(29)-C(28)-C(27)	117.6(7)
C(36)-C(38)	1.48(2)	C(33)-C(28)-C(27)	122.4(7)
C(37)-C(44)	1.48(2)	C(28)-C(29)-C(30)	120.0
C(38)-C(39)	1.39	C(29)-C(30)-C(31)	120.0
C(38)-C(43)	1.39	C(32)-C(31)-C(30)	120.0
C(39)-C(40)	1.39	C(33)-C(32)-C(31)	120.0
C(40)-C(41)	1.39	C(32)-C(33)-C(28)	120.0
C(41)-C(42)	1.39	C(35)-C(34)-C(19)	119.2(11)
C(42)-C(43)	1.39	C(35)-C(34)-W(1)	72.3(7)
C(44)-C(45)	1.39	C(19)-C(34)-W(1)	112.2(7)
C(44)-C(49)	1.39	C(36)-C(35)-C(34)	118.4(12)
C(45)-C(46)	1.39	C(36)-C(35)-W(1)	74.2(6)
C(46)-C(47)	1.39	C(34)-C(35)-W(1)	72.0(7)
C(47)-C(48)	1.39	C(35)-C(36)-C(37)	113.8(14)
C(48)-C(49)	1.39	C(35)-C(36)-C(38)	119.9(12)
C(50)-C(51)	1.32(2)	C(37)-C(36)-C(38)	125.5(13)
C(50)-C(58)	1.446(11)	C(35)-C(36)-W(1)	70.9(7)
C(51)-C(52)	1.48(2)	C(37)-C(36)-W(1)	71.6(7)
C(52)-C(53)	1.39	C(38)-C(36)-W(1)	134.1(8)
C(52)-C(57)	1.39	C(36)-C(37)-C(44)	120.8(14)
C(53)-C(54)	1.39	C(36)-C(37)-W(1)	73.0(6)
C(54)-C(55)	1.39	C(44)-C(37)-W(1)	119.4(8)
C(55)-C(56)	1.39	C(39)-C(38)-C(43)	120.0
C(56)-C(57)	1.39	C(39)-C(38)-C(36)	121.3(9)
C(58)-C(59)	1.39	C(43)-C(38)-C(36)	118.6(9)
C(58)-C(63)	1.39	C(38)-C(39)-C(40)	120.0
C(59)-C(60)	1.39	C(41)-C(40)-C(39)	120.0
C(60)-C(61)	1.39	C(40)-C(41)-C(42)	120.0
C(61)-C(62)	1.39	C(41)-C(42)-C(43)	120.0
C(62)-C(63)	1.39	C(42)-C(43)-C(38)	120.0
		C(45)-C(44)-C(49)	120.0
C(27)-W(1)-C(51)	103.9(4)	C(45)-C(44)-C(37)	116.2(10)
C(27)-W(1)-C(50)	103.7(4)	C(49)-C(44)-C(37)	123.8(10)
C(51)-W(1)-C(50)	37.9(4)	C(46)-C(45)-C(44)	120.0
C(27)-W(1)-C(34)	76.3(4)	C(45)-C(46)-C(47)	120.0
C(51)-W(1)-C(34)	156.4(5)	C(48)-C(47)-C(46)	120.0

C(50)-W(1)-C(34)	165.6(5)	C(49)-C(48)-C(47)	120.0
C(27)-W(1)-C(35)	83.5(4)	C(48)-C(49)-C(44)	120.0
C(51)-W(1)-C(35)	120.7(6)	C(51)-C(50)-C(58)	134.9(11)
C(50)-W(1)-C(35)	158.3(6)	C(51)-C(50)-W(1)	70.0(7)
C(34)-W(1)-C(35)	35.8(4)	C(58)-C(50)-W(1)	154.9(9)
C(27)-W(1)-C(37)	143.7(4)	C(50)-C(51)-C(52)	131.5(10)
C(51)-W(1)-C(37)	102.2(5)	C(50)-C(51)-W(1)	72.1(8)
C(50)-W(1)-C(37)	112.4(4)	C(52)-C(51)-W(1)	155.9(9)
C(34)-W(1)-C(37)	69.8(5)	C(53)-C(52)-C(57)	120.0
C(35)-W(1)-C(37)	61.4(4)	C(53)-C(52)-C(51)	117.0(10)
C(27)-W(1)-C(36)	115.6(4)	C(57)-C(52)-C(51)	122.9(10)
C(51)-W(1)-C(36)	97.6(5)	C(52)-C(53)-C(54)	120.0
C(50)-W(1)-C(36)	127.8(5)	C(55)-C(54)-C(53)	120.0
C(34)-W(1)-C(36)	62.6(5)	C(54)-C(55)-C(56)	120.0
C(35)-W(1)-C(36)	35.0(4)	C(57)-C(56)-C(55)	120.0
C(37)-W(1)-C(36)	35.5(4)	C(56)-C(57)-C(52)	120.0
C(27)-W(1)-P(1)	89.7(3)	C(59)-C(58)-C(63)	120.0
C(51)-W(1)-P(1)	130.9(4)	C(59)-C(58)-C(50)	119.5(6)
C(50)-W(1)-P(1)	93.2(4)	C(63)-C(58)-C(50)	120.5(6)
C(34)-W(1)-P(1)	72.4(4)	C(60)-C(59)-C(58)	120.0
C(35)-W(1)-P(1)	107.4(4)	C(59)-C(60)-C(61)	120.0
C(37)-W(1)-P(1)	91.9(4)	C(62)-C(61)-C(60)	120.0
C(36)-W(1)-P(1)	118.7(4)	C(61)-C(62)-C(63)	120.0
C(13)-P(1)-C(1)	100.7(4)	C(62)-C(63)-C(58)	120.0

Table 7.8 Bond lengths [Å] and angles [°] for **II**.

Atom	U11	U22	U33	U23	U13	U12
W(1)	64(1)	34(1)	69(1)	-5(1)	32(1)	-5(1)
P(1)	58(2)	38(2)	100(3)	-13(2)	32(2)	-5(2)
C(1)	61(8)	36(6)	88(9)	-12(6)	6(7)	-1(5)
C(2)	56(8)	64(9)	152(14)	-38(9)	37(9)	-12(7)
C(3)	100(11)	68(9)	129(13)	-44(9)	35(10)	-9(8)
C(4)	108(12)	68(9)	82(10)	-14(8)	25(9)	20(9)
C(5)	73(9)	94(11)	65(9)	0(8)	9(7)	11(8)
C(6)	58(7)	62(7)	77(8)	-4(8)	12(6)	-8(7)
C(7)	58(8)	45(7)	113(10)	-25(7)	34(7)	-13(6)
C(8)	61(9)	75(10)	157(14)	-29(9)	34(9)	-9(7)
C(9)	62(9)	105(13)	207(19)	-37(13)	51(11)	-24(9)
C(10)	102(13)	97(13)	189(18)	-30(12)	89(13)	-35(11)
C(11)	116(13)	65(10)	210(19)	-28(11)	90(13)	-22(10)
C(12)	73(9)	58(9)	166(15)	0(9)	58(10)	-13(7)
C(13)	62(8)	34(7)	122(12)	-17(7)	24(8)	-1(6)
C(14)	91(11)	60(10)	138(14)	-35(10)	8(10)	11(8)
C(16)	99(12)	87(11)	134(14)	-36(11)	-24(10)	12(10)
C(16)	83(11)	71(10)	164(17)	-28(10)	-15(11)	16(8)
C(17)	60(9)	50(8)	151(14)	-26(9)	-15(9)	6(7)
C(18)	43(7)	55(8)	117(12)	-16(8)	18(8)	2(6)
C(19)	39(7)	50(7)	111(11)	-15(8)	23(7)	0(6)
C(20)	64(7)	33(6)	59(7)	-5(5)	11(6)	-6(5)
C(21)	52(7)	46(7)	71(8)	1(6)	32(6)	2(6)
C(22)	76(9)	33(7)	112(11)	2(7)	33(8)	8(6)
C(23)	107(12)	44(8)	131(14)	-25(9)	68(10)	-13(8)
C(24)	132(15)	61(10)	131(15)	-39(10)	59(12)	-25(10)
C(25)	87(10)	93(12)	107(12)	-26(10)	16(9)	-28(9)
C(26)	83(10)	43(7)	103(11)	-4(8)	16(9)	-8(7)
C(27)	66(8)	35(6)	66(8)	-21(6)	17(6)	-1(6)
C(28)	56(8)	31(6)	64(8)	10(5)	15(6)	1(5)
C(29)	64(8)	44(7)	74(9)	13(6)	14(7)	3(6)
C(30)	97(10)	59(8)	72(9)	17(7)	48(8)	4(7)
C(31)	74(10)	72(9)	116(13)	23(9)	60(9)	10(8)
C(32)	36(7)	72(8)	112(11)	9(8)	16(7)	7(6)
C(33)	52(7)	53(7)	71(8)	13(6)	7(7)	10(6)
C(34)	48(8)	60(8)	95(10)	-27(8)	18(8)	-5(6)
C(35)	73(9)	33(7)	106(11)	-9(8)	45(9)	3(6)
C(36)	89(10)	60(8)	83(10)	-20(8)	57(8)	-3(7)
C(37)	104(10)	50(7)	90(10)	-26(7)	71(9)	-27(8)
C(38)	132(14)	46(8)	102(13)	-6(8)	72(11)	21(8)

C(39)	110(12)	85(11)	75(11)	-10(8)	21(9)	9(9)
C(40)	99(12)	102(12)	129(15)	-7(12)	11(12)	17(10)
C(41)	147(16)	97(13)	70(11)	3(10)	10(11)	52(12)
C(42)	189(19)	64(10)	118(16)	7(10)	84(14)	8(11)
C(43)	207(17)	58(9)	80(10)	-17(9)	75(12)	-3(10)
C(44)	234(23)	48(9)	113(14)	-32(9)	137(15)	-58(12)
C(45)	268(24)	90(12)	145(15)	-62(12)	162(17)	-93(15)
C(46)	478(50)	96(17)	166(22)	-54(15)	220(28)	-139(25)
C(47)	562(58)	58(12)	99(15)	-36(11)	153(26)	-83(23)
C(48)	452(41)	49(10)	62(11)	-20(9)	68(17)	6(17)
C(49)	336(31)	36(9)	76(11)	1(8)	107(16)	0(13)
C(50)	68(8)	32(7)	68(8)	-3(6)	31(6)	-8(5)
C(51)	87(9)	40(7)	67(9)	14(7)	31(8)	0(6)
C(52)	133(12)	54(8)	56(8)	19(8)	34(9)	18(10)
C(53)	193(18)	108(14)	49(9)	4(9)	-19(10)	39(13)
C(54)	237(25)	122(16)	82(13)	5(13)	-1(15)	63(17)
C(55)	146(16)	163(18)	78(13)	52(13)	1(11)	45(16)
C(56)	107(13)	140(18)	78(12)	18(11)	-11(10)	-24(11)
C(57)	79(9)	79(10)	81(10)	-3(10)	10(8)	-8(9)
C(58)	33(6)	40(6)	71(8)	-9(6)	3(6)	3(5)
C(59)	58(8)	58(7)	89(9)	-15(7)	13(7)	16(6)
C(60)	92(11)	84(11)	114(12)	-10(9)	38(9)	26(9)
C(61)	92(11)	69(10)	118(12)	-39(9)	-2(9)	32(9)
C(62)	65(10)	69(10)	288(25)	-90(13)	2(13)	6(8)
C(63)	77(10)	47(8)	251(21)	-67(11)	42(12)	-3(7)

Table 7.9 Anisotropic displacement parameters ($Å^2 \times 10^3$) for **II**.

The anisotropic displacement factor exponent takes the form:

$$-2\,pi^2\,[\,h^2\,a^*\,2\,U11 + ... + 2\,h\,k\,a^*\,b^*\,U12\,]$$

Atom	x	y	z	U(eq)
H(2)	5414(7)	3877(6)	1868(6)	109
H(3)	4746(10)	4620(5)	2655(6)	119
H(4)	3131(11)	4293(6)	3164(4)	103
H(5)	2184(7)	3223(7)	2886(5)	93
H(6)	2852(8)	2480(5)	2099(5)	79
H(8)	7090(10)	2194(5)	1255(6)	117
H(9)	8626(6)	2841(8)	904(7)	150
H(10)	8405(9)	4000(8)	455(7)	155
H(11)	6647(12)	4511(5)	357(6)	156
H(12)	5112(7)	3863(6)	708(7)	119
H(14)	5796(12)	2417(4)	2420(7)	116
H(16)	6738(11)	1524(9)	2984(5)	128
H(16A)	6792(10)	306(7)	2641(6)	127
H(17)	5904(11)	-19(4)	1733(7)	104
H(19)	5045(8)	271(6)	825(6)	80
H(20)	3423(8)	495(5)	1544(5)	62
H(22)	3950(8)	-806(7)	1191(5)	88
H(23)	3193(11)	-1845(4)	721(7)	113
H(24)	1760(11)	-1713(6)	16(6)	129
H(25)	1083(8)	-541(9)	-218(5)	115
H(26)	1839(10)	498(5)	252(6)	92
H(29)	2506(7)	1170(6)	2190(5)	73
H(30)	904(11)	1186(6)	2777(3)	91
H(31)	-806(7)	1359(6)	2308(5)	105
H(32)	-913(5)	1517(6)	1251(6)	88
H(33)	689(9)	1501(6)	663(3)	70
H(34)	5567(38)	1465(58)	439(50)	82
H(35)	3822(83)	725(31)	-122(51)	85
H(37)	5357(47)	2401(72)	-150(55)	97
H(39)	2270(12)	1016(7)	-833(7)	108
H(40)	1568(9)	788(7)	-1809(9)	132
H(41)	2391(15)	1331(9)	-2660(5)	126
H(42)	3916(15)	2102(8)	-2536(6)	148
H(43)	4618(10)	2330(6)	-1560(8)	138
H(45)	6100(10)	3408(10)	-577(8)	201
H(46)	6011(16)	4526(9)	-1104(8)	296
H(47)	4322(22)	4958(5)	-1469(6)	287
H(48)	2721(16)	4273(10)	-1308(7)	225
H(49)	2809(11)	3155(8)	-781(7)	179
H(53)	1019(15)	3904(8)	-44(7)	140

H(54)	-355(16)	4223(7)	-744(9)	177
H(55)	-1175(10)	3315(14)	-1349(6)	155
H(56)	-621(14)	2087(11)	-1254(6)	130
H(57)	753(14)	1768(5)	-554(8)	95
H(59)	498(8)	3077(5)	1342(6)	82
H(60)	-195(8)	4043(7)	1933(6)	116
H(61)	781(11)	5148(6)	2009(6)	112
H(62)	2451(10)	5288(4)	1494(8)	169
H(63)	3144(7)	4322(6)	904(7)	150

Table 7.10 Hydrogen coordinates (x 10^4) and isotropic displacement parameters ($Å^2$ x 10^3) for **II**.